# A New On-Board Imaging Treatment Technique for Palliative and Emergency Treatments in Radiation Oncology

Dissertation with the aim of achieving
a Doctoral Degree
at the Faculty of Mathematics,
Informatics, and Natural Sciences

Department of Physics
University of Hamburg, Germany

Submitted by
Mareike Held

Hamburg
2016

This work is supported by research grants from Siemens OCS and DOSIsoft.

Oral Defense Date:
March 23, 2016

Supervisors:
Prof. J. Pouliot, PhD (UCSF, San Francisco - CA, USA)
Asst. Prof. O. Morin, PhD (UCSF, San Francisco - CA, USA)
F. Cremers, PhD (UKSH, Lübeck, Germany)
Prof. D. Horns, PhD (UHH, Hamburg, Germany)

Reviewers:
Asst. Prof. O. Morin, PhD (UCSF, San Francisco - CA, USA)
F. Cremers, PhD (UKSH, Lübeck, Germany)
Prof. D. Horns, PhD (UHH, Hamburg, Germany)

Research Location:
University of California, San Francisco
Hellen Diller Family Comprehensive Cancer Center
Deptartment of Radiation Oncology
1600 Divisadero Street, San Francisco,
CA 94115-1708

Research Time Frame:
August 2012 - January 2016

*To Jean*

-

*may I some day pay forward the generosity, inspiration, and mentorship I have received from you.*

# Deutsche Zusammenfassung

Diese Dissertation befasst sich mit der Anwendung von on-board-Bildgebungsverfahren als Grundlage für die Bestrahlungsplanung in der Strahlentherapie. Im Laufe des Arbeitsprozesses wurde ein klinischer Arbeitsablauf entwickelt, mit dem innerhalb kürzester Zeit eine einfache Strahlungsbehandlung anhand von 3-dimensionalen CT Bildern simuliert, geplant und durchgeführt werden kann. Dazu werden die verschiedenen Prozesse so verbunden, dass der Patient während der gesamten Zeit auf dem Behandlungstisch liegen bleiben kann. Folglich kann die gesamte Zeit - von der Simulation bis zur Behandlung - auf 30 Minuten reduziert werden.
Die wichtigste Grundlage zur Dosisberechnung anhand von CT Bildern ist die Kalibrierung der abgebildeten CT Grauskala zur Gewebedichte. Diese ist vom Energiespektrum der Photonen abhängig. Die damit verbundenen physikalischen Zusammenhänge sind grundlegend für das Verständnis der Bildqualität und damit für die Bearbeitung der Ursachen von Rausch-, Kontrast- und Uniformitäteigenschaften der verschiedenen on-board Systeme. Die Bildqualität und -stabilität von modernen on-board Bildgebungssystemen, wie z. B. kV und MV Kegelstrahl-CT sowie MV Fächerstrahl-CT, werden in dieser Arbeit charakterisiert. Dazu wird eine Sammlung an Phantom- und Patienten-CT Bildern erstellt, um die Dosisberechnungsgenauigkeit anhand von on-board Bildern zu bestimmen. Das Ziel ist es, lokale Dosisdifferenzen von 5% im Vergleich zu kV CT basierten Behandlungsplänen nicht zu überschreiten.
Eine ausreichend genaue Dosisberechnung anhand von den erstellten on-board Bildern ist in den meisten Fällen gegeben. Die Genauigkeit der Berechnung hängt dabei von der Anatomie des Patienten ab. Behandlungen im Kopfbereich, die mit on-board Bildern geplant werden, sind unabhängig von der Art des on-board Bildgebungsverfahrens mit einer Differenz von $<5\%$ im Vergleich zu kV CT basierten Plänen ausreichend gut zu planen. Lungengewebe hingegen kann Dosisunterschiede von $>5\%$ im Vergleich zu kV CT Plänen verursachen. Da die Bildqualität sich zwischen verschiedenen on-board Systemen unterscheidet, wird die CT-Zahl zur Dichtekalibrierung jedes Systems einzeln erstellt. Im Fall von einigen Bildgebungsverfahren sind die CT-Zahlen außerdem abhängig von der Strahlungsdosis pro Scan und den verwendeten Korrekturfiltern. Somit werden in bestimmten Fällen mehrere Kalibrierungskurven für die genaue Konversion von CT-Zahlen zu Gewebedichte benötigt.
An der UCSF wird diese neue Methode als Ergebnis bereits klinisch verwendet. Besonders die dadurch erreichte verkürzte Behandlungszeit in einfacherer medizinischer Umgebung ist dabei neben den Aspekten von Arbeitszeit, Ressourcenverwaltung und damit auch finanzieller Kalkulationen im Klinikbetrieb der entscheidende Vorteil für den Patienten.

# Abstract

This dissertation focuses on the use of on-board imaging systems as the basis for treatment planning, presenting an additional application for on-board images. A clinical workflow is developed to simulate, plan, and deliver a simple radiation oncology treatment rapidly, using 3D patient scans. The work focuses on an on-line dose planning and delivery process based on on-board images entirely performed with the patient set up on the treatment couch of the linear accelerator. This potentially reduces the time between patient simulation and treatment to about 30 minutes.

The basis for correct dose calculation is the accurate image gray scale to tissue density calibration. The gray scale, which is defined in CT Numbers, is dependent on the energy spectrum of the beam. Therefore, an understanding of the physics characteristics of each on-board system is required to evaluate the impact on image quality, especially regarding the underlying cause of image noise, contrast, and non-uniformity. Modern on-board imaging systems, including kV and megavoltage (MV) cone beam (CB) CT as well as MV CT, are characterized in terms of image quality and stability. A library of phantom and patient CT images is used to evaluate the dose calculation accuracy for the on-board images. The dose calculation objective is to stay within 5% local dose differences compared to standard kV CT dose planning.

The objective is met in many treatment cases. However, dose calculation accuracy depends on the anatomical treatment site. While on-board CT-based treatments of the head and extremities are predictable within 5% on all systems, lung tissue and air cavities may create local dose discrepancies of more than 5%. The image quality varies between the tested units. Consequently, the CT number-to-density calibration is defined independently for each system. In case of some imaging systems, the CT numbers of the images are dependent on the protocol used for on-board imaging, which defines the imaging dose and reconstruction corrections. Consequently, multiple image value-to-density calibration curves are necessary for accurate dose calculation.

UCSF has implemented the new technique clinically for emergency treatments on their patients who stand to benefit from the fast simulation to treatment time frame that is achieved through this on-board imaging workflow.

# Contents

# Acronyms

| | |
|---|---|
| a-Si | amorphous silicon, page 26 |
| ART | adaptive radiotherapy, page 2 |
| CBCT | cone beam computed tomography, page 11 |
| CCC | collapsed cone convolution, page 18 |
| CNR | contrast-to-noise ratio, page 29 |
| CT | computed tomography, page 2 |
| CT# | CT number, page 21 |
| DICOM | Digital Imaging and Communications in Medicine, page 39 |
| eFOV | extended field of view, page 31 |
| ERT | emergency radiation therapy, page 4 |
| FOV | field of view, page 30 |
| IGRT | image-guided radiotherapy, page 2 |
| IVDC | imgae value-to-density calibration, page 17 |
| kV | kilovolt, page 2 |
| kVp | kilovolt peak, page 19 |
| MLC | multileaf collimator, page 4 |
| MRI | magnetic resonance imaging, page 2 |
| MTF | modulation transfer function, page 30 |

| | |
|---|---|
| MU | monitor unit, page 11 |
| MV | Megavolt, page 10 |
| NU | non-uniformity, page 39 |
| PSF | point spread function, page 30 |
| QA | quality assurance, page 1 |
| rFOV | regular field of view, page 31 |
| RT | radiotherapy *or* radiation therapy, page 2 |
| RTTs | radiation therapists, page 93 |
| SAD | source-axis distance, page 16 |
| SCD | source-calibration point distance, page 16 |
| SNR | signal-to-noise ratio, page 25 |
| SSD | source-surface distance, page 15 |
| TFT | thin-film transistor, page 26 |
| TMR | tissue-maximum-ratio, page 15 |
| TPS | treatment planning system, page 15 |
| Tx | treatment, page 5 |

# CHAPTER 1

# Introduction

## 1.1 Radiation Therapy

Radiation Oncology is the medical specialty that prescribes radiation dosage as a treatment. Ionizing radiation damages the DNA of the targeted cells, causing them to reproduce more slowly and eventually necrotize. Radiation is delivered to the patient to induce maximized damage to the tumor cells, while minimizing the dose to the surrounding healthy tissue. A variety of machines can be used to deliver direct and indirect ionizing radiation. Most commonly, radiation is used for malignant cancer treatment. Less commonly, it is also prescribed in some benign conditions. Radiation treatments can be delivered as teletherapy through external beam radiation therapy or as brachytherapy, in which the radiation source is directly on or inside the patient. This study focuses on external beam radiotherapy.

Frequently, cancer treatment involves a combination of multiple treatments that, besides radiation, can be chemical and/or surgical. The order of treatments can affect the outcome. Therefore, all treatments require diligent coordination and a reliable schedule. To prepare for radiation therapy treatments, clinics follow a protocol, which includes a number of steps for patient simulation, treatment planning, quality assurance (QA), and treatment delivery. This involves several people, including doctors, dosimetrists, physicists, and radiation therapists. Besides the coordination of staff, it also requires diagnostic and treatment machines to be available. Thus, workflow optimiza-

tion and clinical coordination are important parts in radiation oncology.

Prior to radiotherapy (RT), images of the patient's anatomy are obtained with X rays from a computed tomography (CT) machine. Treatment planning is based on these images with the intent to localize the tumor and optimize the expected dose distribution. The patient can then be treated on a linear accelerator, for example.

An on-board CT imaging system integrated within the linear accelerator is a standard feature of all modern treatment machines. The imaging tool is commonly used to verify the patient setup immediately before treatment. Other uses include adaptive radiotherapy (ART) to adapt to temporal changes in anatomy and image-guided radiotherapy (IGRT) to account for patient motion during treatment [1, 2]. It is uncommon to use on-board CT images for dose calculation without additional information from kilovoltage (kV) CT or magnetic resonance imaging (MRI) due to their less reliable image quality. Using on-board images for dose-calculation would, in many ways, be an important diversification of on-board imaging systems.

This dissertation is structured as follows: after the introduction to emergency treatments in radiation oncology, Chapter 2 presents the aspects of CT imaging and dose calculation that are helpful for the understanding of the ensuing chapters. Following an introduction to the digital and physical phantoms used throughout the project, Chapter 3 provides specific examples of MV CBCT-based images, which point to the challenges for dose calculation based on on-board images. The new clinical ERT workflow, which was developed as part of the dissertation, is presented in combination with MV CBCT-based dose calculation in Chapter 4. A copy of the recent publication

> Held M, Sneed P K, Fogh S E, Pouliot J, and Morin O, "Feasibility of MV CBCT-based treatment planning for urgent radiation therapy: dosimetric accuracy of MV CBCT-based dose calculations". *J Appl Clin Med Phys* 2015;**16**(6):458-471.

is included to provide detailed documentation of this research. Similarly, Chapter 5 evaluates the suitability of additional kV and MV imaging systems for on-board based dose calculation with regard to emergency treatments. The resulting publication

Held M, Cremers F, Sneed P K, Braunstein S, Fogh S E, Nakamura J, Barani I, Perez-Andujar A, Pouliot J, and Morin O, "Assessment of image quality and dose calculation accuracy on kV CBCT, MV CBCT and MV CT images for urgent palliative radiotherapy treatments". *J Appl Clin Med Phys* 2016; (In press.)

is included to provide details on the methods and results. Chapter 6 reports on the clinical experience of the ERT workflow and evaluates the clinical implementation of MV CBCT-based treatment planning. The first two treatments applying the new ERT workflow are presented in detail. Chapter 7 discusses the challenges, results, and possible future projects related to this work. Finally, Chapter 8 concludes the work of this dissertation.

## 1.2 Emergency vs. Non-Emergency Radiotherapy

The process leading up to radiation treatment usually follows a hospital-specific protocol. Once a patient is diagnosed with a condition that requires radiation therapy, he or she is referred to a radiation oncologist to be advised about treatment options and to prepare for the upcoming therapy, which can last several weeks or months. In non-emergency situations, radiotherapy treatments with a curative aim are scheduled and commonly progress through the following general steps.

1. Patient consultation.
2. Definition of treatment course.
3. Treatment coordination with other departments (i.e. chemotherapy, surgery, radiology, etc.).
4. Patient simulation (kV CT of the treatment site in treatment position).
5. Contouring of regions of interest (ROIs) on the CT.
6. Treatment planning (often complex).
7. Treatment check and approval.
8. Treatment scheduling.
9. Treatment plan quality assurance.
10. Treatment.

In those situations, radiotherapy treatments are planned, simulated, and scheduled over a time span of 1-2 weeks. Many of these treatments are planned as intensity-modulated radiotherapy (IMRT), which is a complex

inverse-planned dose calculation where the multileaf collimators (MLCs) of the machine modulate the photon beam. This not only produces a desirable dose coverage of the treatment target but also offers ways to limit the dose to the surrounding healthy tissues. Several treatment plan checks and approvals are required before the beginning of treatment. To ensure a safe dose delivery to the patient, UCSF follows a "24-hour rule". It requires a full day between the final approval of the treatment plan and the treatment start to allow enough time for quality assurance procedures, which are generally physical dose measurements.

Emergency radiation therapy (ERT) can become necessary for a number of treatment cases when the patient's condition does not allow for the time of a scheduled treatment. Unlike those cases, emergency radiation therapy is prescribed for patients that require immediate or near-immediate radiation [3]. Consequently, the treatment plans are created for simplicity. Emergency radiotherapy treatments often precede a palliative treatment, so they are similar to those in many ways. In both cases, the overall aim is to reduce the targeted tissue quickly to relief pain, while still preventing complications from high dose delivery to healthy tissue surrounding the targeted tumor [4, 5]. Forward-planning of simple delivery fields and opposed beams usually achieve this goal. Other than the computationally complex inverse-planning, forward planning requires fewer staff, less preparation, and less time overall. If necessary, it can be calculated by hand on 2-dimensional patient X-ray images instead of 3-dimensional CT images.

Figure 1.1 outlines the main steps that are taken in preparation for a patient's radiation therapy treatment. The left side summarizes the steps required for emergency radiotherapy while the right side outlines the main procedures in preparation for non-emergency treatments. The arrows on each side indicate the approximate duration of the procedure. These are ideal times. However, processes are regularly delayed, which is especially critical in emergency situations. In contrast to this outline, ERT patients have spent six hours or more in the department previously, waiting to receive treatment. This is mainly due to the limited machine time. To have a streamlined workflow in place with as few interruptions and as short waiting times as possible is crucial for a successful clinical ERT routine.

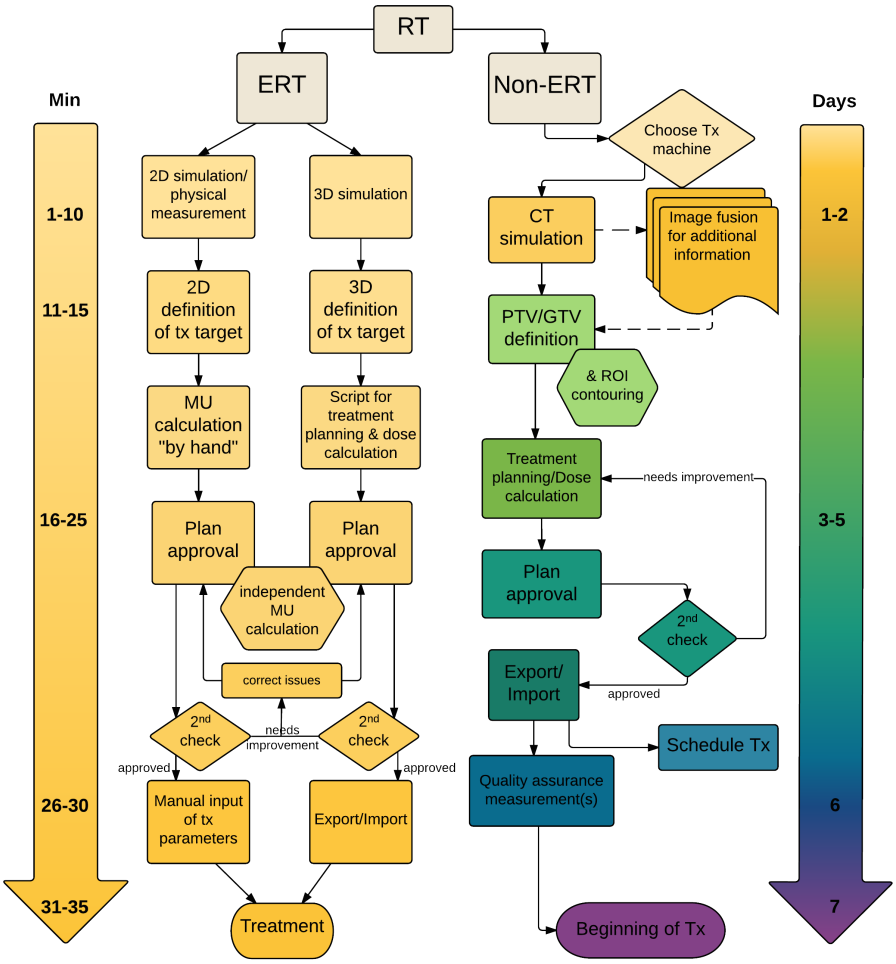


**Figure 1.1:** Approximate (ideal) duration of the clinical course for emergency versus non-emergency radiation therapy. (Tx stands for treatment. )

## 1.3 Workflow for Emergency and Palliative Radiotherapy

In the past, emergency patients were simulated on a kV simulator, which provides 2D information on the patient's anatomy. The treatment dose was planned and calculated based on the information obtained from physical patient measurements, lacking detailed information on the three-dimensional dose distribution. To obtain volumetric dose information, doctors are increasingly inclined to perform an urgent CT scan as a basis for treatment planning. This is highly disruptive to the clinical routine and extends waiting

periods for the patient, as the CT and linear accelerator time is very limited and open treatment times rarely line up. Consequently, the patient has to expect to spend several hours in the radiation oncology department before receiving treatment.

The work of this dissertation is to evaluate on-board image-based dose calculation as a solution to this problem. It provides a 3-dimensional dose distribution for visual evaluation of the treatment volume. In combination with a well integrated treatment workflow, dose calculation based on on-board images is a promising alternative for expedited safe urgent patient care. In brief, the goal here is to image, plan, and treat while the patient remains on the treatment table, which would decrease the time needed between imaging and treatment drastically. Unnecessary waiting times could be eliminated and make the course of treatment more predictable. It would further remove the need to move the patient from the imaging machine to the treatment machine. Keeping the patient in place is ideal when the patient is in pain or immediate treatment is required, which are considered emergency treatments. The dissertation focuses on patients needing ERT with respect to improved dose distributions, increased patient comfort, and minimized complications after treatment.

The challenges of this lie within the quality of on-board images. Depending on the photon energy spectrum of the on-board imaging system, CT images may have low image contrast, an inconsistent or non-uniform grayscale, or other image artifacts caused by patient motion or materials with high atomic numbers. Accurate dose calculation highly relies on consistent image value-to-density conversion. Thus, poor image quality may implicate inaccurate dose calculation.

## 1.4 Examples of Clinical Cases for Emergency and Palliative Radiotherapy

In severe emergency cases, the tumor volume may press on nerves or organs, putting the patient in a considerable amount of pain and at immediate risk to lose mobility or organ function. In other cases, tumor growth and proliferation may progress at such a fast rate that an urgent treatment is necessary. In those situations, an ERT treatment is usually the beginning of a more defined fractionated treatment plan. Although there is a difference in the

urgency between emergency, urgent, and palliative treatments, the clinical procedure is the same and will be referred to as the same in the following. A more detailed aim of palliative therapeutic radiotherapy and the significance of external beam radiotherapy with palliative intent are given in the literature [6, 7].

Besides those, a simple forward-calculated plan is prescribed occasionally, when a patient does not benefit from a complex inverse-planned treatment [8]. Furthermore, any treatments that are necessary outside the regular work hours, which means on weekends or after hours, are also considered emergency treatments as they will be performed by fewer staff and, consequently, are less elaborate.

Common situations that require immediate treatment, such as ERT, include rapidly growing metastases in the brain, near the spine, or near major veins. ERT is also performed to prevent heterotopic ossification after the implementation of prosthetic hardware, such as arthroplasty of the hip, knee, or elbow.

### Whole Brain

Whole brain RT becomes necessary when metastases in the brain occur in such a large number that a treatment of each individual metastasis becomes impractical and invisible spread of the disease throughout the entire brain is expected. A treatment plan generally consists of two opposed lateral beams. The MLCs on the linear accelerator can limit the field size to the brain and spare the skull tissue. The total treatment dose is fractionated and delivered daily over a time span of several weeks.

### Spinal Cord Compression

Metastases near the spinal cord can cause sudden complications during the course of a cancerous disease due to the risk of spinal cord compression, eventually causing vertebrae compression fractions. The treatment can be delivered in a single fraction or fractionated over several treatment deliveries. In case of fractionation, the treatment may be re-planned on 3D CT images after the initial emergency treatment to restrict the dose to the spinal cord, while still being able to target the tumor with the maximum dose possible.

### Heterotopic Bone

Arthroplasty, the surgical replacement of joints, largely increases the risk of heterotopic ossification. It is common practice to use radiation treatment as a measure to prevent ossification. One requirement for the success of this procedure, however, is that radiation is delivered within 72 hours of the surgical intervention [9]. As a result, although treatment can often be scheduled, a treatment plan cannot be made until after the surgery when the area of treatment is known. Thus, clinically, it is considered as an urgent treatment. For these treatments, the total dose is usually delivered in a single fraction as there is no evidence that a fractionated treatment is beneficial [10, 11]. Ideally, two opposed beams deliver the dose.
One difficulty specific to heterotopic bone treatments is that the targeted anatomy, typically near the hip, elbow, or knee, is away from the patient's mid-line. This results in an off-centered treatment position under the gantry and may limit the ability of gantry rotation around the patient, due to clearance between the machine and the patient.

# CHAPTER 2

# Physical Essentials of Imaging and Dose Planning in Radiotherapy

## 2.1 Linear Accelerators in Radiation Oncology

The most important treatment tool of the radiation oncologist is the linear accelerator, also called a linac. Each linac is built into its individual treatment room, which is specifically shielded to prevent radiation leakage to the outside. During treatment, radiation therapists control the machine from a treatment console adjacent to the treatment room while they monitor the patient by camera. Figure 2.1 shows a standard linear accelerator and its parts. For treatment, the patient is positioned on the **treatment couch**. A laser system mounted to the walls and the ceiling guides the patient into position. The gantry attaches to the gantry stand and rotates 360° around the treatment couch. The table itself can rotate in the horizontal plane and move in all three translational dimensions. Special couches, with a total of six degrees of freedom, also offer a 'pitch' and a 'roll' functionality.

The **gantry** contains the waveguide, in which microwaves accelerate electrons to high energies. These electrons are either used directly for treatment, or part of their energy is converted into highly energetic X rays. Electrons are commonly used for superficial treatments near the patient's skin. However, most tumors are several centimeters deep inside the patient, which requires

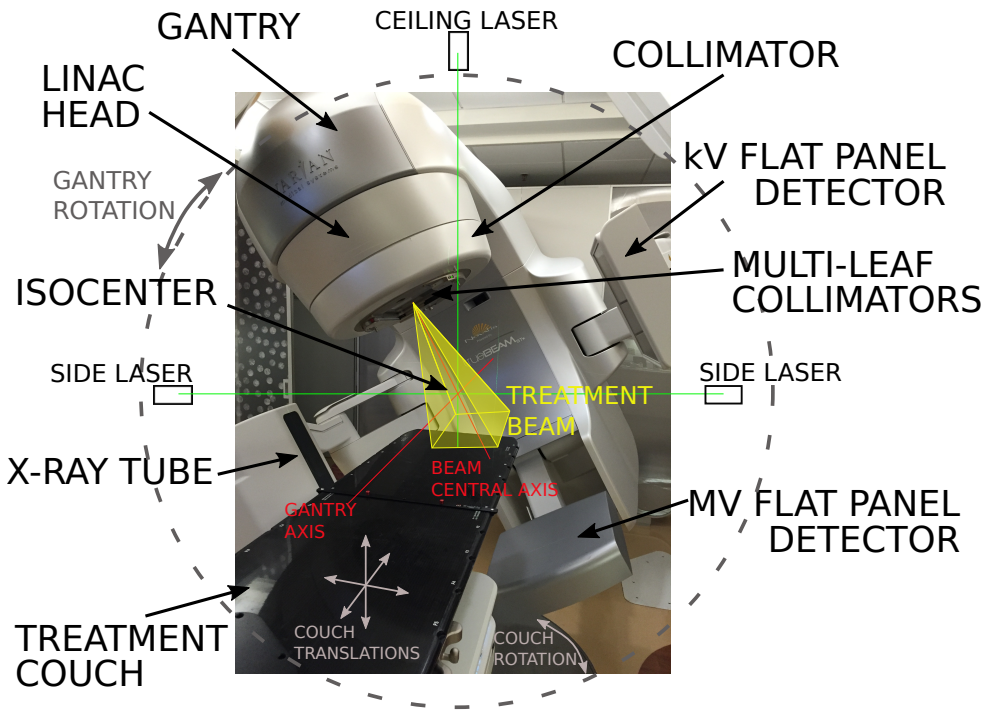


**Figure 2.1:** A modern linear accelerator with the description of parts.

deeply penetrating photons for treatment instead. Commonly, linacs provide photon energy spectra from 6 to 18 megavolts (MV)[1] to treat tumors at different depths. The interaction of the electrons with a metallic target, such as tungsten, creates photons within the **linac head**. A bending magnet redirects the electrons on to the tungsten target. Photons are created through the bremsstrahlung effect in the form of a forward peaking shaped X-ray beam. Before reaching the patient, the beam traverses a primary collimator, a beam flattening filter, ion chambers that monitor the performance of the linac, a secondary collimator, and multileaf collimators to shape the radiation field.

Every linac rotates around one point in space, which is called **isocenter**. It is the intersection of the beam central axis, gantry axis, collimator axis, and table axis. In most modern machines, this point is 100 cm away from the radiation source at all times. Typically, the treatment target is placed at

[1] A 6 MV photon beam is produced by a 6 MeV electron beam. While the electron beam is nearly monoenergetic, the photon beam is not. Is is a continuous Bremsstrahlungs spectrum with 6 MeV as its highest energy. 6 MV refers to the fact that the electrons were gradually accelerated through a potential difference of 6 million volts [12].

isocenter and the room lasers are aligned to indicate this point.

Opposite the head is an **MV flat panel detector** mounted on a retractable arm. It contains rows of detectors that measure the transmitted radiation. This enables the acquisition of patient X-ray images in treatment position and visualization of the treatment area. In addition, some vendors integrate a **kV source** and a **kV flat panel detector** into their linacs. These are also mounted on retractable arms, perpendicular to the gantry. Because of their integration into the linac, these are called on-board imaging systems.

Figure 2.2 shows four modern linear accelerators, each by a different vendor. Figure 2.2(a) and 2.2(b) show the Varian TrueBeam and Elekta VersaHD, respectively, which both provide kV and MV imaging on the machine. 2.2(c) is a photo of the Siemens Artiste, which offers MV cone beam computed tomography (CBCT) on-board imaging. The Tomotherapy by Accuray, displayed in Figure 2.2(d), differs from the other three by using a ring gantry. Here, the radiation source rotates around the patient continuously, while the treatment couch moves through the gantry bore, producing a helical trajectory. MV CT imaging is integrated into the gantry for on-board patient imaging.

For radiation emission, the linac receives a command to deliver a defined number of monitor units (MUs) rather than the target dose. This number is calculated before the delivery based on the characteristics of the machine. The most common way to calibrate linacs defines the delivery of 100 MU to equal the dose of 100 cGy at the point of maximum dose inside a water phantom. In this case, the water surface of the phantom is placed at 100 cm SSD, the radiation field size is 10 cm $\times$ 10 cm at isocenter [13].

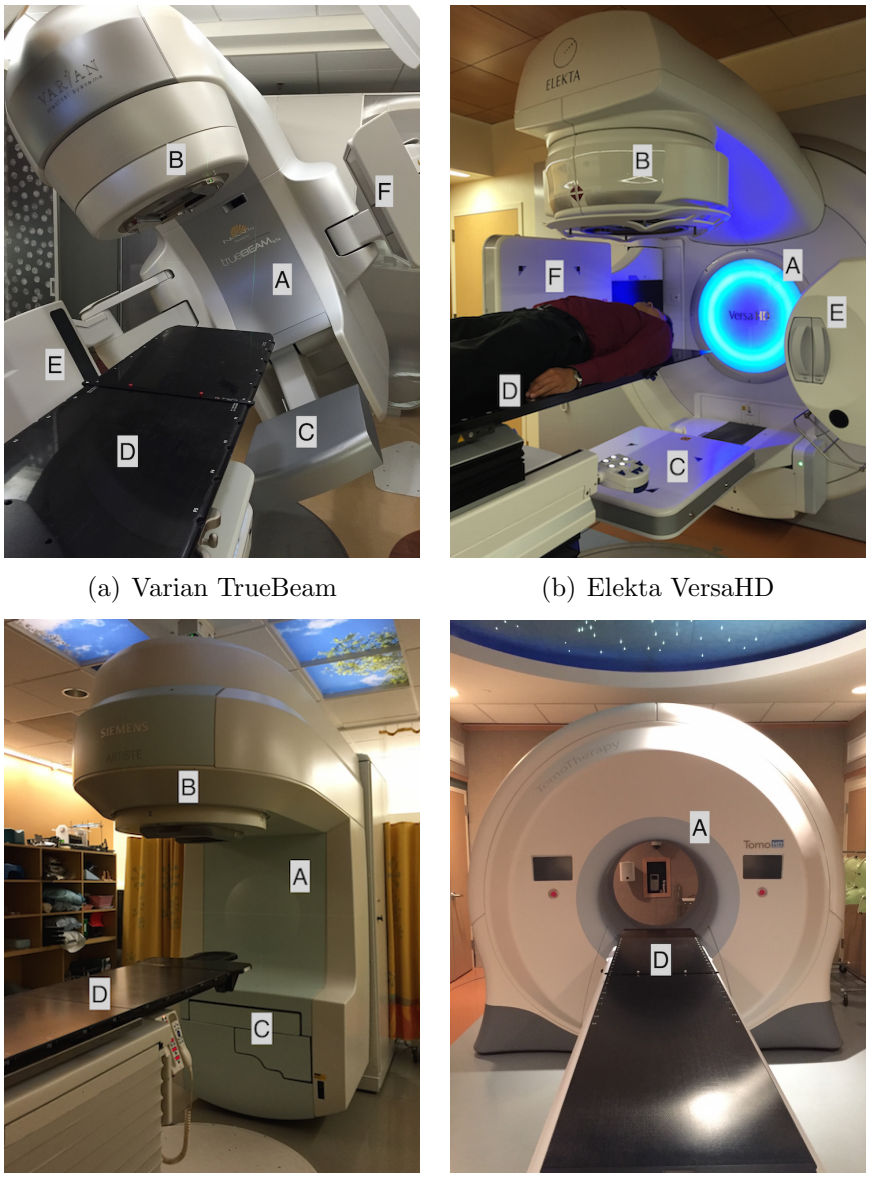


(a) Varian TrueBeam

(b) Elekta VersaHD

(c) Siemens Artiste

(d) Accuray Tomotherapy

**Figure 2.2:** Modern linear accelerators with on-board imaging. Components on the machine are identified by capitalized letters where applicable as (A) gantry, (B) linac head, (C) MV flat panel detector, (D) treatment couch for patient support, (E) kV imaging source, and (F) kV flat panel detector.

## 2.2 X-ray Interaction with Matter

Photons are uncharged particles and, as indirectly ionizing radiation, they interact with matter, such as the patient's body. The most important effects of interaction with respect to the energies used in radiation therapy are the photoelectric effect, the Compton effect, and pair production. When an X-ray beam, consisting of photons, passes through matter, it is attenuated in an exponential decrease in the number of photons. This can be described by

$$I(x) = I_0 e^{-\mu x} \ , \tag{2.1}$$

where $I(x)$ is the transmitted intensity and $I_0$ is the initial transmitted intensity, $\mu$ is the linear attenuation coefficient, and $x$ defines the thickness of the material the photons are traversing. The linear attenuation coefficient is the sum of the contribution of each effect to the photon attenuation,

$$\mu = \sigma_{\text{coh}} + \tau + \sigma_{\text{C}} + \pi \ . \tag{2.2}$$

Here, $\sigma_{\text{coh}}$ denotes the decrease due to coherent scatter, $\tau$ the attenuation contribution by the photoelectric effect, $\sigma_{\text{C}}$ the component attenuated by the Compton effect, and $\pi$ the attenuation due to pair production. $\mu$ is a function of the photon energy $E$, the atomic number $Z$ of the material, and the material density $\rho$. The quotient $\frac{\mu}{\rho}$ is defined as the mass attenuation coefficient.

### Energy Dependence of Indirectly Ionizing Radiation

The predominant photon interaction with matter depends on the photon energy at the time of interaction. The part of the beam attenuated through photoelectric absorption, symbolized by $\frac{\tau}{\rho}$, decreases with increasing photon energies by roughly $\frac{1}{E^3}$. It is the most likely interaction for photons with energies of less than ∼100 keV, prevailing all other effects in the low-energy range [14]. Photons with energies between 100 keV and 10 MeV are most likely to interact with matter through the Compton effect, making it the most important effect for therapeutic photon energies. Pair production is a high-energy phenomena. If a photon enters matter with an excess energy over 1.022 MeV pair production is possible. Its probability increases with increasing photon energy [15]. Figure 2.3(a) shows the contribution of each effect to the total photon attenuation per cm of water for different photon beam energies. Next to it, Figure 2.3(b) is a plot of the attenuation coefficient for clinically relevant materials such as bone, water, and air. The photoelectric absorption increases for materials of high atomic numbers and

is proportional to approximately $Z^3$. In contrast, the Compton effect is almost independent of the atomic number. Pair production increases with the atomic number approximately as $Z^2$. This explains why MV photons produce a linear signal and a lower image contrast for materials of differing $Z$ compared to kV energies.

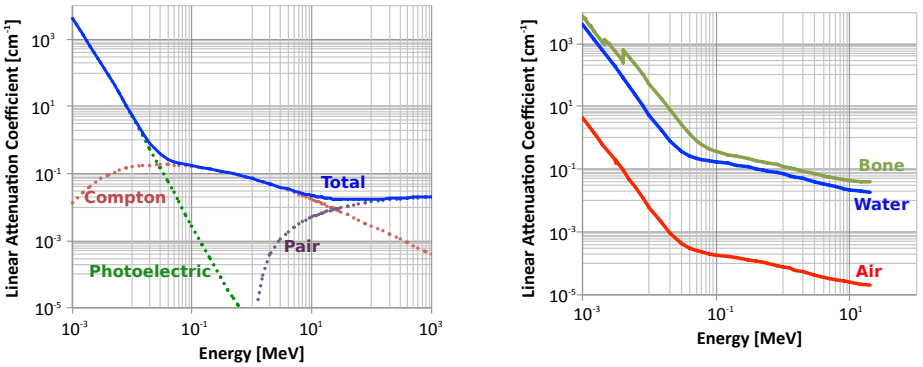


(a) Photon attenuation in water due to photoelectric absorption, Compton effect, and pair production.

(b) Attenuation coefficient for relevant clinical materials and energies.

**Figure 2.3:** Attenuation coefficient for different photon energies.[2] The photon energy determines the dominant effect during X-ray interaction with matter.

## 2.3 2D vs. 3D Treatment Planning

Radiographic 2D images provide anatomical information in one plane. This is sufficient to define the treatment field. However, it does not provide volumetric information, such as the patient thickness, tissue heterogeneity, or depth of treatment, all of which are essential for calculating the treatment dose accurately.

### 2D-based Dose Calculation

When using 2D images for treatment planning, the patient thickness is physically measured with a ruler. To calculate the MUs that are needed to achieve the prescribed dose at a particular point, the medical physicist or dosimetrist uses data tables specific to the linac. Those define the output factors and

[2] According to data from the National Institute of Standards and Technology (NIST).

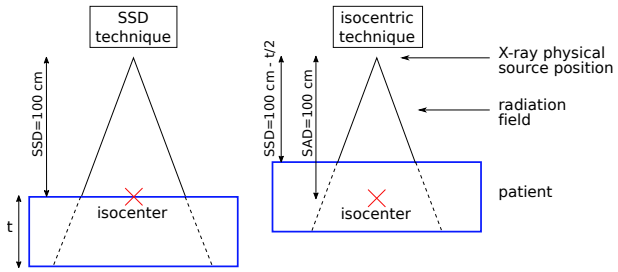


**Figure 2.4:** The patient setup geometry of the SSD technique compared to the isocentric technique.

scatter factors for various field sizes and photon energies. The data tables are generated during the treatment machine commissioning process and entered into the treatment planning system (TPS) and an independent dosimetric validation system. The TPS in this case is Pinnacle[3] by Philips Medical Systems (Eindhoven, NL). The dosimetric validation system is RadCalc by Lifeline Software (Austin, TX). Both systems are used to calculate the amount of MU for a rectangular field and a dose prescription to a specified point inside the patient. The MU calculation depends on the patient setup on the linac.

There are two different techniques to set up the patient on the linac. Figure 2.4 illustrates the different geometries of both techniques. The *SSD technique* positions the patient so that the patient's surface is aligned with the isocenter of the linac. Consequently, for an upright gantry position at a 0° angle the source-surface distance (SSD) is 100 cm. In case of the *isocentric technique*, the isocenter is placed inside the patient. This is the more common setup because of the isocentric gantry rotation around the patient. The isocenter can be placed inside the tumor. Consequently, the target volume remains at the same distance from the source at all times, which simplifies dose calculation for treatments with different gantry positions. In case of treatments with two opposed beams, which is common for ERT, the latter places the isocenter at the patient's mid-plane that is at half the measured patient thickness. Hence, the SSD remains the same for both treatment beams and the calculated amount of MU applies to both.

In case of the isocentric technique, MUs are calculated using the tissue-maximum-ratio (TMR). The TMR is determined by a series of measurements inside a water phantom, depicted in Figure 2.5. It is the ratio of the dose at a given point $d$ in a water phantom to the dose at the same point in space at the reference depth of the maximum dose $d_{\max}$. The maximum dose in water

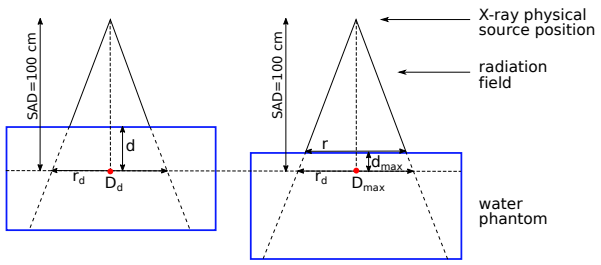


**Figure 2.5:** Sketch of the water phantom setup to measure the TMR on a linac. The water phantom is gradually moved up along the central axis and the dose $D_d$ is measured for each point at depth $d$ and field size $r_d$ measured at isocenter. The TMR is the ratio of the dose $D_d$ and the dose $D_{\max}$ measured at the reference point $d_{\max}$.

of a 6 MV photon beam is commonly at a depth of 1.5 cm [15].

At UCSF, the MUs for ERT treatments are usually calculated with Pinnacle and verified with RadCalc, as shown in the example in Chapter 6. For an isocentric setup, MUs are calculated with Equation 2.3, according to which

$$MU = \frac{D(d, r_d)}{K \times \mathrm{TMR}(d, r_d) \times S_c(r_c) \times S_p(r_d) \times \left(\frac{\mathrm{SCD}}{\mathrm{SAD}}\right)^2} \qquad [15, 16]. \qquad (2.3)$$

$D(d, r_d)$ is the prescribed dose at depth $d$ along the central axis. $K$ is a factor of units cGy per MU, which depends on the reference conditions used during linac commissioning. $S_c$, the collimator scatter factor, is the output factor of the machine in air. It accounts for the primary photon beam and the photons scattered by the linac components. $S_p$ is the phantom scatter factor, which accounts for the scatter within the medium. Both factors are measured under and depend on specific reference conditions. $\left(\frac{\mathrm{SCD}}{\mathrm{SAD}}\right)^2$ is called the source-axis distance (SAD) factor. SAD is the distance from the source to the isocenter, which is commonly 100 cm. SCD describes the source-calibration point distance, which is based on specific reference conditions. $r$ defines the field size at the surface of the water phantom. The field size $r_c$ is the collimator field size, calculated by $r_c = r\left(\frac{\mathrm{SAD}}{\mathrm{SSD}}\right)$, whereas $r_d$ is the field size measured at isocenter (refer to Figure 2.5). The K factor, the collimator scatter factor, and the phantom scatter factor can be combined into one output factor OF. At UCSF, the reference conditions are measured in an SSD setup (Figure 2.4), such that the machine outputs a dose of 1 cGy/MU measured at depth $d_{\max}$ for a photon field of 10 cm $\times$ 10 cm at 100 cm SSD. Thus, for a 6 MV photon beam, the OF is measured at 101.5 cm SCD at the depth of maximum dose. OF is

- $< 1$ for field sizes $< 10$ cm $\times$ 10 cm,
- $= 1$ for field sizes $= 10$ cm $\times$ 10 cm, and
- $> 1$ for field sizes $> 10$ cm $\times$ 10 cm.

Then, Equation 2.3 can be simplified to

$$MU = \frac{D(d, r_d)}{\mathrm{TMR}(d, r_d) \times \mathrm{OF} \times 1.03} \quad .$$

The $\mathrm{TMR}(d, r_d)$ and OF values are listed for a range of square field sizes and treatment depths in a data binder specific to each linac.

To calculate the dose of a rectangular field instead of a square, it can be approximated by the equivalent square method [17,18]. This method equates a rectangular field with a square field by comparing the ratio of the field area $A$ and field perimeter $P$

$$\frac{A}{P} = \frac{a \times b}{2(a+b)}$$

for a rectangular field and

$$\frac{A}{P} = \frac{a^2}{4^a} = \frac{a}{4}$$

for a square field, where $a$ is the field width and $b$ is the field length.

## 3D-based Dose Calculation

MU calculation based on Equation 2.3 only provides results for points along the central axis, neglecting possible dose attenuation differences due to tissue heterogeneity as well as scatter. 3D dose calculation algorithms consider the volumetric CT data provided. With the information of depth at every point, dose can be calculated throughout the entire volume and be displayed digitally on the CT. It provides the ability to account for tissue heterogeneity along the beam path, using the CT grayscale as an indicator of tissue density, which is defined by the image value-to-density calibration (IVDC). 3D images also offer the ability to draw volumes digitally. This opens up the opportunity for multiple other features, such as restrictions on the dose minimum or maximum delivered to a specific region. Lastly, it provides a visual plan quality evaluation tool, referred to as dose-volume histograms [19].

An external beam TPS distinguishes mainly between two algorithm methods, both of which provide clinically acceptable calculation times: the "correction-based" method and the "model-based" method. The correction-based method

is based on measured dose distributions in a water phantom. Independent corrections are applied to account for the beam geometry, beam modifiers, the patient anatomy, and tissue heterogeneity [8]. Correction-based algorithms are limited in the accuracy, particularly in case of 3D heterogeneity in lung tissue. Model-based dose calculation systems use water phantom measurements to model the beam, e.g. the primary photon fluence. Then, the energy absorption and energy transport within the patient are modeled. TERMA, which stands for "total energy released per unit mass", is the product of the mass attenuation coefficient with the primary energy fluence and expresses the absorption of the primary photons [20]. The energy transport within the patient can be modeled by using point dose kernels, which describe the dose distribution around a single interaction point. The superposition method by Mackie et al. [21] provides a model-based algorithm applying TERMA and point dose kernels. It essentially is a convolution of the modeled TERMA with all dose kernels from all primary interaction points [20]. However, the energy distribution varies within the beam, for example due to beam hardening, which is explained in Section 2.6. Thus, dose kernels are not invariant in space. Additionally, in case of tissue heterogeneity, the local TERMA depends on the path of the primary photons. This limits the feasibility of convolution [20]. One approximation can be made by using pencil beam dose kernels to describe the 3D dose distribution of an infinitely narrow photon beam in water. Tissue heterogeneity is accounted for via the effective path length to consider spatial variations in the dose kernels. That way, it correctly accounts for electron scatter in non-water materials. However, it is limited to the longitudinal scaling. Consequently, pencil beam dose kernels do not account for lateral electron variations. Another approximation for the superposition, the collapsed cone convolution (CCC) algorithm, has been suggested by Ahnesjö [22]. The CCC is an analytic kernel represented by a set of cones. The energy deposited within each cone is "collapsed" onto a line [22]. A further simplification to speed up the dose calculation process is the adaptive collapsed cone convolution. This algorithm performs a convolution at every fourth point in the TERMA array when the TERMA gradient between points is below a certain threshold [23]. Throughout this project, the adaptive convolution superposition was applied for all 3D dose calculations.

## 2.4 kV Simulators

Before CT became widely available, simulators were used to plan radiotherapy treatments. The simulator emulates a linac in its dimensions and movement. Similarly, it has a gantry that rotates around the treatment couch. It uses a conventional X-ray tube with diagnostic energies defined at 70 to 120 kilovolt (peak) (kVp) [24]. Opposite the simulator head is an electronic portal imaging device that acquires 2D radiographic images. The simulator can be used to determine the treatment area through the 2D radiographic films or as part of a patient's treatment verification. Figure 2.6 is a photo of the kV simulator at UCSF.

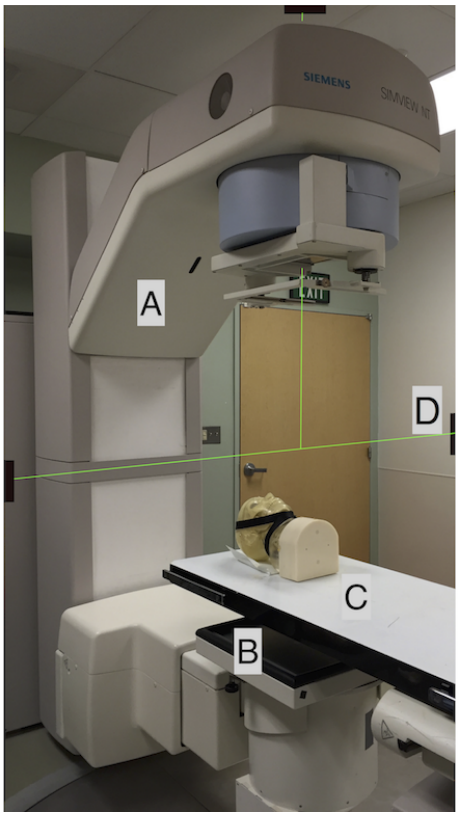


**Figure 2.6:** Siemens kV simulator with (A) gantry, (B) radiographic X-ray film tray, (C) patient couch, and room laser system for patient alignment. For the imaging procedure, the couch is moved up to align the isocenter of the simulator with the treatment target inside the patient.

Figure 2.7 sketches the basic system of a camera-based detector as it is used in older kV simulators. The X-ray beam goes through the patient where

some signal is absorbed. The metal plate on the detector serves as an X-ray converter and produces electrons. There, the generated electrons hit a phosphor screen that serves as a scintillator. The generated light is re-directed by a mirror and captured by a camera lens. The signal generated inside the camera is digitized and displayed on a monitor for review.

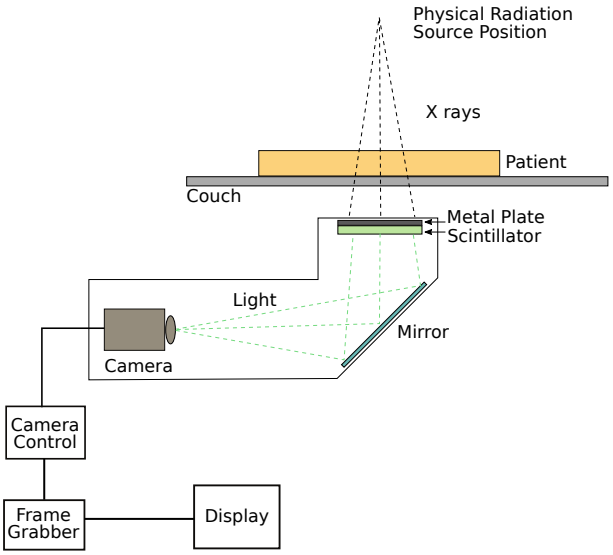


**Figure 2.7:** Schematic setup of a camera-based detector as it is used on the kV simulator. The phosphor screen converts high-energy electrons into light, which creates a video signal inside the camera. The camera is set inside a light-tight case. The mirror reflects the light into the camera, which extends the life-span of the camera by not being exposed to the direct beam. The camera signal is digitized and can be displayed on a monitor inside the control room.

Due to its limited use for patient simulation over the past few years, UCSF has used their kV simulator only in rare occasions when the kV CT was unavailable. Recently, the implementation of the new treatment technique has made the use of the simulator obsolete.

## 2.5 CT and On-Board CT Imaging

Over the last decades, patient imaging has become increasingly important in radiation oncology. Computer technology opens up the possibility to instantly review, send, and use digital images. Its use and functionality has broadened from simple 2D X-ray images, to 3D fan-beam CT images, to

on-board imaging for instant review of patient alignment. Various systems present different advantages and disadvantages.

kV CT scans serve two main purposes in radiation oncology: the definition of the treatment target area and the base for treatment plan dose calculation. Fan-beam CT scanners are a separate machine and operate independently of the treatment machine, whereas on-board CT systems are integrated into the linac. During fan-beam CT, the gantry rotates around the patient continuously while the couch slowly moves the patient forward through the gantry bore. In contrast, cone-beam CT uses a cone-shaped radiation field during acquisition. The gantry rotates around the patient once while acquiring 2D fluence maps at every angle around the patient, which are captured on the electronic portal imaging device (EPID) and subsequently reconstructed to a 3D image. Figure 2.8 illustrates the geometry of both systems. On-board CT imaging is regularly used for patient alignment moments before the treatment delivery and provides a visual tool for tumor positioning inside the treatment field relative to the original planning kV CT. Therefore, requirements on image quality are much lower for on-board systems than for kV CT. Figure 2.2 in Section 2.1 shows examples of the different on-board imaging systems and their integration into the treatment machine.

CT images are generated based on the measurements of the machine-dependent parameters $I_x$ and $I_0$ from Equation 2.1 in Section 2.2. When rearranged to

$$\ln(\mathrm{I_0/I_x}) = \mu \mathrm{x} \ ,$$

$\mu x$ provides important information on the patient anatomy.

The image grayscale on kV CT images is defined in terms of Hounsfield units [15]

$$HU = \frac{\mu_{\mathrm{tissue}} - \mu_{\mathrm{water}}}{\mu_{\mathrm{water}}} \times 1000 \ ,$$

where $\mu$ is the linear attenuation coefficient. Thus, water is, by definition, represented as $HU = 0$. However, the grayscale of on-board images is not necessarily set up with this definition. To avoid confusion and to match the notation of the TPS used here, the grayscale of CT images is referred to as CT numbers (CT#) in the following, which is defined as

$$CT\# = HU + 1024 \ .$$

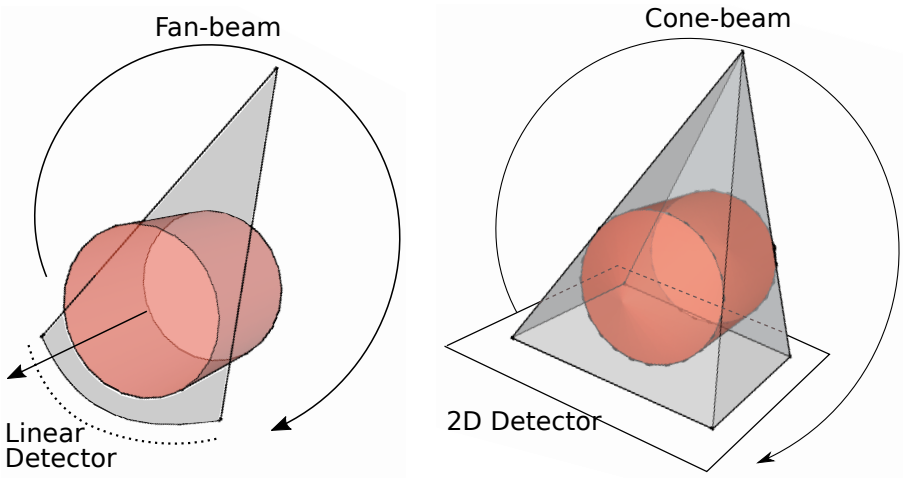


(a) During a fan-beam CT, the detector captures one image slice at a time.

(b) During a cone-beam CT, the detector, which is a 2D array, captures projection images of the object.

**Figure 2.8:** Fan-beam and cone-beam CT geometry.

CT simulation began to replace conventional simulation in the early 1990s. As radiation delivery devices become increasingly precise, demands for more accurate CT simulation increase [25]. CT simulation presents the conjunction between the CT scanner, the laser system, the workstation, and the treatment planning system [26]. The vertical and horizontal room lasers help to align the patient such that the cross section of the laser is placed as close to the treatment target as possible. The patient is imaged in the same position as during treatment. Occasionally, patient immobilization devices are also used during patient simulation. The patient position is documented in precise detail since it is crucial for correct re-positioning on the treatment machine.

Aside from serving as a tool for patient alignment before treatment, on-board CT imaging has become increasingly interesting to use for dose calculation. Being able to use the information of regularly acquired images during the course of treatment is very desirable for multiple reasons. Applications include adaptive radiotherapy (ART), image-guided radiotherapy (IGRT), and dose-guided radiotherapy (DGRT) [1, 2, 27]. The objective of these applications is to use the daily patient images to define the treatment status. Due to tumor shrinkage over the course of treatment, re-planning sometimes becomes necessary. On-board images could be used as a guide to decide when an adjustment of the treatment plan should occur.

## kV CT

CT scanners use X rays in the kV range for patient imaging. Each CT scanner contains an X-ray generator, a gantry, a detector system, a patient table, a control console, and a computer system. Compared to conventional diagnostic CT scanners, CT scanners for radiotherapy simulation require precise couch alignment, a high tube rating, sufficient disk storage capacity, and an image geometric scale [28]. The patient couch is made of low-$Z$ material, usually carbon fiber, and has a flat surface to mimic the treatment couch of the linac [24]. The gantry is a ring, which contains a rotating X-ray tube and detectors. The tomographic acquisition consists of several transmission measurements, which are called rays or projections. For a single axial CT image, the system takes about 800 rays at 1,000 projection angles, which totals to 800,000 transmission measurements [29]. Figure 2.9 shows a CT scanner used in Radiation Oncology.

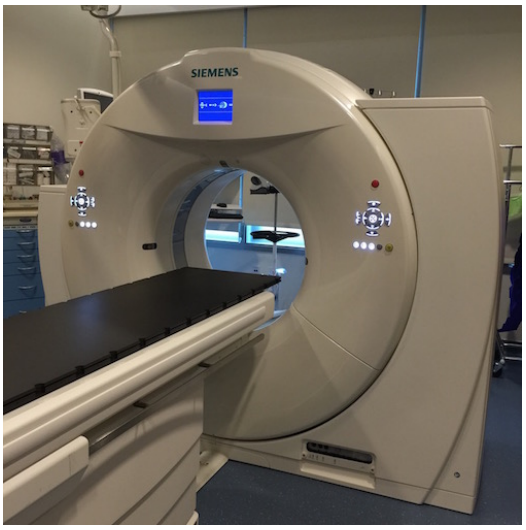


**Figure 2.9:** A modern CT scanner for patient simulation in radiation oncology. This particular model was recently installed at UCSF but was not used for this work.

The CT scanner that provides all images in this dissertation is the MX8000 by Philips Medical Systems. It falls into the category of third-generation CT scanners. It uses an array of solid-state detectors, which rotate around the patient opposite of and at the same time as the X-ray tube. The solid-state detectors use a scintillator, often $Gd_2O_2S$, to generate light, similar to the

one described in Section 2.4, which is coupled to a photodiode. The electronic signal from the photodiode is used to generate the CT image [29].

## kV CBCT

KV CBCT systems use a cone-shaped beam geometry as introduced in Figure 2.8(b). These on-board imaging systems are currently included in linacs of different vendors, for example in those by Varian (Palo Alto, CA, USA) and Elekta (Crawley, UK). The kV source is attached to the gantry of the linac, perpendicular to the central axis of the linac. Opposite the kV source is an amorphous silicon portal imager. Both, the kV source and the detector panel, are mounted on retractable arms. During image acquisition, both parts need to be fully extended. However, during treatment, the kV source and panel can be stored in a resting position on the side of the gantry, outside the patient's view.

For kV CBCT acquisition, the gantry rotates around the patient while capturing projection images at each gantry angle, whereupon the 3D image is reconstructed. Image processing filters are applied to reduce image artifacts and improve its display. Additionally, different imaging protocols can be chosen for the image acquisition. These improve the field of view and kV CBCT results based on the targeted anatomic site.

## MV CBCT

MV CBCT acquires projection images of the patient using the treatment source while rotating the gantry around the patient. Consequently, no additional radiation source and panel are required. Instead, the images are acquired with energies in the MV range. Projection images of each angle are reconstructed to a full 3D image. An amorphous silicon portal imager is installed opposite to the MV source as the detector. It is mounted on a retractable arm that allows it to be stored flush against the gantry when not in use.

MV imaging shows little to no image artifact when scanning across metal. This is especially desirable when acquiring images of the patient's head during the presence of dental fillings or prosthetic metal implants. kV photons are absorbed easily in metal due to its high atomic number $Z$, leading to photon starvation and a lack of signal on the detector. Consequently, these spots

shine bright white, leading to streaking artifacts around the metal object. MV photons, however, still pass through the metal and produce undisturbed signal [30].

## MV CT

An MV CT system is integrated into the Tomotherapy linac by Accuray (Sunnyvale, CA, USA). It is a fan-beam CT; thus, images are acquired slice-by-slice while the patient is translated through the bore, resting on the treatment couch. In contrast to the planning CT scans, however, images are acquired using the treatment beam with an energy of 6 MV. Experience shows that, while image contrast in soft tissue is displayed similarly poor as in MV CBCT images, the reduced scatter due to the fan-beam technology is advantageous and reduces motion and Cupping artifacts.

## Electronic Portal Imaging Device - EPID

Electronic Portal Imaging Devices - EPIDs - are commonly used for digital radiography on linacs as a replacement of portal imaging films. The digital image processing provides instant digital 2D images. EPIDs are used for volumetric CBCT images and provide a tool for on-line verification [31, 32].

The performance of an EPID can be defined by the detective quantum efficiency (DQE). It describes the efficiency with which incoming data with a signal-to-noise ratio (SNR) of $\mathrm{SNR}_{in}$ produces an image with a SNR of $\mathrm{SNR}_{out}$. Thus,

$$\mathrm{DQE} = \frac{\mathrm{SNR}_{out}^2}{\mathrm{SNR}_{in}^2} \ .$$

SNR is defined in more detail in Section 2.6. Flat panels that are currently in use for MV detection have a DQE of $\sim$1%. For kV detectors, the DQE is much higher at about 60% [33]. Consequently, MV imaging requires a higher imaging dose than kV to produce a sufficient SNR.

### Indirect Detection Systems

The structure of an EPID is shown in Figure 2.10. An indirect detection system is analogous to a screen-film system, with the exception that an electronic sensor replaces the light-sensitive film emulsion. Each image pixel is

represented by a detector element, which contains a light-sensitive area and electronics. In this example, MeV photons first strike a metal plate, commonly copper, which converts the incident X rays to light. The generated Compton electrons then interact with the subsequent phosphor screen. That process generates light photons in the green spectrum that are registered by amorphous silicon (a-Si) photodiodes. The charge is stored in capacitors before it is read out for each detector element with the help of thin-film transistors (TFT). The EPID is made up of a series of horizontal and vertical electrical lines. This design reduces the number of connections that are required to read out the signal of each individual pixel [29]. Figure 2.11 shows the read-out process of the detector elements. For the read-out process, the system applies a negative voltage during exposure to switch off the transistor. The charge remains in the capacitor until a positive voltage is sequentially applied to open the switch that connects the detector elements.

For indirect detection systems, the spatial resolution is determined by the size of the detector element. Therefore, decreasing the size of each detector improves the spatial resolution. However, that also increases the fraction of area covered by electronics, which is not sensitive to light. Consequently, the light collection efficiency decreases with smaller detector elements, which results in a lower contrast resolution. The ratio of light-sensitive area to the entire detector element area is defined by the fill factor. In summary, an increase in spatial resolution creates a lower fill factor, which leads to a lower SNR [29].

To improve the image quality, three corrections are performed. An offset correction is used to correct the dark current of each pixel for a specified frame time, a gain correction is used to homogenize different pixel sensitivities, and a dead pixel correction allows a software repair of defected pixels to enhance image quality by averaging the values of the adjacent pixels instead [34].

## In-Line kView System on Siemens Artiste

The Artiste is the most recent linac produced by Siemens. It offers MV CBCT as an on-board imaging system. Compared to kV CBCT, MV CBCT provides better images when scanning across metal, due to the Compton effect being independent of the atomic number $Z$. However, MV CBCT consistently produces less image contrast due to its higher energy, especially in soft tissue regions. To maintain the benefits of MV imaging but to also improve image quality while reducing the radiation dose per CBCT scan, Siemens

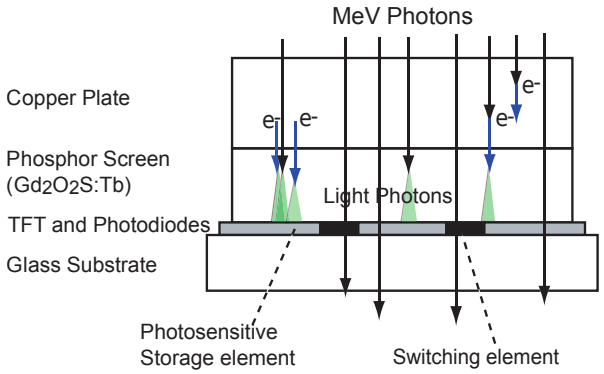


**Figure 2.10:** The layers of an EPID for MV photon detection (not to scale). (Reproduced from [35] with permission.)

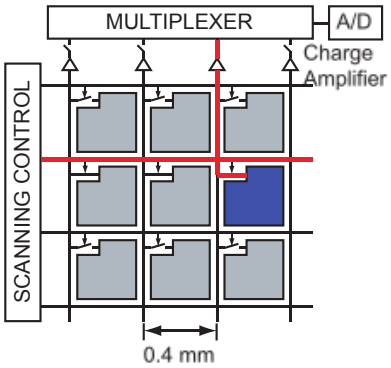


**Figure 2.11:** Detector elements of an EPID. The red line indicates the read-out process of the charge for the highlighted blue pixel. (Reproduced from [35] with permission.)

invented a specific low-MV imaging application that can be integrated into their linac. Such a system was implemented on the Siemens Artiste at UCSF in the Spring of 2013. A summarizing report of the installation is included in Appendix E.

Section 2.2 explains the energy dependence of physical effects. This is exploited in the In-Line kView system. During patient imaging, the metallic tungsten target ($Z = 74$) is replaced with a low-atomic number carbon target ($Z = 6$). To avoid electron leakage through the target, the energy of the electron beam is lowered to 4 MeV. Additionally, the flattening filter is removed, which would usually filter low-energy photons. The resulting X-ray beam is effectively described as a 1 MV beam. Consequently, the energy spectrum is shifted towards the kV range, which results in improved image contrast.

Without the flattening filter, the beam profile is peaked instead of flat. Figure 2.12 shows this for the crossline beam profile. While the treatment beam of 6 MV and 18 MV is flattened out across the entire field size of $40 \times 40$ cm$^2$, the imaging beam with an energy of 1 MV peaks towards the center.

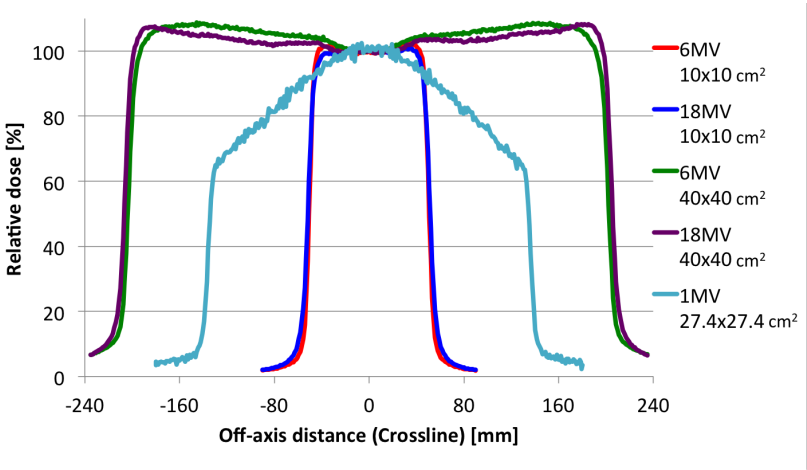


**Figure 2.12:** Crossline profiles of the InLine kView system using 1 MV energy in comparison with the treatment beam for 6 MV and 18 MV energies. 6 MV and 18 MV energy beams are shown for field sizes $10 \times 10$ cm$^2$ and $40 \times 40$ cm$^2$. The 1 MV InLine kView beam profile is shown for a field size of $27.4 \times 27.4$ cm$^2$, which is used during CBCT imaging. The latter also shows an increase in noise along the profile, which is owed to the lower dose per pulse. Due to the removed flattening filter, the profile peaks towards the center.

## 2.6 CT Performances

### Image Quality

The amount of noise, contrast, image non-uniformity, and spatial resolution of an image are measures for image quality. They can be used to compare the performance of different CT machines. In Chapter 5, each of these are defined for CT system evaluation. The radiation source, energy, dose, and detector affect CT performance. The imaged object geometry and size can further cause image artifacts and decrease image quality.

#### Contrast

Image contrast defines the difference in the image grayscale. In medical imaging, different steps during the acquisition produce contrast. Subject contrast

is the difference in some aspect of the signal before being detected. It is dependent on the absorption differences of different object tissues. Subject contrast decreases with increasing energy due to the decrease of photoelectric absorption probability with $\frac{1}{E^3}$.

**Noise**
Image noise adds a stochastic component to the image. It is due to uncertainties in the detected signal. X-ray detectors register discrete X-ray quanta, which introduces a statistical uncertainty. Quantum noise is an important contributor to image noise for X-ray detectors. It follows a Poisson distribution, according to which the variance $\sigma^2$ in the number of detected X-ray quanta is equal to the mean number of detected photons N:

$$\sigma^2 = N \ , \tag{2.4}$$

where $\sigma$ is the standard deviation or noise [29]. Additional sources of noise include energy absorption noise, electronic or film noise, and noise by the human visual system [31].

**Contrast-to-Noise Ratio**
The contrast-to-noise ratio (CNR) is used to measure the contrast potential in digital images. With the possibility of digital image postprocessing, contrast itself can be increased or decreased. Thus, the CNR is a more suitable image characterization for digital images. It is defined as

$$\mathrm{CNR} = \frac{\mathrm{A} - \mathrm{B}}{\sigma} \tag{2.5}$$

for two different signals A and B and the image noise $\sigma$.

**SNR**
The SNR describes how large a signal difference is compared to the uncertainty of the detected signal. As the number of detected photons N increases, $\sigma$ increases by the square root according to Equation 2.4. For processes following a Poisson statistic, the SNR is defined as

$$\mathrm{SNR} = \frac{N}{\sigma} = \frac{N}{\sqrt{N}} = \sqrt{N} \ . \tag{2.6}$$

The relative noise, $\sigma N$, which is perceived by the human observer, decreases with an increase in signal by the square root.

**Spatial Resolution**
The spatial resolution describes the ability of an image system to delineate

two adjacent objects in the spatial dimensions of an image. It can be measured by stimulating the detector with a single point input. The resulting signal is referred to as the point spread function (PSF), which may detect directional image blurring. Alternatively, the spatial resolution of an imaging system can be calculated in the spatial frequency domain. The modulation transfer function (MTF) plots the signal modulation versus spatial frequency. Mathematically, it is the Fourier transform of the PSF $s(r)$, defined as

$$S(k) = \mathcal{F}\{s(r)\} = \int_{-\infty}^{\infty} s(r)e^{-2\pi irk}dr \ , \tag{2.7}$$

where $k$ and $r$ are the conjugate variables in the frequency domain and the spatial domain, respectively. The MTF can be practically determined by measuring the ability of an on-board system to resolve an image with sinusoidal intensity lines [36]. Appendix F contains an example where the MTF is measured for different CT systems.

**Image Non-Uniformity**
Image non-uniformity refers to the varying CT number nonlinearities in reconstructed 3D CT images [37]. This image degradation is known as Cupping artifact. Due to photon scatter, the signal that is captured by the EPID increases for some areas of the object. Thus, those areas appear to be less dense than others of the same tissue density. X-ray scatter is described to be the main physical factor for the degradation of CBCT image quality [38]. Image uniformity can also be diminished due to beam hardening. Beam hardening occurs for polychromatic X-ray sources. When the photon beam traverses an object, it absorbs low-energy photons more easily than the high-energy photons. Consequently, the radiation beam becomes "harder", making photon attenuation less likely.

## Field of View

The field of view (FOV) describes the area that can be visualized in one image. Ideally, the image is large enough to display the entire cross-section of the patient. However, the larger the field of view, the more scatter from within the patient contributes to the image.

The FOV is especially important when images are used for dose calculation. To calculate the dose of a particular beam, all anatomical information along the beam path needs to be accessible. Thus, a beam can only be placed at

angles around the patient for which the entire anatomy is displayed. This especially becomes difficult for large patients and images acquired of the pelvis.

Fan-beam kV CT scanners commonly have a bore diameter of 50 cm or more. Consequently, the field of view is sufficiently large for almost any patient. Recently, efforts have been made to increase CT scanner bore diameters up to 90 cm, to also provide clearance for patient's immobilization devices, without decreasing image quality significantly [26,39]. For on-board systems, the FOV is limited by the radiation field and the area of the detector. Furthermore, the scatter contribution from within the patient is higher for CBCT scans. Therefore, small objects are commonly acquired using the regular (r)FOV, which allows for minimal radiation dose and acquisition time. Instead of a full gantry rotation, it requires only 200deg rotation with one projection per degree. Images are reconstructed using the Parker Weighting [40]. The extended (e)FOV is used to image larger anatomy only when necessary. One way to achieve the eFOV is to shift the flat panel laterally by a few centimeters, in which case a full rotation becomes necessary.

The Siemens Artiste once provided a CBCT FOV of up to 37 cm. However, with the introduction of the In-Line kView system, the FOV was decreased to maintain image quality, mainly due to the forward-peaked beam profile (see Figure 2.12). To limit the effect of the forward-peaked beam, the maximum flat panel offset was decreased to 5.5 cm, resulting in an eFOV diameter of 31 cm.

# CHAPTER 3

# Requirements for MV CBCT-based Dose Calculation

This chapter introduces the phantoms that are used to evaluate image quality and define the image value-to-density calibration. It also summarizes different approaches to optimize MV CBCT image quality on the Siemens Artiste for dose calculation. MV CBCT image quality is presented with respect to the imaging dose. Finally, the system stability is measured.

## 3.1 Digital and Physical Phantoms

### Digital Phantoms

Digital phantoms present a tool to quantify the effect that artifacts have on dose calculation as presented in Section 3.3. The digital phantom used here is generated in MATLAB (The MathWorks, Natick, MA). It contains 100 slices of $512 \times 512$ pixel each. The voxel size is set to measure 0.5 mm $\times$ 0.5 mm $\times$ 2 mm. It is assigned a cylindrical shape of 40 cm in diameter. The original phantom contains circular regions with three different CT numbers of 200, 1024, and 1400, corresponding to those of air, water, and bone, respectively. Figure 3.7 shows the axial view of this phantom with increasing image degradation from left to right. First, the contrast-to-noise ratio is decreased by introducing random noise across the entire image. This is achieved by multiplication of the image with the *randn function* in Matlab, which is a normal

distribution of pseudorandom numbers. Then, the image non-uniformity is increased by increasing the CT Numbers towards the phantom edges and lowering the CT Numbers towards the center of the phantom. In order to do this, a ring function with increasing radii and correction factors is multiplied with the original image. The spatial resolution of the image is degraded by applying a Gaussian filter to the image using the Matlab function *imfilter*.

## Water Phantoms

Four physical water phantoms were built throughout the course of this project. The first one is a plastic cylinder filled with water, which has a diameter of 17 cm to roughly resemble the size and shape of a human head. A high density insert, made from a mineral-filled epoxy to simulate the density of bone, is fixed to a plastic plate centered inside the cylinder. On the opposite side, an air cavity is created using a small plastic cup. Figure 3.1 is a photo of this phantom. The intention was to use the phantom for defining the IVDC, which is required for dose calculation. However, it was uncertain whether or not three inserts would provide sufficient data to produce an accurate calibration curve. Instead, the phantom was used to show the relationship between image quality and imaging dose in Section 3.4.

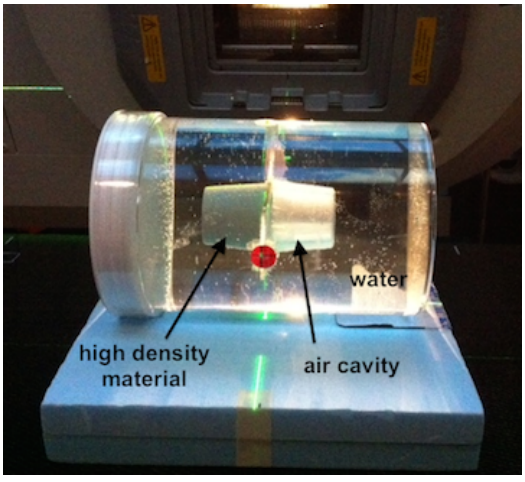


**Figure 3.1:** Phantom 1 is a cylindrical water phantom containing inserts of bony material and air. The red markers on three sides are used for subsequent re-alignment on the linac.

Another phantom was built using various inserts of a commercial kV CT calibration phantom (Model 062M, CIRS, Norfolk, VA), which provides a data

sheet of the insert densities. Each insert is wrapped air-tight in vacuum-sealed plastic to avoid damage when submerged in water. They are placed inside a cylinder filled with water and are held in place by a circular plastic piece with round cut-outs. Figure 3.2 shows the placement of the inserts. Seven different inserts image ca used: lung inhale (mass density: 0.195 g/cm$^2$), lung exhale (0.495), adipose (0.967), water(1.0), trabecular bone (1.161), dense bone (1.609), and air (0.0). The rFOV MV CBCT image values are calibrated to physical density using this phantom.

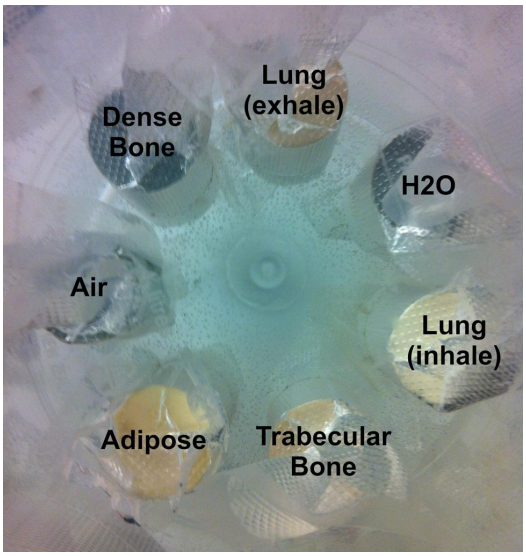


**Figure 3.2:** For phantom 2, inserts of different densities are positioned inside a cylindrical water phantom. The inserts are held in place by an acrylic disk with circular cut-outs. Each insert is wrapped in vacuum-tight plastic wrapping to prevent water damage to the inserts.

A plot of the IVDC obtained from measurements with each cylindrical phantom appears in Figure 3.3. A comparison between the IVDC curves shows a difference in CT number of 19, 0, and 56 at densities of 0.0, 1.0, and 1.56 g/cm$^3$. This corresponds to a relative difference of 4%, 0%, and 5.5% in CT numbers, respectively.

For the eFOV, which is used to image larger anatomy, another phantom was built, resembling the size and shape of a pelvis. Figure 3.4(a) shows the making of the phantom. Acrylic sheets were bent under heat to form a round shape, avoiding any sharp edges which may cause unnatural image artifacts. Despite the differences in the IVDC curves in Figure 3.3, inserts similar to the ones of phantom 1 from Figure 3.1 are included to provide CT informa-

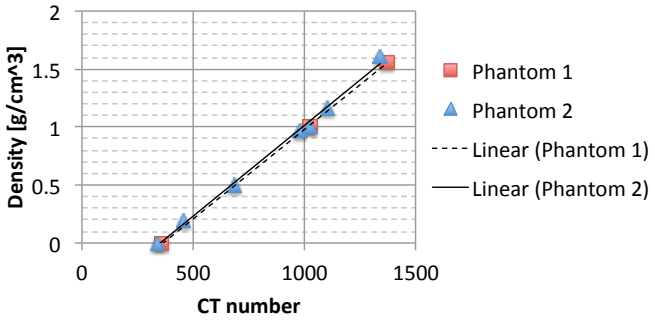


**Figure 3.3:** Image value-to-density calibration obtained with phantom 1, introduced in Figure 3.1, and Phantom 2, introduced in Figure 3.2. A relative difference of up to 5% between both IVDC curves shows the limits of the self-made inserts of phantom 1.

tion on different densities. An additional phantom with the same properties of this pelvis phantom but without density inserts was later built to define the image quality of large objects imaged with the eFOV.

There are some commercial phantoms that are intended to be used for image value to dose calibration. Nevertheless, this option of self-made phantoms presented a cost-efficient alternative.

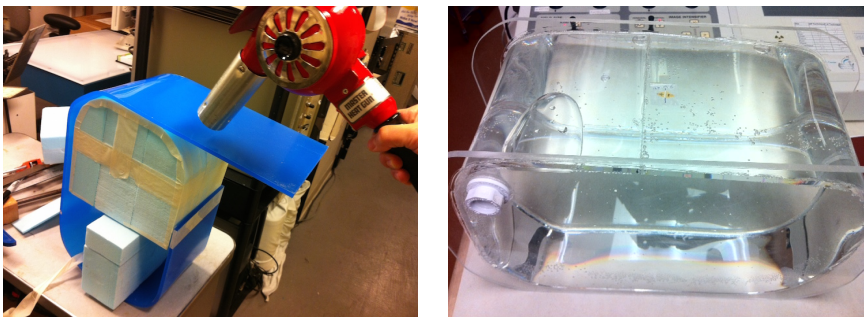

(a) Acrylic sheets are bent under heat to form a round pelvis-like shape.

(b) The finished pelvic phantom filled with water.

**Figure 3.4:** The making of a pelvic water phantom from acrylic sheets. The phantom is used to define the image value to density calibration of large objects in the eFOV.

### Anthropomorphic Head Phantom

An anthropomorphic head phantom appears in Figure 3.5. The phantom is used for dose planning in Chapter 4 and 5 as well as for CT number profiles on kV CT and MV CBCT images in the following section. The anatomy and tissue density of the phantom is based on the real anatomy of a human head.

**Figure 3.5:** Photo of the anthropomorphic head phantom that is used to compare dose calculation differences between kV CT-based treatment plans and on-board CT-based treatment plans.

## 3.2 IVDC

Image contrast is an important image attribute to distinguish between different structures within an object. It can be measured as the difference in grayscale intensities for different material densities. The anthropomorphic head phantom from Figure 3.5 is imaged on the kV CT and the MV CBCT In-Line kView beam line. Figure 3.6(a) and 3.6(b) show the CT scans, respectively. The dotted line shows the path of the intensity profile that is depicted below in Figure 3.6(c). The green and purple arrows show the positions within the CT images. Differences in image intensities become obvious when looking at the kV CT intensity profile, shown in blue, and the MV CBCT intensity profile, shown in red. While tissues containing air result in low CT numbers compared to other tissues, high Z tissues, such as bone, cause high intensity signal. The absolute difference, however, varies for the different CT modalities. The range of CT numbers is more narrow for the MV CBCT profile, suggesting less image contrast overall. Consequently, a specific IVDC becomes necessary to accurately convert the CT grayscale of MV CBCT images to physical densities. Thus, the kV CT and MV CBCT are converted to density using machine-specific IVDCs. Figure 3.6(d) plots

the resulting density profiles in blue and red on the left axis of the plot. The difference between both density profiles, normalized to their respective mean, is plotted in green in the same figure with the percentage difference values on the right axis. This shows that once the images are converted to density, the profiles agree better in terms of amplitude. The peaks of the density difference plot, with differences up to 63%, appear in regions of a high tissue density gradients within the image. This may result from the lower spatial resolution in MV CBCT images compared with kV CT images [41, 42]. Nevertheless, high dose differences of 20 - 38% also appear in the region of densities below 0.5 g/cm$^3$, indicating inaccuracies of the IVDC for low density tissues. Bony anatomy is calibrated to about 20% lower than its actual density in this case. Implications of these discrepancies are discussed in the following chapters.

The IVDC plays an essential role for CT-based dose calculation. It provides a look-up table that assigns density values to specific CT numbers. Every TPS is based on the correctness of this table. Some TPS ask for a calibration to physical density, others for a calibration to electron density, and each calibration table is specific to one CT machine. Periodic measurements are performed for quality assurance. Therefore, commercial QA products are available for kV CT calibration. They usually consist of a 5 cm thick solid water slice with circular cut-outs as placeholders. Interchangeable density inserts can be placed inside the cut-outs to represent tissues of various densities. These phantoms, however, are unsuitable for CBCT image value to density calibrations as it requires an extended phantom to account for scatter in the Z-direction, perpendicular to the direction of gantry rotation. To calibrate CT numbers to electron densities on a CBCT unit, the phantoms presented in the previous Section 3.1 were built containing different density inserts.

The results of the image value-to-density calibration for the rFOV and eFOV are documented in detail in Chapter 4.

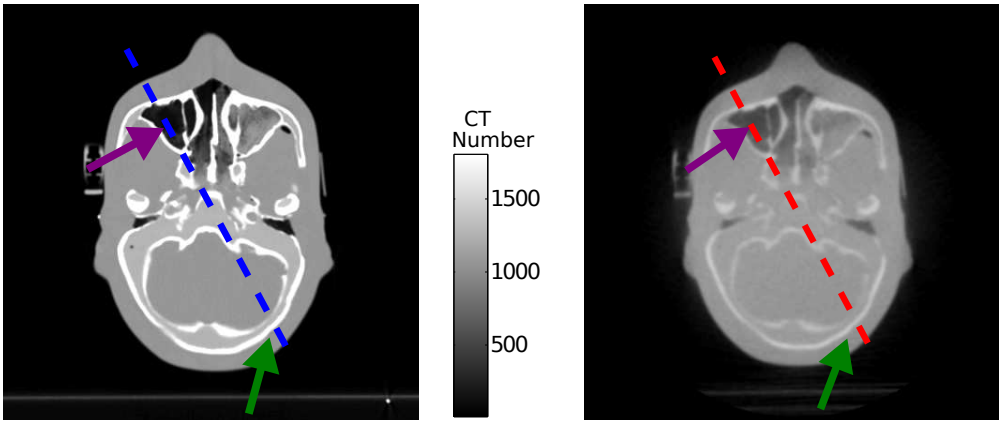


(a) kV CT image of an anthropomorphic head phantom.

(b) MV CBCT image of the same anthropomorphic head phantom as in (a).

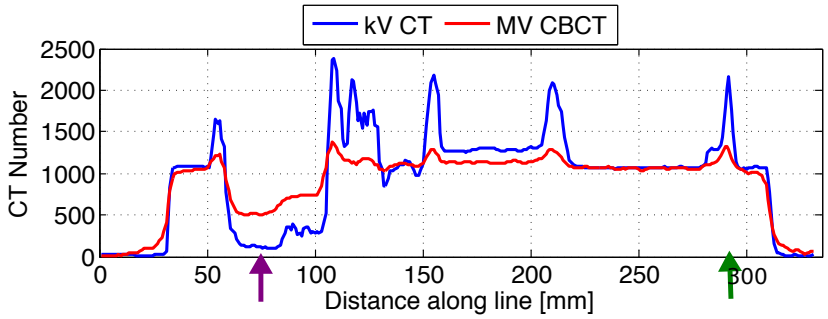


(c) Intensity profile for the kV CT (blue) and MV CBCT (red) image along the line indicated in 3.6(a) and 3.6(b). The purple and green arrow mark the positions along the profile as indicated by the same arrows in (a) and (b).

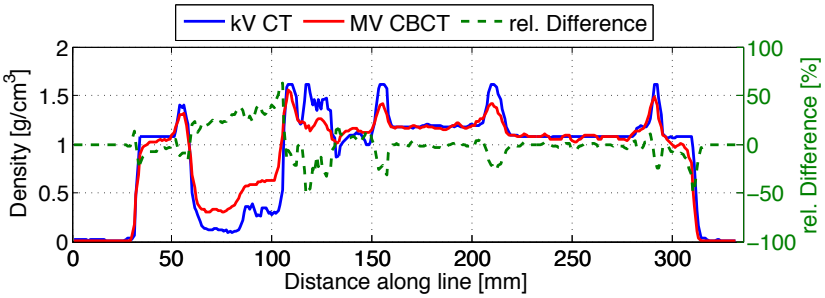


(d) Profile from (c) converted into density values using the machine-specific IVDC for kV CT (blue) and MV CBCT (red). The green plot marks the density difference between both density plots normalized to their respective mean value in percent.

**Figure 3.6:** Image intensity varies for different CT modalities. This example shows the intensity and tissue density across a kV CT and an MV CBCT image of an anthropomorphic head phantom.

## 3.3 Digital Image Manipulation

The overall goal in radiation therapy is a dose delivery accuracy of 5% [25]. This considers deviations that may be introduced throughout the treatment planning process, including inaccuracies arising from the contouring of the treatment target, the patient set up, and dose calculation. Emergency and palliative treatments may not fulfill these strict requirements mainly due to the fact that, to a certain extend, immediate treatment is more important than the treatment accuracy. The aim here is to provide dose calculation accuracy within 5% inside soft tissue and near critical structures.

A simplified digital cylindrical phantom was generated as described in Section 3.1. Figure 3.7 presents a series of this phantom with increasing image degradation from left to right. The contrast-to-noise ratio, image uniformity, and spatial resolution are independently altered as described above. For dose calculation, the original image and each modified digital phantom is converted to a dicom (Digital Imaging and Communications in Medicine) file format and imported into the TPS. A single IVDC is used for all images. The dose of a single anterior-posterior beam is calculated and the dose grid exported for evaluation. Figure 3.7(a) shows the original digital phantom and the dose distribution of the beam. Below each modified digital phantom, the 2D dose difference map shows the relative difference to the original dose distribution. The CNR value listed in Figure 3.7(a) describes the difference in contrast-to-noise ratio between the bone insert and the surrounding water calculated by

$$\mathrm{CNR} = \frac{\mu_{\mathrm{bone}} - \mu_{\mathrm{water}}}{\sigma_{\mathrm{water}}} \quad .$$

$\mu_{\mathrm{bone}}$ and $\mu_{\mathrm{water}}$ are the mean CT number of a region of interest within each medium, respectively, and $\sigma_{\mathrm{water}}$ is the standard deviation of the same region in water. The non-uniformity (NU) factor is given in % in Figure 3.7(b). It is defined as the quotient of the difference between the minimum and maximum CT number for water and the CT number range between water and air:

$$\mathrm{NU} = \frac{\max(CT\#)_{\mathrm{water}} - \min(CT\#)_{\mathrm{water}}}{\max(CT\#)_{\mathrm{water}} - \min(CT\#)_{\mathrm{air}}} \quad .$$

Image blurring is introduced by using a Gaussian filter, whose magnitude is defined by the standard deviation parameter $\sigma_{\mathrm{NU}}$ and included in Figure 3.7(c).

The figure shows that an increase in noise and consequently a decrease in the contrast-to-noise ratio has a relatively small effect on dose calculation

accuracy. It requires an unrealistically high noise level for dose differences up to 4%. However, a decrease in contrast, which would also decrease the contrast-to-noise ratio, would require a revised image value-to-density calibration to preserve correct dose calculations. A non-uniformity factor of 7% causes an average dose difference of less than 2% with local dose differences of less than 4%. Similarly, 13% and 37% of non-uniformity increase the average dose difference up to 3% and 5% with local dose differences up to 6% and 13%, respectively. A low spatial resolution causes dose calculation discrepancies in the area of transition between different tissue densities as well as at the surface of the object, which is facing the beam. This leads to local dose differences. Nevertheless, the level of image blurring that it takes for dose differences of 5% or more is higher than what is usually observed in clinical images. Here, the bigger issue would be the inability to capture small objects.

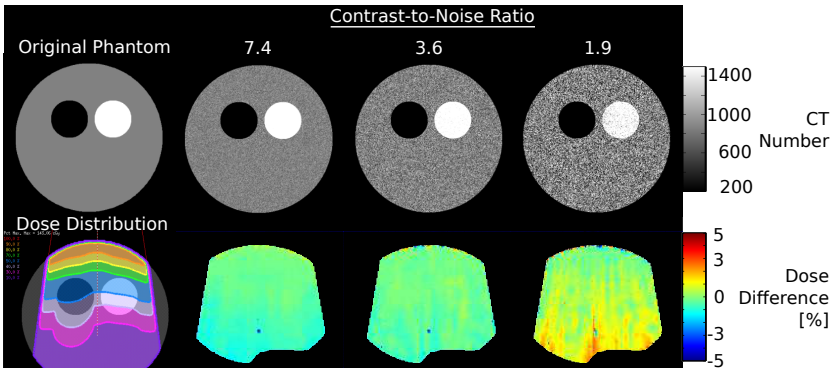


(a) The original phantom without image noise, non-uniformity, or image blurring is shown on the left. Below is the dose distribution of a single anterior-posterior beam. To the right, the contrast-to-noise ratio decreases, resulting in dose calculation differences relative to the original dose distribution. The color red indicates dose differences up to 5%. The noise in the examples with a CNR of 3.6 and 1.9 is higher than what is seen in clinical images.

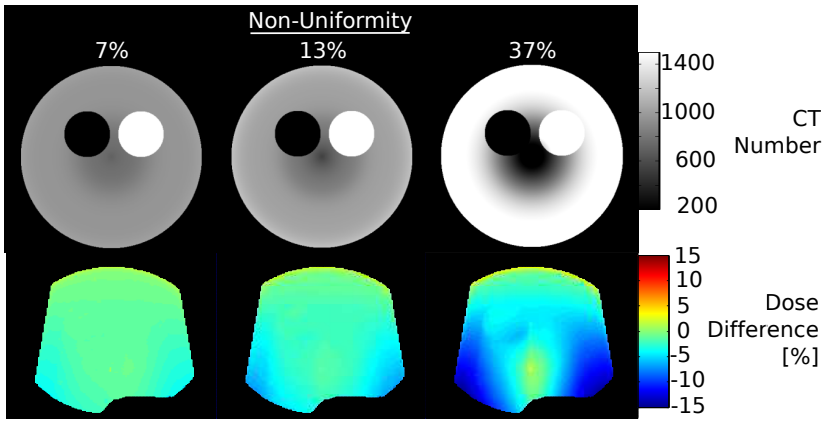


(b) Image non-uniformity is increased for the digital phantom from left to right. Blue indicates dose differences of 15% compared to the original image. The example of 37% non-uniformity does not usually occur clinically.

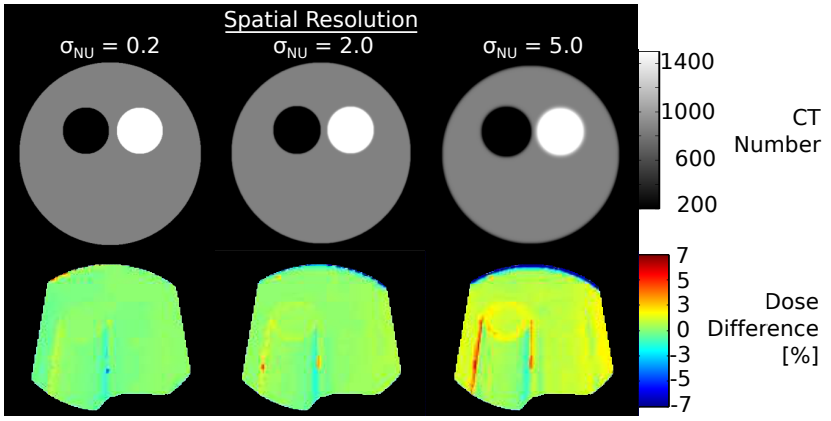


(c) The image is blurred by the application of a Gaussian filter, decreasing the spatial resolution for the digital phantom from left to right. This causes local dose differences in regions of density gradients. Dose calculation inaccuracies also occur at the surface of the phantom that is facing the beam. Blue indicates an underdosage of up to 7%.

**Figure 3.7:** A digital phantom is modified by individually decreasing the contrast-to-noise ratio, increasing the non-uniformity factor, and decreasing the image spatial resolution. The dose calculation difference is plotted below each phantom relative to the original dose distribution.

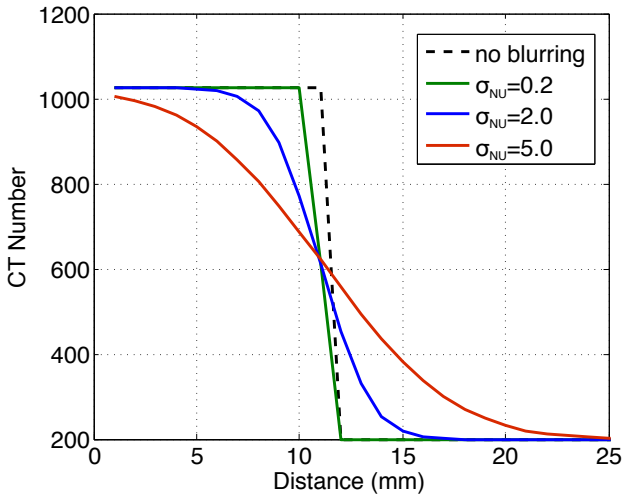


**Figure 3.8:** The transition of CT Numbers between water and air for different $\sigma_{\mathrm{NU}}$ values to illustrate the variations of image blurring in Figure 3.7(c).

## 3.4 Image Quality vs. Imaging Dose

The detective quantum efficiency of EPIDs for MV photons is ∼1% [33]. Increasing the imaging dose yields more signal, thus improving image quality. Figure 3.9 shows an example using the cylindrical water phantom presented in Section 3.1, which is imaged on an MV CBCT system. The total dose delivered per MV CBCT acquisition is increased, using an exposure of 3 MU, 15 MU, and 60 MU. The kV CT image is acquired with 120 kVp and shown for comparison.

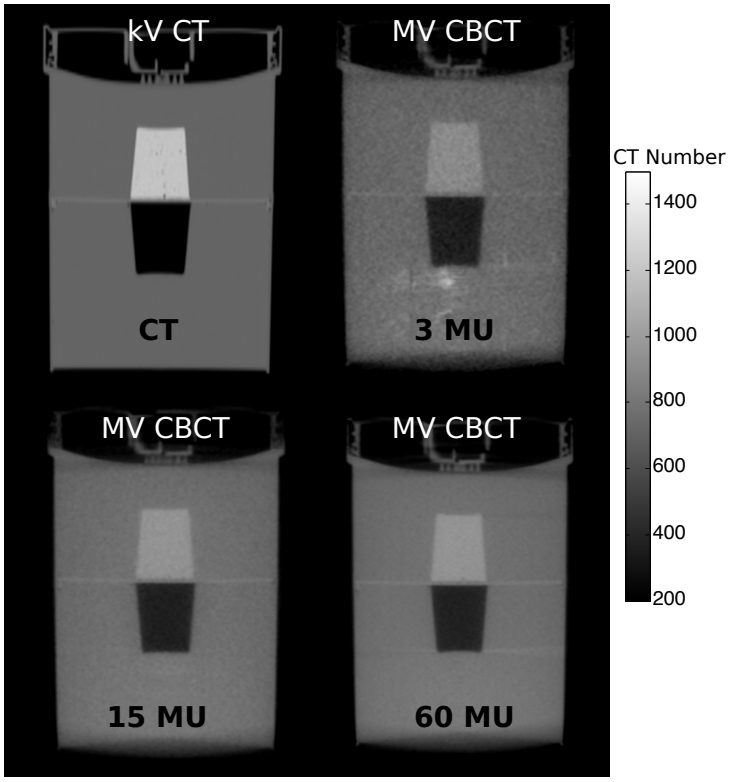


**Figure 3.9:** kV CT image in comparison to MV CBCT images of different dose exposures per scan. The object is a water phantom with inserts of different densities. On the upper left is the coronal view of the kV CT image. The other three images are MV CBCTs acquired on the treatment beam line of the Siemens Artiste. The dose per image is modified by increasing the MU per scan from 3 MU to 15 MU and 60 MU. All images are displayed at the same contrast level.

To be able to use images for dose calculation, the displayed CT number should not change when increasing the imaging dose. The system uses a calibration factor, $I_{0perMU}$, which is the detector sensitivity at 1 MU exposure of the

non-attenuated X-ray beam [35]. To verify the linearity of the flat panel response, four MV CBCT scans are acquired in air with an increasing total exposure of 5 MU, 10 MU, 15 MU, and 20 MU per acquisition, using a full gantry rotation. This results in 360 projection images per scan. Figure 3.10(a) plots the MU per frame for each projection and each acquisition. Similarly, Figure 3.10(b) plots the corresponding flat panel intensity for each projection and acquisition.

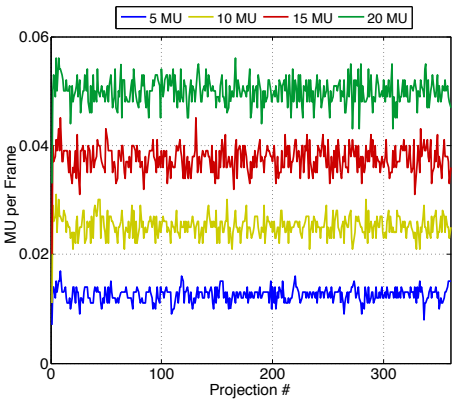


(a) MU per projection for four eFOV MV CBCT scans in air with a total dose per scan of 5 MU, 10 MU, 15 MU, and 20 MU.

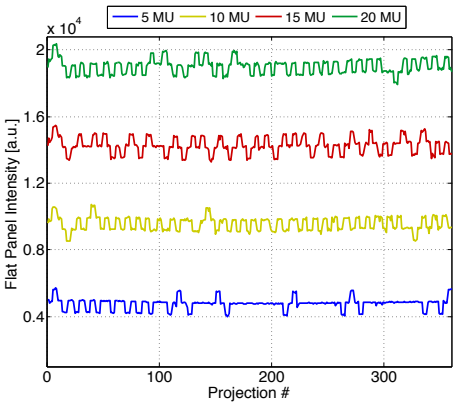


(b) Mean flat panel intensity per projection for the same eFOV MV CBCT scans as in (a).

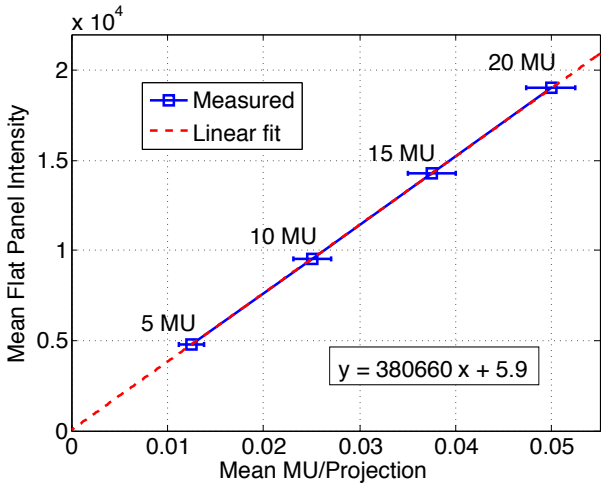


(c) For each MV CBCT acquisition in air, the mean flat panel intensity is plotted against the mean number of MU per projection. The equation for the linear fit is added inside the plot. The slope of the curve equals an increase in mean flat panel intensity of $3.81 \times 10^5$ units for every MU per projection .

**Figure 3.10:** The $I_{0perMU}$ calibration factor is defined by the slope of the flat panel response curve shown in (c).

The mean number of MU and the mean flat panel intensity value for each acquisition are extracted from each graph and plotted against each other in Figure 3.10(c). The linear fit describes the data well ($r^2 = 1$) and lies within

the margin of error, which is the standard deviation of the mean MU per projection. The slope of the regression line is $3.81 \times 10^5$. This should equal the calibration factor $I_{0perMU}$ of the machine.

The $I_{0perMU}$ factor is saved in the image dicom header of the file, which provides a lot of valuable information on the acquired image such as patient data, acquisition date and time, file format and size, machine parameters, etc. The $I_{0perMU}$ value listed in this example is $3.7882 \times 10^5$. In comparison to the value obtained from the plots in Figure 3.10, the difference between them is 0.58%. Consequently, CT numbers are expected to be the same for same tissue densities, regardless of the total imaging dose. This is verified with Figure 3.11. A water cylinder is imaged with a total exposure of 3 MU, 5 MU, 10 MU, and 20 MU. The CT numbers are plotted for a cross section profile of each scan. The mean CT number and standard deviation of water are $1010 \pm 16$, $1021 \pm 12$, $1019 \pm 9$, and $1016 \pm 8$, respectively. This proves the linear response of the flat panel.

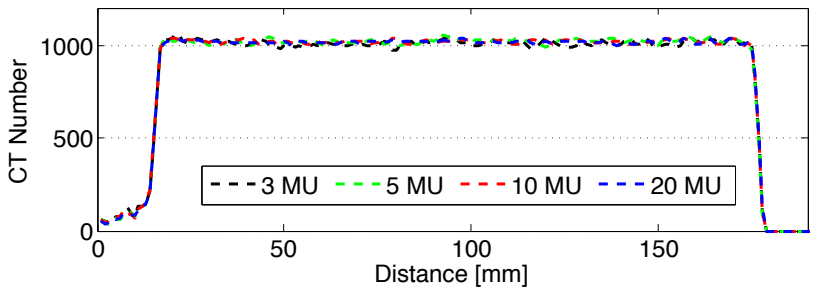


**Figure 3.11:** Image intensity profiles across an axial slice of the cylindrical water phantom MV CBCT images for different imaging doses. The total exposure per acquisition is 5 MU, 10 MU, 15 MU, and 20 MU.

In another study, the small cylindrical phantom and the large pelvic phantom are imaged with the rFOV and the eFOV of an MV CBCT system, respectively. The exposure per scan is increased from 1 MU up to 20 MU. The relative noise and CNR are evaluated for each scan. The results are plotted in Figure 3.12.

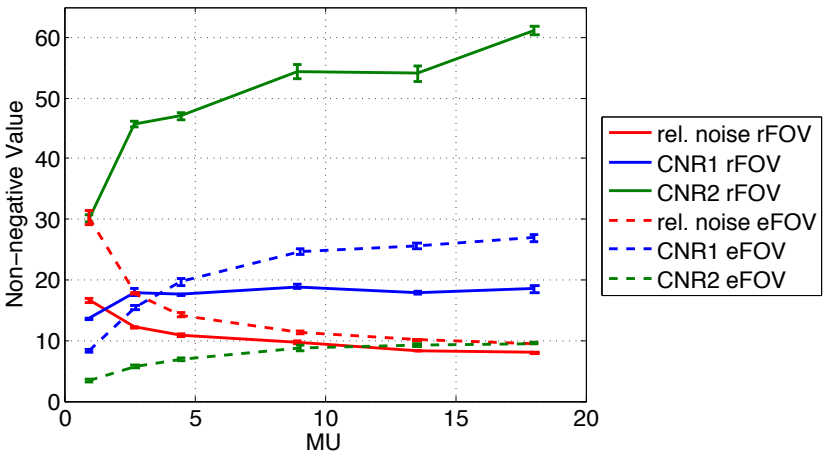


**Figure 3.12:** The relative noise and CNR are measured for MV CBCT images of exposures between 1 and 20 MU, which results in an effective exposure of 10% less than the value entered. CNR1 and CNR2 describe the contrast-to-noise ratio between water and air and water and bone, respectively. The CNR is plotted in non-negative values.

The signal increases linearly with the MU, as shown in Figure 3.10(c). According to Equation 2.4, the absolute noise increases for an increase in signal, but only by $\sqrt{N}$. Thus, the SNR, defined in Equation 2.6, increases with an increase in signal, also by $\sqrt{N}$. Consequently, the relative noise decreases with increasing MU. When the signal is tripled by raising the MU from 1 MU to 3 MU, the dose to the patient is also tripled. Then, the SNR ideally increases by a factor of $\sqrt{3} = 1.73$. Due to the quantum noise, it can never increase more than that. In that example, the noise relative to the signal equals $\frac{\sqrt{3}}{3}$ or 57.74%, which is a relative decrease of 42.3%. To triple the SNR, the MUs would need to be increased by a factor of 9, which also increases the patient dose by that factor.

The relative noise, that appears in the plot in Figure 3.12, is measured as the standard deviation of the CT numbers inside a ROI in water, averaged over ten image slices per CT scan. The plot shows a decrease of relative noise by $38.0 \pm 3.4\%$ and $42.7 \pm 1.5\%$ for an increase from 1 MU to 3 MU for the rFOV and the eFOV, respectively. The differences in the decrease of the relative noise may be explained by noise contributions other than those following the Poisson statistic.

The CNR is calculated as the difference in CT numbers between water and air, and water and bone, divided over the standard deviation of the CT numbers for water. Like the SNR, the CNR is expected to increase by $\sqrt{N}$. The

plot in Figure 3.12 shows that for an increase from 1 MU to 3 MU, CNR1 and CNR2 increase by a factor of $1.30 \pm 0.04$ and $1.50 \pm 0.03$ for the rFOV, and by a factor of $1.9 \pm 0.04$ and $1.7 \pm 0.10$ for the eFOV, respectively. The increase in CNR1 for the eFOV is outside the margin of error for the expected increase in CNR. This may be due to image reconstruction filters that perform image averaging to correct for noise. Although the reconstruction settings were the same for all image acquisitions, the averaging filters (such as the diffusion filter) may be unable to reduce image noise in case of this very low signal of 1 MU. For this particular case, the expected increase in CNR1 when doubling the signal from 5 MU to 10 MU is a factor of $\sqrt{2} = 1.41$. The measured increase is $1.23 \pm 0.05$, which is a realistic increase in CNR when doubling the signal and may present a better example here.

## 3.5 System Stability

The flat panel stability is verified over a period of 18 weeks with no sign of significant drift in the flat panel response. For this purpose, a water cylinder with an air and a bone insert is imaged repeatedly in the same setup using the same image protocol. An ROI is assigned to each insert and the mean value is calculated for every acquisition. The data of day 1 is used as a reference. Figure 3.13 summarizes the results in a bar plot and shows the relative difference to the mean CT number of Day 1 for every ROI and day.

The relative difference is less than 2% for all days measured. This is well within the expected fluctuations to consider the flat panel response stable over an extended period of time. It also agrees with similar findings that were reported previously [35]. Consequently, image value to density calibrations do not require other quality assurance checks in addition to the recommended protocol, which suggests quarterly QA and calibration of the flat panel.

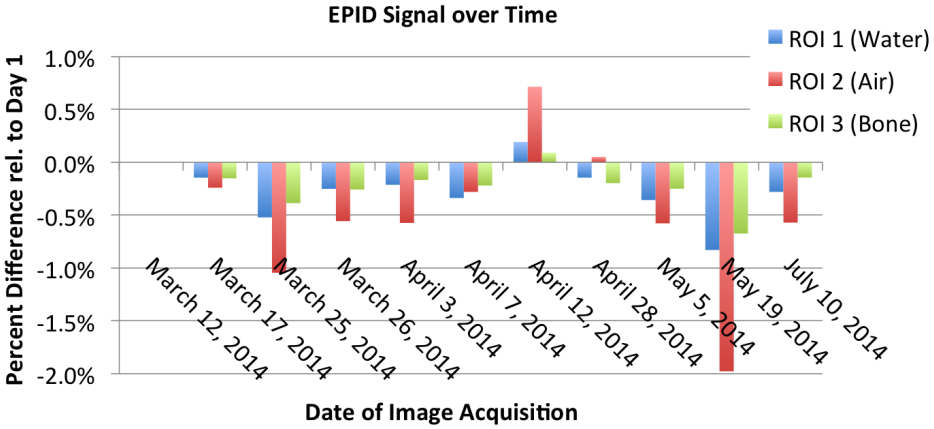


**Figure 3.13:** Percent difference of the flat panel intensity values for different density inserts. The difference is relative to the EPID intensity of the first measurement from March 12, 2014.

# CHAPTER 4

## Developing a Workflow for ERT based on MV CBCT

The clinical routine at the department of radiation oncology follows a treatment schedule that typically has each patient fixed in the same time slot from day to day. An unexpected emergency treatment can be disruptive to the clinical flow, causing delays for the scheduled patients and crowded waiting areas. To minimize this burden on the patients and staff, a streamlined workflow is developed with the aim to simulate and treat patients urgently without causing undesired disruptions and delays to others.

3D dose calculation has become the standard in radiation therapy, causing physicians to be reluctant to use 2D images for treatment planning. However, available machine time on the kV CT scanner and the linear accelerator rarely line up, preventing a smooth transition from simulation to treatment and requiring the patient to wait until machine time is available. The workflow developed uses on-board imaging instead of a kV CT scan for patient simulation. This minimizes patient setup time, which is difficult and time-consuming for the staff, and can be painful for the patient. The CT images are instantly loaded into the treatment planning system. There, software facilitates the treatment planning process. Depending on the treatment site, automated input gatherings carry out specific commands, minimizing the need for entering redundant information.

The key to the success of this procedure is the availability of all staff involved

at the time the linear accelerator is available for treatment. This includes the patient's physician, a radiation therapist, and a dosimetrist or physicist. Experience shows that it is less disruptive for everyone involved when they agree on a set time frame during which they need to be available rather than having to expect interruptions throughout the day. This alone reduces unwanted waiting times.

The workflow is scheduled to be implemented for the on-call linear accelerator, which, at UCSF, is a Siemens Artiste. Therefore, accurate dose calculation based on MV CBCT images is a prerequisite for the success of this project. The resulting publication

> Held M, Sneed P K, Fogh S E, Pouliot J, and Morin O, "Feasibility of MV CBCT-based treatment planning for urgent radiation therapy: dosimetric accuracy of MV CBCT-based dose calculations". *J Appl Clin Med Phys* 2015;**16**(6):458-471.[3]

is included below. It first appeared in the Journal of Applied Clinical Medical Physics in November 2015. The manuscript presents the new integrated workflow for emergency radiotherapy treatments that combines simulation, planning, and treatment. The paper evaluates the feasibility of the workflow and considers the physics aspects for dose calculation on MV CBCT for different anatomic sites. Following previous publications on the matter of MV CBCT-based dose calculation [43–45], it verifies results from previous papers for commercially available systems.

[3]Reproduction of the publications is in accordance with the Creative Commons Attribution 4.0 International License.

JOURNAL OF APPLIED CLINICAL MEDICAL PHYSICS, VOLUME 16, NUMBER 6, 2015

# Feasibility of MV CBCT-based treatment planning for urgent radiation therapy: dosimetric accuracy of MV CBCT-based dose calculations

Mareike Held, Penny K. Sneed, Shannon E. Fogh, Jean Pouliot, Olivier Morin[a]
*Department of Radiation Oncology, University of California San Francisco, San Francisco, CA, USA*
*Olivier.Morin@ucsf.edu*

Received 20 February, 2015; accepted 26 May, 2015

Unlike scheduled radiotherapy treatments, treatment planning time and resources are limited for emergency treatments. Consequently, plans are often simple 2D image-based treatments that lag behind technical capabilities available for nonurgent radiotherapy. We have developed a novel integrated urgent workflow that uses onboard MV CBCT imaging for patient simulation to improve planning accuracy and reduce the total time for urgent treatments. This study evaluates both MV CBCT dose planning accuracy and novel urgent workflow feasibility for a variety of anatomic sites. We sought to limit local mean dose differences to less than 5% compared to conventional CT simulation. To improve dose calculation accuracy, we created separate Hounsfield unit–to–density calibration curves for regular and extended field-of-view (FOV) MV CBCTs. We evaluated dose calculation accuracy on phantoms and four clinical anatomical sites (brain, thorax/spine, pelvis, and extremities). Plans were created for each case and dose was calculated on both the CT and MV CBCT. All steps (simulation, planning, setup verification, QA, and dose delivery) were performed in one 30 min session using phantoms. The monitor units (MU) for each plan were compared and dose distribution agreement was evaluated using mean dose difference over the entire volume and gamma index on the central 2D axial plane. All whole-brain dose distributions gave gamma passing rates higher than 95% for 2%/2 mm criteria, and pelvic sites ranged between 90% and 98% for 3%/3 mm criteria. However, thoracic spine treatments produced gamma passing rates as low as 47% for 3%/3 mm criteria. Our novel MV CBCT-based dose planning and delivery approach was feasible and time-efficient for the majority of cases. Limited MV CBCT FOV precluded workflow use for pelvic sites of larger patients and resulted in image clearance issues when tumor position was far off midline. The agreement of calculated MU on CT and MV CBCT was acceptable for all treatment sites.

PACS numbers: 87.55.D-, 87.57.Q-

Key words: dose calculation, emergency treatments, MV CBCT, radiation therapy, treatment techniques

## I. INTRODUCTION

Cone-beam CT acquisition has become a routine procedure in radiation oncology. It provides a 3D image of the patient in treatment position immediately before treatment and is regularly used as a method to increase precision of patient alignment. Recently, there has been a growing

[a] Corresponding author: Olivier Morin, Department of Radiation Oncology, UCSF, 505 Parnassus Avenue, L08-D, San Francisco, CA 94143 – 0226, USA; phone: (415) 353 9302; fax: (415) 353 8679; email: Olivier.Morin@ucsf.edu

interest in using cone-beam CT images for other purposes, such as dose calculations and monitoring of patient anatomy, during the course of treatment. Dose calculations using MV CBCT images are feasible.[1,2] However, consistently converting CT numbers to electron density can be difficult.[3–6] Previous research studies reported a gamma index of 98% for 3% and 3 mm criteria that described dose calculation accuracy on MV CBCT for head-and-neck cases, using in-house developed image correction filters.[7] However, this was based on a limited patient population and dose calculations needed verification in more anatomical sites to be clinically relevant. Aubry et al.[8] presented similar results for phantom studies of the pelvic region. These research studies focused on dose calculation to improve the accuracy for image-guided radiation therapy (IGRT). Other applications include emergency treatments using CBCT- and MV CT-based planning to reduce patient setup and waiting time.[9,10] Here, similar results to our initial experience with head-and-neck cases[7] have been verified for commercially available systems. Furthermore, MV CBCT-based dose calculation was investigated for different anatomical sites using a lateral flat-panel offset for an extended FOV.

MV CBCT imaging has advanced considerably, providing better image quality while still lowering dose to the patient. The most recent commercially available systems are considered second-generation MV CBCT systems. This study combines both approaches mentioned above: reduce patient setup and planning time while still providing accurate dose calculation that considers inhomogeneity corrections.

The objective of this study was to investigate the feasibility of emergency radiotherapy treatment (ERT) dose planning on selected anatomical sites based on MV CBCT images acquired on a commercial treatment machine.

## II. MATERIALS AND METHODS

### A. ERT workflow

A streamlined workflow was developed to reduce the amount of time the patient spends from the time a decision is made to undergo emergency radiation therapy to the delivery of the treatment. The workflow combined simulation, planning, QA, and treatment into a single session so that the patient is set up once on the treatment machine and remains on the linac couch until after treatment delivery. Ideally, this would be done within a 30 min time slot to avoid delaying other patients. Figure 1 outlines the suggested workflow. The goal was to automate the process

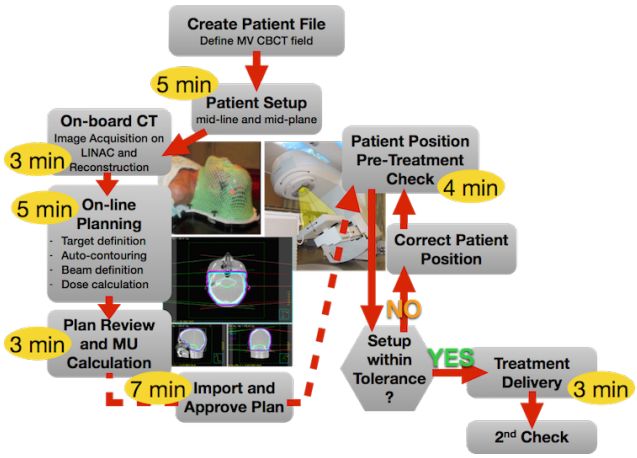


FIG. 1. ERT workflow. Flowchart to describe the workflow for combined simulation, planning and treatment of emergency patients in one session with the expected times for each step.

as much as possible by using scripting within the planning software to quickly produce a simple treatment plan, and by merging each person's responsibilities into one step.

Dose calculation accuracy on MV CBCT images was the other focus of this study. First, phantom studies were performed to determine the reconstructed intensity for different tissue densities. This resulted in two different calibration curves, which were added to a commercial planning system. Then, simple dose calculations on phantom and patient images were performed. The plans included clinically relevant examples of emergency and palliative treatments. All MV CBCT based treatment plans were compared to the simulation CT-based plans as the gold standard and were displayed in percent difference relative to the simulation CT. All CT were acquired on a Philips MX8000 CT scanner (Philips Healthcare, Andover, MA).

### B. MV CBCT imaging

The cone-beam images used in this study were acquired on the Siemens Artiste and the In-Line kView cone-beam system (Siemens, Munich, Germany). This commercially available in-room imaging system was integrated into the treatment machine. It used a low-energy treatment beam of 1 MV with a carbon target and no flattening filter. More detailed information on the system has been described in the literature.[11–13] The system includes two available imaging modes: regular field of view (FOV), and extended FOV. The In-Line kView MV CBCT system acquired images with a FOV of approximately $27 \times 27 \times 27$ cm$^3$ when using the regular FOV mode. It acquired images at 1° increments for a 200° rotation around the patient. The FOV for MV CBCT systems was one of the main limitations. To perform dose calculation, the entire anatomy had to be captured along the beam path. Furthermore, truncating the anatomy caused missing data artifacts.[4] To obtain a larger FOV, two approaches have been previously reported. The first approach fuses the kV CT reference image with the MV CBCT.[14,15] Alternatively, the FOV can be extended during the image acquisition.[1] The aim of this study was to perform simple dose planning without the acquisition of a CT image. Thus, a lateral flat-panel offset of 5.5 cm and a full rotation around the patient was used to capture larger anatomy, such as the chest or the pelvis. This allowed for an extended FOV up to $31 \times 31 \times 27$ cm$^3$. Due to the uneven beam profile, the image corrections varied based on which imaging mode was used. The system applied binning, averaging, and diffusion filters automatically to reduce image artifacts, such as cupping artifacts, ring artifacts, and noise.[16] The exposure used during an image acquisition was measured in monitor units (MU) and could be as low as 1 MU. The exposure range of interest for this study, however, was between 3 and 15 MU (equivalent to about 3–15 cGy), depending on the treatment site, to improve image quality.

### C. Electron density calibration

Most treatment planning systems use a lookup table that converts the reconstructed gray-level intensity of each CT image voxel into a physical or electron density value, thereby mapping the tissue inhomogeneity of the imaged object. Consequently, the reconstructed intensity of tissues has to remain constant over space and time in order to perform dose calculation accurately. Due to the energy dependence of X-ray interaction with matter,[17,18] the reconstructed intensity-to-physical-density calibration for fan-beam CT scanners was invalid for MV CBCT images. Thus, the MV CBCT system had to be calibrated independently. Two water phantoms with density inserts were used to calibrate the Hounsfield units (HU) to physical density for both the regular FOV (rFOV) and extended FOV (eFOV). Phantom 1, used to calibrate the rFOV, was a commercially available head-sized cylindrical container filled with water. The phantom dimensions were 17 cm in diameter and 25 cm in length. A similar phantom was used for MV CBCT dose calibration in previous studies.[4,7] A plastic disc with cutouts was glued inside the center to hold seven different density inserts (air, lung inhale, lung exhale, adipose, water, trabecular bone, and dense bone) (CIRS Inc. model 062, Norfolk, VA) in place. Phantom 2, used to simulate the dimensions of a pelvis patient, measured approximately $38 \times 25 \times 25$ cm$^3$ and was used to calibrate the eFOV. To avoid sharp edges that could cause unnatural artifacts during

imaging, acrylic sheets were bent under heat to form a human-like pelvis object. The inserts of phantom 1 are routinely used for clinical HU calibration of the departmental CT scanner. Thus, the physical and electron density were well known. For phantom 2, customized inserts made from epoxy 670 HT (Reynolds Advanced Materials, Brighton, MA) were glued to the inside. Each insert contained between 10% and 30% of $CaCo_3$ to vary its density.

Both phantoms were imaged on both the standard kV CT and the MV CBCT. A region of interest (ROI) was defined across several center slices for each insert. The MV CBCT calibration curve was obtained by plotting the average HU of each ROI against the respective physical density. Afterwards, the value for air was adjusted slightly based on ROIs within air cavities of patient MV CBCT images. The original MV CBCT curves were extrapolated linearly to 0 density and extended to the origin of the plot, as required by the planning software.

### D. CT and MV CBCT dose planning on phantom images

To determine the feasibility of accurate dose calculation on CBCT images using commercially available software, dose predictions were compared on phantom CT and CBCT images. All treatments were planned using the treatment planning software Pinnacle 9.2 (Philips Healthcare, Andover, MA), which is our clinical standard planning system for treatments on the Siemens Artiste. Each CT and CBCT image pair was rigidly aligned prior to treatment planning. A new patient file was created for each image set. During the dose planning process, the density calibration was chosen accordingly to the imaging mode that was used during the acquisition of that specific image series (CT or rFOV MV CBCT or eFOV MV CBCT). Single beams with field sizes between 5 cm × 5 cm and 10 cm × 10 cm were applied to each CT and the plan was copied to the MV CBCT. It was verified that the isocenter, dose grid, beam, and other parameters were identical for each CT and the matching MV CBCT. Once the dose distribution was calculated, the 3D dose of each CT and MV CBCT pair was exported and compared using MATLAB (MathWorks, Natick, MA).

### E. CT and MV CBCT dose planning on patient images

Over a period of several months, patient cone-beam CT images were collected to build a case library based on clinical cases. For dose comparison purposes, the MV CBCT images were rigidly aligned to the patient's planning CT. Each scan was associated with a new patient in the planning system. A simple emergency treatment plan was created on the CT and copied to the aligned MV CBCT with two different prescriptions. Prescription 1 prescribed the treatment dose to a point at mid-plane to find the percentage difference of MU. Prescription 2 was set to 100 MU per plan. The dose distribution was analyzed in MATLAB, using a voxel-by-voxel comparison. The mean dose difference and standard deviation (SD) were determined for dose regions of 20% and more of the prescription dose. Additionally, the dose distribution was analyzed using the gamma index criterion for 2D axial plane in the SNC patient software (Sun Nuclear, Melbourne, FL). The various sites imaged during this period included seven brain, nine thoracic, and nine pelvis cases, as well as two extremities, one knee, and one foot.

## III. RESULTS

### A. ERT workflow feasibility

Prior to clinical implementation, several test runs were performed on phantoms. The general workflow required to first register the patient/phantom in the patient-management software (MOSAIQ; Elekta AB, Stockholm, Sweden). A diagnosis, prescription, site setup, and MV CBCT treatment field were entered before the patient arrived. Once the patient/phantom was set up on the treatment machine, the MV CBCT was acquired. The reconstructed image was sent to the treatment planning software. Three scripts were used to define the desired treatment plan and export the fields to verify the MU calculation. These scripts were treatment site specific. The only action required during planning was the field definition and adjustment of the prescribed dose. The QA process involved an independent MU calculation using RadCalc (LifeLine Software Inc., Austin, TX). Once the plan was checked and approved, it was imported into MOSAIQ, from where it was forwarded to the treatment machine. The correct patient setup was confirmed using portal imaging immediately before the treatment delivery and the patient position was corrected where necessary. These workflow tests on phantoms showed that the simulation, treatment planning, QA, and delivery could be achieved within 30 min of machine time. The average time for each step is shown in yellow in Fig. 1. Additionally, it required about 5 min to register the phantom and set up the prescription and MV CBCT field before the phantom was set up for treatment. Another 20–30 min were spent on the second check of the treatment plan, uploading of all documents, and billing.

### B. Density calibration

Figure 2 shows the reconstructed intensity-to-physical-density calibration curves for standard CT and MV CBCT, the latter using regular field of view and extended field of view. They were entered into the planning software to convert the reconstructed intensity into density values. These calibrations were used for all of the study treatment plans, according to the image mode used for acquisition. The stability of the MV CBCT system was validated previously by Morin et al.[16] It was also verified for this specific system over a three-month period during which Hounsfield units and image quality (noise, contrast-to-noise ratio) remained stable.

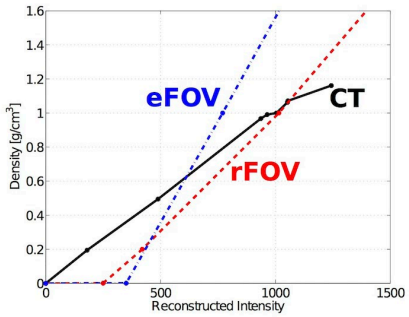


FIG. 2. HU calibration. Reconstructed intensity-to-density calibration curves for standard CT (solid black), regular FOV (dashed red), and extended FOV (dash-dot blue) MV CBCT. The MV CBCT curves were extended to an intensity of 0, as required by the planning system.

### C. Dose difference for CT and MV CBCT dose planning on phantoms

Figure 3 displays CT versus extended FOV MV CBCT horizontal and vertical density profiles in an image slice of the pelvis-sized water phantom using the calibrations shown in Fig. 2. The eFOV density calibration curve was used to convert the reconstructed intensity into density values. While water was displayed with a density of 1 for both image modalities, the air insert on MV CBCT appears to have a higher density of around 0.28 than on CT, where it was close to 0. Contrarily, the density values for the other inserts appear less dense than on CT. On MV CBCT the densities for the inserts display as 1.40, 1.35, and 1.33 g / $cm^3$ compared to CT densities of 1.46, 1.50, and 1.36 g / $cm^3$. The comparison of the profiles also shows that the transition between different densities was not as distinct on MV CBCT as it was on CT and that the MV CBCT profiles show more noise compared to the CT image.

The same phantom and intensity-to-density conversion was used to compare dose calculation accuracy, ultimately studying dose calculation errors from inaccurate density conversion. Figure 4 compares the dose distribution for a single beam calculated based on CT and MV CBCT for the same phantom as above, but on a different image slice. On the left, Fig. 4(a) shows the planned dose distribution within the phantom. The low-density region (black circle) displays the air insert in the phantom. Figure 4(b) on the right shows the planned dose difference on the eFOV MV CBCT in percent, relative to the CT planned dose. The percentage difference was less than 2% in most of the beam field. The surface region (0.5 cm) of the phantom showed dose differences around 5%.

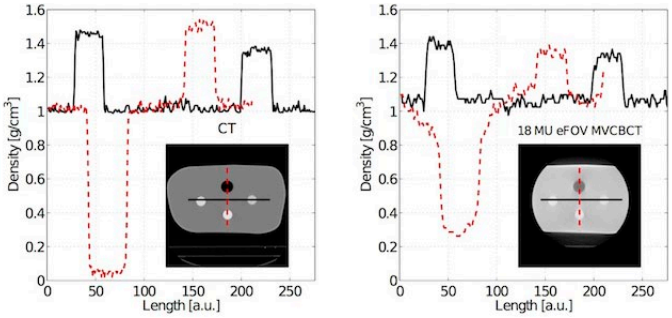


FIG 3. CT and MV CBCT image comparison. Reconstructed density values along a horizontal (solid black) and vertical (dashed red) profile on a CT and extended FOV MV CBCT of a pelvis-sized water phantom are shown. The phantom included inserts of air and bony materials. The inset images show the standard CT and the eFOV MV CBCT. The sides on the cone-beam image were truncated due to a limited FOV.

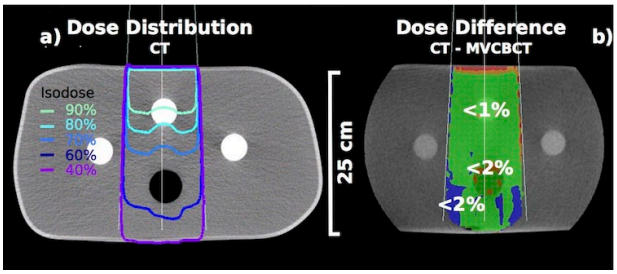


FIG. 4. Dose plan comparison in a phantom: (a) dose distribution from one open-field beam as planned on a CT of a pelvis-sized water phantom with air and density inserts; (b) percentage dose difference on an eFOV MV CBCT of 18 MU exposure for the same plan relative to the CT-based planned dose.

## D. Clinical patient cases

### *D.1 Whole brain*

Figure 5 maps the dose difference between a whole-brain treatment planned on CT and a 4.5 MU MV CBCT using the rFOV. Figure 5(a) shows a transverse view of the patient's MV CBCT. For prescription 2, the dose difference was less than 3% everywhere except in the nasal cavity, where the dose difference was more than 5%. Similarly, Fig. 5(b) shows a sagittal center slice of the patient with the dose difference distribution less than 1% in the center of the treatment field and less than 3% everywhere else in the brain, except for the nasal air cavity. Prescription 1 showed 1.2% less MU calculated for 300 cGy at a mid-plane calculation point.

Differences in MU calculated for each plan varied between 0% and 1.2% to achieve the prescription dose of 300 cGy at mid-plane. Mean dose differences for all studied brain treatments were within 3%. Some cases showed local dose differences higher than 5% in the nasal air cavities. The gamma index for a 2D axial plane was 95% or more for 2% and 2 mm criteria in the SNC patient software.

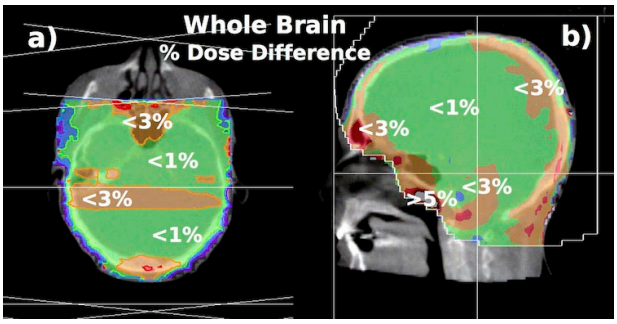


FIG. 5. Dose difference for a whole-brain plan: (a) axial view and (b) sagittal view of the relative dose difference of a whole-brain treatment with opposed lateral beams. The displayed dose difference is relative to the CT planned dose distribution. The plan used MLCs to shape the PTV.

### *D.2 Thoracic spine treatment*

Figure 6(a) shows the dose distribution of a thoracic spine treatment with opposed AP/PA beams on a CT. The relative dose difference between the CT and the 13.5 MU eFOV MV CBCT was calculated and is presented in Figs. 6(b) through 6(d) (transverse, sagittal, and coronal views, respectively). The local dose difference in soft tissue was less than 3% and up to 5% in some areas close to lung tissue. Dose differences of more than 5% were visible within and beyond lung tissue. The MU for this treatment and a prescribed dose of 700 cGy to mid-plane were 1.4% lower when calculated on the MV CBCT compared to the CT.

For three out of seven thoracic spine treatments, the gamma index was above 97% for 3% and 3 mm criteria. Two treatments had dose calculation accuracy with a gamma index of 100% for increased criteria of 5% and 3 mm. Locally, the gamma index failed the given criteria within lung tissue. Large dose differences between the CT and MV CBCT also occurred within the 5 mm buildup region near the skin. The difference of MU calculated on CT and MV CBCT for a prescribed dose of 700 cGy to mid-plane using two opposed beams ranged between 1.4% and 3.6%.

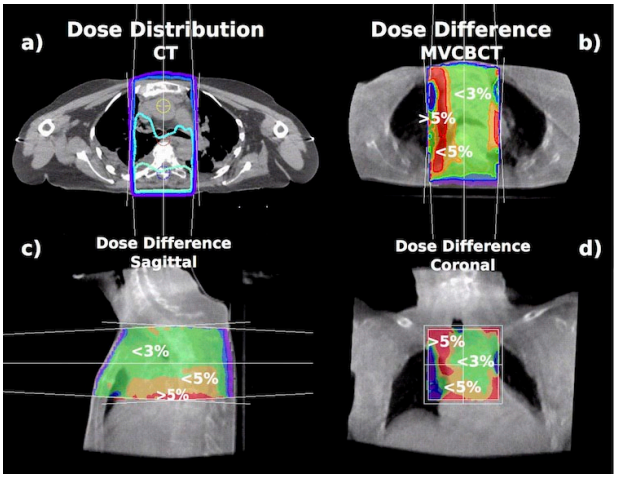


FIG. 6. Dose difference for a thoracic spine plan: (a) dose distribution of a thoracic spine treatment with opposed AP/PA beams, planned on a standard CT. Relative dose difference planned on a 13.5 MU exposure eFOV MV CBCT in the transverse (b), sagittal (c), and coronal (d) views.

### *D.3 Pelvis treatment*

Figure 7 presents the dose distribution of opposed AP/PA beams in a pelvis (a) and the relative dose difference in percent of the same plan calculated based on an eFOV MV CBCT (b). The dose difference resulting from this comparison was less than 3% in about two-thirds of the volume. The dose difference was less than 5% in the bowel area, which contains air cavities. Due to the time difference of the image acquisition, the size and location of the air cavities were not identical. The dose calculated based on the MV CBCT was underestimated in the posterior skin area where the dose difference was about 5%. The number of MU calculated on the CT and the MV CBCT were the same for a prescribed dose to mid-plane.

For all studied simple pelvis treatments, the gamma index was between 90% and 98% for 3% and 3 mm criteria. Local dose discrepancies that failed the gamma index were within air cavities and, in some cases, within the 5 mm buildup region near the skin surface. For a prescription point at mid-plane, MU were calculated within -1% and +1.9% accuracy for MV CBCT-based images.

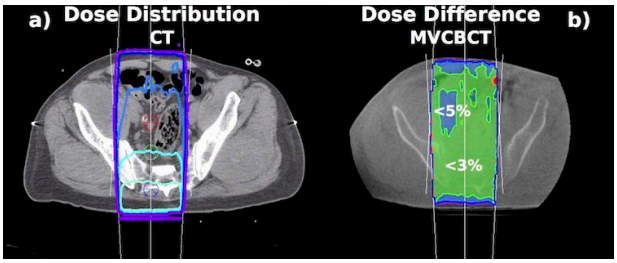


FIG. 7. Dose difference for a pelvis plan: (a) the CT planned dose distribution and (b) relative dose difference planned on a 13.5 MU exposure eFOV MV CBCT of a pelvis patient. The treatment plan consisted of opposed AP/PA, with a one-third to two-thirds beam weighting.

### *D.4 Extremities — knee treatment*

The dose difference between the same CT and MV CBCT treatment plan for a knee is presented in Fig. 8. It shows the transverse (a) and coronal (b) views of a 4.5 MU exposure rFOV MV CBCT. The plan consisted of opposed lateral beams. The dose differences were less than 3% in most areas. The transverse view shows a small area within the knee in which the MV CBCT dose was overestimated up to 5%. The dose within 0.5 cm of the lateral sides of the knee was underestimated on the MV CBCT by more than 5%. The MUs obtained from the MV CBCT were 2.2% lower than those from the CT for a dose of 700 cGy at mid-plane using opposed lateral beams.

All patient case results are summarized in Table 1.

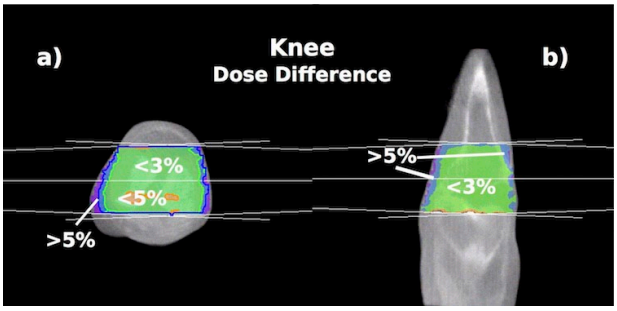


FIG. 8. Dose difference for a knee plan: (a) transverse and (b) coronal views of a knee showing the dose difference relative to a standard CT planned on a 4.5 MU exposure rFOV MV CBCT. Opposed lateral beams with equal weighting were used in this plan.

TABLE 1. The range of calculated dose plan accuracies on MV CBCT for each treatment site is shown. The number in parentheses in the left column indicates the quantity of patient cases in each group.

| *Treatment Site* | *Difference in MU* ($MU_{CT}/MU_{CBCT}$) | *Gamma Index (3%/3 mm)* |
|---|---|---|
| Brain (7) | ≤1.2% | 99%–100% |
| Thorax (9) | ≤1.4% | 47%–100% |
| Pelvis (9) | ≤1.9% | 90%–99% |
| Extremity (2) | ≤2.2% | 92% and 99% |

## IV. DISCUSSION

### A. Workflow

To accomplish the entire workflow within 30 min, it required well-trained staff, good communication, and focus of the entire group. It was key that, prior to the 30 min machine time, the patient was registered in the system, the prescription was entered, and the MV CBCT was set up. The most critical and time-consuming part was the plan import into MOSAIQ. Also crucial for a smooth workflow was the physician's presence to review and approve the portal images for patient verification immediately before treatment.

The fact that this workflow requires a minimum of 30 min uninterrupted machine time was seen skeptically at first by all the staff involved. However, the benefits outweighed these concerns, one of which is the guarantee of treatment within 30 min after the patient is set up on the treatment couch, minimizing patient waiting times. In the previous setting, urgent-treatment patients often spent several hours in our department. If a CT was required, available time on

the CT scanner for patient simulation rarely aligned with free time on the treatment machine, causing delays and long waiting times for the patient. The entire process was highly disruptive for the physician, physicist, and dosimetrist, who had to be available based on the schedule of two machines. The advantage of the streamlined workflow is to be able to schedule the patient on the treatment machine so that everyone involved knows when his or her work is required. Furthermore, this workflow minimizes patient setup. Especially in cases of heterotopic bone or spine compression treatments, the movement from the bed onto the treatment couch can be extremely painful and difficult for the patient and should be avoided if possible.

In the past, an alternative treatment approach for urgent radiotherapy has been to calculate the dose by hand, solely based on physical patient measurements instead of CT images. The target was defined using 2D portal images. However, physicians are becoming increasingly reluctant to treat patients without sufficient image guidance so as to avoid delivering high doses to normal tissues surrounding the target. The suggested new workflow allows us to view a 3D treatment plan of equal or better quality than from treatment planning without CT simulation.

### B. Extended field of view CBCT

The lateral flat-panel offset presented several challenges. Due to the uneven beam profile and energy fluence, the reconstructed intensity of an image changed, based on whether the image was acquired with the regular FOV or the extended FOV. During the course of this study, rFOV and eFOV MV CBCT calibration curves were developed independently of each other. The MV CBCT calibration curves were linear due to the energy to attenuation coefficient relation in the MV range.

### C. Dose calculation accuracy for phantoms

MV CBCT of differently sized water and anthropomorphic phantoms were used for initial dose planning. The results show that dose predictions on MV CBCT were within 3% mean difference relative to plans based on standard CT for all tested phantoms. Dose differences can be up to 5% locally within 0.5 cm of the phantom surface facing the beam. The phantoms do not deform, thus image alignment was accurate. The homogeneous dose difference distribution for the water phantoms showed that the HU calibration for water was accurate in rFOV and eFOV for the measured calibration curves and that image nonuniformity was negligible. Although density differences for individual inserts can be observed based on the location within the phantom, this did not prove to cause notable dose calculation inaccuracies.

### D. Considerations for choosing the MV CBCT protocol

Certain cone-beam properties, as well as properties of the imaged object, can negatively affect image quality. The need for different calibration curves based on the imaging modality showed that the values for reconstructed intensities were not as uniform as for kV CT but rather depend on the object size. This was mostly due to the scatter characteristics of an MV beam. The reconstructed intensity for water changed depending on whether rFOV or eFOV mode was used during the acquisition. Hence, two different calibration curves were used in this study. Within the distinction of the imaging mode used, the size of the object also affected the image quality. Each protocol provided the option to choose from “small,” “medium,” and “large” settings, referring to the object size, to optimize the applied filters. To be consistent, only “medium” scan settings have been used in this study. However, the additional differentiation may improve image quality and consequently dose calculation accuracy, if found to be necessary. Furthermore, truncated anatomy caused missing data artifacts and altered the HU values, causing reduced image quality. Additionally, movement during the acquisition caused motion artifacts. Lastly, the position within the FOV can affect accurate image reconstruction and should be considered. The image reconstruction, which uses certain imaging filters to improve image quality, was optimized with the anatomy centered in the beam field. MV CBCT imaging with patients far off-center may cause these to be less accurate, altering image intensity locally.

In addition to these considerations during patient setup, cone-beam imaging may be restricted due to the limited FOV and, especially for extremities, clearance between the machine and the patient.

### E. Expected dose calculation accuracy for treatment site

To assess the described limitations and potentialities for MV CBCT-based dose planning, the patient library was created considering a wide range of patient sites. Based on clinical experiences, treatment sites were categorized in four groups as follows and studied for dose planning: brain, thorax/spine, pelvis, and extremities.

Within the brain group, all treatments to the brain were predicted accurately using MV CBCT. The bone and soft tissue density were clearly identifiable on all brain scans. Nasal cavities caused the highest local dose differences within the dose calculation comparison.

The highest mean differences in dose predictions were within or beyond lung tissue in the thoracic spine group. The dose calculation accuracy largely depended on whether or not the beam traversed lung tissue. Motion due to breathing during the image acquisition caused streaking artifacts, which provided difficulties for correct intensity display. The static air inserts used during the reconstructed intensity-to-density calibration were not comparable to lung tissue in MV CBCT. Thus, the density of lung tissue varied significantly between patients, causing large local dose differences. Nevertheless, besides the general awareness of these discrepancies, they are not clinically relevant in palliative treatment situations. While it might be difficult to build an adequate phantom, a collection of patient images could be used to further assess the density for lung tissue and improve dose calculation predictions within lung tissue.

All pelvic images within the scope of this study were acceptable for treatment planning, provided that the patient was centered within the beam field during imaging. Difficulties for this group included truncation of the anatomy for patients exceeding the extended FOV. Capturing the entire anatomic site along the beam path was prerequisite for dose calculation and had to be considered during patient setup. In certain cases, only a single beam treatment was possible.

Extremities can often cause problems for machine clearance and patient safety. Although the rFOV was usually sufficient to image an arm, a knee, or a foot, clearance was difficult to achieve for a shoulder or a thigh, due to the target's off-center position. For these cases, alternative CBCT protocols might be necessary to change the gantry start and end position to provide machine clearance. Due to a limited number of clinical cases for the duration of this study, the dosimetric evaluation for extremities will need further attention.

Despite local dose differences, the total number of MU per plan did not change significantly between dose calculations to the mid-plane on CT and MV CBCT images. It shows the ability to use MV CBCT for simple dose planning. However, it is important to keep in mind which anatomical characteristics decrease the local dose calculation accuracy to prescribe to a point outside these areas.

### F. kV CBCT and MV CT imaging

Within the scope of this paper, only MV CBCT-based treatment plan accuracy was assessed. Nevertheless, the workflow described here is adaptable to kV CBCT- and MV CT-equipped linacs, which makes it versatile. kV CBCT image characteristics vary from MV CBCT images. Consequently, the feasibility for the treatment sites listed here would need to be verified separately through an additional dose comparison study.

A similar workflow as presented above has previously been described in the literature in combination with TomoTherapy (Accuray Corp., Sunnyvale, CA) and StatRT, commercial software specifically developed for TomoTherapy.[10] Additional research for a similar procedure on TomoTherapy exists for the treatment of spine metastases.[19–22] Although StatRT offers advanced capabilities for urgent treatments, it is limited to TomoTherapy. The workflow described here is independent of commercial software, such as StatRT. It provides a technically advanced, fast, and safe option for machines using kV CBCT or MV CBCT on-board imaging

systems to perform urgent radiation therapy on different treatment sites, thus offering a unique alternative to palliative treatments on TomoTherapy.

## V. CONCLUSIONS

We have developed and implemented a clinical workflow to enable rapid and safe urgent treatments. All steps (CT simulation, dose planning, patient verification and quality assurance, and dose delivery) can be performed in one session with the patient on the linac couch. Dose calculation based on MV CBCT images can be used for a large number of palliative and emergency treatment cases. Sufficient dose precision was demonstrated for brain, pelvis, and extremity fields, as well as the accuracy of calculated MU for all thoracic spine treatments in palliative treatment situations. However, dose plan accuracy depends on the prescription point in these cases. A separate CBCT protocol and a thorax-specific HU-to-density calibration curve for thoracic scans should be considered to improve dose calculations within and around lung tissue.

The clinical use of this technique for whole-brain treatment is underway in our clinic. The results obtained in this study are promising to make MV CBCT-based dose calculation possible for other emergency treatments, as well. Additional pelvic cases and extremity radiotherapy cases need to be studied to assess the full range of site-specific planning accuracies before the clinical implementation of this technique. Once this has been established, a detailed workflow description will be written. Additional clinical experience will allow for a quantitative evaluation of the time, patient comfort, and dosimetric benefits that can be reached through this workflow.

## REFERENCES

1. Morin O and Pouliot J. Megavoltage cone-beam IGRT. In: Bourland JD, editor. Image-guided radiation therapy. Boca Raton (FL): CRC Press, Taylor & Francis Group; 2012.
2. Chen J, Morin O, Aubin M, Bucci MK, Chuang CF, Pouliot J. Dose-guided radiation therapy with megavoltage cone-beam CT. Br J Radiol. 2006;79:S87–98.
3. Petit SF, van Elmpt WJ, Nijsten SM, Lambin P, Dekker AL. Calibration of megavoltage cone-beam CT for radiotherapy dose calculations: correction of cupping artifacts and conversion of CT numbers to electron density. Med Phys. 2008;35(3):849–65.
4. Cheung J, Aubry JF, Yom SS, Gottschalk AR, Celi JC, Pouliot J. Dose recalculation and the dose-guided radiation therapy (DGRT) process using megavoltage cone-beam CT. Int J Radiat Oncol Biol Phys. 2009;74(2):583–92.
5. Thomas TH, Devakumar D, Purnima S, Ravindran BP. The adaptation of megavoltage cone beam CT for use in standard radiotherapy treatment planning. Phys Med Biol. 2009;54(7):2067–77.
6. Hughes J, Holloway LC, Quinn A, Fielding A. An investigation into factors affecting electron density calibration for a megavoltage cone-beam CT system. J Appl Clin Med Phys. 2012;13(5):93–107. Retrieved February 19, 2014 from http://www.jacmp.org
7. Morin O, Chen J, Aubin M, et al. Dose calculation using megavoltage cone-beam CT. Int J Radiat Oncol Biol Phys. 2007;67(4):1201–10.
8. Aubry JF, Cheung J, Morin O, Gottschalk A, Beaulieu L, Pouliot J. Correction of megavoltage cone-beam CT images of the pelvic region based on phantom measurements for dose calculation purposes. J Appl Clin Med Phys. 2009;10(1):33–42. Retrieved March 21, 2012 from http://www.jacmp.org
9. Létourneau D, Wong R, Moseley D, et al. Online planning and delivery technique for radiotherapy of spinal metastases using cone-beam CT: image quality and system performance. Int J Radiat Oncol Biol Phys. 2007;67(4):1229–37.
10. McIntosh A, Dunlap N, Sheng K, et al. Helical tomotherapy-based STAT RT: dosimetric evaluation for clinical implementation of a rapid radiation palliation program. Med Dosim. 2010;35(4):280–86.
11. Faddegon BA, Wu V, Pouliot J, Gangadharan B, Bani-Hashemi A. Low dose megavoltage cone beam computed tomography with an unflattened 4 MV beam from a carbon target. Med Phys. 2008;35(12):5777–86.
12. Beltran C, Lukose R, Gangadharan B, Bani-Hashemi A, Faddegon BA. Image quality & dosimetric property of an investigational imaging beam line MV-CBCT. J Appl Clin Med Phys. 2009;10(3):37–48. Retrieved February 19, 2014 from http://www.jacmp.org
13. Gayou O. Influence of acquisition parameters on MV-CBCT image quality. J Appl Clin Med Phys. 2012;13(1):14–26. Retrieved January 13, 2015 from http://www.jacmp.org
14. Langen KM, Meeks SL, Poole DO, et al. The use of megavoltage CT (MVCT) images for dose recomputations. Phys Med Biol. 2005;50(18):4259–76.

15. Aubry JF, Pouliot J, Beaulieu L. Correction of megavoltage cone-beam CT images for dose calculation in the head and neck region. Med Phys. 2008;35(3):900–07.
16. Morin O, Aubry JF, Aubin M, et al. Physical performance and image optimization of megavoltage cone-beam CT. Med Phys. 2009;36(4):1421–32.
17. Battista JJ and Bronskill MJ. Compton scatter imaging of transverse sections: an overall appraisal and evaluation for radiotherapy planning. Phys Med Biol. 1981;26(1):81–99.
18. Rogers M, Kerr A, Salomons G, Schreiner LJ. Quantitative investigation of megavoltage computed tomography [proceedings paper]. In: Flynn MJ, editor. Medical Imaging 2005: Physics of medical imaging. Bellingham (WA): SPIE; 2005. p. 685–94.
19. Mahan SL, Ramsey CR, Scaperoth DD, Chase DJ, Byrne TE. Evaluation of image-guided helical tomotherapy for retreatment of spinal metastasis. Int J Radiat Oncol Biol Phys. 2005;63(5):1576–83.
20. Kim B, Soisson ET, Duma C, et al. Image-guided helical tomotherapy for treatment of spine tumors. Clin Neurol Neurosurg. 2008;110(4):357–62.
21. MacPherson M, Montgomery L, Fox G, et al. On-line rapid palliation using helical tomotherapy: a prospective feasibility study. Radiother Oncol. 2008;87(1):116–18.
22. Rong Y, Yadav P, Paliwal B, Shang L, Welsh JS. A planning study for palliative spine treatment using StatRT and megavoltage simulation. J Appl Clin Med Phys. 2011;12(1):97–107.

# CHAPTER 5

## Evaluating the Feasibility of Different On-Board Imaging Systems

The workflow procedure has been successfully implemented on the Siemens Artiste, using the MV CBCT on-board imaging system of the linac. The next question is whether this workflow can be applied to linacs from other vendors as well, making it applicable to all major commercial systems that are currently available. These systems differ fundamentally from the Siemens Artiste on-board imaging system. The on-board imaging system currently available from Varian and Elekta is a kV CBCT, as described in Chapter 2, whereas Accuray offers MV CT on-board imaging with their linac.

The suitability of these other on-board imaging systems has been examined in detail for the ERT workflow. The Journal of Applied Clinical Medical Physics accepted the corresponding study for publication and will publish it in Spring 2016. The manuscript

> Held M, Cremers F, Sneed P K, Braunstein S, Fogh S E, Nakamura J, Barani I, Perez-Andujar A, Pouliot J, and Morin O, "Assessment of image quality and dose calculation accuracy on kV CBCT, MV CBCT and MV CT images for urgent palliative radiotherapy treatments". *J Appl Clin Med Phys* 2016; (In press.)

is included below. The study presents the image quality and dose calculation suitability for simple treatment plans on four different on-board imaging systems in comparison to kV CT. The feasibility of the urgent RT workflow

is evaluated for each imaging system. Furthermore, the paper considers the physical aspects for dose calculation on each system for different anatomic sites.

Held, et al.: Comparison of on-board imaging systems

**Assessment of image quality and dose calculation accuracy on kV CBCT, MV CBCT, and MV CT images for urgent palliative radiotherapy treatments**

Mareike Held,[1] Florian Cremers,[2] Penny K. Sneed,[1] Steve Braunstein,[1] Shannon E. Fogh,[1] Jean Nakamura,[1] Igor Barani,[1] Angelica Perez-Andujar,[1] Jean Pouliot,[1] and Olivier Morin[1a]

*Department of Radiation Oncology,[1] University of California San Francisco, CA, USA; Department of Radiation Oncology,[2] Universitätsklinikum Schleswig-Holstein, Lübeck, Germany*

Olivier.Morin@ucsf.edu

Received 2 September, 2015; accepted 18 November, 2015

[a] Corresponding author: Olivier Morin, Department of Radiation Oncology, University of California San Francisco, 505 Parnassus Ave., L08-D, San Francisco, CA 94143 – 0226, USA; phone: (415) 353 9302; fax: (415) 353 8679; email: Olivier.Morin@ucsf.edu

ABSTRACT

A clinical workflow was developed for urgent palliative radiotherapy treatments that integrates patient simulation, planning, quality assurance, and treatment in one 30-minute session. This has been successfully tested and implemented clinically on a linac with MV CBCT capabilities. To make this approach available to all clinics equipped with common imaging systems, dose calculation accuracy based on treatment sites was assessed for other imaging units. We evaluated the feasibility of palliative treatment planning using on-board imaging with respect to image quality and technical challenges. The purpose was to test multiple systems using their commercial setup, disregarding any additional in-house development. kV CT, kV CBCT, MV CBCT, and MV CT images of water and anthropomorphic phantoms were acquired on five different imaging units (Philips MX8000 CT Scanner, and Varian TrueBeam, Elekta VersaHD, Siemens Artiste, and Accuray Tomotherapy linacs). Image quality (noise, contrast, uniformity, spatial resolution) was evaluated and compared across all machines. Using individual image value to density calibrations, dose calculation accuracies for simple treatment plans were assessed for the same phantom images. Finally, image artifacts on clinical patient images were evaluated and compared among the machines. Image contrast to visualize bony anatomy was sufficient on all machines. Despite a high noise level and low contrast, MV CT images provided the most accurate treatment plans relative to kV CT-based planning. Spatial resolution was poorest for MV CBCT, but did not limit the visualization of small anatomical structures. A comparison of treatment plans showed that monitor units calculated based on a prescription point were within 5% difference relative to kV CT-based plans for all machines and all studied treatment sites (brain, neck, and pelvis). Local dose differences > 5% were found near the phantom edges. The gamma index for 3%/3 mm criteria was > 95% in most cases. Best dose calculation results were obtained when the

treatment isocenter was near the image isocenter for all machines. A large field of view and immediate image export to the treatment planning system were essential for a smooth workflow and were not provided on all devices. Based on this phantom study, image quality of the studied kV CBCT, MV CBCT, and MV CT on-board imaging devices was sufficient for treatment planning in all tested cases. Treatment plans provided dose calculation accuracies within an acceptable range for simple, urgently planned palliative treatments. However, dose calculation accuracy was compromised towards the edges of an image. Feasibility for clinical implementation should be assessed separately and may be complicated by machine specific features. Image artifacts in patient images and the effect on dose calculation accuracy should be assessed in a separate, machine-specific study.

PACS numbers: 87.55.D-, 87.57.C-, 87.57.Q-

Key words: dose calculation, palliative radiation therapy, IGRT, MV CBCT, kV CBCT

## I. INTRODUCTION

Modern linear accelerators offer the capability to use on-board imaging for patient position verification. The intended purpose of the imaging system for 3D pretreatment verification is consistent across linac platforms;[1] however, implementation of different imaging systems is fundamentally different with advantages and disadvantages inherent in each system. Imaging systems differ in the X-ray source energy used (kV or MV), the acquisition technique (cone beam (CB) or fan beam (FB)), and the reconstruction algorithm.[2] Image quality of these systems has improved significantly over time,[1] presenting the opportunity to use the on-board imaging systems not only for patient alignment but also for dose verification. Numerous studies have explored the dose calculation suitability of these systems,[3,4,5,6,7] including studies that focus on rapid planning with palliative intent.[8,9] For adaptive radiotherapy (RT), some studies combined information from on-board images and CT images and calculated the dose on the resulting modified image that contained kV CT Hounsfield units (HU).[10]

We developed a novel workflow for urgent treatments that consists of patient setup and on-board CT imaging on the treatment machine, simple planning based on that image set, and treatment delivery (Fig. 1). This workflow is in clinical use on our linac used for on-call radiotherapy. The current study evaluated dose calculation accuracies for simple plans (one or two beams) on four different treatment machines to determine whether or not each imaging system would be suitable for our urgent treatment workflow.

The aim of palliative therapeutic radiotherapy and the significance of external beam radiotherapy with palliative intent are given in the literature.[11,12]

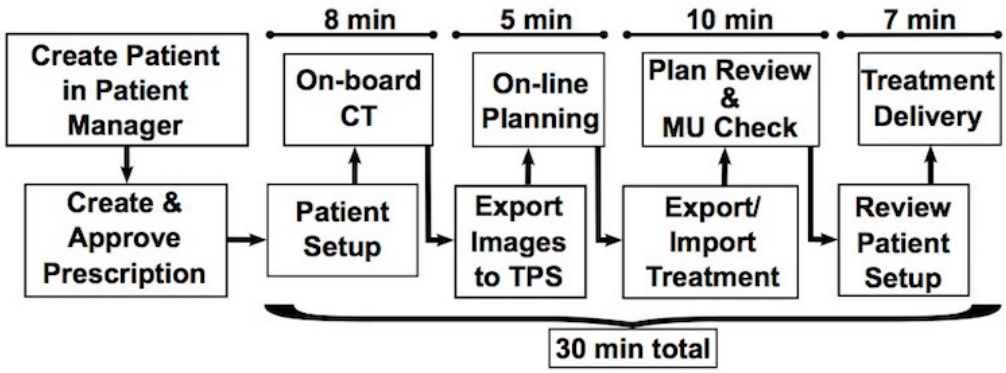


FIG. 1. Outline of the workflow for urgent radiotherapy treatments. Approximate times per steps are indicated above each section.

## II. MATERIALS AND METHODS

### A. Phantoms

Five different site setups were evaluated using two water phantoms and two anthropomorphic phantoms. For Setup 1, we used a 17 cm diameter and 25 cm in long plastic cylinder. Setup 2 was designed to mimic a pelvis made from acrylic sheets bent into a rounded container measuring 38 cm by 25 cm by 25 cm. Setup 3 utilized the head section of a sliced anthropomorphic phantom, and Setup 4 used the thorax section of the same phantom. Setup 5 was a solid anthropomorphic pelvis phantom.

### B. Imaging systems

Four on-board imaging systems were evaluated and compared to conventional CT: kV CBCT on the TrueBeam (Varian, Palo Alto, CA), kV CBCT on the VersaHD (Elekta, Crawley, UK), MV CBCT on the Artiste (Siemens, Munich, Germany), and MV CT on the TomoTherapy (Accuray, Sunnyvale, CA). Each imaging system had its own artifacts, and

vendors provided different choices of filters for reconstruction, usually based on the treatment site and size. These imaging protocols were used as suggested by the vendors and no additional in-house filters or image corrections were applied.

**B.1 kV CBCT**

Two different linear accelerators were used for kV CBCT image acquisition. The Varian TrueBeam provided a different imaging protocol for each treatment site. Small phantoms were imaged using a full-fan and half-trajectory setting. For head-sized phantoms, 100 kV tube voltage and 150 mAs tube current were recommended. The thorax protocol specified a half-fan and full trajectory to increase the field of view up to 45 cm in diameter, using 125 kV and 270 mAs. The pelvis protocol used the same settings with a higher tube current of 1080 mAs. Beam collimation was accomplished with dynamic X and Y jaws.[13] The reported weighted CT dose index ($CTDI_w$) was between 0.29 and 1.43 cGy per acquisition.

Similarly, the VersaHD provided different protocols based on the treatment site and size. Each protocol used a matching collimator cassette, similar to previous Elekta linac models and described in prior reports.[13] The reconstructed fields of view (FOVs) were up to 27 cm, 41 cm, or 50 cm, depending on the lateral flat panel offset, which can be set to small (S, no offset), medium (M, 11.5 cm lateral offset), and large (L, 19 cm lateral offset).[13] Here, three different protocols were used for phantom image acquisitions: "Head and Neck S20" for the cylinder and head phantom (100 kV and 10 mA, no filter), "Chest M20" for the thorax phantom, and "Pelvis M20" (both 120 kV and 40 mA, with bow-tie filter) for the water pelvis and anthropomorphic pelvis phantom. The letter S, M, or L denotes the amount of lateral flat panel offset, the number 20 indicates the scan length in Z direction in cm. The physical bow-tie filter is a filtration cassette that "can significantly change the

x-ray beam spectrum".[13] Nominal scan doses were reported between 0.12 and 2.20 cGy (Elekta Instructions for use, XVI R4.5)

**B.2 MV CBCT**

MV CBCT images were acquired on a Siemens Artiste that was equipped with the In-Line kView system. Instead of using the treatment beam, it used a low MV energy and a carbon target during imaging to improve image contrast.[14] Images were acquired using between 5 and 15 monitor units (MUs) (about 5–15 cGy per acquisition). Imaging protocols were chosen based on the phantom size. For small objects (size of a head), the regular field of view (rFOV) was sufficient to capture the entire anatomy and the system used a half-arc of 200°. For larger objects (the size of a thorax or pelvis), the extended field of view (eFOV) was used. This mode used a 5.5 cm lateral flat-panel offset during the acquisition and a 360° gantry rotation. Similar to the other machines, one of three different imaging protocols was chosen based on the treatment site.

**B.3 MV CT**

MV CT images were acquired on the Accuray TomoTherapy machine. Unlike CBCT, it acquires axial image slices on a ring gantry while the patient is translated through the treatment bore. This makes the system extremely stable and prevents reconstruction artifacts.[2] The imaging parameters during image acquisition were set to a normal pitch with a 2 mm reconstruction interval and a dose rate of 45 MU/min for all phantoms, which results in about 1 to 2 cGy dose to the patient per acquisition.[2]

**B.4 Diagnostic kV CT**

Standard treatment planning CT images were acquired on the diagnostic kV CT scanner MX8000 by Philips (Philips Healthcare, Andover, MA). All phantoms were imaged using

120 kV tube voltage, 209–244 mA tube current and a slice thickness of 2 mm. The delivered dose per scan was about 0.20 cGy. Treatment plans based on these diagnostic CT images were used as the reference to evaluate the treatment plans based on the four on-board systems described above.

**C Image noise, contrast, uniformity, spatial resolution**

Image quality, noise, contrast-to-noise ratio (CNR), and uniformity (UN) were assessed for phantom images on each machine, using the definitions:

$$Noise = 100 * \frac{\sigma_{(Water)}}{\mu_{(Water)}}, \quad (1)$$

$$CNR = \frac{\mu_{(ROI_{bone})} - \mu_{(Water)}}{\sigma_{(Water)}}, \quad (2)$$

and

$$UN = 100 * \frac{\mu_{(Water_{periphery})} - \mu_{(Water_{center})}}{\mu_{(Water_{pelvis})}}. \quad (3)$$

Regions of interest (ROIs) were drawn to obtain the mean image value for water, $\mu_{(Water)}$ , and bone, $\mu_{(ROI_{bone})}$ , and the standard deviation (SD) $\sigma_{(Water)}$ . $\mu_{(Water_{periphery})}$ included the mean value of the ROI on the lateral edges of the pelvic water phantom. $\mu_{(Water_{center})}$ was the mean value of the ROI in the center of the same phantom, and $\mu_{(Water_{pelvis})}$ was the mean image value of the ROI covering the entire area inside the phantom.

The spatial resolution of each system was defined using the Catphan504 phantom (The Phantom Laboratory, Salem, NY) with the CTP528 high resolution module, which contains resolution sections ranging from 1–21 lps/cm. The phantom was imaged on all five imaging systems, using the same image protocol as the one that was used for the anthropomorphic head phantom. The modulation transfer function (MTF) was calculated

for each machine and the 50% critical frequency (50% cf) was defined for a comparison of the spatial resolution among all systems.

**D. Density calibration**

Initial attempts to use a single image value to density calibration phantom across all five machines failed. Thus, phantom images acquired on each machine were used to calibrate the physical density to the image values, as required by the treatment planning system. ROIs were drawn for different densities on each image set. The mean HU value of each ROI was assigned to the according density of the same ROI on the kV CT image. A separate image value to density calibration (IVDC) was created for each image acquisition protocol.

Accurate dose calculation requires consistent IVDCs all throughout the phantom. Nonuniformity could cause objects to appear more or less dense than they actually were in parts of the images. Before using the IVDCs for dose calculation, they were used to display the object in density values, highlighting areas in which artifacts changed the density value of the object.

**E. Dose planning on phantom images**

A simple treatment plan was created on each image set (Table 1). For Setup 1 and 2, a single posterior–anterior (PA) beam with an open field was planned. Two opposed beams were used for Setups 3 to 5. Each plan used two different prescriptions. In prescription 1, a set number of MUs were prescribed. In prescription 2, a dose to a point at mid-plane was prescribed. All calculated plans were compared to the plan on the standard kV CT. Prescription 1, with a set number of MUs, was used to compare the dose distribution within the phantoms. The mean dose difference and gamma index for 3%/3 mm criteria

were assessed, including all values above the low-dose threshold of 30% of the maximum dose. Prescription 2 evaluated the plan dose by looking at the total number of MUs that were prescribed resulting from treatment plans based on kV CBCT, MV CBCT, or MV CT images compared to kV CT images.

## III. RESULTS

### A. Image noise, contrast, uniformity, spatial resolution

Visually, image quality was sufficient for emergency type treatment plans on all machines and bony anatomy was displayed with enough contrast to define its structure. Among all phantom images in this study, MV CT images had the highest noise level, six times higher than the noise in the kV CT images. MV CBCT images showed the lowest CNR between bone and water. kV CBCT images on the VersaHD overcorrected the image nonuniformity such that the image center appeared at a higher image value than on the edges of the image. Similarly, but less pronounced, MV CBCT images showed image nonuniformity with slightly lower image values left and right of the image center. Out of all five imaging systems, spatial resolution was worst on Artiste images, with a 50% critical frequency about 2.5 times less than for kV CT and TrueBeam kV CBCT images. The dose per scan was comparable on all imaging systems, except the Artiste. Here, dose was up to seven times higher for eFOV acquisitions. All values describing image quality are summarized in Table 2 for comparison.

TABLE 2. Image dose, noise, CNR, uniformity, and spatial resolution.

| | $CTDI_{vol}$ (cGy) rFOV/eFOV | Noise | CNR (bone/water) | Uniformity | Spatial Resolution 50% cf (1/cm) |
|---|---|---|---|---|---|
| kV CT (MX 8000) | 0.20 | 0.53 | 161.5 | 0.1 | 4.1 |
| kV CBCT (TrueBeam) | 0.29/1.43[a] | 2.10 | 52.2 | -1.0 | 4.1 |
| kV CBCT (Versa) | 0.12/2.20[a] | 3.07 | 36.7 | 6.7 | 2.1 |
| MV CBCT (Artiste) | 5.00/15.00[b] | 1.91 | 14.9 | -4.5 | 1.6 |
| MV CT (Tomo) | ~ 2.00[b] | 3.14 | 15.7 | 0.0 | 2.1 |

[a]$CTDI_w$, [b]dose,

**B. Density calibration**

In previous studies, Thomas[15] reported a resulting dose difference of 1% for an electron density difference of 8% for typical radiotherapy beams, and Hatton et al.[16] similarly showed that 21% difference in electron density resulted in 2.6% dose difference. Thus, IVDCs for the same machine that were within 8% difference in density were combined into one curve. For the CT, TrueBeam and TomoTherapy units, all calibration points were within 8% of each other, which resulted in less than 1% dose difference according to Thomas.[15] Thus, the TrueBeam and Tomotherapy units required only one IVDC each, despite using different imaging protocols. The Versa required two different curves, one for small objects (such as the head) and one for large objects (such as the thorax or pelvis). The Artiste was assigned three calibrations, which included separate IVDCs for images of the head, thorax, and pelvis. In the end, eight different IVDCs were entered into the treatment planning system for five different machines. All IVDC curves are plotted in Fig. 2.

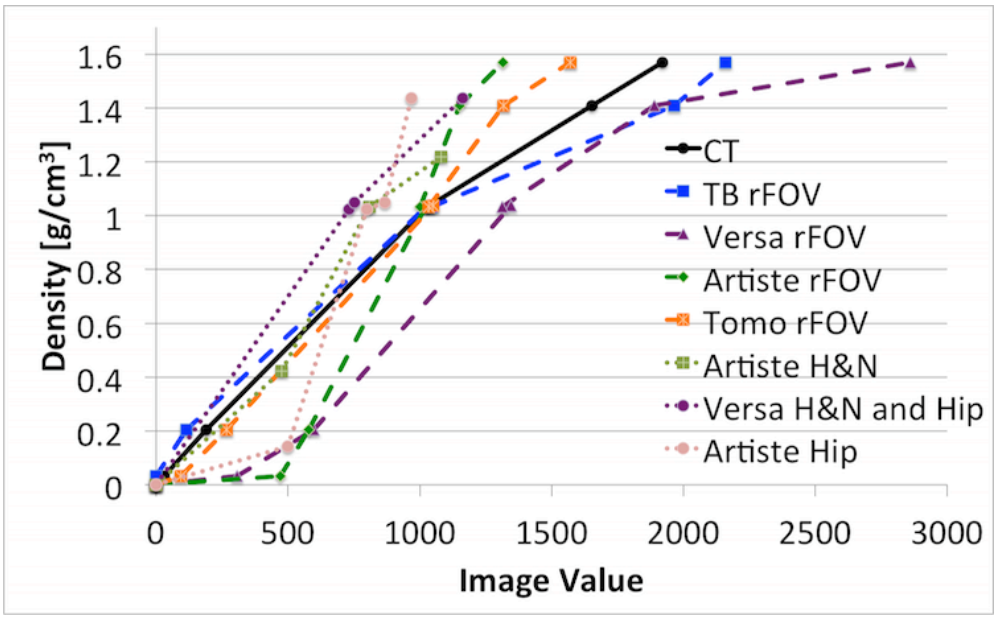


FIG. 2. IVDC curves for kV CT and on-board imaging systems. The VersaHD required two separate curves for rFOV and eFOV imaging protocols. The Artiste required three protocols, one for rFOV and two for eFOV.

Using the resulting IVDCs, the images were converted into physical density. Figure 3 shows a density profile (solid line) for the water cylinder and the pelvic water phantom. The same profile was plotted for all imaging machines studied here. The image noise in MV CT images was clearly visible. Versa images showed an inconsistency in image value to density conversion in the image center in case of the water cylinder phantom. This appears to be due to the image nonuniformity.

Table 3 lists a summary of the mean density difference in percent relative to the kV CT density along each profile and one standard deviation.

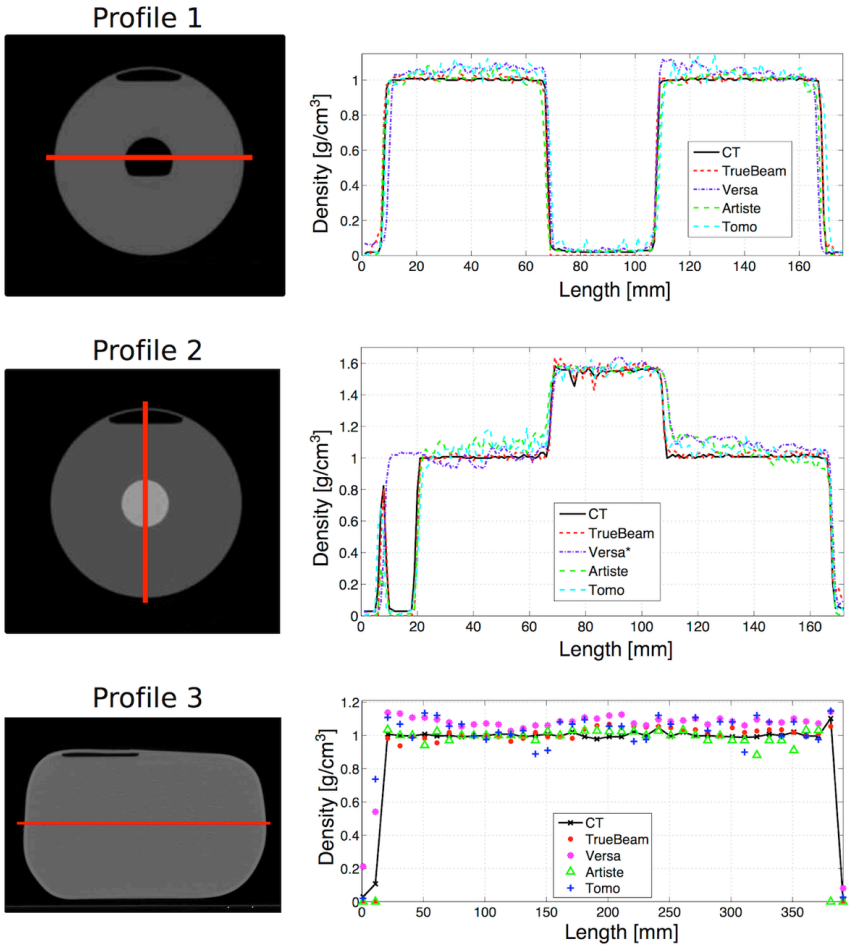


FIG. 3. Density profiles for the cylindrical and the pelvic water phantom. (left) CT image slice of the water phantoms. The red line indicates the path of the profile. (right) Density profiles for the acquired CT on each imaging system. The HU values are converted to density values using the machine-specific IVDC. (*The air bubble in the cylindrical phantom was removed before image acquisition on the VersaHD.)

TABLE 3. Density difference along image profiles from Fig. 3. Values are the relative difference to kV CT in percent.

| | **Profile 1** | **Profile 2** | **Profile 3** |
|---|---|---|---|
| kV CBCT (TrueBeam) | 0.70±1.38 | 0.71±2.13 | 0.85±3.32 |
| kV CBCT (Versa) | 4.86±3.32 | 3.99±6.61 | 8.05±2.77 |
| MV CBCT (Artiste) | 0.80±2.74 | 4.76±6.83 | 0.06±3.73 |
| MV CT (Tomo) | 3.30±4.49 | 3.01±4.69 | 3.40±7.00 |

### C. Dose calculation accuracy

Based on prescription 1, local dose calculation errors were identified. Figure 4 summarizes the percentage dose calculation differences in a color map. The left column shows the diagnostic CT center slice of each phantom with the planned dose distribution in percent, relative to the maximum dose. The four columns to the right map the local dose differences relative to the kV CT plan for the according image slice, which resulted from the treatment plan based on the on-board images of all four systems. The color map is scaled from -5% (blue) difference to +5% (red) difference, with green indicating good agreement between both plans. The calculated dose differences, expressed by the gamma index with 3%/3 mm criteria, the overall mean difference, and standard deviation, are summarized in Table 1.

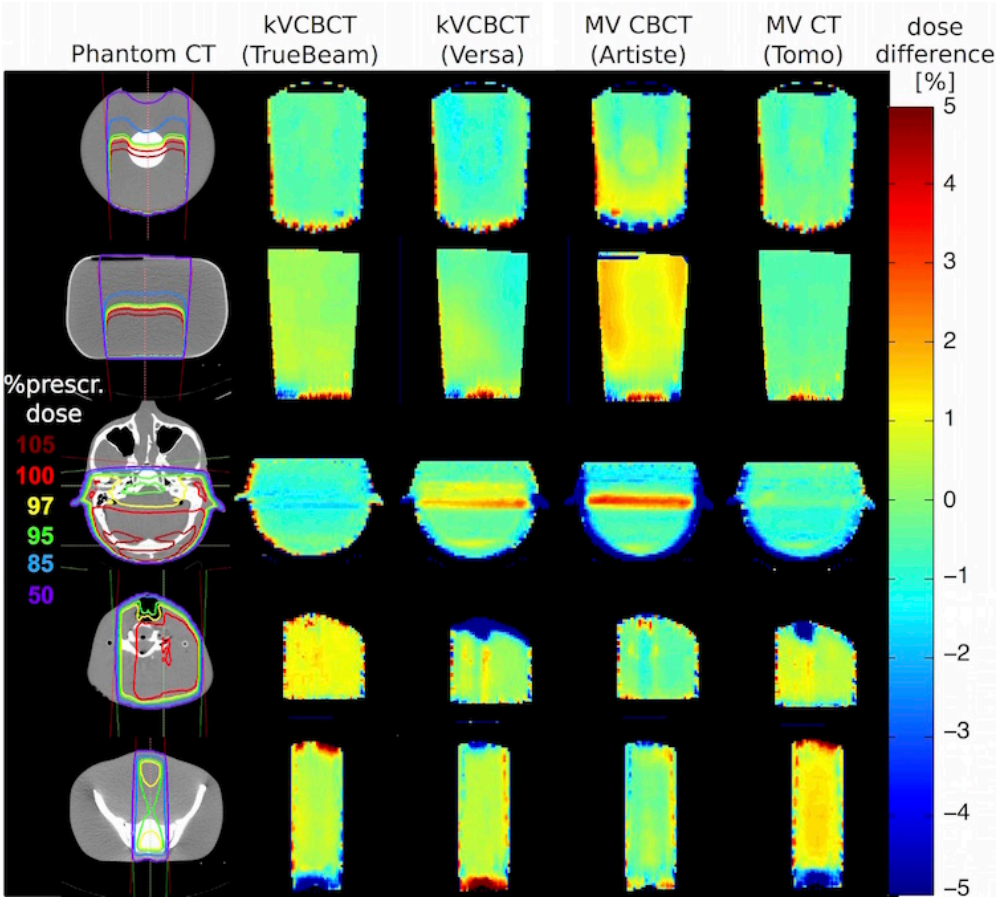


FIG. 4. Dose difference maps. Percentage difference of simple dose plans based on kV CBCT, MV CBCT, and MV CT images compared to diagnostic kV CT-based images. The left column bar shows the dose distribution within the CT image as percentage of the maximum dose. The columns to the right show the relative percentage differences where green is no difference, blue is underdosing, and red is overdosing on the linac's on-board images.

TABLE 1. Difference in calculated dose for prescription 1 relative to the treatment planning CT.

| | **kV CBCT (TrueBeam)** | | **kV CBCT (Versa)** | | **MV CBCT (Artiste)** | | **MV CT (Tomo)** | |
|---|---|---|---|---|---|---|---|---|
| Phantom | γ-index (3%/ 3mm) | Mean (%) SD | γ -index (3%/3 mm) | Mean (%) SD | γ -index (3%/3 mm) | Mean (%) SD | γ -index (3%/3 mm) | Mean (%) SD |
| Water Cylinder | 97.28 | -0.28<br>2.38 | 97.20 | -0.59<br>2.69 | 96.74 | -0.71<br>6.46 | 97.03 | -0.44<br>3.71 |
| Water Pelvis | 99.37 | 0.27<br>0.80 | 99.35 | -0.05<br>0.82 | 99.13 | 0.21<br>5.42 | 100.00 | -0.29<br>0.63 |
| Head | 94.36 | -1.93<br>4.28 | 99.67 | -1.15<br>6.25 | 96.70 | -3.74<br>12.52 | 99.47 | -1.73<br>6.08 |
| Neck | 99.62 | 0.64<br>4.99 | 97.88 | -3.54<br>15.15 | 99.51 | -0.32<br>6.78 | 99.25 | -0.96<br>8.99 |
| Hip | 99.99 | -0.15<br>4.74 | 99.81 | 0.59<br>2.37 | 99.86 | -0.22<br>3.78 | 99.99 | 0.18<br>4.92 |

Another approach to evaluate the outcome of the treatment plans was the comparison of MUs per plan. These were obtained based on the treatment dose prescribed to a point inside the phantom. In all cases, calculated MUs were within 5% of the number of MUs for the same kV CT-based plan. The relative differences of MUs for each imaging system and treatment site are listed in Table 4.

TABLE 4. Percentage difference in MUs compared to the kV CT plan prescribed to a point at mid-plane.

| | **kV CBCT (TrueBeam)** | **kV CBCT (Versa)** | **MV CBCT (Artiste)** | **MV CT (Tomo)** |
|---|---|---|---|---|
| Water Cylinder | -0.82 | 2.46 | 0.82 | 0.00 |
| Water Pelvis | -0.13 | 0.00 | -0.93 | 0.66 |
| Head | 2.35 | -0.59 | -0.59 | 0.00 |
| Neck | -0.62 | -1.23 | 1.23 | -1.23 |
| Hip | -3.02 | -2.63 | -2.10 | -3.15 |

## IV. DISCUSSION

Despite the reported differences in image quality, each machine produced sufficient image contrast to identify bony anatomy, which is important for defining the treatment target in many emergency setups. Further reduction in imaging dose is not necessary on the TrueBeam and VersaHD, since imaging protocols are preset and already optimized for low dose delivery. Imaging dose for the TomoTherapy could possibly be lowered by using a 3 mm pitch instead of 2 mm. Reducing the MUs per MV CBCT acquisition on the Artiste may also be possible, if requested. However, in both cases, it is important to ensure this would not affect the IVDC.

In case of the VersaHD and Artiste, the IVDCs obtained were dependent on the image protocol and object size. The TomoTherapy and TrueBeam systems produced spatially stable image values regardless of these two factors. For the Artiste, all image value to density calibrations have been tested for stability over time before clinical implementation. This remains to be done for all other systems.

Although the contrast to noise ratio and spatial resolution for Artiste images were about a tenth and a third less than that of kV CT images, respectively, MV CBCT images were still adequate for simple treatment plan dose calculation. Overall, this study on water and anthropomorphic phantoms showed that image acquisition on all four on-board imaging systems provided acceptable dose calculation accuracy for simple treatment plans of single or opposed beams in case of head, head and neck, and pelvis treatments. Prescription 1 revealed areas of local dose differences of up to 5% within the phantom, showing the largest dose differences in MV CBCT-based treatment plans. Local differences of more than 5% were observed only on the field edges, irrespective of the field size. Our

recommendation based on these observations is that areas of relative differences > 5% should be avoided when choosing a prescription point.

Prescription 2 was used as an additional test to determine the overall difference in treatment plans. Based on a dose prescription to a point at mid-plane, the total number of MUs was within the objective of ± 5% relative to the kV CT-based plan for all imaging machines and all treatment sites. In the end, this would be the difference in delivered dose for these treatments. Nevertheless, knowledge of where dose calculation may be less accurate was important to correctly prescribe the treatment dose and make judgments regarding dose distribution.

With this accuracy, all treatment fractions could be delivered using this setup and treatment plan. However, this should be decided on a case-by-case basis, taking into account patient-specific factors and treatment plan details.

Figure 5 shows a CT slice of the phantoms used in Setups 3 to 5, which were acquired using each of the linac's on-board imaging system. In comparison, Fig. 6 is a collection of patient images. These images demonstrate that the phantoms used provided good representation of realistic image quality. Many of the image artifacts could be observed in phantom as well as patient images. For example, nonuniformity caused by the transition from the neck to the shoulders was present in all cone-beam images. Images using energies in the MV range showed a much lower CNR than kV images. This is mainly due to the dominant Compton effect for MV energy photon interaction with matter, in which case photon attenuation is independent of the atomic number Z. For photons with energies in the kV range, photoelectric attenuation is dominant, which is proportional to $Z^3$, resulting in higher contrast, especially for soft tissues. kV CBCT images presented brighter shades of gray-level around bony anatomy. Nevertheless, artifacts caused due to organ motion

are not captured in phantom images. Consequently, streaking artifacts were much more pronounced in pelvic images of actual patients than in the phantom images. A separate study that compares treatment plans based on patient images of each of the on-board imaging systems to the same plans based on the kV CT would be advised. Also of interest may be another study that investigates artifacts specific to patients with metal implants or prostheses.

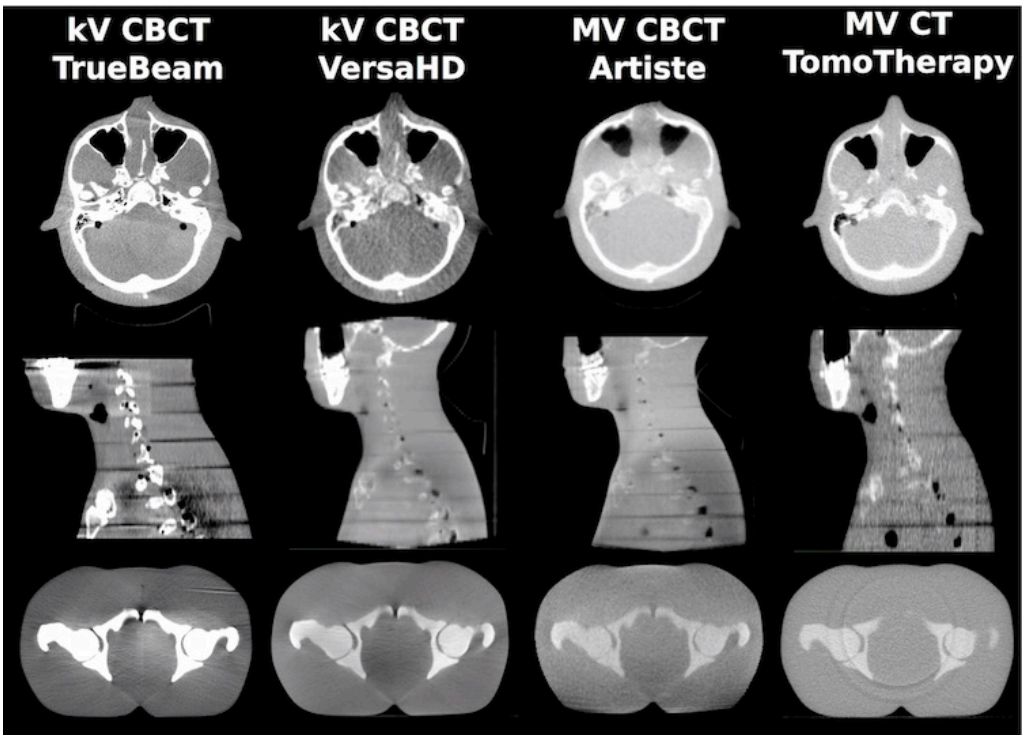


FIG. 5. CT images of the phantom used in Setup 3, 4, and 5.

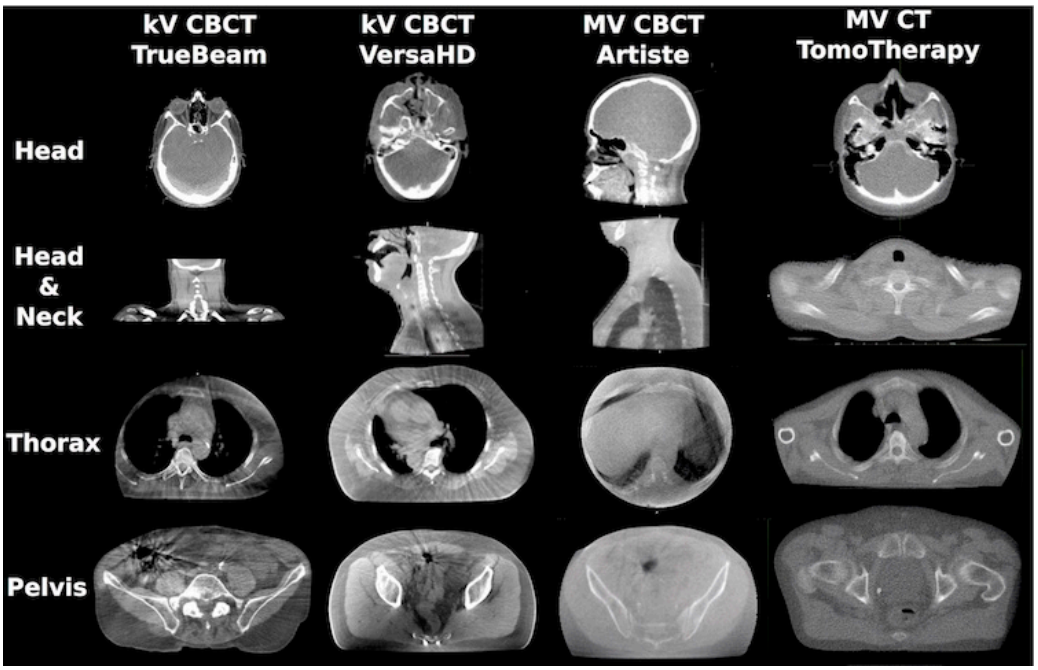


FIG. 6. Patient CT images of different treatment sites. The images were acquired using the indicated machines' on-board imaging system.

**A. Field of view**

The field of view remained a limitation for this application. In case of the TrueBeam, the 15 cm scan length might be insufficient to capture the anatomy for a whole brain treatment. Artiste images were limited to 31 by 31 $cm^2$ for an axial FOV, which was sufficient in most cases; however, opposed beam planning might present a problem for large patients. The VersaHD allowed a FOV up to 50 by 50 $cm^2$ for axial slices when using the largest lateral flat panel offset, but image uniformity was reduced compared to the medium FOV size of 42 by 42 $cm^2$, which was used here. Additionally, in all cases, the dose calculation accuracy is diminished towards the edges of the image. Consequently, it is important that the patient setup point and image isocenter were in close proximity to the treatment isocenter.

**B. Clinical implementation**

Another potential limitation is that DICOM export to the treatment planning system might require extra time if it was not integrated into the linac software. This may depend on the combination of linac and patient management software used in the clinic. Furthermore, MV CT acquisition times on the TomoTherapy were known to extend the duration of the workflow by a few minutes. Upon clinical implementation, a procedure that ensures the choice of the correct IVDC within the treatment planning system is strongly recommended.

Previous research reported on a similar workflow for palliative treatments on the TomoTherapy linac, using the commercial software StatRT, which was created specifically for this purpose on the TomoTherapy.[9,17,18,19] However, this software was not available in our clinic at the time of this study.

A summary of clinically important factors for each machine is provided in Table 5.

The dosimetric prerequisites to accurately and rapidly simulate, plan, and treat were given on each machine studied. Nevertheless, initial individual dose verification using patient images instead of phantoms is still recommended for each machine.

TABLE 5. Summary of clinically important factors for each on-board imaging system.

| | kV CBCT (TrueBeam) | kV CBCT (Versa) | MV CBCT (Artiste) | MV CT (Tomo) |
|---|---|---|---|---|
| Multiple IVDC calibrations necessary | no | yes | yes | no |
| Mean dose calculation accuracy < 5% / < 10% including 1 SD? | | | | |
| Head | no/yes | no/yes | no/no | no/yes |
| Neck | no/yes | no/no | no/yes | no/yes |
| Pelvis | yes/yes | yes/yes | yes/yes | no/yes |
| Difference of prescribed MU to mid-plane < 5%? | yes | yes | yes | yes |
| Max. field of view (diameter, length (cm)) | 45, 15 | 50, 27 | 31, 25 | 40, 26[c] |
| Acquisition & reconstruction time | < 2 min | < 2 min | < 2 min | ~ 5 min[a] |

[a]Scan length variable – acquisition time estimated for 26 cm scan length.

This study compared dose calculations for treatment sites of the head, neck, and pelvis. Treatments of the thorax specifically were not studied here, as rigid phantoms seemed inappropriate for the purpose. In those particular cases, the main challenge would be artifacts caused by tissue motion during the image acquisition, which does not occur in rigid phantoms and in some cases the need for sufficient image quality to count vertebral bodies reliably. A collection of patient images for each machine will be required before making any qualified recommendations on dose calculation accuracy around and within lung tissue.

## V. CONCLUSIONS

On-board imaging provided a useful tool to simulate patients in urgent treatment situations for a simplified and streamlined treatment procedure. Although implementation of the workflow may involve additional work, the prerequisites for dose calculation based on on-board images were given. With machine-specific IVDCs, the calculated MUs per plan were within the objective of ± 5% difference relative to kV CT-based planning. Local dose differences were identified for three treatment sites (head, neck, and pelvis).

In contrast to urgent hand calculation based treatments, if CT-simulation is unavailable outside of regular work hours, this approach offers an enormous advantage through 3D CT-based treatment planning that makes use of modern digital capabilities. Compared with the challenges of expedited kV CT-based urgent plans, the workflow suggested here reduces patient waiting and setup times and provides a predictable treatment timetable, combining simulation, planning, and treatment into one session.

## ACKNOWLEDGMENTS

We would like to thank Atchar Sudhyadhom, Christopher McGuinness and Aaron Garcia, all from UCSF, for their help acquiring the images on the various imaging systems.

**REFERENCES**

1. Mutaf YD. Electronic portal imaging devices. In: Mundt AJ and Roeske JC, editors. Image-guided radiation therapy. Shelton, CT: People's Medical Publishing House-USA; 2011. p. 74–98.

2. Mackie TR, Morin O, Olivera GH, Pouliot J. Megavoltage imaging systems. In: Mundt AJ and Roeske JC, editors. Image-guided radiation therapy. Shelton, CT: People's Medical Publishing House-USA; 2011. p. 123–29.

3. Yoo S and Yin FF. Dosimetric feasibility of cone-beam CT-based treatment planning compared to CT-based treatment planning. Int J Radiat Oncol Biol Phys. 2006;66(5):1553–61.

4. Yang Y, Schreibmann E, Li T, Wang C, Xing L. Evaluation of on-board kV cone beam CT (CBCT)-based dose calculation. Phys Med Biol. 2007;52(3):685–705.

5. Morin O, Chen J, Aubin M, et al. Dose calculation using megavoltage cone-beam CT. Int J Radiat Oncol Biol Phys. 2007;67(4):1201–10.

6. Petit SF, van Elmpt WJ, Nijsten SM, Lambin P, Dekker AL. Calibration of megavoltage cone-beam CT for radiotherapy dose calculations: correction of cupping artifacts and conversion of CT numbers to electron density. Med Phys. 2008;35(3):849–65.

7. Guan H and Dong H. Dose calculation accuracy using cone-beam CT (CBCT) for pelvic adaptive radiotherapy. Phys Med Biol. 2009;54(20):6239–50.

8. Létourneau D, Wong R, Moseley D, et al. Online planning and delivery technique for radiotherapy of spinal metastases using cone-beam CT: image quality and system performance. Int J Radiat Oncol Biol Phys. 2007;67(4):1229–37.

9. MacPherson M, Montgomery L, Fox G, et al. On-line rapid palliation using helical tomotherapy: a prospective feasibility study. Radiother Oncol. 2998;87(1):116–18.

10. Thomas TH, Devakumar D, Purnima S, Ravindran BP. The adaptation of megavoltage cone beam CT for use in standard radiotherapy treatment planning. Phys Med Biol. 2009:54(7):2067–77.

11. Konski A, Feigenberg S, Chow E. Palliative radiation therapy. Semin Oncol. 2005;32(2):156–64.

12. van Oorschot B, Rades D, Schulze W, Beckmann G, Feyer P. Palliative radiotherapy – new approaches. Semin Oncol. 2011;38(3):443–49.

13. Ishikawa M, Kamath S, Saw CB, Sethi A, Shirato H, Song WY. Kilovoltage imaging systems. In: Mundt AJ and Roeske JC, editors. Image-guided radiation therapy. Shelton, CT: People's Medical Publishing House-USA; 2011. p. 110–22.

14. Faddegon BA, Wu V, Pouliot J, Gangadharan B, Bani-Hashemi A. Low dose megavoltage cone beam computed tomography with an unflattened 4 MV beam from a carbon target. Med Phys. 2008;35(12):5777–86.

15. Thomas SJ. Relative electron density calibration of CT scanners for radiotherapy treatment planning. Br J Radiol. 1999;72(860):781–86.

16. Hatton J, McCurdy B, Greer PB. Cone beam computerized tomography: the effect of calibration of the Hounsfield unit number to electron density on dose calculation accuracy for adaptive radiation therapy. Phys Med Biol. 2009;54(15):N329–N346.

17. Mahan SL, Ramsey CR, Scaperoth DD, Chase DJ, Byrne TE. Evaluation of image-guided helical tomotherapy for retreatment of spinal metastasis. Int J Radiat Oncol Biol Phys. 2005;63(5):1576–83.

18. Kim B, Soisson ET, Duma C, et al. Image-guided helical tomotherapy for treatment of spine tumors. Clin Neurol Neurosurg. 2008;110(4):357–62.

19. Rong Y, Yadav P, Paliwal B, Shang L, Welsh JS. A planning study for palliative spine treatment using StatRT and megavoltage CT simulation. J Appl Clin Med Phys. 2010;12(1):97–107. Retrieved January 22, 2015 from http://www.jacmp.org

# CHAPTER 6

# Implementation into the Clinical Routine

## Initial Experiences with ERT patients

The new ERT workflow was first used clinically in January 2015. Within its initial year of clinical implementation, the procedure has been used to treat over 20 patients. During that time, its application was restricted to whole brain and heterotopic bone treatments that were requested during clinical hours, where heterotopic bone RT formed the majority of treatments. This restriction was necessary to give the radiation therapists (RTTs) time to adapt to the new workflow while performing each step confidently without having to consult the procedure book. Both whole brain and heterotopic bone treatments are common emergency situations, providing opportunities for the RTTs to improve the workflow. Furthermore, whole brain treatments use a simple patient setup. Their prescribed MUs are expected to be within a small range for the same prescription, due to similar head separations for patients. This fact can be used as a simple check to ensure treatment safety as shown in Appendix A. Here, it is important to mention that heterotopic bone treatments do not usually use 3D treatment planning due to the fact that CBCT acquisition may be infeasible for the off-axis treatment area in most cases. The ERT workflow was modified for heterotopic bone treatments to use the on-board imaging system for 2D imaging instead. The treatment dose is calculated based on the required field size and patient thickness, as shown in the example below. Consequently, 3D dose calculation on CBCT images is not available for heterotopic bone treatments. Although the work-

flow has been used on over 20 patients, CBCT based dose calculation was used for the treatment of four whole brain patients only.

## First Whole Brain Treatment

The first patient treated with the new ERT workflow required urgent whole brain RT. The patient was already in the department for another scheduled treatment when the urgency of a whole brain treatment became evident. Since it was a Friday afternoon and the RTT responsible for patient CT simulation had already left, the next possible treatment day was Monday.[4] The new ERT workflow provided an alternative to avoid that the patient had to come back for treatment on a later day. Thus, the patient was scheduled for treatment on the machine immediately. The course of simulation, planning, and treatment is listed below in Table 7.1., including the duration of each step. The treatment was prescribed using two opposed later beams to deliver a total dose of 300 cGy at isocenter. It was simulated, planned, and treated within 42 minutes.

[4]The need for treatment was not urgent enough to justify an after-hour treatment.

| Step | Time |
|---|---|
| 1. Fitting the immobilization mask to the patient's head (Figure 6.1(a)). | 5 min |
| 2. Acquisition of the MV CBCT for patient simulation. | 4 min |
| 3. Importing the patient CT into the TPS. | 1 min |
| 4. Treatment planning (Figure 6.1(b)). | 8 min |
| 5. MU check using RadCalc. | 2 min |
| 6. 2nd check of treatment plan parameters. | 5 min |
| 7. Importing the treatment plan into the patient management system. | 6 min |
| 8. Image association of the digitally reconstructed radiograph (DRR) with the according treatment field for portal image verification (Figure 6.1(c)). | 1 min |
| 9. Portal image verification for each beam to verify correct patient setup (Figure 6.1(d)). | 7 min |
| 10. Treatment delivery for a prescription of 300 cGy. | 3 min |
| **TOTAL** | **42 min** |

**Table 6.1:** Steps outlining the first patient treatment with the new ERT workflow.

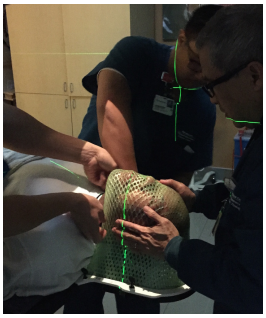

(a) The fitting of the patient immobilization mask.

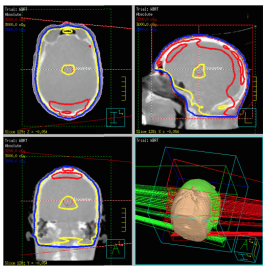

(b) Treatment plan and dose distribution.

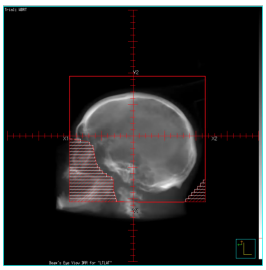

(c) Digitally reconstructed radiograph from the TPS.

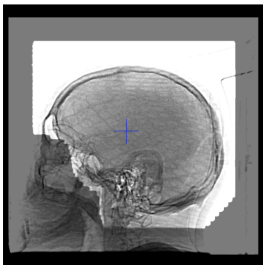

(d) Portal image for patient setup verification.

**Figure 6.1:** Photos illustrating some of the steps listed in Table 7.1.

## First Heterotopic Bone Treatment

The anatomic treatment site of the first heterotopic bone treatment was a hip. CBCT acquisition was unfeasible in this case due to the off-centered patient position. Instead, 2D portal images are used to define the treatment field size. The MUs per beam are calculated as presented in Chapter 2. The course of treatment is outlined in Table 7.2. The prescription defined the treatment to be delivered using two opposed beams for a total dose delivery of 700 cGy to the patient's mid-plane. The patient separation at the treatment site was physically measured to be 22 cm. Consequently, the prescription point was at 11 cm depth.

A first portal image was acquired to visualize the anatomy (Figure 6.2(b)). The collimator angle and treatment field size were subsequently altered and a portal image was acquired each time to visualize the desired treatment field (Figure 6.2(c) and 6.3(a)). Before the treatment delivery, a portal image was also acquired for the opposed beam to verify the correct treatment field and patient position (6.3(b)). The treatment was planned with the TPS using a planning option that allows the user to add a treatment plan to a patient's folder without importing CT images. Consequently, tissue heterogeneity was not considered in the dose calculation. Figure 6.4 is a screenshot of the interface. After selecting the patient positioning and photon beam energy based on the prescription, the dosimetrist defined a point at the iso center depth, which is at half of the measured patient separation. The dosimetrist then entered the prescription dose of one beam, which is half of the total prescription dose in case of a two beam treatment, as in Figure 6.4(a). Next, the treatment field size was entered in another tab, shown in Figure 6.4(b), according to what was defined previously with the portal images.

The total time of the procedure was 60 minutes in this case, which was owed to a confusion about the definition of the treatment field unrelated to the new workflow. This added about 12 minutes to the time needed otherwise.

| Step | Time |
|---|---|
| 1. Setting up the patient on the linac (Figure 6.2(a)). | 10 min |
| 2. Taking the first portal image (Figure 6.2(b)). | 6 min |
| 3. Adjusting the collimator angle on the linac. | 1 min |
| 4. Taking the second portal image (Figure 6.2(c)). | 11 min |
| 5. Adjusting the field size and taking the third portal image. | 8 min |
| 6. Final field size adjustment and fourth portal image. | 2 min |
| 7. Measuring the patient thickness at the central treatment axis. | 1 min |
| 8. MU calculation in Pinnacle. | 2 min |
| 9. MU verification with RadCalc. | 9 min |
| 10. Portal image verification of the opposed beam. | 5 min |
| 11. Treatment delivery. | 5 min |
| **TOTAL** | **60 min** |

**Table 6.2:** Steps outlining the first heterotopic bone treatment using the new ERT workflow.

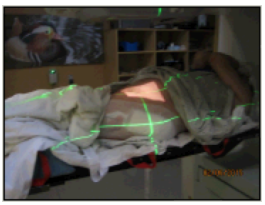

(a) The patient setup on the linac for heterotopic bone RT.

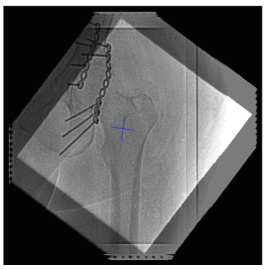

(b) 1st portal image to determine the field size and collimator angle for the correct treatment field.

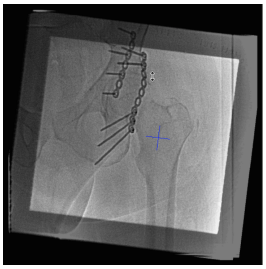

(c) 2nd portal image with an adjusted collimator angle.

**Figure 6.2:** Photos illustrating some of the steps listed in Table 7.2.

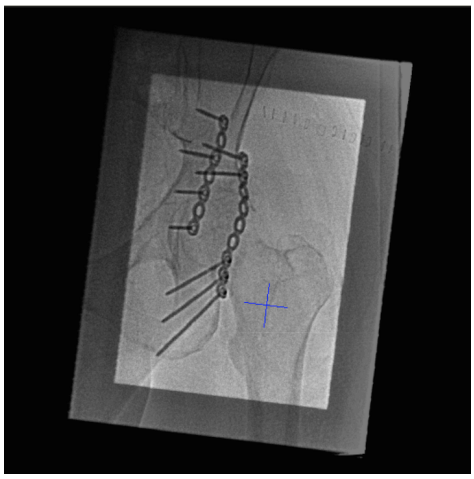

(a) Final portal image with the correct field size and collimator angle. The lighter square indicates the actual radiation field.

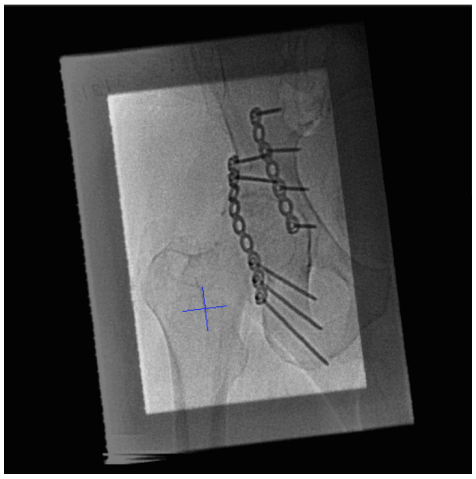

(b) Verification of the treatment field for the opposed beam at 180° gantry angle.

**Figure 6.3:** Portal images visualizing the final treatment field.

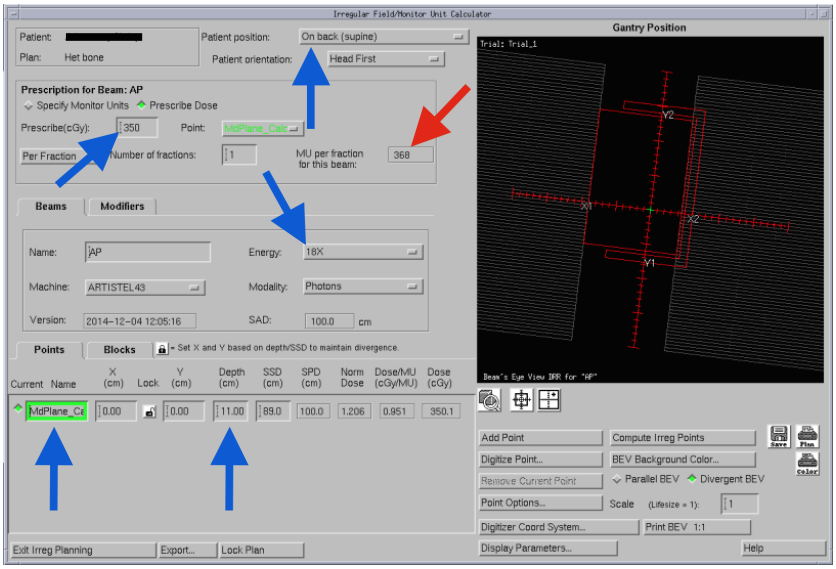


(a) The blue arrows mark those fields that need to be filled in by the dosimetrist. The red arrow indicates the output of the calculated number of MU for the desired treatment setup and prescription dose.

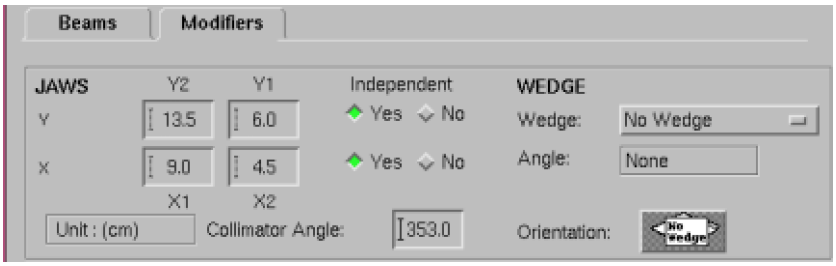


(b) The second tab, where the treatment field size and collimator angle are set.

**Figure 6.4:** TPS interface for the dose calculation of a heterotopic bone treatment.

## Clinical Workflow Duration

The ERT treatment can be simulated and planned within a 30-35 minute time span. Clinically, the average treatment time was longer for the cases that were logged. The first 10 treatments took between 40 and 67 minutes from the time the patient was brought into the treatment room to the point the patient left the room. There are several reasons for this extended time frame. One is the learning curve of every radiation therapist and physician. Another is that the linac has experienced a very low patient load over the past year. This makes it a suitable machine to use for clinical implementation. However, it does not reflect the back-to-back treatment schedule other machines have to comply with. Although not confirmed, the lack of treatment time restrictions may be unintentionally prolonging the duration of the treatment. Figure 6.5 plots the treatment time required for the first 10 patients that were treated according to the new protocol. Circumstances that were found to extend the overall treatment time included who was performing the treatment and whether the physician and second check person were available when requested. In cases of immobile patients, their setup required additional time.

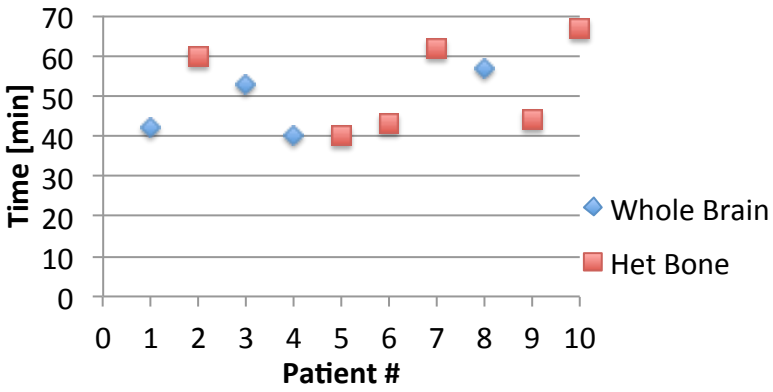


**Figure 6.5:** Clinical treatment time of the first ten ERT patients.

Based on these first cases, the mean treatment time was 48 min for whole brain treatments and 53 min for heterotopic bone treatments. The clinical treatment time for the first ten patients shows a slight upward trend. This may be explained by the receding assistance by the physicists who are very familiar with the workflow. The last treatment plotted in Figure 6.5 was the first treatment that was completed without the help of physicists during patient simulation and planning, which is a first step towards the implemen-

tation of this workflow on weekends. A decrease in the mean treatment time is expected throughout the next year. Overall, personnel not being present was the main reason treatment times extended past the targeted 35 min treatment duration. It also occurred that the patient's folder was taken to a different office for the second check, which regularly caused delays. Presumably, general distraction causes delays in the return of the documents, which are required at the beginning of treatment. This shows that a raise of awareness about the new procedure is required. The staff needs to be focused and aware that the patient is on the treatment couch the entire time.

Despite the aim of 35 min total not being met, the ERT workflow procedure reduced the time that patients, who require urgent treatment would spend in the department, drastically. As mentioned in Chapter 1, the previous workflow offered 2D simulation based on film only. The evasion to urgent kV CT regularly caused delays for the patient in question as well as other patients scheduled on the kV CT or linac. Regardless of whether the kV simulator or the kV CT was used for patient simulation, the patient had to expect to spend a minimum of an hour in the radiation oncology department. More often 4-6 hours would pass between patient simulation and treatment. In case of emergency patients, who are often in a large amount of pain, any minute spent waiting is an imposition. Now, 3D dose calculation is made available where necessary, providing better or equal treatment plan quality as before while minimizing patient waiting time to a maximum of an hour.

# CHAPTER 7

# Discussion

The idea of using on-board imaging to assist with patient simulation in ERT situations has been proposed before, for example by Létourneau et al. [46]. Their approach, to plan the dose based on an equivalent thickness of water instead of the actual patient images, does not consider tissue density heterogeneity. The novelty of this work here is that on-board CT images are used for dose planning as they are reconstructed, without additional image modifications. Being able to use on-board images for dose calculation is desired for many reasons and extensive research has been done to improve it [44, 47–50]. However, most of the approaches aim for high dose calculation accuracy as required for ART and IGRT, using specific image corrections, for example by combining kV CT and on-board CT information [51]. This process requires time that ERT treatments do not allow for. Instead, a requirement for this work was to use commercially available and clinically feasible on-board imaging systems only, which limits dose calculation accuracy on on-board images.

## IVDC

The prerequisites for dose calculation on CT images are verified for the Siemens Artiste MV CBCT system by measuring the linear response of the flat panel and verifying its stability in Chapter 3. As a result, the on-board system requires QA measurements no more frequent than the 3-month intervals recommended for gain calibration and dead-pixel map updates. Figure

3.6 illustrates the importance of IVDC for CT-based dose calculation. Four phantoms were built to assist with the IVDC. To consider photon scatter along the Z-axis in CBCT, the phantoms need to extend over the entire length of the field, perpendicular to the gantry rotation, which is an important difference compared to fan-beam CT calibration phantoms. The tested phantoms present a cost-efficient alternative to commercial products. Nevertheless, using the density inserts of a commercial system instead of those made from mineral-filled epoxy can provide more accurate information on the density of the insert. The image value-to-density calibration curves were adjusted later on by using CT number information of real patient images. This improves the representation of air and soft tissue CT numbers in particular. An increase in signal increases the SNR and CNR of an image by the square root, which is shown in Section 3.4 on the example of MV CBCT images. However, an increase in signal also increases the dose to the patient, which is of clinical concern. For phantoms that are comparable in size to a human's head and pelvis, an increase in exposure above 5MU for the rFOV, and above 10MU for the eFOV, respectively, shows no relevant increase in CNR that could justify the additional dose to the patient. These MU values are chosen for ERT specific imaging protocols on the MV CBCT system, which is about a factor 2 more than the daily cone-beam CT protocols in use. This is acceptable since the scan is only acquired once. Subsequent CBCT images for patient setup use the usual clinical protocols.

## kV and MV CT-based Dose Calculation

Digital phantoms are generated to separate the effects of image degradation on dose calculation. Figure 3.7 shows that non-uniformity has the most serious effect on degrading dose calculation accuracy. Reduced spacial resolution effects the dose calculation at the beam-facing surface of the phantom and near large tissue density gradients. Nevertheless, compared with image artifacts observed in clinical on-board CT images, dose calculation is feasible within 5% compared to kV CT-based treatment plans. Chapter 4 is a study on the feasibility of MV CBCT-based dose calculation for real phantom and patient images in case of simple ERT treatments. The choice of image protocol - rFOV or eFOV, optimized for head, thorax, or pelvis anatomy - influences the grayscale of the CT image. Consequently, different IVDCs are required based on the image protocol that is used. Dose calculation on other on-board systems, including kV CBCT and MV CT, shows that not every system requires multiple IVDCs. Although each on-board system pro-

vides different imaging protocols, only the Elekta VersaHD kV CBCT and the Siemens Artiste MV CBCT require more than one IVDC for accurate dose calculation across different treatment sites. This increases the calibration and QA work load for those systems. Another difference between the IVDCs of the different systems is that for MV systems, the calibration curves are linear, whereas for kV CT systems, they have a kink at the density of water. The proportional dependence of the photoelectric effect on the atomic number by $\sim Z^3$ explains this phenomenon.

Based on the study presented in Chapter 5, the largest dose differences occur in MV CBCT-based treatment plans. Still, for all on-board systems, local dose differences remain under 5% within soft tissues compared to the same plan calculated based on kV CT images. Local dose differences of more than 5% may occur within or beyond lung tissue. For both MV systems, the lower spatial resolution also causes relative dose differences larger than 5% along the surface of the imaged object. Based on these observations, one recommendation is that areas of relative differences >5% should be avoided when choosing a prescription point. For a dose prescription to a point at mid-plane, the total number of MUs is within the objective of ±5% relative to the kV CT-based plan for all imaging machines and all treatment sites. In the end, this would be the overall difference in the delivered dose for these treatments.

A similar workflow as presented in Chapter 4 has previously been described in the literature in combination with a TomoTherapy linac (Accuray, Sunnyvale, CA) and StatRT (also by Accuray), commercial software specifically developed for TomoTherapy [52]. Additional research for a similar procedure on TomoTherapy exists for the treatment of spine metastases [53–55]. Although StatRT offers advanced capabilities for urgent treatments, it is limited to TomoTherapy. The advantage of the workflow described here is that it is independent of commercial software, such as StatRT. It provides a technically advanced, fast, and safe option for machines using kV CBCT or MV CBCT on-board imaging systems to perform urgent radiation therapy on different treatment sites, thus offering a unique alternative to palliative treatments on TomoTherapy.

## Advantages and Disadvantages of MV and kV CT Systems

The largest advantage of MV imaging systems is that they provide the ability to image high $Z$ materials without suffering from photon starvation, which can cause bright streaking artifacts on CT images due to a lack of signal reaching the detector. These artifacts can degrade image quality severely, making them unsuitable for dose calculation without overriding the image density. Density override is undesired because it takes time to do accurately and also introduces unknown inaccuracies into the image. kV imaging systems, on the other hand, provide a superior image contrast at a much lower imaging dose to the patient. That is due to the photoelectric effect, which is the dominant effect of photon interaction with matter for kV energetic photons, and its proportionality to approximately $Z^3$. While the image contrast is the poorest for MV CBCT images, it is still sufficient to visualize bony anatomy and count the vertebrae of a spine on the image, which is essential in ERT.

Based on these results, each system provides an adequate solution for on-board CT-based dose calculation. In the end, the clinic will utilize whatever system is available for ERT. However, if there is a choice, MV CT imaging will provide the best dose calculation results while providing a sufficiently large FOV. Especially in connection with the StatRT software [56], the MV CT system provides a good solution for a streamlined ERT workflow. At UCSF specifically, the Tomotherapy unit is a machine with high demand for complex treatments and long treatment times. Unless multiple Tomotherapy systems were available, this makes it unsuitable as an emergency treatment machine at UCSF. Furthermore, there remains a lot of room for image quality improvements. As a suggestion, a superior system could be a low-MV CBCT with a limited field width in the Z-direction along the patient's longitudinal axis. Then, two or three scans could be merged to produce a large enough FOV. This would decrease photon scatter, which is the main cause of image non-uniformity, while only moderately increasing scan times. The low-MV energy would provide better image contrast than the MV CT system that uses the 6 MV treatment beam. Still, it would prevent artifacts caused by kV photon interaction with high $Z$ materials. Combining multiple CBCT scans would require as little patient movement as possible in between scans, otherwise image concatenation may be difficult. Thus, a speedy image reconstruction algorithm is necessary to make this clinically feasible. The FOV would ideally be around 31 - 42 $cm^2$ to be large enough to capture the entire

anatomy of most patients, but small enough to limit scatter.

## MV CBCT using the In-Line kView System

The In-Line kView imaging system provides improved image contrast at the same imaging dose compared with the original treatment beam line. Initial adjustments of the MV CBCT on-board imaging system are made to optimize the image reconstruction. Among other small adjustments, the float value, a machine-specific reconstruction parameter, is tuned to assign the CT number of 1024 to the density of water, similar to kV CT imaging. The human body consists primarily of water equivalent tissues. Thus, the adjustment minimizes the overall dose calculation error in case that the wrong IVDC curve was ever applied for dose planning. Furthermore, imaging protocols are created and named to be easily identifiable as ERT protocols. The new In-Line kView imaging system was successfully installed on the Siemens Artiste in 2013. The main benefit of this low-energy beam line is improved image contrast while maintaining the same rate of dose exposure per scan. A detailed analysis of the image quality between the original treatment beam line and the newly installed imaging beam line is presented by Faddegon et al. [57] He and his colleagues demonstrated the increased soft tissue contrast that results from the lower photon energy.

## Evaluation of the Success of the Project

The aim of the dissertation, to develop a new treatment technique for emergency radiotherapy treatments using on-board imaging, has been achieved. Furthermore, it has been clinically implemented for a large number of emergency cases. Based on the initial experience of patient treatments presented in Chapter 6, the new workflow benefits the patients and staff. It reduces the amount of time the patient spends in the department of radiation oncology immensely by optimizing individual patient simulation and treatment planning steps. Nevertheless, additional work is necessary to optimize the clinical routine. Ideally, the time the patient spends inside the treatment room should be reduced to the time of a treatment slot on the machine, which is usually 30 minutes. The ultimate goal is to use the procedure outside of clinical hours and eliminate the need for 2D-based dose calculation, where favorable. This requires the commitment of the radiation oncology

team. On-call radiation therapists must feel comfortable with mastering the tasks without the support of physicists.

Currently, this workflow is limited to simple treatments that in the past were prescribed using 2D dose calculations. Yet, it is possible to also use it for more complex treatments, which require more than two beams per plan and are optimized using intensity modulation. For those plans, the plan QA may be more difficult to perform than the current QA, which is described in Appendix A. IMRT treatments require physical measurements for plan verification. This means that the patient would have to be moved off the table between simulation and treatment, eliminating one large advantage of this treatment procedure. In-vivo dosimetry may present a solution to that problem. A number of companies are currently exploring new ways to perform QA on RT plans using either entrance or exit dosimetry [58, 59]. In cases of non-emergency situations, the workflow may also become beneficial. It could make 3D planning available for clinics that cannot afford a CT scanner in addition to a linear accelerator or the additional workload and staff necessary for 3D treatment planning. For them, on-line imaging, planning, and treatment using on-board CT could become the new standard of radiation therapy.

# Future Projects

The treatment workflow has proven itself to be beneficial for the patients as well as for the physicians and staff. Over the next year, we will continue to work with the physicians and RTTs to improve the procedure in terms of flow with the aim to minimize the time the patient spends on the treatment couch. This is also necessary to limit precious machine time and make the procedure clinically financially efficient. Eventually, the procedure will be extended to spinal cord compression treatments. Once the staff feels confident to perform the workflow on their own, it will go into effect after clinical hours, including on the weekend. However, this requires thorough understanding of the procedure by the on-call RTT. Another question that needs to be answered is whether or not a dosimetrist or physicist would be required to be present or if the therapist and physician would feel comfortable to perform the workflow on their own. Currently, only RTTs and physicians are on-call for weekend emergencies, which limits the dose planning capabilities in those situations.

We plan to expand this workflow to other linear accelerators. An expan-

sion to systems made by major linac vendors would increase the platform for clinical implementation. This involves several technical challenges. Dose planning must be optimized for modalities other than MV CBCT imaging, as suggested in Chapter 5. The linac systems must be set up in a way that can integrate the workflow. The first implementation of this ERT procedure was for the Siemens Artiste, with the Pinnacle treatment planning system by Philips Healthcare (Andover, MA), and the Mosaiq record-and-verify system by Elekta (Crawley, UK). This implementation required many workarounds to connect each of the different vendor systems. Thus, the need for new workarounds would certainly be expected for linacs by other vendors.

Furthermore, this workflow may become an important treatment approach in clinics and departments that do not have the necessary resources for standard CT simulation and planning. In particular, developing countries could adopt this workflow and hugely benefit from 3D dose calculation. Over the past years, the main linac vendors Varian (Palo Alto, CA) and Elekta (Crawley, UK) have shown an increasing interest in low-MV on-board imaging. In Spring 2015, Varian unveiled their new product named VitalBeam™, designed specifically for cost-efficient advanced radiotherapy [60].

# CHAPTER 8

## Conclusion

A new and complete workflow for the treatment of emergency radiation therapy was developed and implemented within the framework of this dissertation. An important part of this work is the reliable dose calculation based on kV and MV on-board CT images. Several phantoms and patient on-board images were used for dose calculation of different treatment sites. The research shows that image quality is sufficient and consistent in almost all cases with dose calculation errors of <5% compared to standard kV CT-based planning. Treatments on anatomic sites such as a head and extremities are calculated most accurately for all systems. Lung tissue and air cavities may result in local dose calculation inaccuracies larger than 5%. This must be considered especially for treatments close to the spinal cord.

The main advantage of kV systems over MV systems is the superior image contrast of soft tissues at a comparably low dose to the patient. MV systems, on the other hand, provide better image quality when metal or other materials of high atomic numbers are within the field of view. Generally, fan beam CT images are preferred for treatment planning because of the reduced scatter contribution to the image, which degrades image quality. Thus, the Tomotherapy MV CT on-board system provided the most suitable conditions for accurate dose calculation. However, when good image contrast and a low dose are important, the TrueBeam kV CBCT on-board system offers a good alternative in terms of dose calculation accuracy.

The total amount of time spent on simulation, planning, and treatment is

reduced by several hours compared to previous ERT treatments. Instead of kV portal images, on-board imaging is used for patient simulation, enabling 3D information on the patient's anatomy and 3D dose planning. This makes a 3D dose distribution available to the physicians for review, which helps to protect critical structures near the targeted treatment site and minimizes post-treatment complications. Additional staff experience is expected to further decrease the time spent between patient simulation and treatment. Currently, the field of view of some on-board systems remains a technical limitation for some treatment cases. Additionally, the suitability of a specific on-board imaging system for the workflow depends also on the integrity of the software in use. Some software requires additional work to enable a smooth connection to send data between different systems. Scripting within the treatment planning software is a necessary tool to streamline the planning process, which saves valuable time. Overall, the commitment of the radiation oncology team is essential to the success of this procedure.

Besides emergency cases, this ERT procedure opens up 3D-image-based treatments for other simple radiotherapy patients. The workflow can potentially become an important treatment alternative to clinics that cannot afford CT simulation due to cost, space, or staff limitations.

In conclusion, a new procedure has been developed from its basic idea through clinical qualification to the full implementation as a standard clinical procedure for ERT treatments. An oral presentation of this work was given in Århus, Denmark at the EPI2K14 (Electronic Patient Imaging 2014) conference in September 2014 and in Anaheim at the AAPM annual meeting in August 2015. Posters on this topic were presented at the AAPM meetings in 2013 and 2014 in Indianapolis, IN and Austin, TX, respectively, as well as at the ASTRO (American Society for Radiation Oncology) annual meeting 2014 in San Francisco.

# APPENDIX A

## Quality Assurance and Safety Procedures

The ERT workflow presented previously aims to provide patient care within a short period of time. The planning process is optimized to require as little time and as few steps as possible. Overall patient safety remains the most important requirement. This is particularly crucial when using automated scripting for treatment planning. There are two requirements for patient safety: 1) the dose delivered to the patient is within non-lethal limits and 2) the treatment is delivered according to the treatment plan. The first one is a gross check of the total MU delivered. The second one is a detailed verification of every treatment parameter, also called "second check".

## Workflow Safety Procedures

The three main concerns, all of which may be deadly for the patient if applied incorrectly, are

- patient-machine collision,
- incorrect patient alignment, and
- a lethal amount of dose.

To avoid any of these occurrences, the necessary safety steps before every treatment involve:

- A dry run from within the room to ensure that the gantry can be rotated around the patient without collision.
- Patient ID verification and anatomical treatment site verification before patient setup.
- MU check before the beginning of treatment.

These controls are in place to avoid situations dangerous to the patient. In addition, we implemented frequent checkpoints within the procedure for the radiation therapist, physicist, dosimetrist, and physician involved to ensure a safe and accurate treatment delivery. These were identified during test runs that were performed with three different teams of radiation therapists. A detailed workflow procedure was written for the three most common tretment sites. It is included in the Appendices B, D, and D. Any questions that came up during the test runs were added to the procedure.

Emergency treatments occur on short notice, leading to rushed treatments. Even a streamlined workflow cannot prevent every human error. Thus, a certain amount of redundancy is maintained to catch any errors before treatment delivery. To raise awareness of possible sources for errors, Table A lists actions and associated risks during simulation, planning, and before dose delivery, providing possible consequences and methods to avoid errors.

| **Action** | **Risk** | **Error/Solution** |
|---|---|---|
| *Simulation* | | |
| Setup Patient | Treatment target not at isocenter | Treatment area may be outside of the radiation field size.<br>⇒ Re-position patient and re-acquire simulation. |
| In case of heterotopic bone RT: Measuring the patient thickness | Not measured at central axis | Wrong treatment depth, causing treatment target underdosage (when assuming smaller separation) or overdosage (when assuming larger separation).<br>⇒ Re-measure patient separation at central axis. |

| Action | Risk | Error/Solution |
|---|---|---|
| 3D simulation | Using the wrong simulation protocol | Possible errors include<br>– insufficient image quality.<br>– unnecessary dose exposure.<br>– insufficient FOV.<br>⇒ Re-acquire simulation if necessary. |
| *Planning* | | |
| Loading the patient CT | Choosing the wrong HU calibration protocol | Possible errors include<br>– over- or under-dosing treatment target.<br>– inaccurate overall dose calculation.<br>⇒ Change HU calibration protocol in TPS and re-calculate dose. |
| Defining the treatment target | Not identifying the tumor sufficiently | Insufficient target coverage or unnecessary irradiation of healthy tissue.<br>⇒ Delete treatment beams, adjust the treatment target ROI and re-run scripts to set beams and re-compute the dose distribution. |
| *Before Treatment* | | |
| MU calculation | Calculated MUs from TPS and RadCalc™ disagree by >5% | Incorrect MU delivery for desired dose.<br>⇒ Review the IVDC applied during planning and the treatment plan for possible errors. |

**Table A.1:** A list of workflow actions and their associated risks, which could potentially lead to erroneous treatments. The arrow indicates possible solutions to correct the error.

## Whole Brain MU Verification

The variation in the lateral width of a person's head is relatively small between different people. Since the dose calculation is highly dependent on the anatomic separation, a guidance for the expected amount of MU is given based on data of previous whole brain treatments. Therefore, the head sepa-

ration is measured on 15 patient CTs at treatment isocenter. The delivered MUs of the treatment are divided by the prescribed dose in cGy and the quotient is plotted versus the head separation. Figure A.1 shows the results. A similar approach could be used to verify the range of MUs for other treatment sites as well. However, it is important to note that this is only recommended as an additional fast and easy safety check but does not replace any of the other QA.

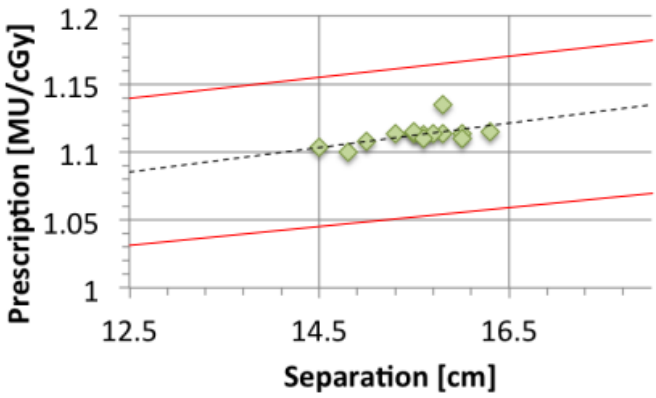


**Figure A.1:** The MU per cGy versus the measured patient separation can be used as a guide for correct dose calculation in case of whole brain radiotherapy. The dotted line is the linear fit ($R^2 = 0.32$) and the red solid lines indicate $\pm 5\%$ of that.

## Discussion of ERT Safety Procedures

Two main requirements for safety are included in the ERT workflow procedure, both of which aim to prevent treatment errors before the first treatment delivery. Another option that was discussed in connection with the workflow procedure are in-vivo QA devices, which record the dose during treatment. The measurement is then, after the first treatment, compared to the treatment plan to verify correct dose delivery. For now, the second check and RadCalc™ MU calculation provides a sufficient level of safety. However, in the future additional in-vivo dose verification may be included. This would add another level of QA, in particular for fractionated treatments. Should a treatment plan be delivered incorrectly, the in-vivo QA device would catch those errors and prevent further harm.

# APPENDIX B

## Clinical Procedure for Whole Brain ERT

The procedure has been written into a clinical protocol with detailed description of every step. Screenshots are included to describe important supplementary details visually. This procedure was printed and placed on the shelf above the treatment console for everyone to consult, should difficulties arise. The document is included below as attachments B - D.

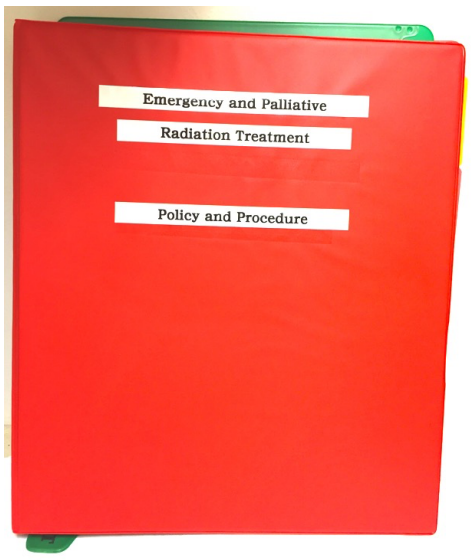


**Figure B.1:** The red binder containing the written clinical procedure for emergency radiotherapy at UCSF.

# Emergency and Palliative Radiation Treatment

## Policy and Procedure

University of California San Francisco
Department of Radiation Oncology
Long Hospital Room L43

Olivier Morin, PhD
Mareike Held, MSc
Version 1.0
Last revised: Jan 23, 2015






## Table of Contents

## History of the document

| Author(s) | Date | Version | Modifications |
|---|---|---|---|
| Olivier Morin, PhD<br>Mareike Held, MSc | 12/07/2014 | 1.0 | Original document with details for WBRT, AP/PA and heterotopic bone. |
| Olivier Morin, PhD<br>Mareike Held, MSc | 07/02/2015 | 1.1 | Included 'print pdf' and more detailed comments where necessary. |

## Purpose

The UCSF Medical Center and the Radiation Oncology Department are committed to providing outstanding care for patients receiving emergency and palliative treatments. This document outlines the procedure for preparing, delivering and documenting an emergency patient treatment.

## Definition

1. Emergency treatment – urgent radiation treatment delivered without sufficient time to perform CT simulation and/or radiation due to be delivered outside of treatment hours
2. Palliative treatment – simple treatment plan of usually ≤2 beams with the intend to minimize pain or other complications
3. MU – Monitor Unit
4. AP/PA treatment – treatment consisting of two beams with anterior-posterior and posterior-anterior placement
5. WBRT – whole brain radiotherapy
6. 2D approach – DRR/film based planning with simple MU calculation based on patient separation
7. 3D approach – volumetric dose calculation





## Overview of the process

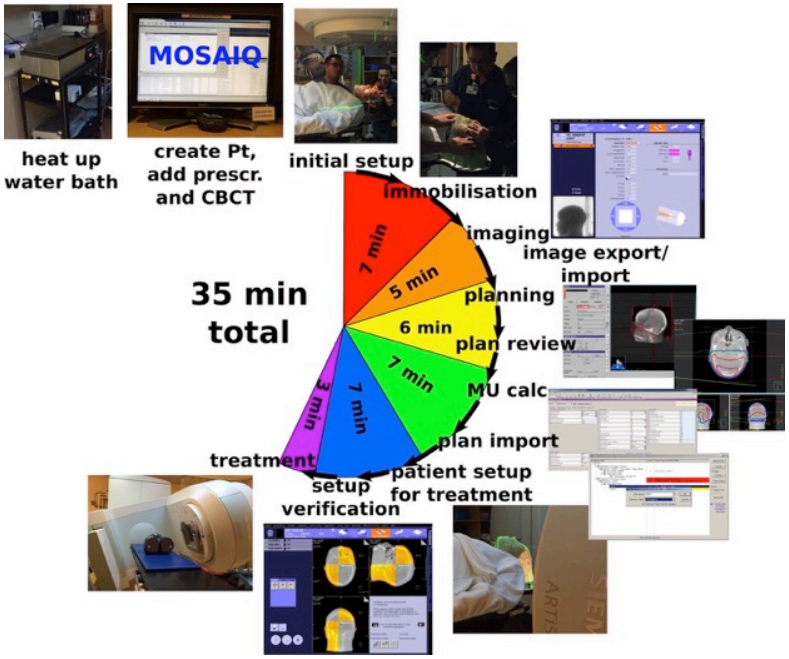


Overview of the emergency and palliative radiation treatment procedure.

**For 2D approach:**

**A. Prepare prescription**

- In MOSAIQ, create a new patient if necessary.
- Have the doctor add & affirm a diagnosis and add & approve a prescription.
- Add & approve a site setup.

**B. Setup patient**

- Measure the patient separation at the treatment area.
- Setup the patient with the center of the target as close to the machine isocenter as possible.
- Adjust the table position, field size, gantry and collimator angle using the light field.

- Use the red laser distance measurement to verify the SSD (SSD = 100 – patient thickness / 2).

**C. Add treatment field**

- Add a treatment field based on the machine parameters.
- Fill in field name and ID, tolerance, type (static), modality, energy, 1MU, dose rate, dose (prescription dose divided by number of beams).
- Choose Portal Image planned: 1 MU, open: 1 MU.
- Approve the field and add to the dosimetry record by clicking on *Dosimetry*.
- Schedule the field using Only:Plan – Open portal imaging.

**D. Image**

- Acquire PI with 1.0 UF as imaging segment energy.
- Adjust the treatment field and re-image until the correct field is reached.
- Save image as a reference image and mark the patient.

**E. Verify plan**

- After the physician accepts the field, perform an MU check:
- In Pinnacle, add the patient to the Emergency_V9.8 institution and manually enter the field parameters.
- Print the plan for review.
- In RadCalc, add the patient, enter the field parameters and the MUs calculated in Pinnacle.
- Print the RadCalc comparison to pdf in the eSCAN folder (MOSAIQ).
- Compare the MU from Pinnacle and RadCalc. The difference should be less than 5%. If not, review HU to density calibration and treatment plan parameters.

**F. Prepare for treatment**

- Adjust the MU in the treatment field.
- Copy and oppose the treatment field.
- Create the dose coefficient by clicking on *Dosimetry*.
- Schedule the fields and add a pre-treatment check if necessary.

**G. Treat**

**For 3D approach:**

**A. Prepare prescription**

- In MOSAIQ, create a new patient if necessary.
- Have the doctor add & affirm a diagnosis and add & approve a prescription.
- Add & approve a site setup.
- Create a treatment field of type “MVCT” with a longitudinal couch position of 50. Approve the field.
- Click on *Dosimetry* to add the field to the record.
- Schedule the treatment field to be ready for patient imaging.

**B. Setup patient**





- Setup the patient with the center of the treatment target as close to the machine isocenter as possible. The machine isocenter will be the imaging isocenter and the beam isocenter.

**C. Image**

- Acquire an MV CBCT using one of the ERT imaging protocols based on the treatment site.
- Export the cone beam CT from the patient browser to Pinnacle.

**D. Plan**

- Use a remote Pinnacle log in to plan the treatment.
- Choose the Emergency_V9.8 Institution.
- Add a new patient and import the images from the patient directory.
- Add a new patient plan.
- Adjust the couch position and use scripts to plan the treatment.

**E. Verify plan**

- After the physician accepts the plan, export it to RadCalc for an MU check.
- Print the plan from RadCalc to pdf in the eSCAN folder (MOSAIQ) (and from Pinnacle for review if necessary).

**F. Export/Import Plan**

- Export the plan from Pinnacle.
- Import the plan into MOSAIQ.
- Verify the treatment field parameters.
- Approve the Site Setup and treatment field.
- Add fields to the dosimetry record by clicking *Dosimetry*.
- Schedule the treatment field for delivery.
- Send reference data if necessary.

**G. Verify Setup**

- Verify the correct patient position using portal images or a low-MU CBCT.

**H. Treat**

# WBRT

| | |
|---|---|
| **1. Select or create Patient in MOSAIQ**<br><br>Click on “Select Patient” in the upper right corner. Choose “Add” on the ‘Select Patient Window’ if the patient isn’t already in MOSAIQ. | 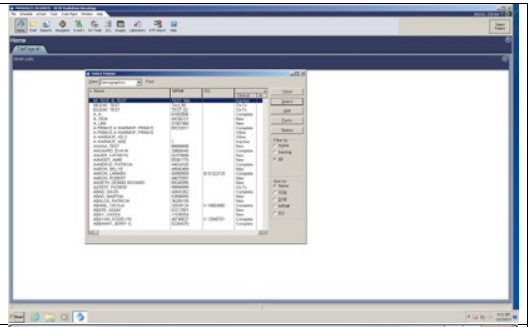 |
| Fill in the Demographics marked in red:<br><br>Last Name<br>First Name<br>MRN#<br>Birth Date<br>Gender | 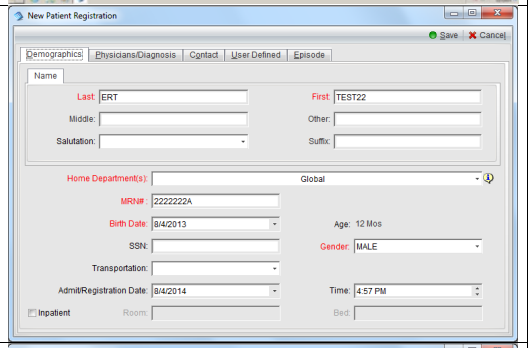 |
| On the next tab, fill in the Physician’s Diagnosis marked in red:<br><br>Attending Physician Category<br><br>Click “Save” on the upper right. | 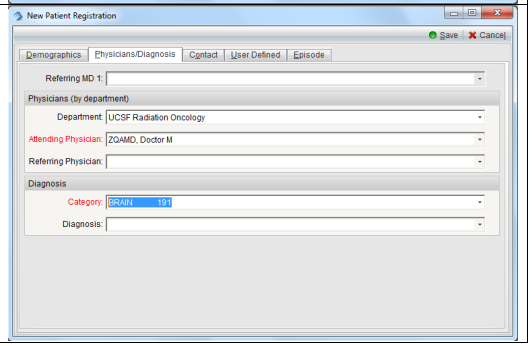 |





| | |
|---|---|
| Click “No”. | 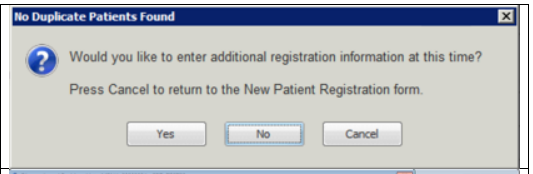 |
| **2. Add Diagnosis, Care Plan, Rad Rx, Site Setup, Tx Field**<br>Choose the “D&I” tab from the toolbar<br>  <br><br>or open it through eChart I Diagnosis and Interventions.<br><br>**The MD will do the part in gray:**<br>On the right hand side, click on “Diagnosis”.<br>Click on “Change” in the ‘Diagnosis and Problem List Window’.<br><br>Enter the diagnosis and click on “Save and Affirm”.<br><br>Then “Close”. | 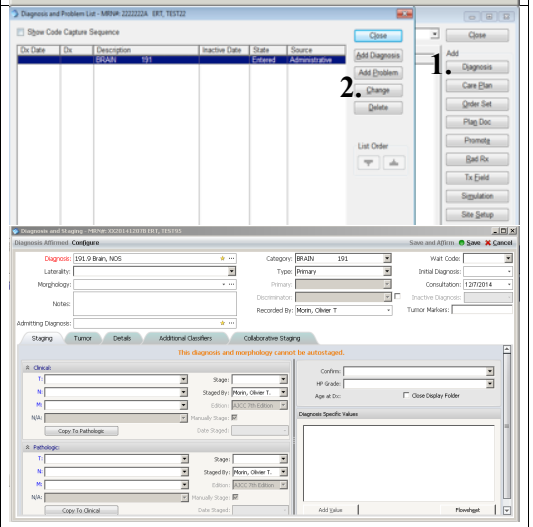 |

| | |
|---|---|
| Create a treatment course by clicking on “Care Plan”. | 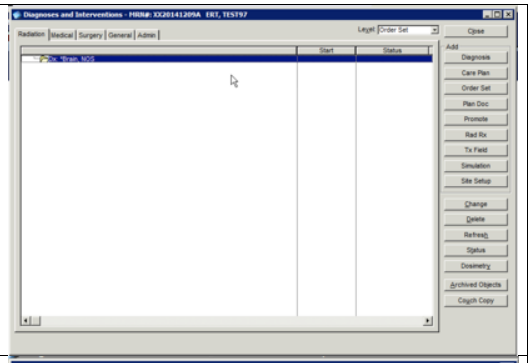 |
| Confirm with “Ok”. | 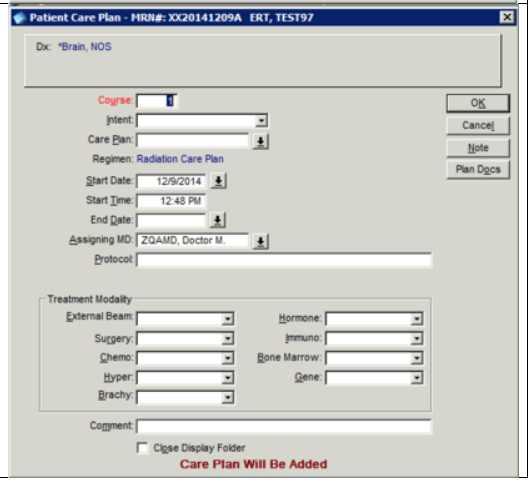 |





| | |
|---|---|
| On the ‘Diagnosis and Intervention List’, click on “Rad Rx” and this window opens up.<br><br>Fill in the prescription for the treatment.<br>Example:<br>Rx Site: WBRT<br>Technique: Opposed Laterals<br>Modality: 6 MV Phot<br>Dose Spec: MID-PLANE, 100%<br>Rx Dose 3000 cGy<br>Fractional Dose 300 cGy<br><br>Click on the drop down error under ‘Fractionation Pattern’ | 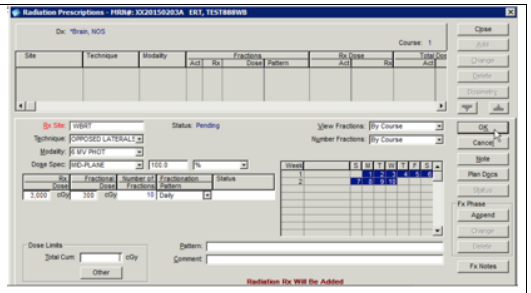 |
| If treatment is on the weekend or over the holidays, include ‘Saturday’, ‘Sunday’, or ‘Holidays’ on the bottom by clicking the according check mark.<br><br>Confirm this Setup Form with “OK”. | 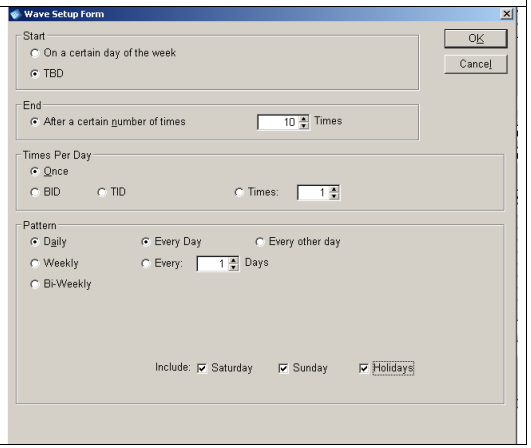 |

| | |
|---|---|
| Right click inside the Radiation Prescription window, choose ‘Status’ and approve the prescription. | 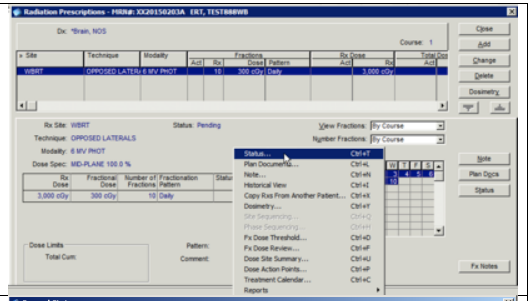 |
| Check “Approved”, sign with your password and close the window using “OK”. | 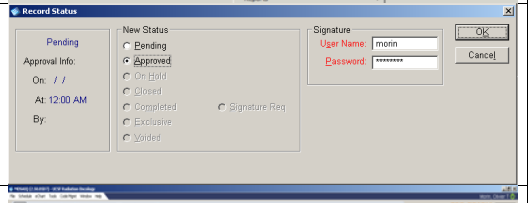 |
| In the ‘Diagnoses and Interventions’ window, click on “Site Setup” and this window opens up.<br><br>Fill in the fields in red:<br>Patient Orientation<br>Machine<br>Tolerance<br><br>Right-click into the window to approve the Site Setup. | 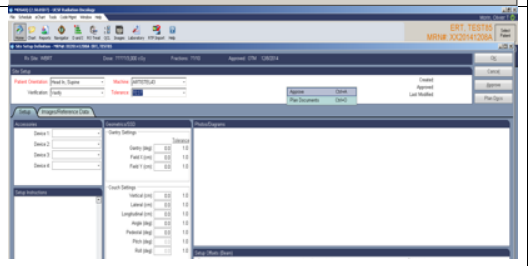 |
| In the ‘Diagnoses and Interventions’ window, click on “Tx Field” and this window opens up. Select “ARTISTEL43”. | 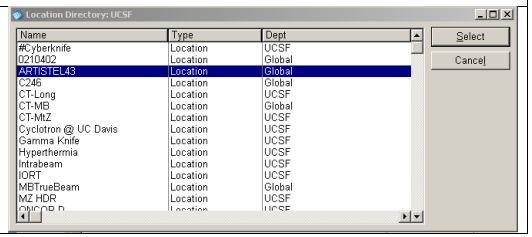 |





| | |
|---|---|
| Fill in the red fields:<br><br>Field: E900 planCBCT<br>Tolerance: Emergency<br>Type: MVCT<br><br>Also fill in:<br>Monitor Units: 5<br>Couch Longitudinal: 50.0<br><br>Right-click into the window to approve. | 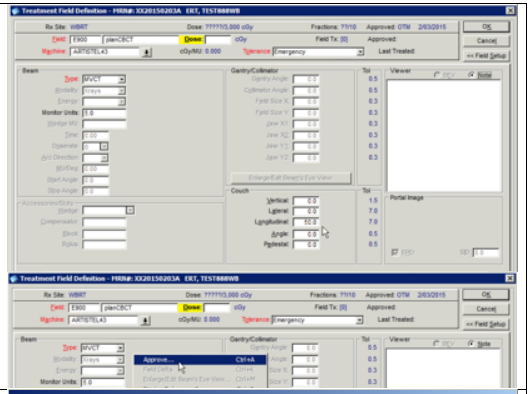 |
| Confirm the warning window with “Yes”.<br><br>Enter password to approve the field. Exit window with “OK”. | 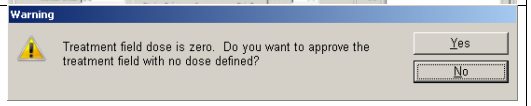 |
| In the ‘Diagnoses and Interventions’ window, click on “Dosimetry” and this window opens up.<br><br>Confirm with “OK”.<br><br>Close the next window. | 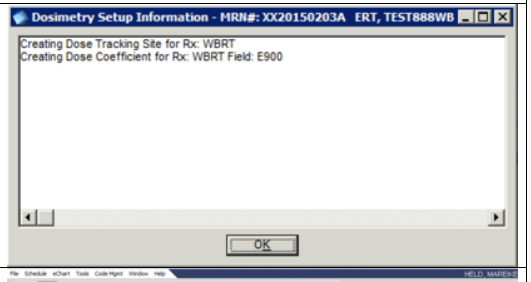 |
| **3. Schedule MV CBCT**<br>In the main tabs on top, choose “RO Treat”.<br><br>Click on “Tx Calendar”. | 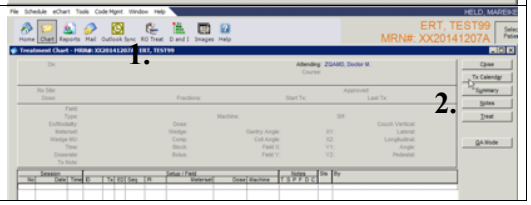 |

| | |
|---|---|
| Click on “Add” on the right side. | 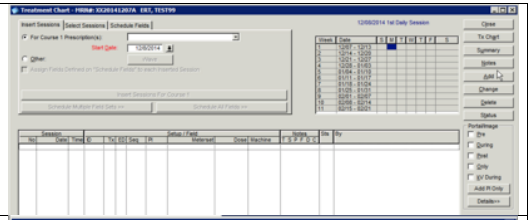 |
| Click on the arrow (1.) to open the calendar. Choose ‘Today’ and confirm with “OK”.<br><br>Then, click on “Define” (2.) | 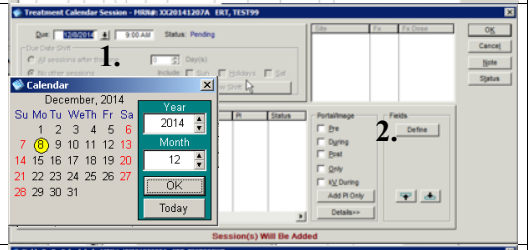 |
| Highlight the field E900 – planCBCT – MVCT on the left and add it to the right side.<br>Confirm with “OK”, and the next window with “OK”. |  |
| Then click “Tx Chart” in the ‘Treatment Chart Window’.<br><br>This brings you back to the original RO Treat window.<br><br>At this point, the CBCT is ready to be delivered on the machine. The patient can be brought into the room at this point.<br><br>Click on “Treat”. | 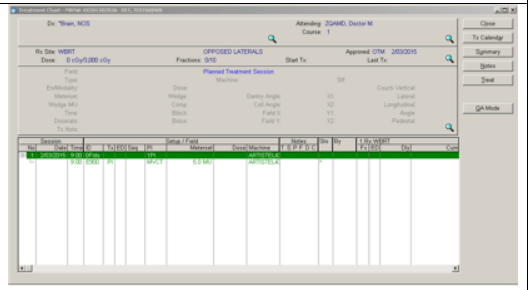 |





| | |
|---|---|
| Click “Continue” in this window.<br><br>Make sure that the Syngo computer is logged in and ready to receive the treatment field. | 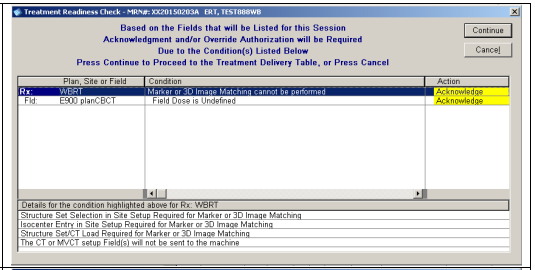 |
| Hit “Send Plan” to send the field to Syngo. | 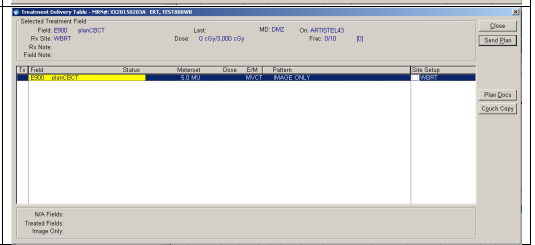 |
| Acknowledge the conditions in this window and “Continue”. | 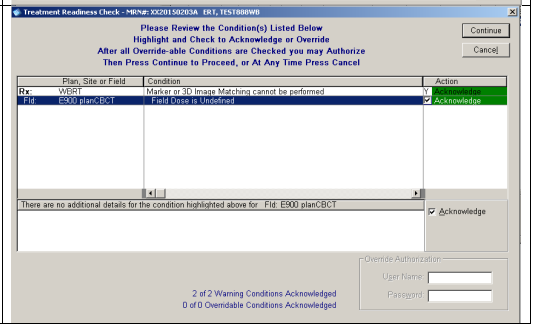 |

| | |
|---|---|
| Cancel this screen and confirm with “Yes”.<br><br>MOSAIQ is now sending the field to Syngo. | 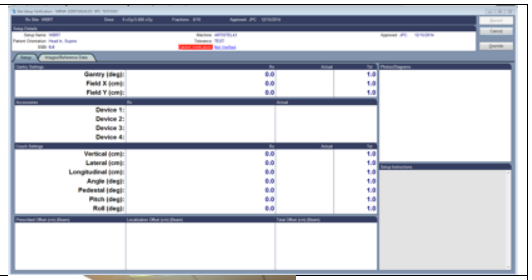 |
| **4. Setup patient**<br>Set up the patient as you expect they will be positioned during treatment.<br><br>Prepare a patient immobilization mask if necessary. |  |
| **5. Acquire MV CBCT**<br>On the Syngo computer, confirm to receive the treatment field with “OK”.<br><br>Click on the chart symbol at the bottom to select an imaging protocol.  | 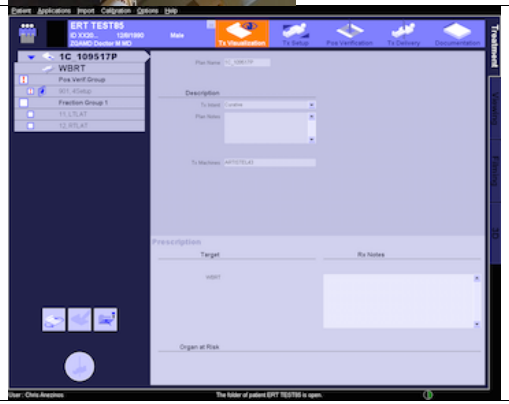 |





| | |
|---|---|
| Right mouse click on to the treatment field and choose “Imaging Options”. |  |
| Choose the imaging protocol from the drop down menu, in this case ERT_Head_5MU_256.<br><br>Choosing this imaging protocol is important for the correct dose calculation in the TPS.<br><br>The patient size is defaulted to Medium. Keep this setting.<br><br>Click ‘OK’ and  on the bottom left to confirm selection. |  |

Check the box next to Pos.Verif.Group and click the round treatment button on the bottom.

On the treatment console, use F12 to adjust the gantry and MV flat panel position.

Double-click Accept. If necessary, override Longitudinal and Vertical table positions.
Wait for the machine to turn to a green ready light, turn the right key and hit RAD-ON.

The bottom left shows the projection image of the patient during CBCT acquisiton.

The cone beam uses 5 MU and a clock-wise gantry rotation from 270° to 110°.





Wait until the image acquisition is completed and the images are loaded in Syngo.

Confirm this warning with “OK” and abort treatment on the X at the bottom.

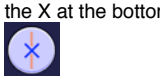

**6. Export images to Pinnacle**

To export the images, open the patient browser by clicking on the “3 people symbol” in the top left corner.

Find the Patient in the Local Database and highlight the latest Cone Beam CT.

Only choose “Cone Beam CT”. Do **NOT** export any of the other fields.

In the toolbar on top, find “Transfer”, “Send to…”

| | |
|---|---|
| Choose ‘Pinnacle’ from the list and click “Send”.<br><br>You can now close the patient in Syngo. Save changes before the unload. | 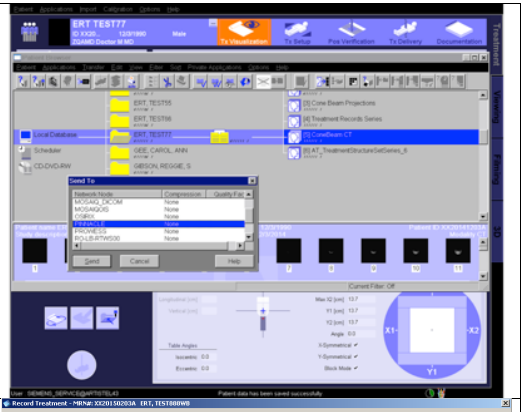 |
| On the MOSAIQ computer, record the delivered field by clicking on “Record”. | 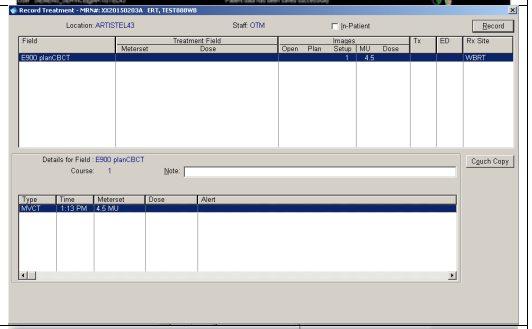 |
| Confirm to exit the dose delivery. | 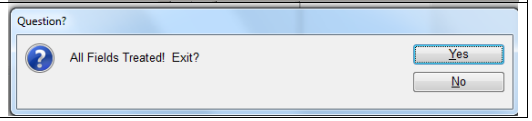 |







| | |
|---|---|
| **7. Treatment planning**<br>On the MOSAIQ CLIENT/DAILY QA computer:<br>Start up Oracle Virtual Desktop Client from the Desktop.<br>Log in to Pinnacle and click on the triangle icon to get to the home screen. | 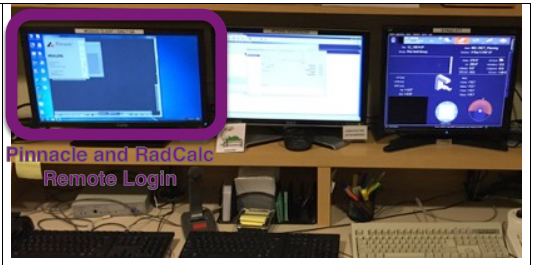 <br> 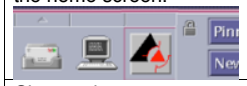 |
| Choose the Emergency_V9.8 Institution by clicking on “Institutions”.<br><br>  <br><br>Close window with “Dismiss”. | 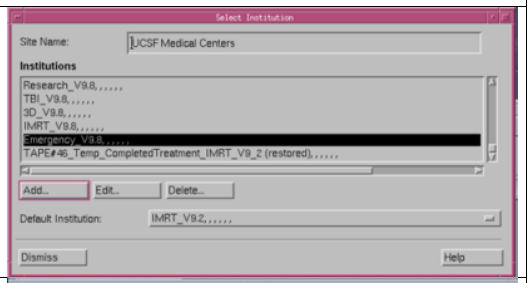 |
| Go to Planning.<br><br>  <br><br>Add a patient by clicking on the “Add” button under ‘Patients’. | 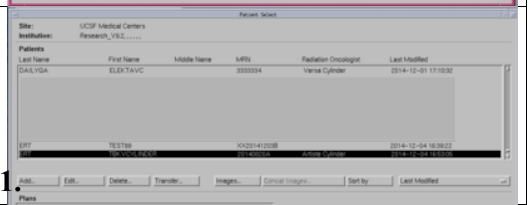 |
| Click on “Import Images”. | 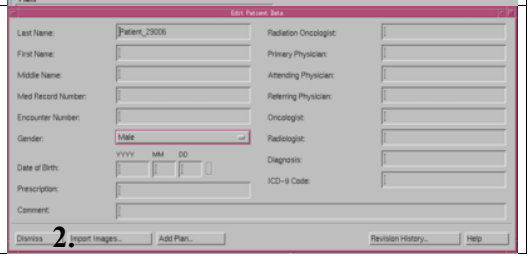 |

| | |
|---|---|
| Click “Add”.<br><br>Be patient, it might take a moment for the image library to pop up. | 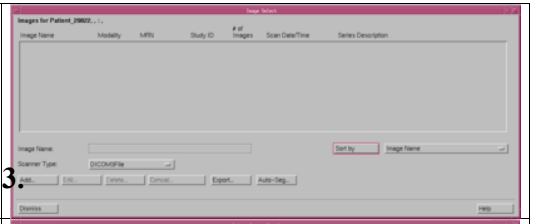 <br>3. |
| Select the Patient and check the box next to the image set to import.<br><br>At the bottom, click “Import Images and Add Plan”. | 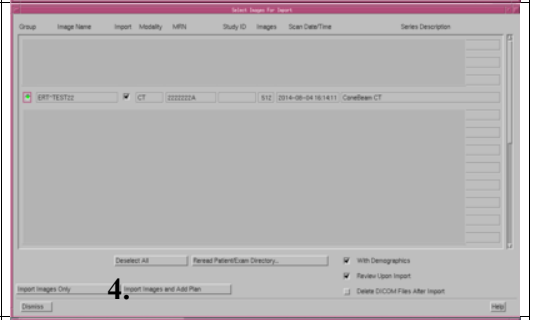 <br>4. |
| Click on “Save and Exit” on the bottom left. | 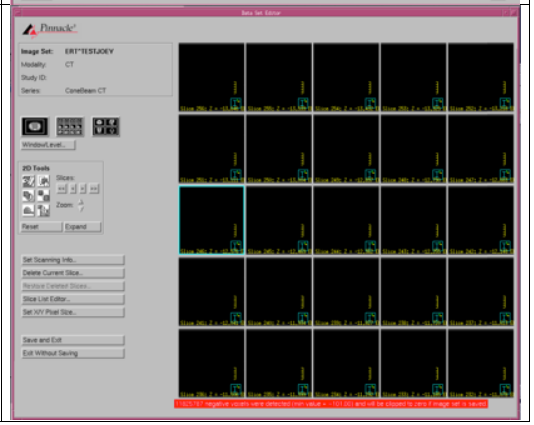 |





| | |
|---|---|
| Change the Plan Name to ‘WBRT’.<br><br>Under ‘Primary Image Set’, choose the CBCT image from the drop down menu.<br><br>Click “Planning” at the bottom. | 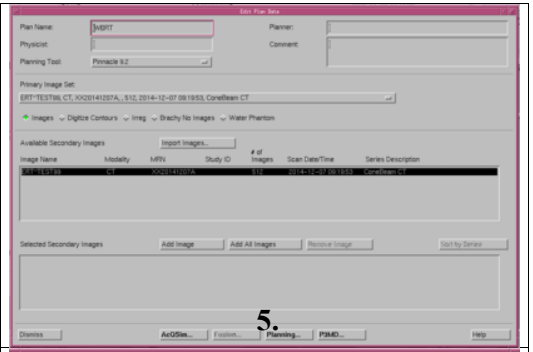 <br>5. |
| Choose the ‘CT-Density Table’ corresponding to the imaging protocol that was used during the CBCT imaging.<br><br>For WBRT, that would be Artiste rFOV Head.<br><br>“Accept” at the bottom. |  |

| | |
|---|---|
| Change selection under ‘Remove couch from scan’ to “Yes”.<br><br>Click on the little icon next to ‘Location’<br>  <br>and place the couch (red line) below the posterior end of the patient. | 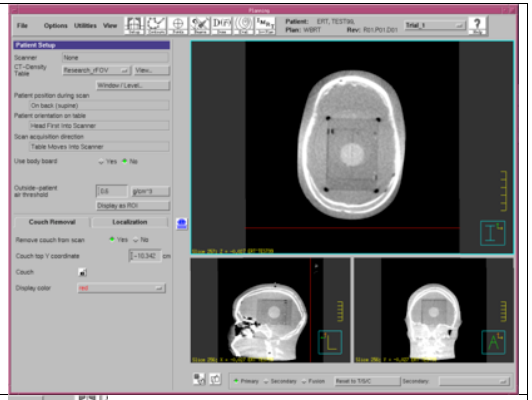 |
| At the top, under ‘Utilities’, choose ‘Scripting’. | 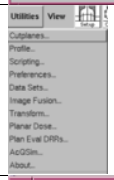 |
| Click on the HotScript “ERT_WB_ONE” *1)<br><br>For detailed info on what happens within the script, refer to **Note1** at the end of this procedure.<br><br>The script places necessary points, LTLAT beam, changes the prescription, and jumps into BEV. | 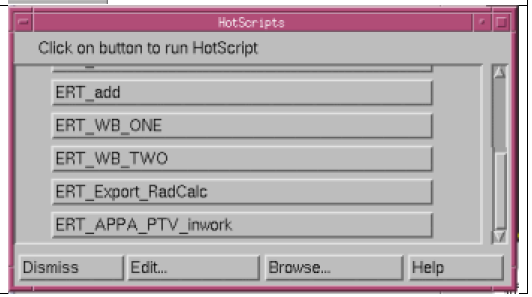 |





| | |
|---|---|
| *1)<br>If the script is not on your HotScripts list, click on “Browse”. Enter the directory<br><br>/home/heldma/Scripts<br><br>Select the script on the left hand side and click on “OK” at the bottom.<br><br>Wait for the script to run. | 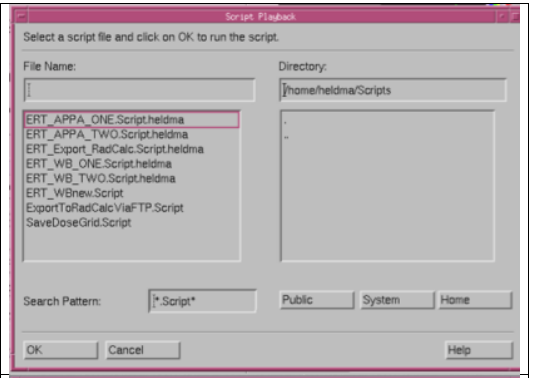 |
| At this point, the system is ready to draw the block.<br><br>**NOTE:** You can use a right mouse click onto the image to choose to zoom in.<br> 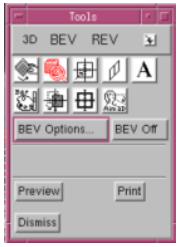 | 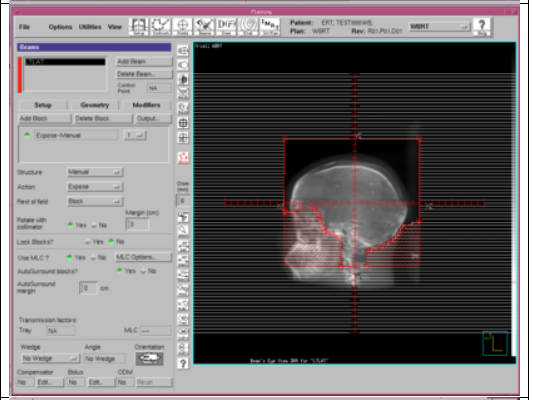 |
| Once ready, run the second script ERT_WB_TWO.<br><br>Again, use the browse button if the script is not on the HotScripts list.<br><br>For detailed info on what happens during this script, refer to **Note2** at the end of this procedure. | 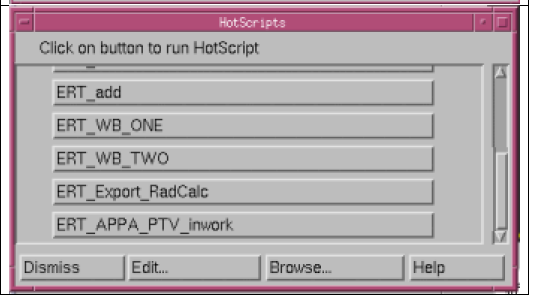 |

| | |
|---|---|
| The script uses Copy & Oppose for beam RTLAT, adjusts the beam weighting to 50/50, and computes the dose for both beams.<br>**Isodose lines** are absolute values of 3200 (red), 3000 (yellow), 2800 (green), 2400 (blue).<br><br>It opens the 'Eval' tab and shows the prescription, MU, and beam weighting window.<br><br>The default prescription is set to 300 cGy per fraction to 100% of point dose at "MdPlane_CalcPt" for 10 fractions. | 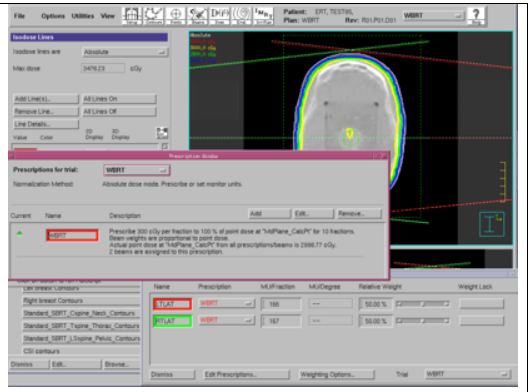 |
| Verify the prescription, beam weighting, dose distribution and MU per beam.<br><br>**NOTE: If the patient has already received <u>emergency radiation treatment</u> before, make sure that the field ID E11 and E12 are unique. MOSAIQ does not allow to import beams with the same field ID.**<br><br>Change the Field ID if necessary (check in MOSAIQ) to unique IDs under the beam tab.<br>  <br>Do so for both LTLAT and RTLAT beams. | 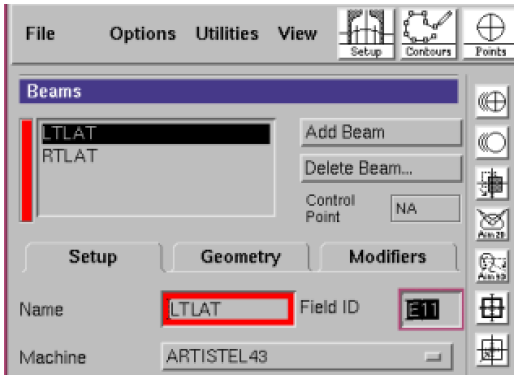 |





| | |
|---|---|
| Suggestion: E21 and E22 | |
| Once the plan is ready for second dose check and export, use a script to export the plan to RadCalc.<br><br>Under 'Utilities', 'Scripting', choose 'ERT_Export_RadCalc' or use the 'Browse' button to call the script.<br><br>It chooses the MdPlane_CalcPt as the reference point. | 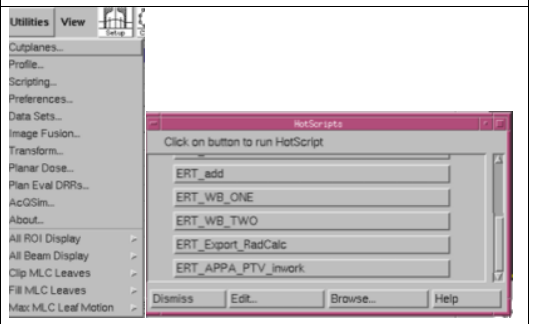 |
| Minimize the Pinnacle window for now. | |
| **8. MU verification**<br>Open RadCalc using the RadCalc Shortcut on the Desktop.<br> 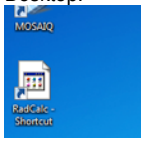 <br>Confirm the security warning with "Run". | 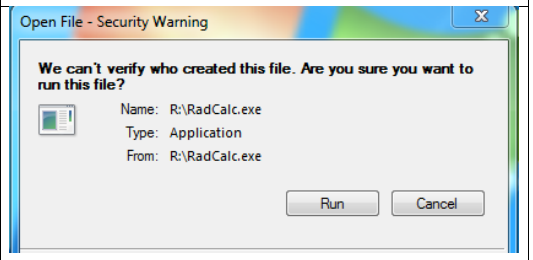 |
| Log in to RadCalc with your username and password.<br><br>Click on "Import" to import the patient plan.<br>  | 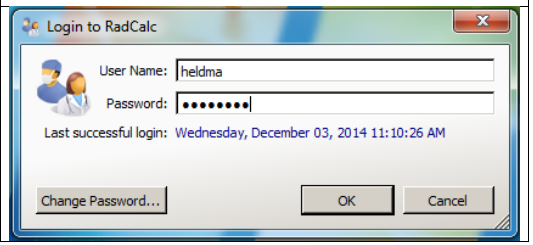 |

| | |
|---|---|
| Select patient and click on “Import Selected” at the bottom. | 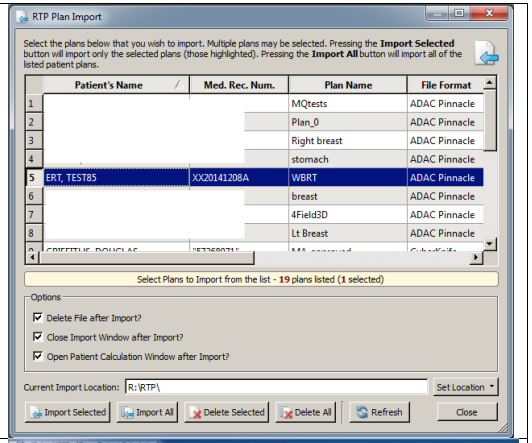 |
| Double-click on the plan to open. | 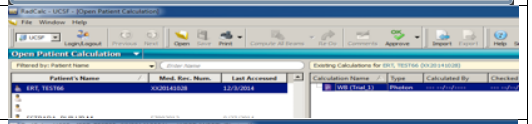 |
| The first window summarizes the prescription.<br><br>Prescription Isodose and Scatter Dose are not required. | 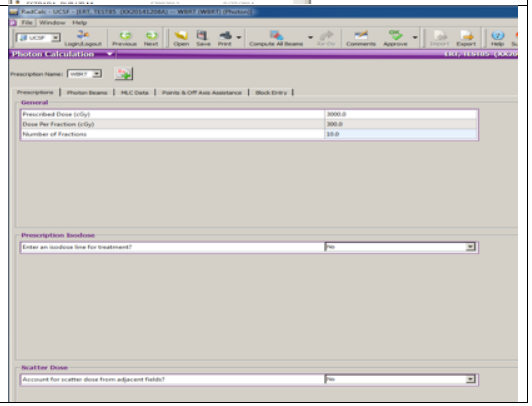 |





| | |
|---|---|
| Open the second tab ‘Photon Beams’.<br><br>Verify that all the information is correct. Under Beam Setup, ‘Calc Pt’ should be set to ‘MdPlane_CalcPt’.<br><br>In the yellow window in the upper right corner are the MUs calculated for this beam by RadCalc, by Pinnacle, and %Diff. | 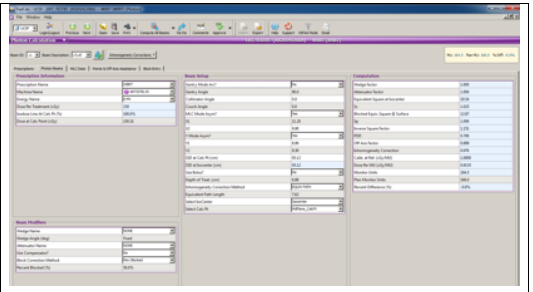 |
| Under ‘Beam Description’, choose the second beam “RTLAT” from the drop down menu and verify the same way as the first beam.<br><br>The %Diff should be less than 5% for both beams.<br><br>(In case %Diff > 5%, change the placement of the point in Pinnacle away from sharp dose gradients and export to RadCalc again.) | 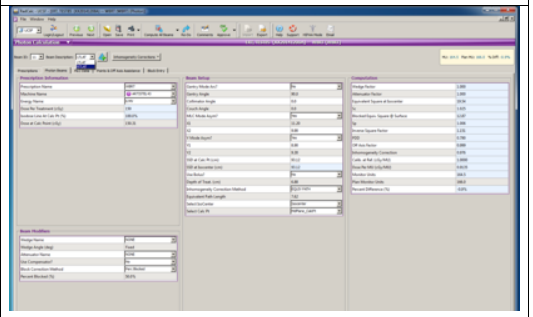 |
| Print the RadCalc check. Under File → Print → Print… | 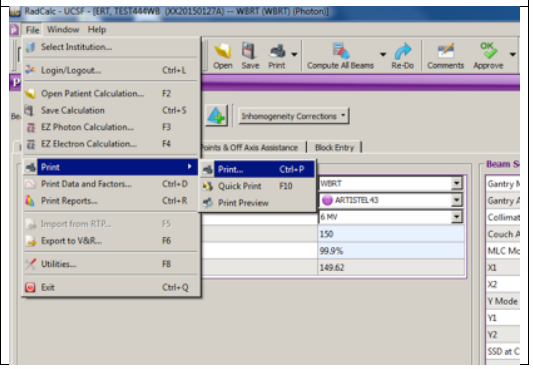 |

This window opens up:

Click the check box at the bottom: ☑Print to file

The path is: \\mosaiqapp\ MOSAIQ_APP\ UCSF_APP\ESCAN

Close RadCalc and maximize the Pinnacle Virtual Desktop Window again.

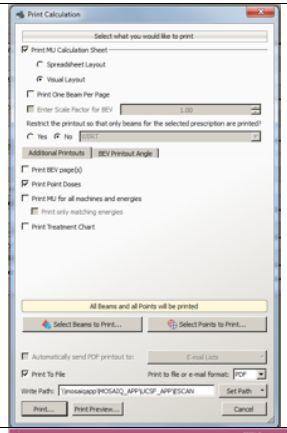

**9.A Export plan from Pinnacle to MOSAIQ**

The 'ERT_Export_RadCalc' script also prepares the export to MOSAIQ and automatically checks the following checkboxes for export:
RT Plans
Prescription WBRT
RT Structures
RT Images
DICOM Image

Destination AE Title: IMPAC_DCM_SCP

Click on "Transmit Data" and wait until finished.

Transmit Data

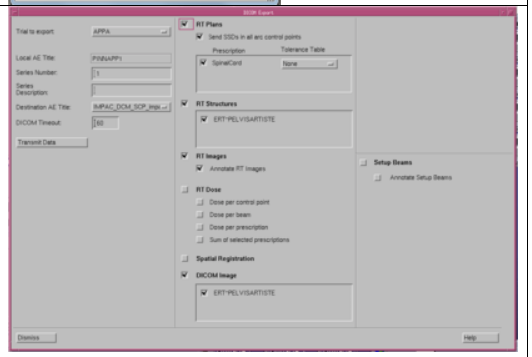

Click "OK" in the pop-up box.

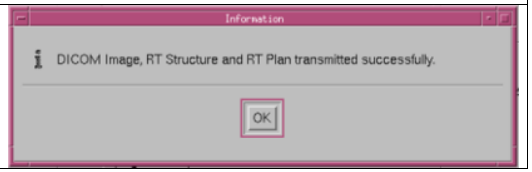






**9.B Create PDF for MOSAIQ**

In case you need a paper version to verify:

Print the plan.
Got to File → Print Plan

Make sure to select Long Ricoh printer.

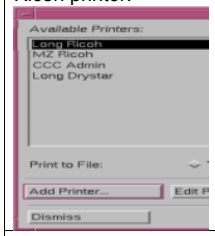


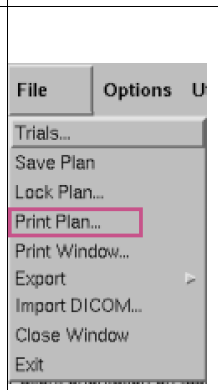


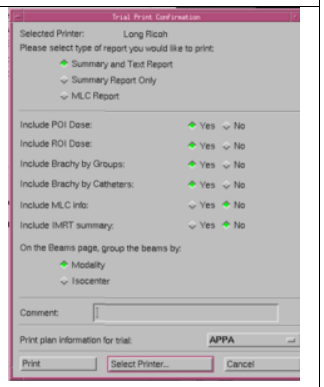


**10. Import plan to MOSAIQ**

In MOSAIQ, go to RTP Import. Either click the symbol on the tool bar


or find it under File I Import/Export I RTP Import..

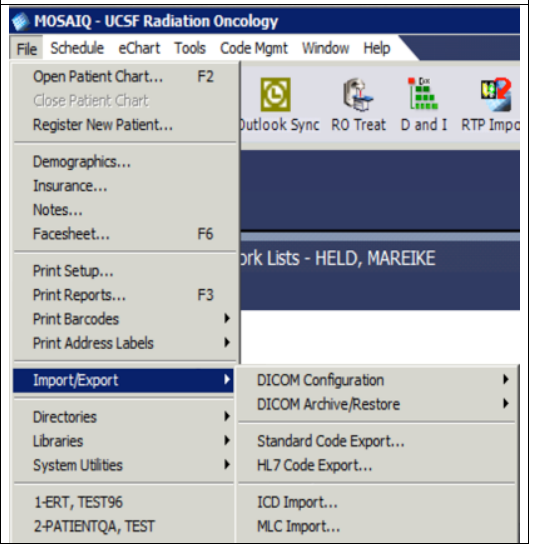

| | |
|---|---|
| Choose \\Mosaiqapp\ MOSAIQ_APP\UCSF_ APP\RTP from the drop down menu.<br><br>Select the patient to import. | 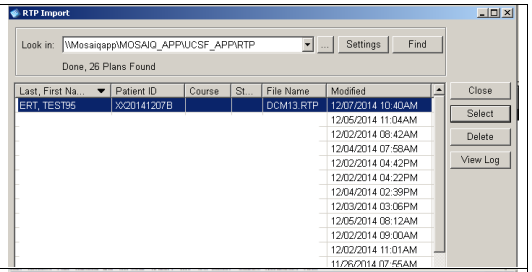 |
| Click on the red highlighted ?? in the column ‘Action’ next to ‘Radiation Oncology Course’.<br>Choose ‘XX – Ignore’ to ignore this field during import.<br>  | 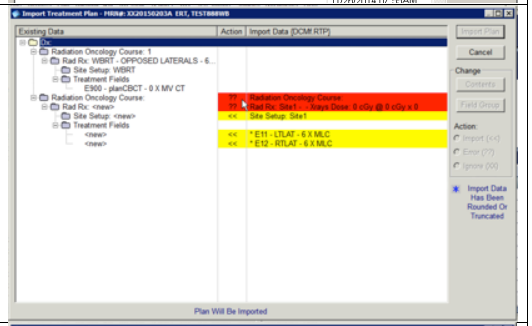 |
| Click on the green << in the column ‘Action’ next to Rad Rx: Site1.<br>Choose ‘XX – Ignore’ to ignore this field during import.<br>  <br><br>Double click on the yellow field “Site Setup: Site1” | 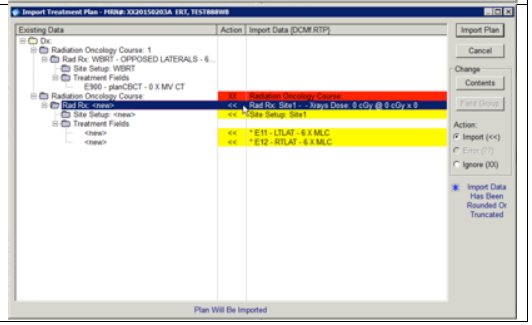 |





| | |
|---|---|
| In the yellow highlighted line, click on the empty field in the column ‘Import Data’ and choose ’11 TEST’.<br><br>In the top row ‘Rx Site Name’ replace Site1 under ‘Import Data’ with the Rx Site name entered previously when creating the prescription. In this case it is “WBRT”. | 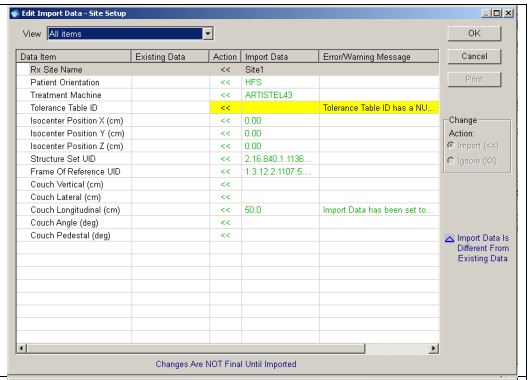 |
| Make sure that the Rx Site Name is identical to the previously entered site name.<br><br>Confirm with “OK”. | 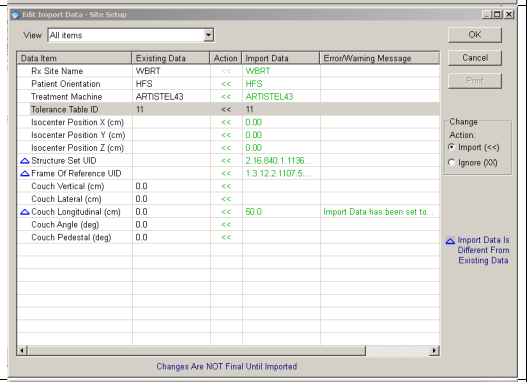 |
| Highlight the first treatment field. On the right hand side, click on “Field Group”.<br><br>Choose the site name ‘WBRT’ entered previously from the drop down menu and select the Tolerance Table ‘8 Emergency’.<br><br>Finalize the import by clicking “Import Plan”. | 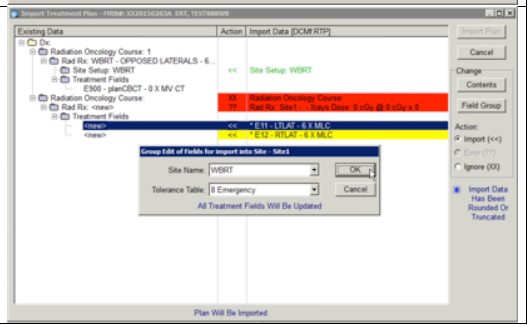 |

| | |
|---|---|
| Close the RTP Import Window | |
| **11. Associate DRR images**<br>Go to Images<br>  <br><br>Double-click on the treatment field LTLAT. | 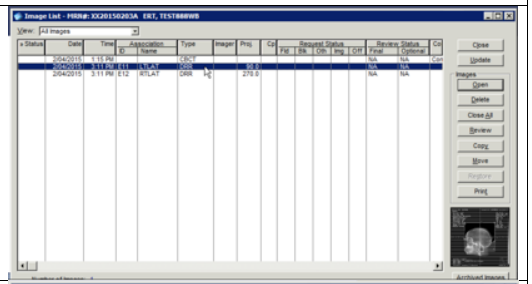 |
| Click the check-box “Use for Tx Definition” and select “OK”.<br><br>Repeat the same for the other beam RTLAT. | 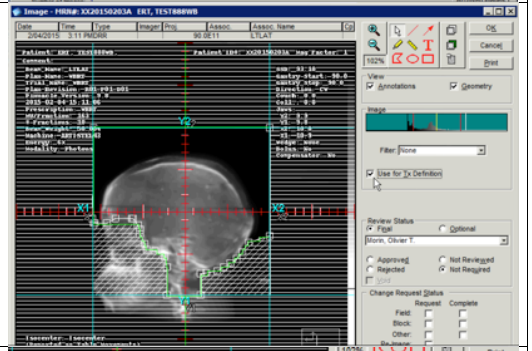 |
| In case you need to verify/change the image association, use a right-mouse-click into the image and select “Image Information”. | 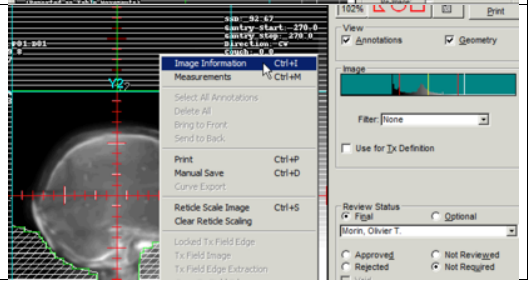 |





| | |
|---|---|
| This shows the information of the associated images. Confirm with OK. | 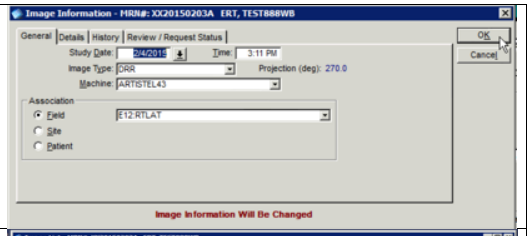 |
| The fields should now have a “T” in the status column. | 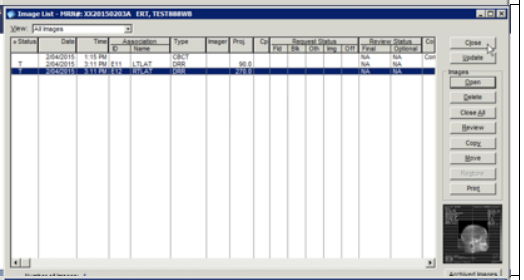 |
| **12. Approve Site Setup and Treatment Fields**<br>Open D&I.<br>  <br><br>Double click on Site Setup. | 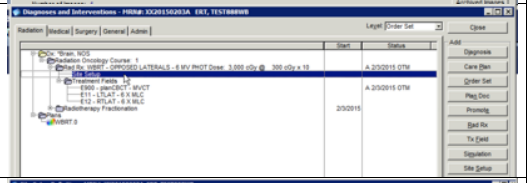 |
| Verify that the correct Patient Orientation and Machine are entered and approve the Site Setup. |  |
| Highlight treatment field E900 planCBCT MVCT.<br><br>Click on “Tx Field” on the right side. | 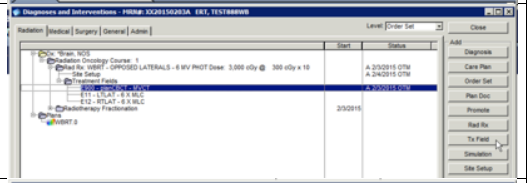 |
| Confirm to copy treatment field with “Yes”. | 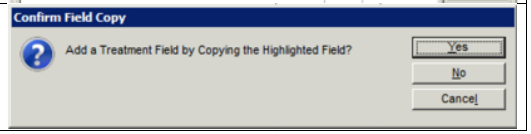 |

| | |
|---|---|
| Enter beam ID E901 setupCBCT under Field:<br><br>Verify that all beam parameters are correct and Longitudinal Couch Position is 50.00.<br><br>Right click into the window to approve beam E901. Confirm the warning about no dose entered with “Yes”. | 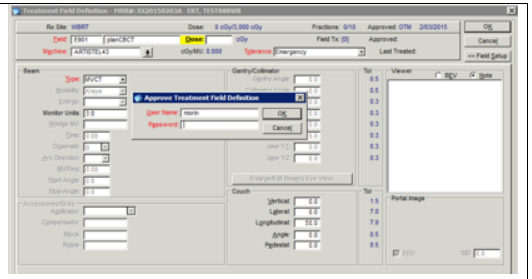 |
| Highlight and right click on the previous treatment field E900. Choose ‘Hidden Tx Field’ to hide this field for delivery.<br><br>It should now have “AH” before the approval stamp under ‘Status’ in the D&I window. | 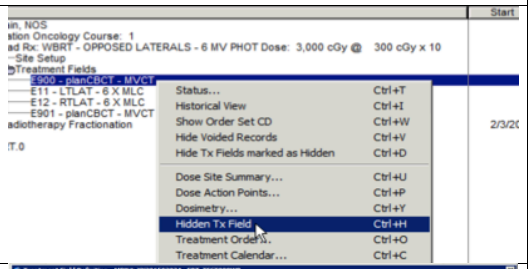 |
| Double click on the treatment field E11 – LTLAT.<br><br>Verify all beam, Gantry/Collimator, and Couch parameters.<br><br>Then, right click into the window to approve the field.<br><br>Close window with “OK”. | 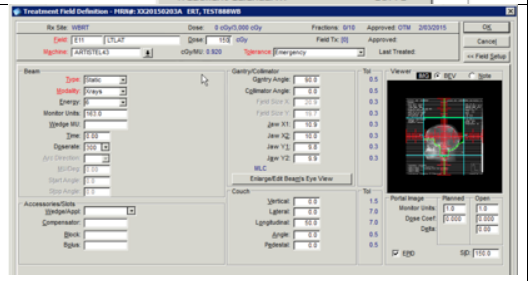 |





| | |
|---|---|
| Accept the new field. | 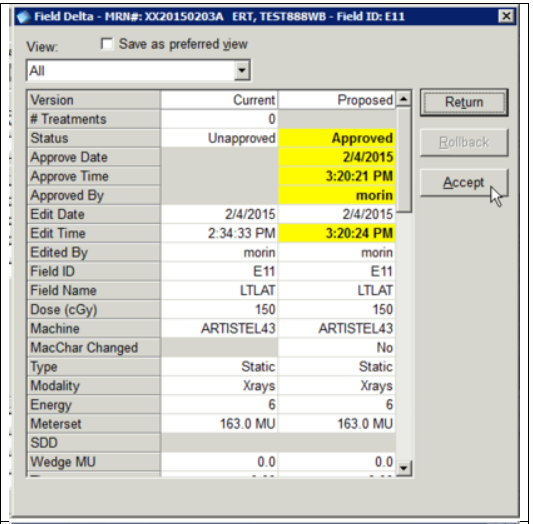 |
| Repeat the same for treatment field 12.<br><br>Double click on the treatment field E12 – RTLAT.<br><br>Verify that all beam parameters are correct and approve the field. Accept the Field Delta window as above. | 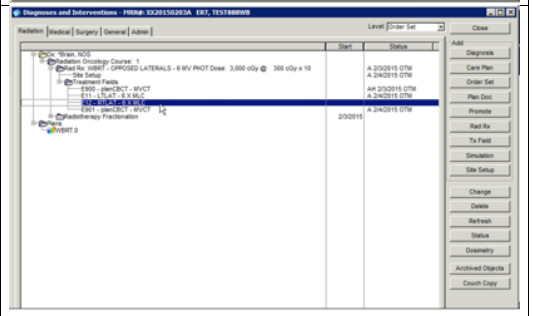 |
| Make sure that **the dose sum of both fields equals the total dose per fraction**. You can adjust this inside the tx field and is important for dose tracking. You need to approve the field again if you change this. | 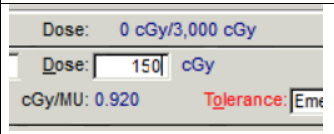 |

| | |
|---|---|
| For dose tracking, create the dose coefficient for the new beams by clicking on “Dosimetry”.<br><br>Confirm the Dosimetry Setup Information with “OK”. | 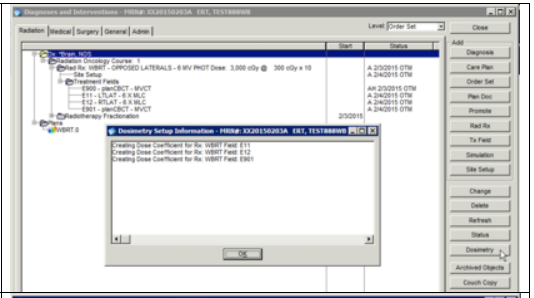 |
| Double-check in the dose column that the dose per beam is correct. The sum of all beams has to equal the total dose per prescription.<br><br>Close the Dosimetry Setup window. | 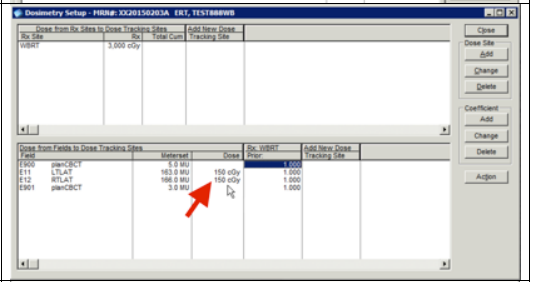 |
| **13.A Verify patient position and treatment field delivery**<br>Open the Treatment Chart window by clicking on the “RO Treat” tab.<br>  <br>Open ‘Tx Calendar’ on the right. | 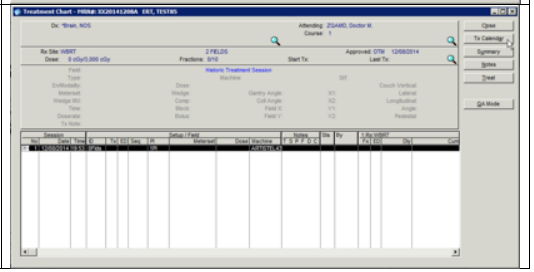 |





| | |
|---|---|
| Click on “Add” on the right side to add a new treatment session. | 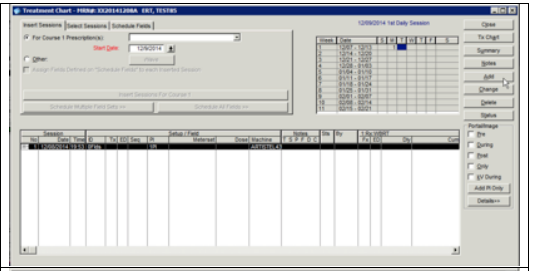 |
| Choose today’s date under ‘Due’ and confirm with “OK”.<br><br>Then, click on “Define”. | 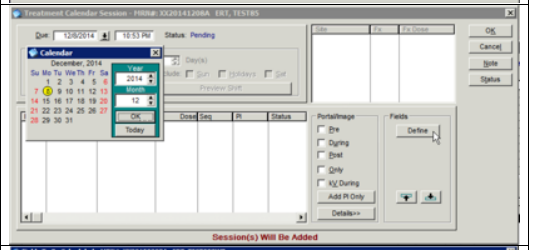 |
| Add all treatment fields under the prescription WBRT from the left to the right by using the “Add>>” button.<br>Confirm with “OK”. | 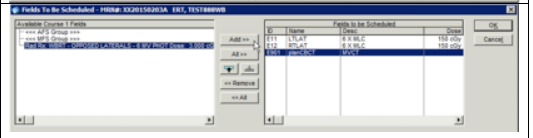 |
| Click on “Details” in this window to enable port imaging. | 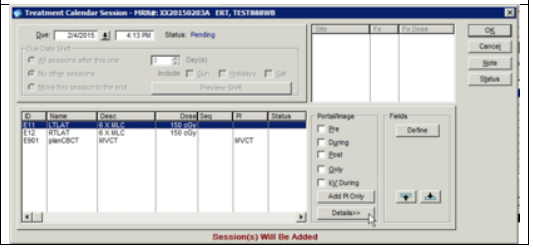 |

| | |
|---|---|
| Check the box next to ‘Only’ and choose “Plan-Open”.<br><br>Confirm with “OK”. | 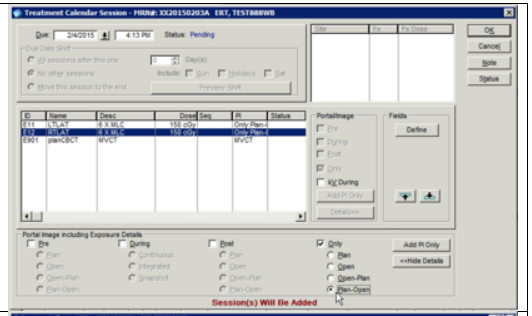 |
| Confirm the next window with “OK”. Return to ‘RO Treat’ by clicking on “Tx Chart”. | 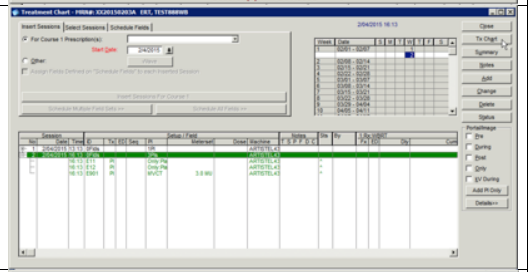 |
| | 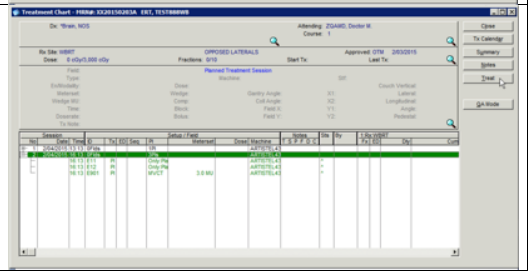 |





| | |
|---|---|
| **13.B Confirm patient setup with MV CBCT**<br>If you need to acquire a cone beam for setup, you can do that as normal. Choose any CBCT protocol that is suitable.<br><br>  | 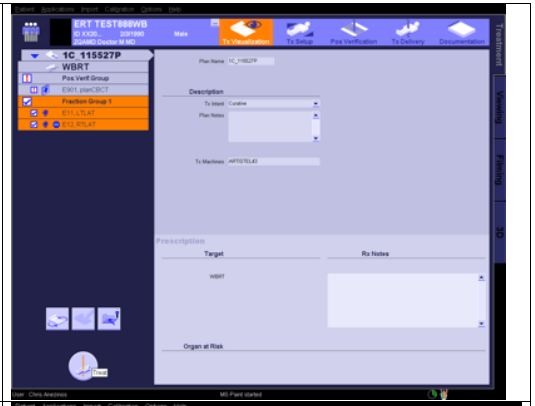 |
| Right click onto the E901 treatment field and choose ‘Imaging Options’. |  |

| | |
|---|---|
| Choose any protocol that you think is suitable for patient setup verification. For example ‘3MU Head Bony Alignment’.<br><br>Verify with ‘OK’ and click the chart symbol again to return to the field delivery window.<br><br>  |  |
| Check the boxes next to both ‘Pos.Verif.Group’ and ‘Fraction Group 1’.<br><br>On the treatment console, move the gantry, collimator, and MV flat panel into position. Double click “Accept”.<br><br>In Syngo, override the table position if necessary and approve with password.<br><br>Acquire the cone beam CT. |  |





| | |
|---|---|
| Once the cone beam is taken, it automatically goes into the ‘Pos Verification’ tab on the Syngo computer.<br><br>Change the view using any of the tools on the left side of the screen. |  |
| Use automatic alignment or align the cone beam image manually to the reference image.<br><br>Once complete, ‘accept offset’.<br><br>  |  |

| | |
|---|---|
| Apply offset<br>  <br>and confirm to ‘apply offset’ that is shown in the small window. | 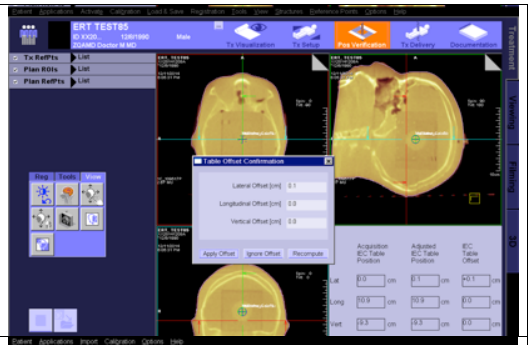 |
| **13.C Acquire portal images for both beams.**<br><br>Click on the chart check symbol. Right click on the field to open the imaging options. Choose 1.0 UF as energy for the PI. |  |





| | |
|---|---|
| |  |
| After the acquisition of portal images for both beams, the patient position can be verified in the Pos Verification. |  |
| Exit out of the patient. | |

| | |
|---|---|
| **14. Schedule treatment fields**<br>Open the Treatment Chart window by clicking on the “RO Treat” tab.<br>  <br><br>Open ‘Tx Calendar’ on the right. | 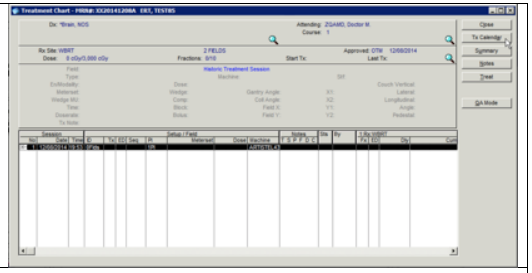 |
| Click on “Add” on the right side to add a new treatment session. | |
| Choose today’s date under ‘Due’ and confirm with “OK”.<br><br>Then, click on “Define”. | |
| Add all fields under the prescription WBRT from the left to the right by using the “Add>>” button.<br>Confirm with “OK”. | 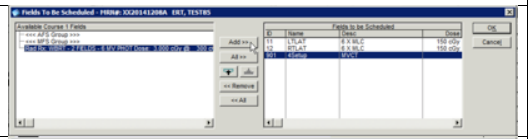 |
| Confirm the next window with “OK”. Return to ‘RO Treat’ by clicking on “Tx Chart”. | 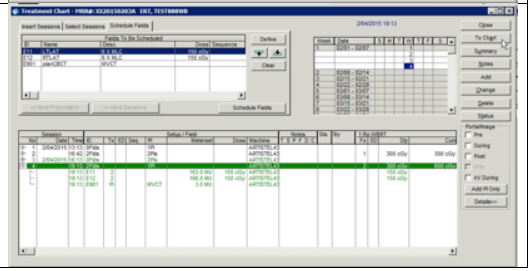 |





| | |
|---|---|
| All scheduled treatment fields should be green.<br><br>Click “Treat” to proceed. | 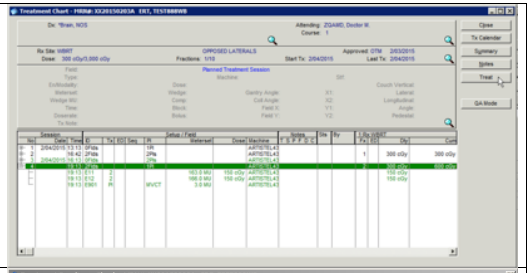 |
| Continue. | 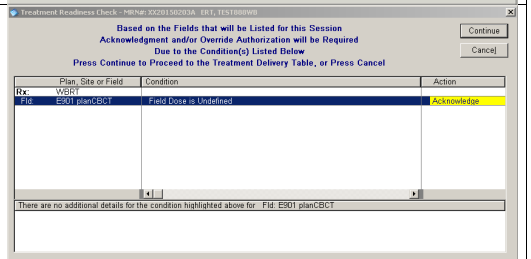 |
| Send Plan. | 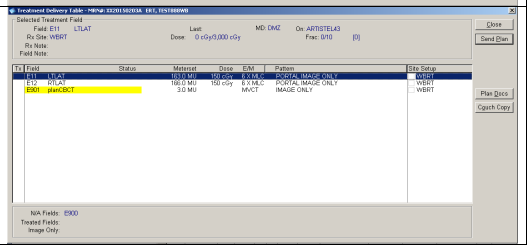 |

| | |
|---|---|
| Acknowledge the condition in the Treatment Readiness Check window and click “Continue”. | 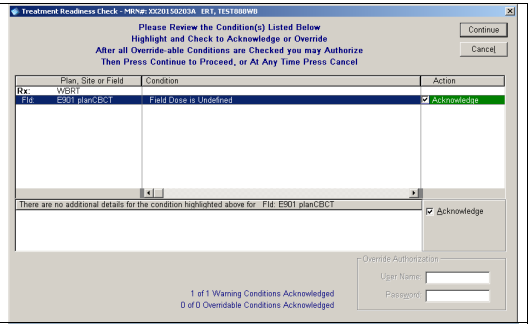 |
| Cancel the Site Setup Verification. | 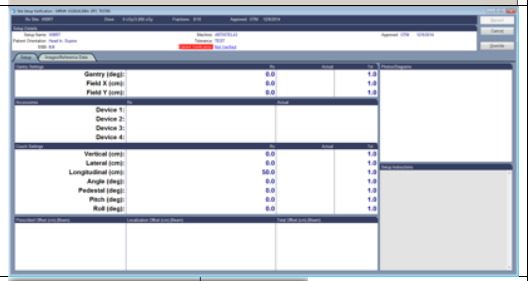 |
| Confirm to cancel. | 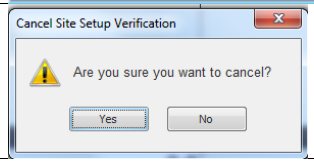 |





| | |
|---|---|
| **16. Treatment**<br>Press RadOn on the treatment console to proceed with the treatment delivery. | 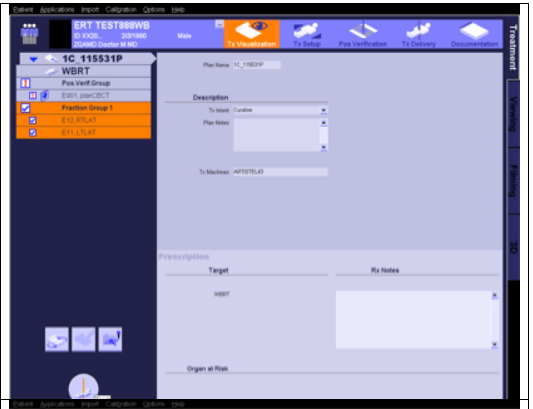 |
| Once all fields are delivered, close out the patient from Syngo<br>  <br>and record the delivered dose in MOSAIQ. | 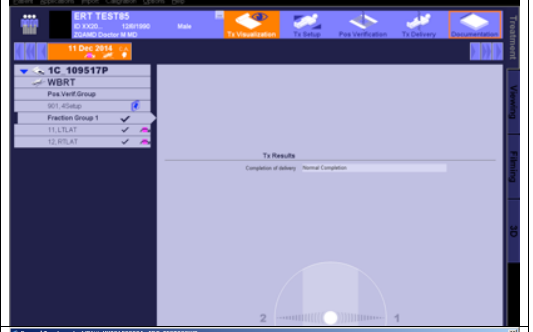 |
| | 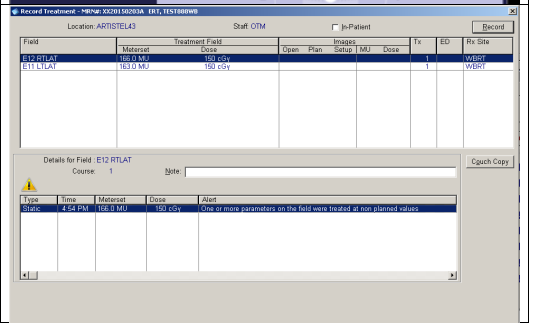 |

| | |
|---|---|
| **17. 2nd Check request and documentation**<br><br>On you task bar, click on<br><br>  <br><br><br>or go to eChart → Documents.<br><br>On the top left, click on Add → eSCAN | 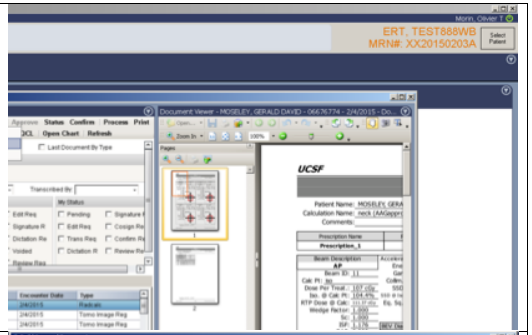 |
| This window opens up. Find your document on the left under “Documents Available” and highlight it.<br><br>On the right, choose “RadCalc” as document type and fill in the encounter date.<br><br>Then, click and drag the document into the “Documents Saved” window below it. | 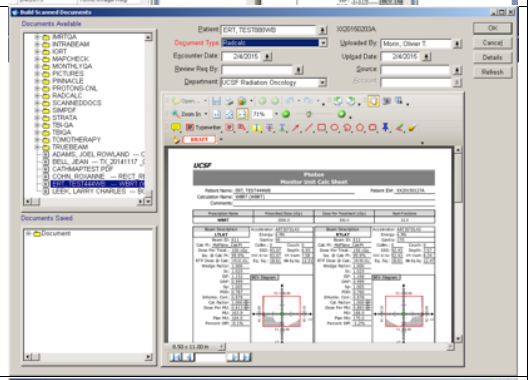 |
| The document is now saved to the patient folder in MOSAIQ. | 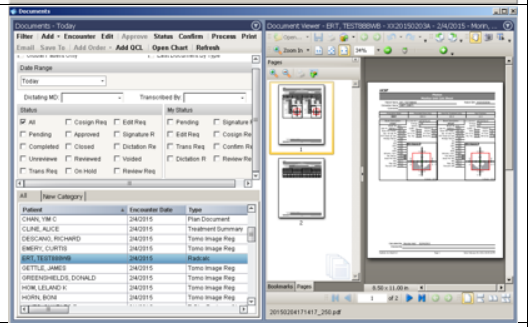 |
| Make sure you close out of the patient in Pinnacle. | |





| | |
|---|---|
| Under File → exit. Save and exit to close patient plan. | |

**Note1:**
**What script #1 ERT_WB_ONE does:**

- Changes Trial name to ‘WBRT’
- Sets localization to 0, 0, 0
- Places point at 0, 0, 0, and names it Isocenter
- Changes POI type to Isocenter
- Places a second point at 0, 0, 0
- Names point MdPlane_CalcPt
- Adjusts window level for CBCT view
- Contours external ROI and names it ‘Tissue’, ROI type ‘External’
- Cleans up contour
- Adds LTLAT beam on the Artiste, 6 MV, with gantry at 90°, Isocenter is ‘Isocenter’
- Jaws are asymmetric and automatically adjust to MLCs
- MLCs are enabled
- Jaws are open to 20 cm x 20 cm
- Dose grid is drawn on tissue contour
- Adds a default prescription of 300 cGy to dose point ‘MdPlane_CalcPt’
- Prescription name is ‘WBRT’
- Adjusts window level for BEV
- Increases BEV resolution to 555
- Displays DRR in BEV automatically
- Jumps into BEV and is ready to draw the block

**Note2:**
**What script #2 ERT_WB_TWO does:**

- Copy & Oppose beam
- Beam name, beam ID
- Adjusts beam weighting to 50/50.
- Computes dose for both beams.
- Adjust isodose lines to absolute values of 3200 (red), 3000 (yellow), 2800 (green), 2000 (blue)
- Draws thick lines
- Opens prescription window and beam weighting window
- Jumps to the Evaluation tab for plan review

# APPENDIX C

## Clinical Procedure for Heterotopic Bone ERT

## Heterotopic Bone

| | |
|---|---|
| **1. Select or create patient in MOSAIQ**<br><br>Click on “Select Patient” in the upper right corner. Choose “Add” on the ‘Select Patient Window’ if the patient isn’t already in MOSAIQ. | 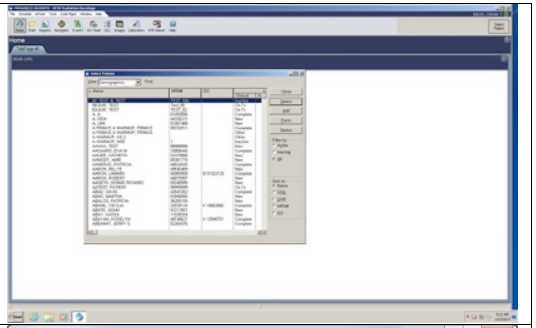 |
| Fill in the Demographics marked in red:<br><br>Last Name<br>First Name<br>MRN#<br>Birth Date<br>Gender | 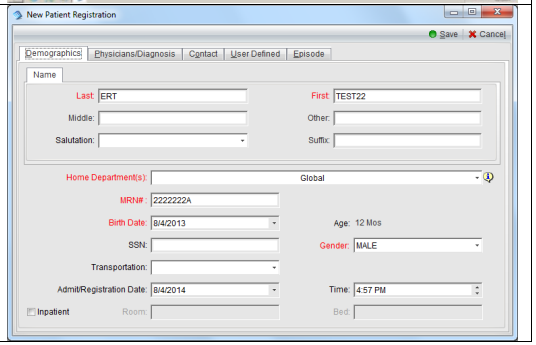 |





| | |
|---|---|
| On the next tab, fill in the Physician’s Diagnosis marked in red:<br><br>Attending Physician<br>Category<br><br>Click “Save” on the upper right. | 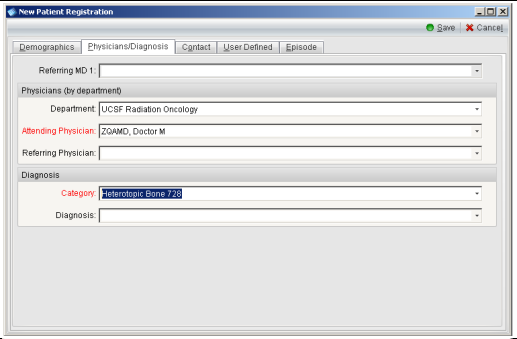 |
| Click “No”.<br><br>Inform the MD to change the diagnosis and create and approve the prescription. | 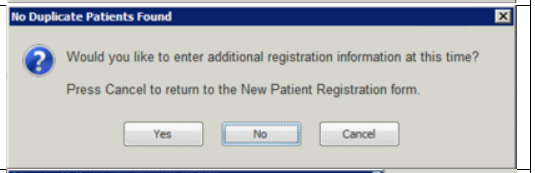 |
| **2. Add Diagnosis, Care Plan, Rad Rx, Site Setup**<br>Choose the “D&I” tab from the toolbar<br>  <br>or open it through eChart I Diagnosis and Interventions.<br><br>**The MD will do the part in gray:**<br>On the right hand side, click on “Diagnosis”.<br>Click on “Change” in the ‘Diagnosis and Problem List Window’.<br><br>Change the diagnosis and click on “Save and Affirm”.<br><br>Then “Close”. | 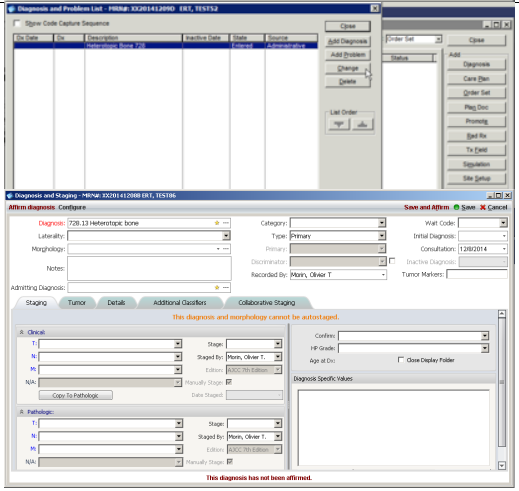 |

| | |
|---|---|
| Create a treatment course by clicking on “Care Plan”. | 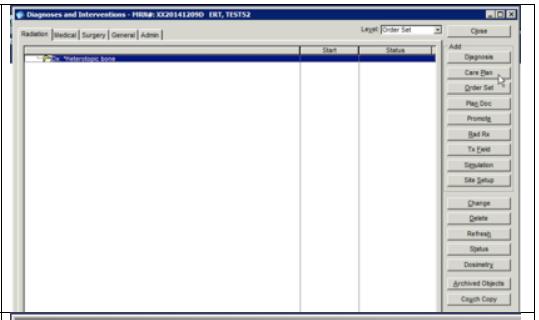 |
| Confirm with “Ok”. | 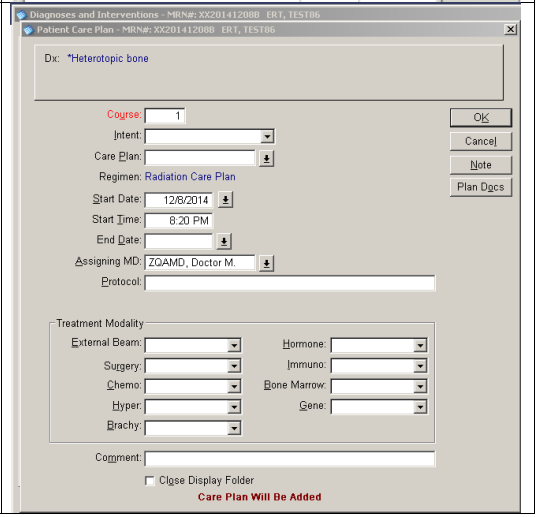 |





| | |
|---|---|
| In the ‘Diagnoses and Interventions’ window, click on “Rad Rx” and this window opens up.<br><br>Fill in the prescription for the treatment.<br>Example:<br>Rx Site: Lhip<br>18 MV PHOT<br>AP/PA<br>Dose to MID-PLANE, 100%<br>700 cGy total, 700 cGy per fraction | 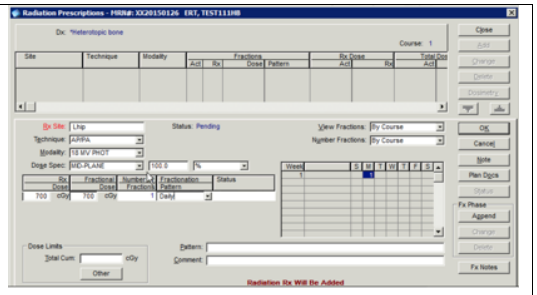 |
| If treatment is on the weekend or over a holiday, include ‘Saturday’, ‘Sunday’, or ‘Holidays’ on the bottom by clicking the according check mark.<br><br>Confirm the Setup Form with “OK”. | 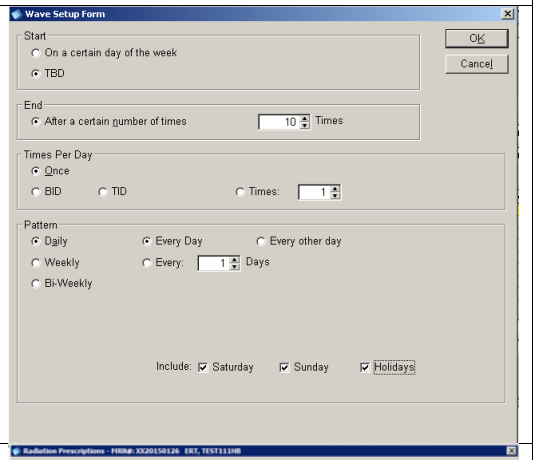 |
| Right click inside the Radiation Prescription window, choose ‘Status’ and approve the prescription. | 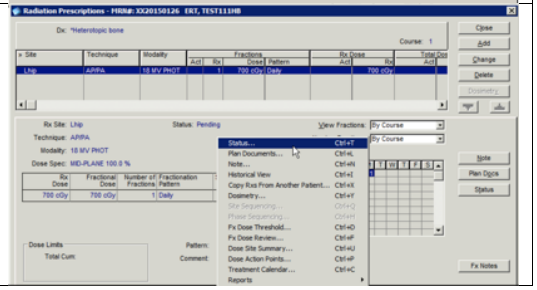 |

| | |
|---|---|
| Check “Approved”, sign with your password and close the window using “OK”. | 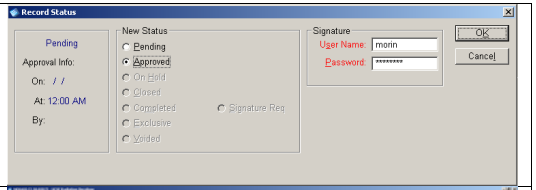  |
| In the ‘Diagnoses and Interventions’ window, click on “Site Setup” and this window opens up.<br><br>Fill in the fields in red:<br>Patient Orientation<br>Machine<br>Tolerance | 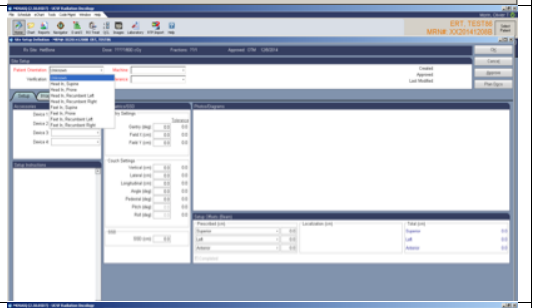 |
| Right-click into the window to approve the Site Setup. | 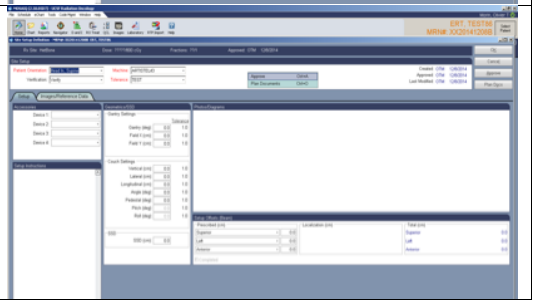 |





| | |
|---|---|
| **3. Patient Setup**<br>Measure the patient thickness at the treatment area and set up the patient at mid-plane on the treatment couch. |  |
| Adjust the table position, gantry angle, collimator angle, and field size using the light field to cover the approximate treatment area. Use the red SSD distance measurement to measure the SSD.<br><br>It should be<br>SSD = 100 – $PT_d/2$, with $PT_d$ being the patient thickness at the treatment location.<br><br>Leave the patient set up on the machine and go to the treatment console to set up the field for image verification. | 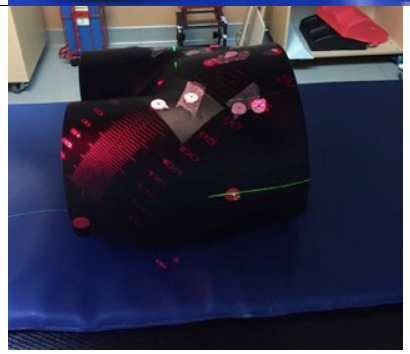 |
| **4. Add Tx Field**<br>In the ‘Diagnoses and Interventions’ window, click on “Tx Field” and this window opens up. Select “ARTISTEL43”. | 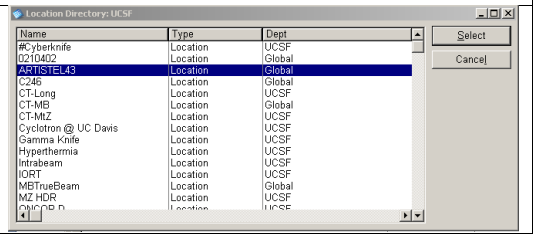  |

Fill in the red fields:

Field: E11 AP
Tolerance: Emergency
Type: Static
Modality: Xrays

Also fill in:
Energy: 18
Monitor Units: 1
Dose Rate: 500
Dose: 350 cGy (half of total prescription if AP/PA)

Below the BEV window, choose Portal Image
Monitor Units:
Planned: 1.0 and
Open: 1.0 on

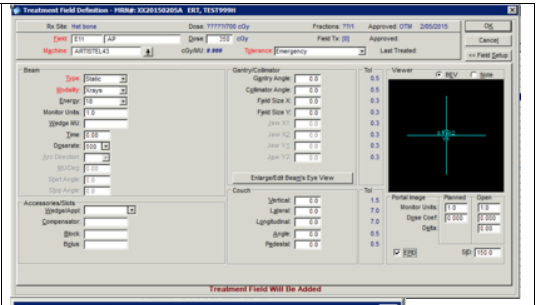

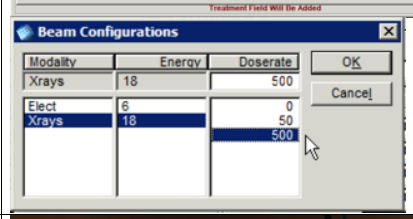


Adjust the Gantry and Collimator based on the Linac settings that were made using the light field.

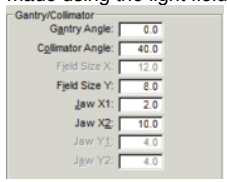


You can copy these from the Control Console monitor.




NOTE: If needed, you can set asymmetric jaws by doing a right mouse click, 'Asymmetric Jaws', and choosing 'ASY X' and/or 'ASY Y'.

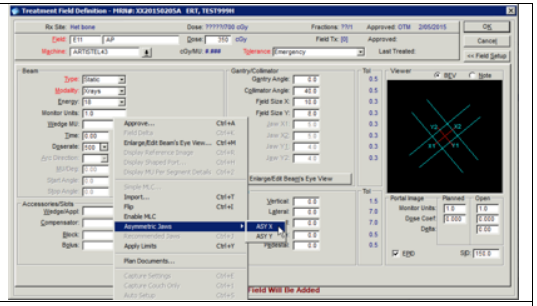

To approve the field, right-click into the window. Enter password to approve the field. Exit window with "OK".

In the 'Diagnoses and Interventions' window, click on "Dosimetry" and this window opens up.

Confirm with "OK".

Close the Dosimetry Setup window.

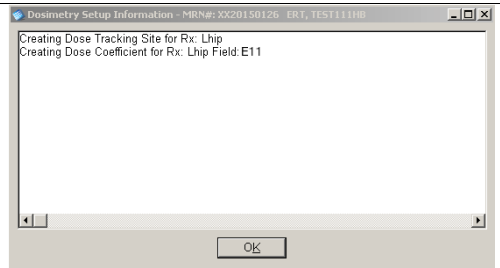


**5. Schedule Tx to acquire portal image**
In the main tabs on top, choose "RO Treat".


Click on "Tx Calendar".

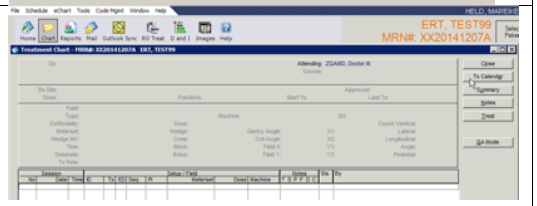

| | |
|---|---|
| Click on “Add” on the right side. | 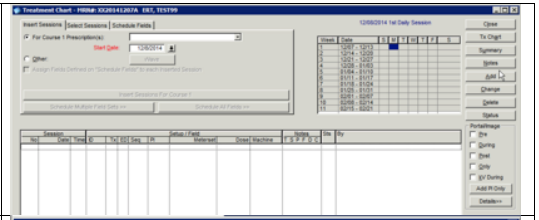 |
| Click on the arrow (1.) to open the calendar. Choose ‘Today’ and confirm with “OK”.<br><br>Then, click on “Define” (2.) | 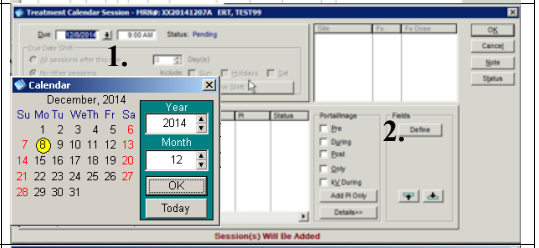 |
| Highlight the field 11 – AP on the left and add it to the right side.<br>Confirm with “OK”, and the next window with “OK”. | 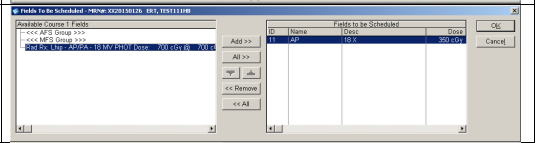 |
| Click on “Details” in this window to enable port imaging. | 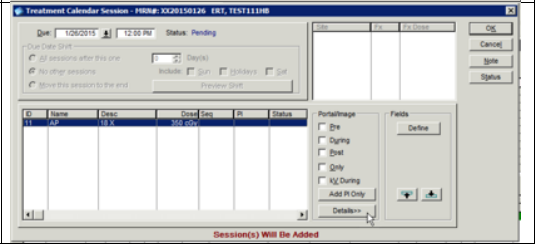 |





| | |
|---|---|
| Check the box next to ‘Only’ and choose “Plan-Open”.<br><br>Confirm with “OK”. | 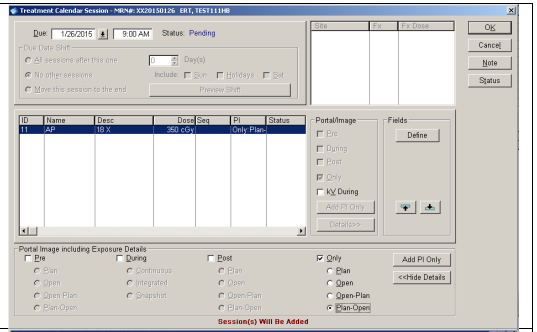 |
| Under ‘Setup/Field’ in column PI it should say ‘Only:Plan – Open’ in green.<br><br>Click on “Tx Chart”. | 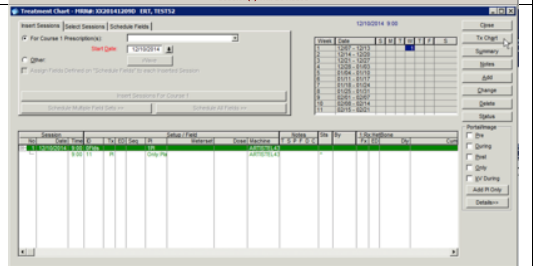 |
| Proceed to treatment by clicking on “Treat”. | 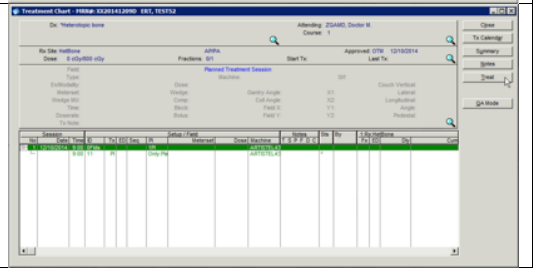 |

| | |
|---|---|
| Send the field to Syngo by clicking on “Send Plan”. | 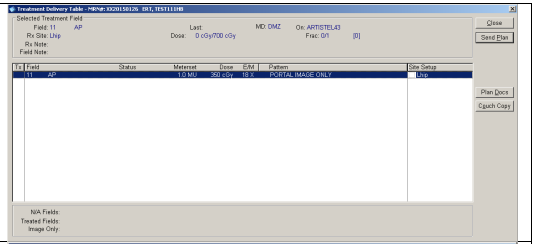 |
| Acknowledge the Fx Dose Mismatch and hit “Continue”. | 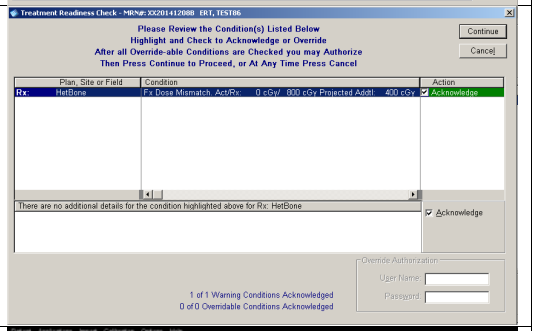 |
| **6. Acquire Portal Image**<br>Receive the plan in Syngo. This is what you should see in Syngo now.<br><br>The blue head symbol next to the treatment field indicates that an image will be taken.<br><br>Click on the chart symbol at the bottom.<br>  | 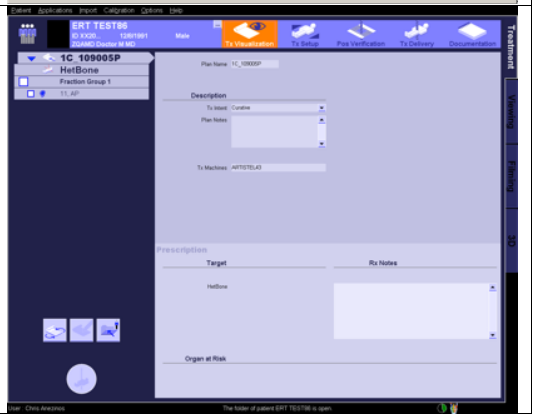 |





| | |
|---|---|
| Use a right mouse click on the treatment field to open the ‘Imaging Options’. |  |
| Exposure MUs are set to 1.0. Keep this setting, as it is the maximum for kView Inline portal imaging.<br><br>Choose ‘1.0 UF’ from the drop down menu for Imaging Segment Energy [MV]. This uses the kView Inline function with lower energy during imaging for better image quality and contrast.<br><br>Use a double exposure. You can specify the Beam Delta. |  |

| | |
|---|---|
| If your port field is too large for the flat panel, the beam may affect the electronics in the flat panel. The field limit is indicated by the inner square. In this case, the SID turns red. |  |
| You have to either reduce the SID or check ‘Clipping’ to enable portal imaging.<br><br>Confirm the imaging options with “OK”.<br><br>Click the check mark to return to the treatment delivery window.<br>  |  |





| | |
|---|---|
| Check the box next to ‘Fraction Group 1’ and send the field to the machine using the round ‘Treat’ button.<br>  |  |
| The machine delivers two fields with the specified number of 1.0 MU: the planned treatment field and an expanded field defined by the beam delta. |  |

| | |
|---|---|
| Once the portal image is completed, go to the 'Pos Verification' tab on the top.<br>  <br>The inner square is what the treatment field currently looks like. |  |
| To use the graticule, the image has to be saved as a reference image first.<br><br>Save the Image as a reference image under 'Load & Save', select "Save As Reference".<br><br>(This will only be a reference for future images. The treatment field can look different from this field.) | |
| Take notes on how to change the field. You can use the table printed on a separate sheet of paper to take notes. | 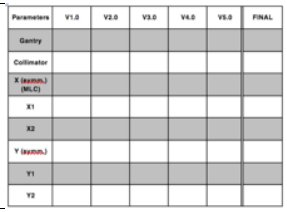 <br> 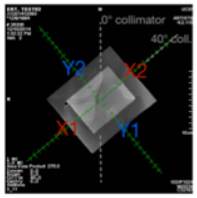 |





| | |
|---|---|
| To adjust the treatment field, exit the patient and modify the field size. Then, you can re-image using a portal image. | 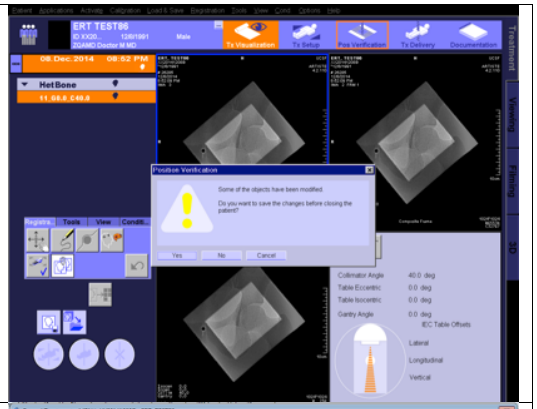 |
| After exiting the patient in Syngo, record the delivered field on the MOSIQ SEQUENCER. | 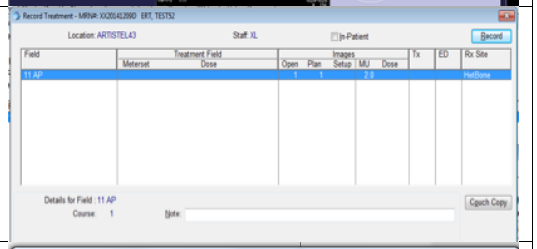 |
| Confirm to exit the dose delivery. | 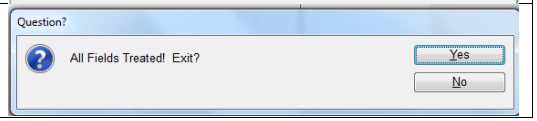 |

| | |
|---|---|
| **7. Adjust field size**<br>To change the image field size:<br>In D&I, double click the treatment field to open. Change the field size to the desired parameters.<br><br>You can enter an asymmetric jaw by doing a right mouse click and choosing 'Asymmetric Jaws'.<br><br>Approve the beam once you're done. | 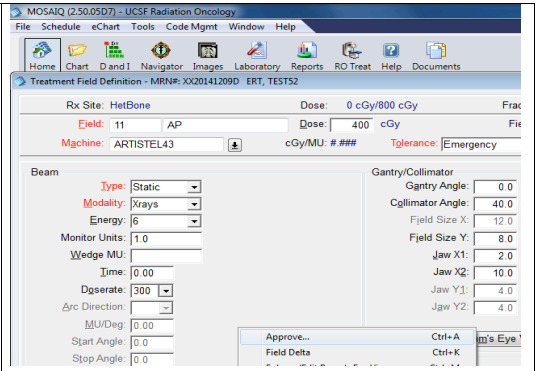 |
| Accept the change. | 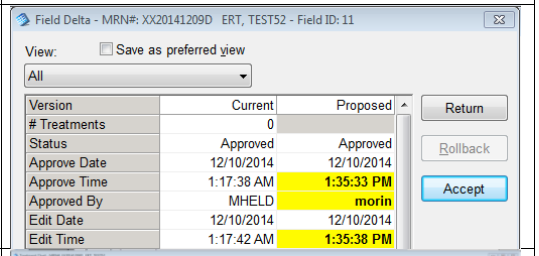 |
| Go to RO Treat.<br>  <br>Click on "Tx Calendar". | 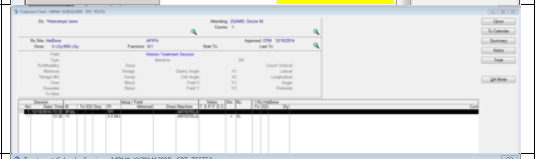 |
| As before in **step 5.**, choose today's date from the drop down calendar. Then, click on "Define".<br><br>Add the beam from the left to the right to 'Fields to be scheduled'. Confirm with "OK". | 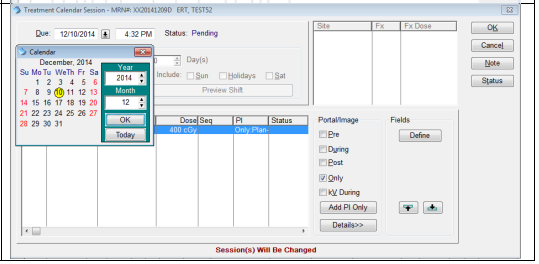 |





| | |
|---|---|
| Click on 'Details' and check the box next to 'Only' and 'Plan-Open'. | 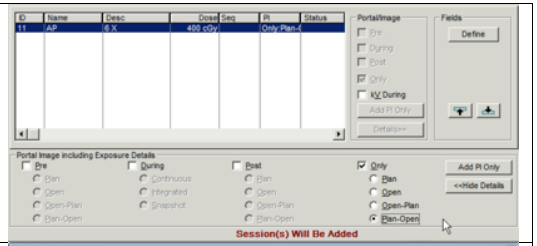 |
| Go to 'Tx Chart' and send the plan to treat. | 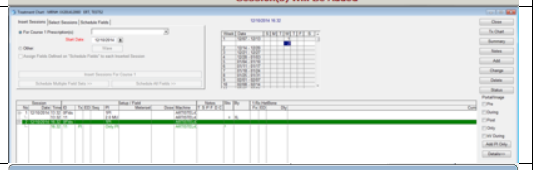 |
| Confirm the Verification Image Status window with "OK". | 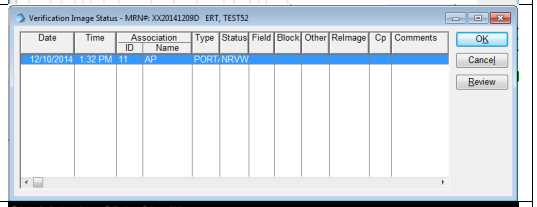 |
| In Syngo, confirm the warning with "OK".<br><br>Again, go to Imaging Options to choose 1.0 UF | 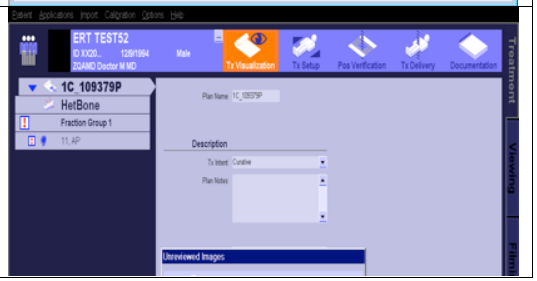 |

| | |
|---|---|
| If the field Lateral turns red, you can adjust the flat panel position manually or by clicking on “Best Fit”.<br><br>Confirm the changes with “OK” and click on the chart symbol to take the portal image. |  |
| Under the tab ‘Pos Verification’, you can compare your current field to the previous one.<br><br>Or you can save your new field as the reference.<br><br>**Repeat the same steps as above until you have the correct and final treatment field.** |  |





| | |
|---|---|
| **8. Mark final field**<br>Save the Image as a reference image under ‘Load & Save’, select “Save As Reference”.<br><br>Confirm the Position Verification with “Yes”.<br><br>Mark the patient position on the patient’s skin. | 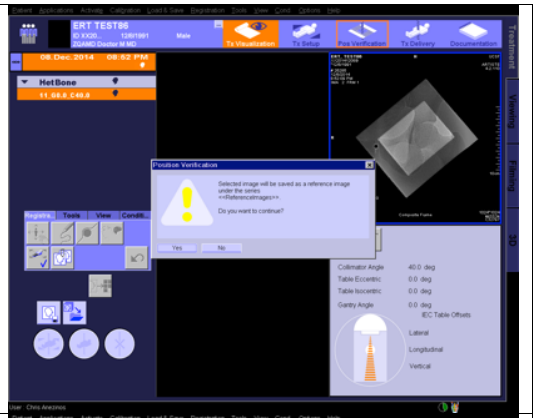 |
| You can turn on the digital graticule for the reference image under “Tools” on the left hand side.<br>  <br><br>Once you know the field size, you need to do an MU calculation. | 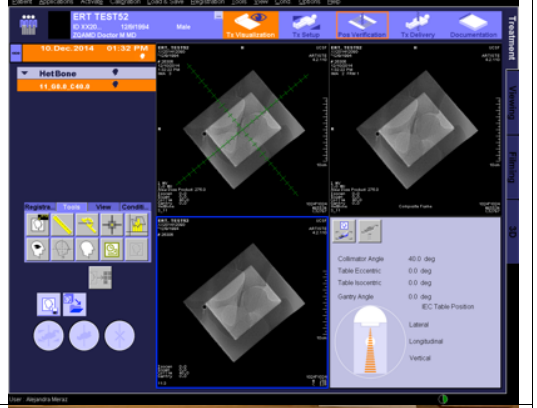 |
| **9. MU calculation (This will be done by physics or dosi)**<br>On the MOSAIQ CLIENT/DAILY QA computer:<br>Start up Pinnacle from the Desktop. Log in to Pinnacle and click on the triangle icon to get to the home | 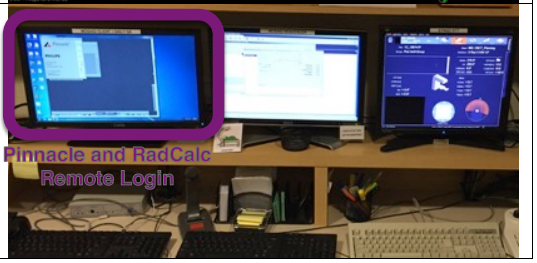 |

| | |
|---|---|
| screen.<br>  | |
|  <br>Highlight the Emergency_V9.8 Institution and dismiss the window.<br><br>Click on planning<br>  <br>Add a new patient using the “Add” button on the top half of the screen. | 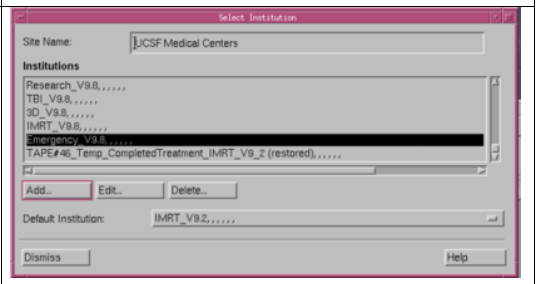 |
| Enter the patient data:<br><br>Last Name<br>First Name<br>Middle Name<br>Med Rec Number<br>Gender<br><br>Click on “Add Plan…” | 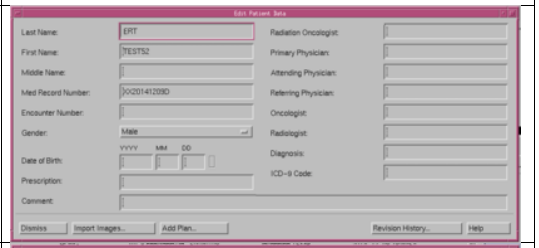 |
| Change the Plan Name to the prescription name in MOSAIQ.<br><br>Choose “Irreg”.<br><br>Click on “Planning…”. | 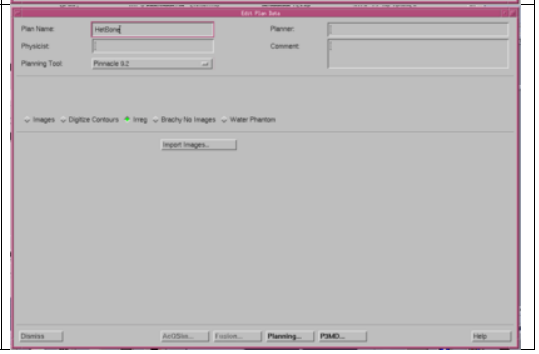 |





| | |
|---|---|
| Fill in all necessary fields:<br>Patient position<br>Patient orientation<br><br>Prescription dose for one beam. (In case of AP/PA, enter 50% of the total prescription dose.)<br><br>Beam Name<br>Machine<br>Energy<br>Modality<br><br>Add a point using the button on the right.<br>Name the point MdPlane_CalcPt. based on prescription.<br>Adjust the Depth and SSD. | 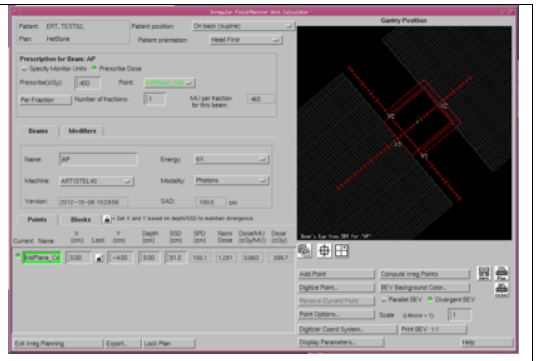 <br>Depth: patient separation / 2<br>SSD: 100 – patient separation / 2 |
| In the Modifiers tab, set the jaws to match the final treatment field.<br><br>Adjust the Collimator Angle. | 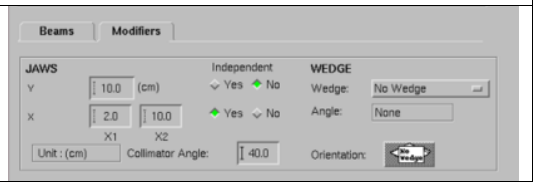 |

Move the point position to the center of the field. If jaws are asymmetric, this point is not at the center of the graticule.
Use this button

to move it away from the graticule center.

Click on “Compute Irreg Points” to calculate the MU.

The MUs per fraction for this beam appear in the ‘Prescription for Beam’ section.

If needed, print this page and save the plan for the record.

Exit the plan and Pinnacle.

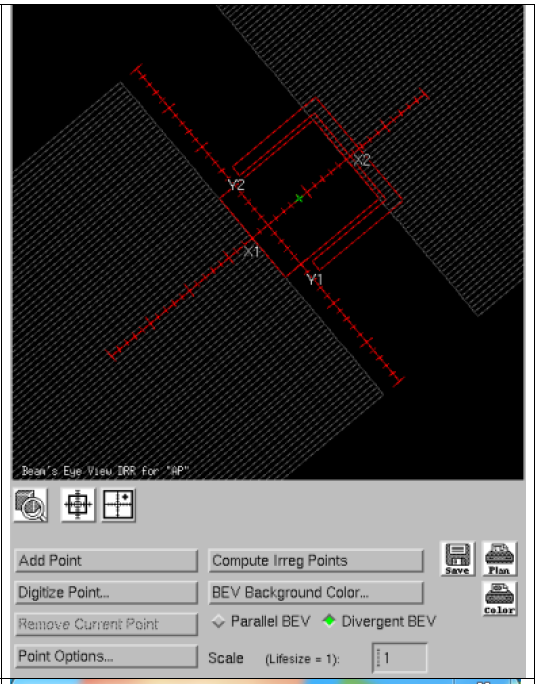


**10. 2nd MU check**
Open RadCalc using the RadCalc Shortcut on the Desktop.

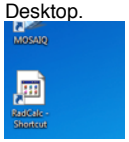


Confirm the Security Warning with “Run”.

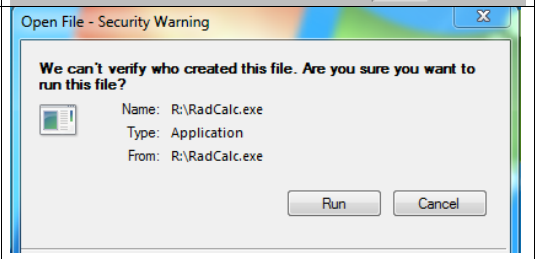






Log in to RadCalc with your username and password.

username: therapist

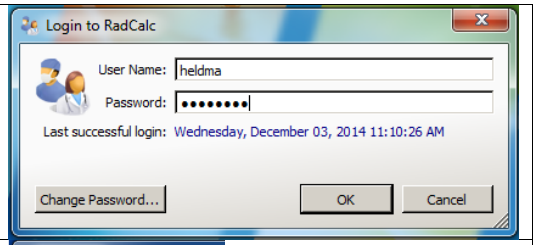


Click on File to open “EZ Photon Calculation…”

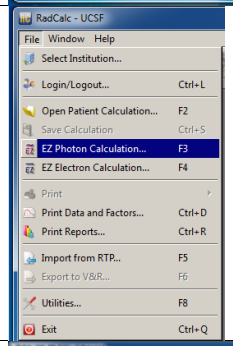


Enter the Patient Information:
Patient ID
Last Name
First Name
Middle Initial

Change the Beam ID and Beam Description to match MOSAIQ.
Choose the calculation mode (SSD).

Adjust the Beam Setup:
Machine Name
Energy
Field Size
SSD
Depth

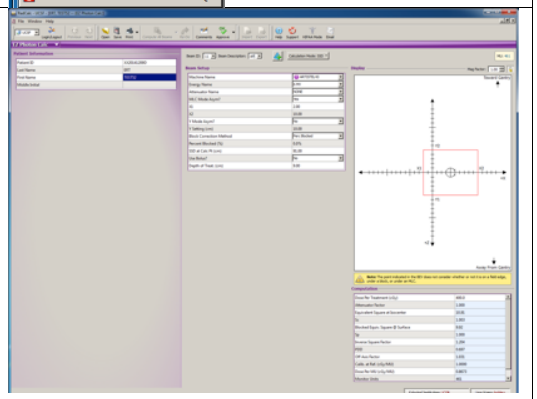

| | |
|---|---|
| In the computation window, enter the dose per beam and treatment.<br>(Enter only 50% of the total prescription dose if it is AP/PA.) | 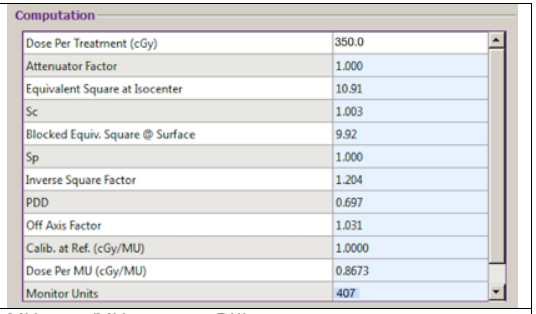 |
| Compare the MU from Pinnacle and RadCalc. The %Diff should be less than 5%. | $MU_{Pinnacle}/MU_{RadCalc}$ = %Diff<br><br>412MU/407MU = 1.2%. |
| Print the dose calculation. Then, save dose calculation and close RadCalc. | |
| **11. Adjust MU and create PA field**<br>Now that you know the treatment field and MU, go to D&I on the MOSAIQ SEQUENCER.<br><br>Open the treatment field E11 AP and enter the MU you received from the RadCalc EZ photon calculation.<br><br>Approve the field and confirm with “OK”. | 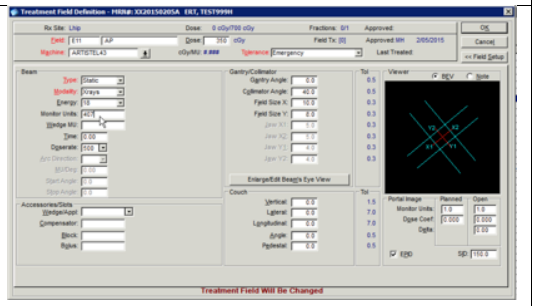 |





| | |
|---|---|
| Copy the treatment field by highlighting it in the ‘Diagnoses and Interventions’ window. Then click on “Tx Field” on the right. | 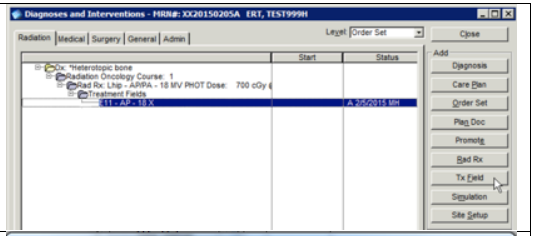 |
| Confirm to copy the treatment field with “Yes”. | 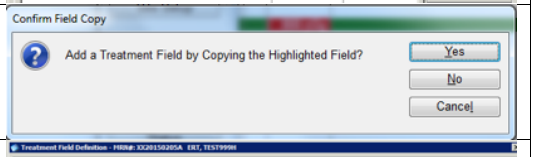 |
| Enter the field ID 12 PA. Verify the MU.<br><br>Right click into the window to ‘Flip’ the beam. | 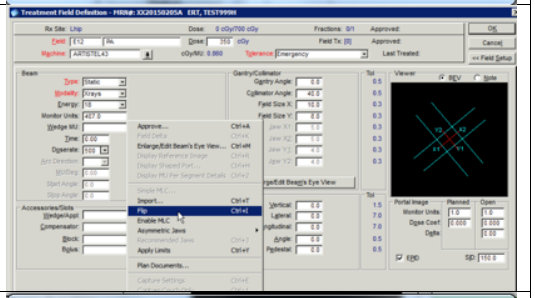 |
| Confirm to flip the beam with “Yes”. | 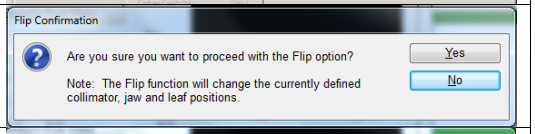 |
| Confirm to convert the gantry angle to the opposing angle with “Yes”. | 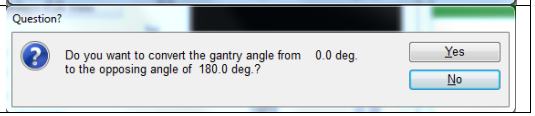 |

| | |
|---|---|
| The resulting beam is an opposed copy of the AP field.<br><br>Right click to approve the field. | 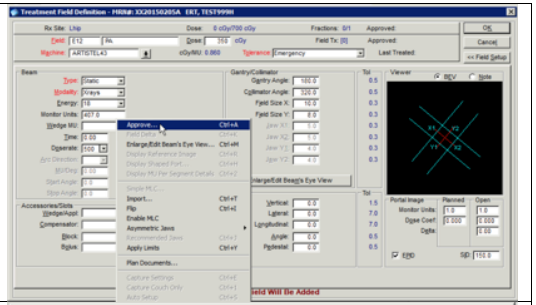 |
| Create the dose coefficient for field 12 by clicking on “Dosimetry” in the ‘Diagnoses and Interventions’ window. | 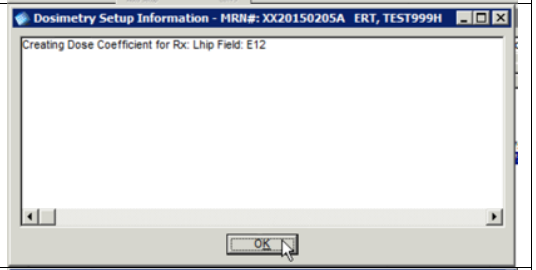 |
| **12. Verify patient setup**<br>Schedule the PA field as before in **step 5.**<br>Go to RO Treat, Tx Calender, Add, Define. | 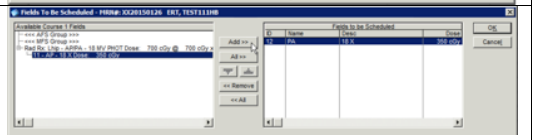 |
| Under Details, add Portal Imaging “Only : Plan-Open”. | 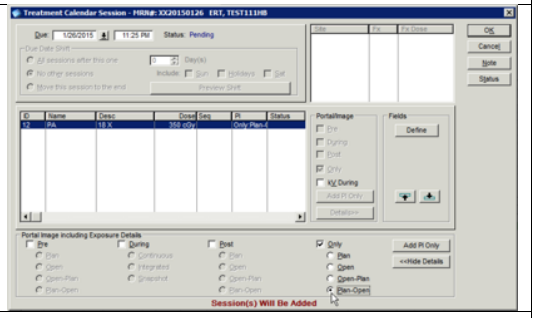 |
| Take a portal image to verify the PA beam | |





| | |
|---|---|
| delivery.<br>Once the doctor approves the setup, the fields are ready for treatment. | |
| **13. Treatment**<br>To schedule the fields, go to ‘RO Treat’, ‘Tx Calendar’, ‘Add’ and ‘Define’ as before. Make sure to choose the correct date from the calendar. | 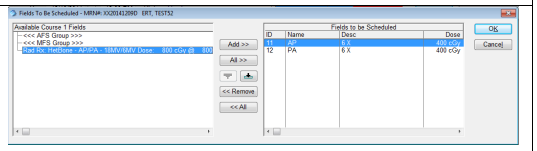 |
| Add Portal Imaging to each field by clicking on “Details”. If necessary, | 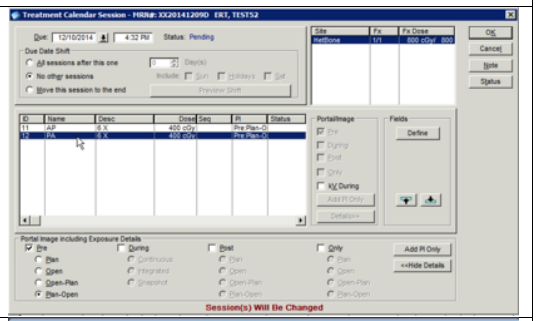 |
| Click on “Tx Chart”, then “Treat”. | 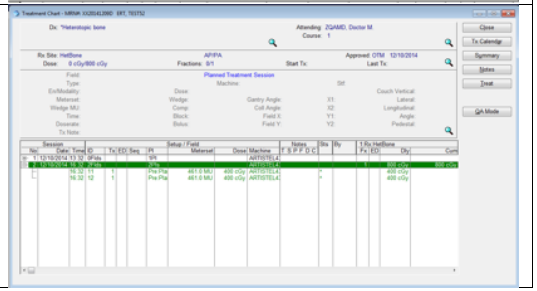 |

| | |
|---|---|
| Continue. | 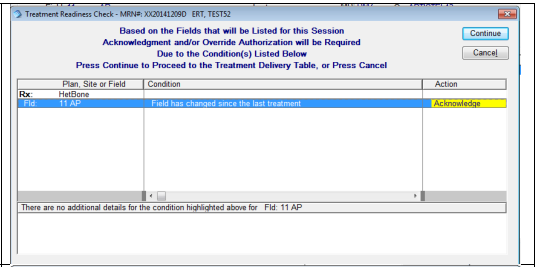 |
| Acknowledge the Verification Image Status window with “OK”. | 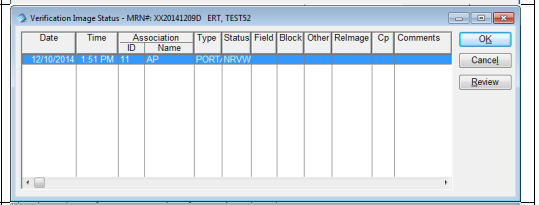 |
| Send the plan to Syngo. | 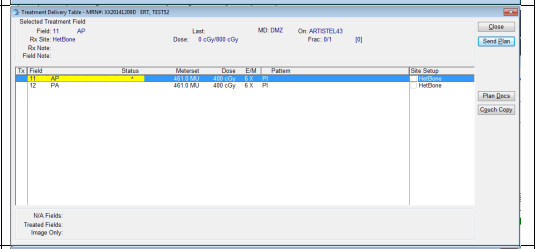 |
| Acknowledge that the treatment field 11 AP has changed since the last treatment. | 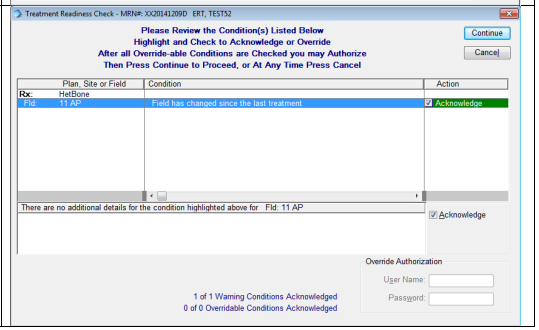 |





| | |
|---|---|
| Cancel the Site Setup Verification and confirm with yes. | 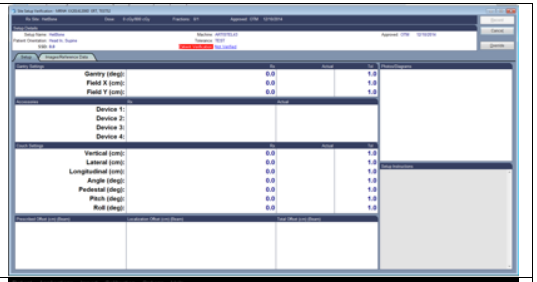 |
| | 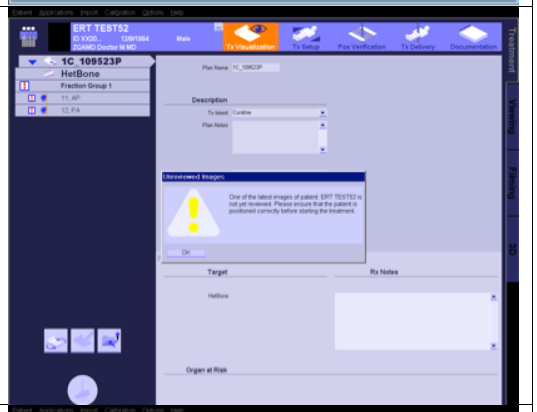 |
| As before (**step 6.**), click on the Chart symbol, then right click on field 11 AP for imaging options.<br><br>Choose 1.0 for Imaging Segment Energy [MV]. Adjust the flat panel position if necessary by clicking “Best Fit”. |  |

| | |
|---|---|
| Repeat the same thing for beam 12 PA.<br><br>Confirm with “OK” and click on the chart symbol to return to the treatment window.<br>  |  |
| Deliver both fields.<br><br>The system will acquire a portal image before each beam with an open portal to see the anatomy, just like before.<br><br>After acquiring the plan and open field for imaging, it will continue to treat. This is only a way to record the patient position, not to verify. |  |





| Parameters | V1.0 | V2.0 | V3.0 | V4.0 | V5.0 | FINAL |
|---|---|---|---|---|---|---|
| Gantry | | | | | | |
| Collimator | | | | | | |
| X (symm.) (MLC) | | | | | | |
| X1 | | | | | | |
| X2 | | | | | | |
| Y (symm.) | | | | | | |
| Y1 | | | | | | |
| Y2 | | | | | | |

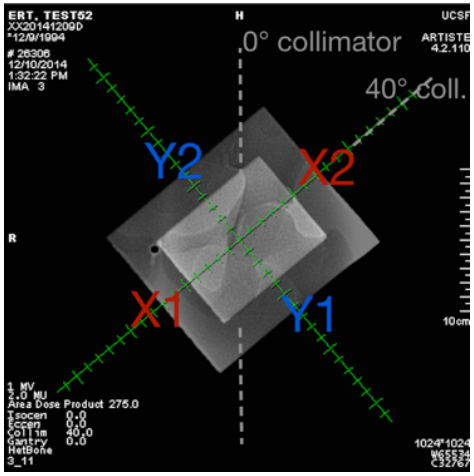

# APPENDIX D

## Clinical Procedure for Spinal Cord Compression ERT

# AP/PA Treatments

| | |
|---|---|
| **1. Select or create patient in MOSAIQ**<br><br>Click on “Select Patient” in the upper right corner. Choose “Add” on the ‘Select Patient Window’ if the patient isn’t already in MOSAIQ. | 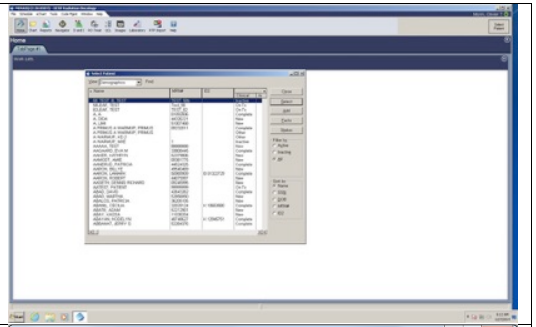 |
| Fill in the Demographics marked in red:<br><br>Last Name<br>First Name<br>MRN#<br>Birth Date<br>Gender | 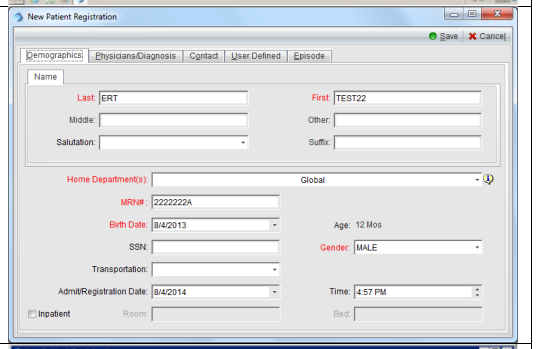 |
| On the next tab, fill in the Physician’s Diagnosis marked in red:<br><br>Attending Physician Category<br><br>Click “Save” on the upper right. | 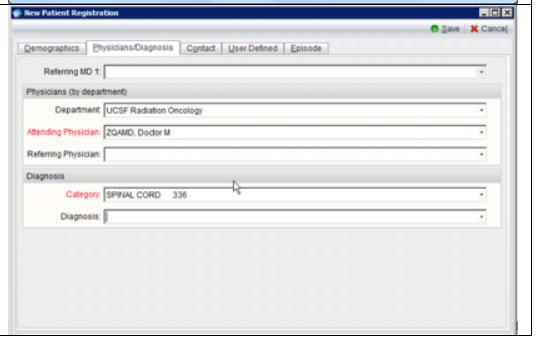 |





| | |
|---|---|
| Click “No”. | 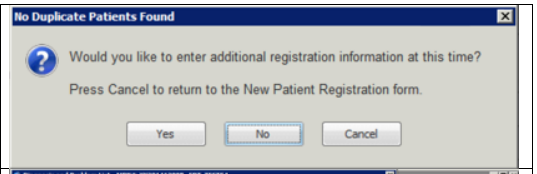 |
| **2. Add Diagnosis, Care Plan, Rad Rx, Site Setup, Tx Field**<br>Choose the “D&I” tab from the toolbar<br>  <br>or open it through eChart l Diagnosis and Interventions.<br><br>**The MD will do the part in gray:**<br>On the right hand side, click on “Diagnosis”.<br>Click on “Change” in the ‘Diagnosis and Problem List Window’.<br><br>Change the diagnosis and click on “Save and Affirm”.<br><br>Then “Close”. | 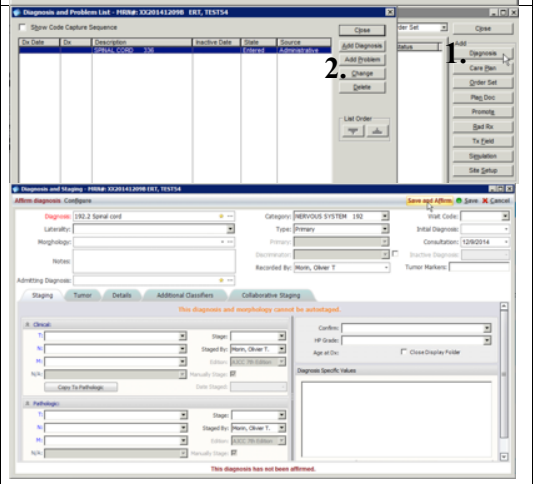 |
| Create a treatment course by clicking on “Care Plan”. | 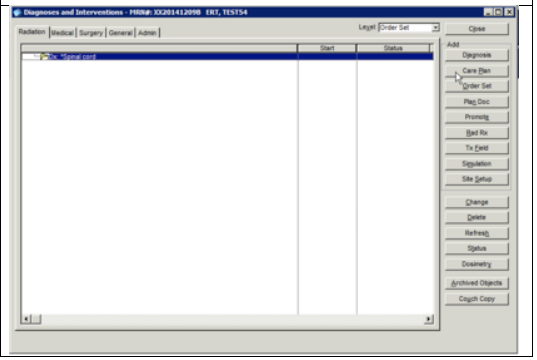 |

| | |
|---|---|
| Confirm with “Ok”. | 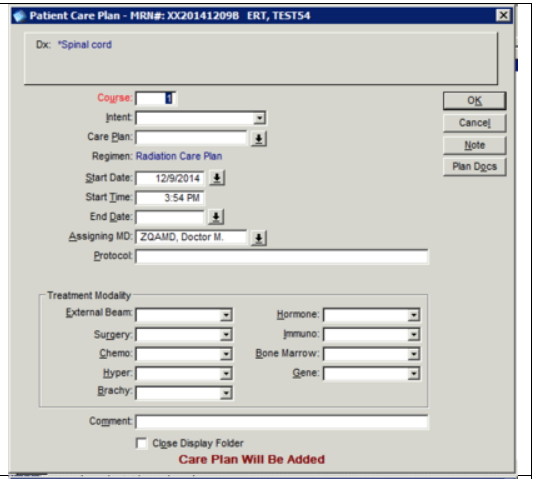  |
| In the ‘Diagnoses and Interventions’ window, click on “Rad Rx” and this window opens up.<br><br>Fill in the prescription for the treatment.<br>Example:<br>Rx Site: HetBone<br>Technique: AP/PA<br>Modality: 18MV/6MV<br>Dose Spec: CalcPoint, 100%<br>Rx Dose 1200 cGy<br>Fractional Dose 400 cGy<br><br>Click on the drop down arrow under ‘Fractionation Pattern’. | 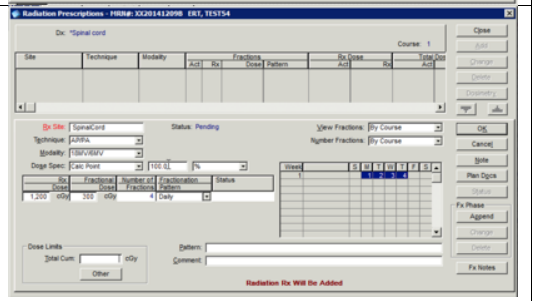  |





| | |
|---|---|
| If treatment is on the weekend or over a holiday, include ‘Saturday’, ‘Sunday’, or ‘Holidays’ on the bottom by clicking the according check mark.<br><br>Confirm the Setup Form with “OK”. | 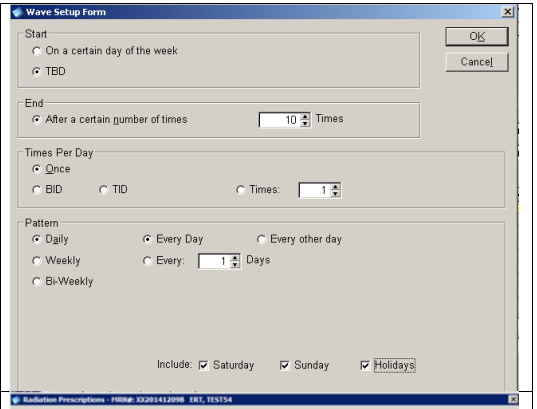  |
| Right click inside the Radiation Prescription window, choose ‘Status’ and approve the prescription. | 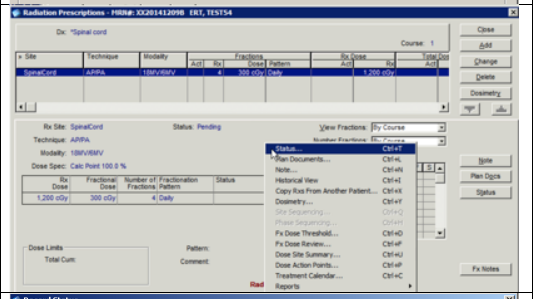  |
| Check “Approved”, sign with your password and close the window using “OK”. | 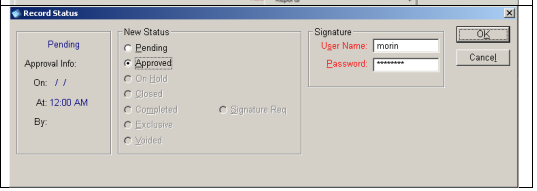  |

| | |
|---|---|
| In the 'Diagnoses and Interventions' window, click on "Site Setup" and this window opens up.<br><br>Fill in the fields in red:<br>Patient Orientation<br>Machine<br>Tolerance<br><br>Right-click into the window to approve the Site Setup. | 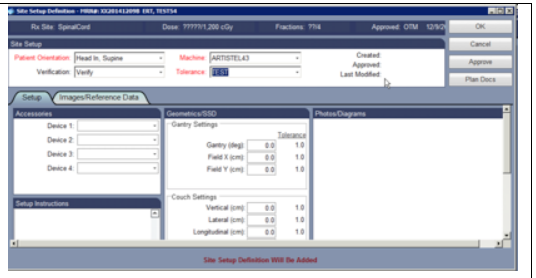 |
| In the 'Diagnosis and Interventions' window, click on "Tx Field" and this window opens up. Select "ARTISTEL43". | 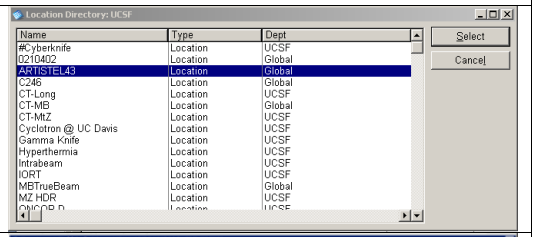 |
| Fill in the red fields:<br><br>Field: 900 4Planning<br>Tolerance: Emergency<br>Type: MVCT<br><br>Also fill in:<br>Monitor Units: 15<br>Couch Longitudinal: 50.0<br><br>Right-click into the window to approve. Confirm the warning window with "Yes".<br><br>Enter password to approve the field. Exit window with "OK". | 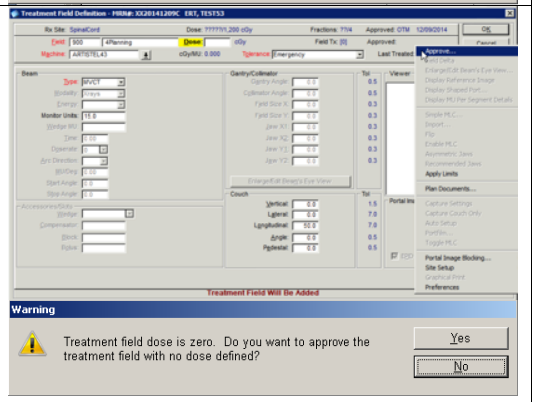 |







| | |
|---|---|
| In the 'Diagnoses and Interventions' window, click on "Dosimetry" and this window opens up.<br><br>Confirm with "OK".<br><br>Close the next window. | 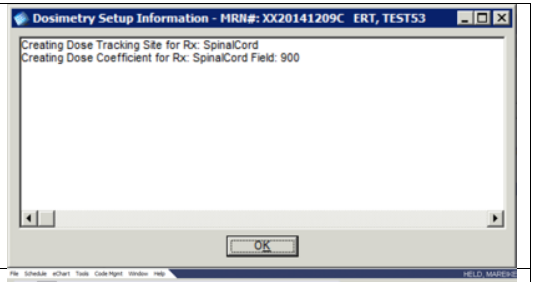 |
| **3. Schedule MV CBCT**<br>In the main tabs on top, choose "RO Treat".<br><br>  <br><br>Click on "Tx Calendar". | 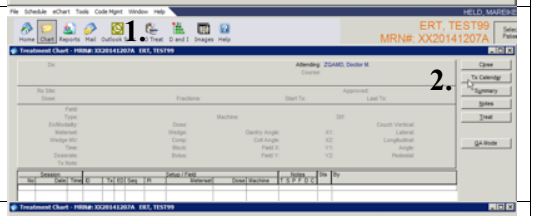 |
| Click on "Add" on the right side. | 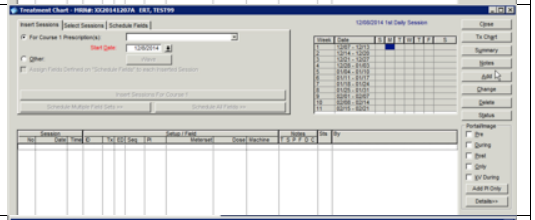 |
| Click on the arrow (1.) to open the calendar. Choose 'Today' and confirm with "OK".<br><br>Then, click on "Define" (2.) | 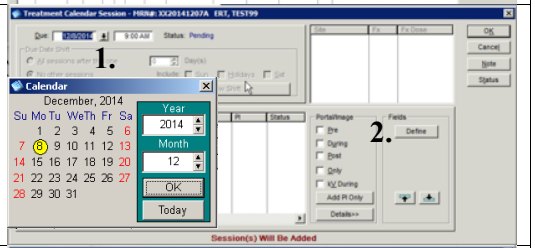 |
| Highlight the field 900 – 4Planning – MVCT on the left and add it to the right side.<br>Confirm with "OK", and the next window with "OK". | 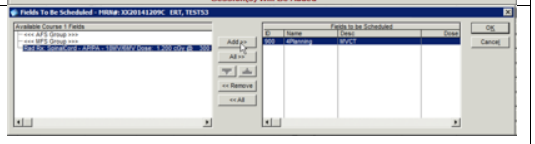 |

| | |
|---|---|
| Then click Tx Chart in the ‘Treatment Chart Window’.<br><br>This brings you back to the original RO Treat window.<br><br>At this point, the CBCT is ready to be delivered on the machine. The patient can be brought into the room at this point.<br><br>Click on “Treat”. | 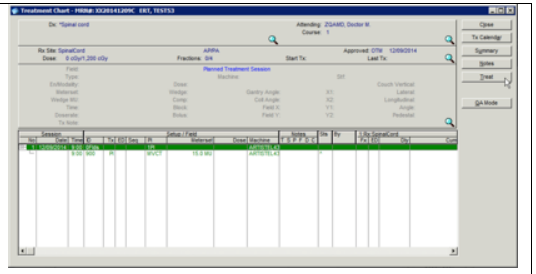 |
| Click “Continue” in this window.<br><br>Make sure that the Syngo computer is logged in and ready to receive the treatment field. | 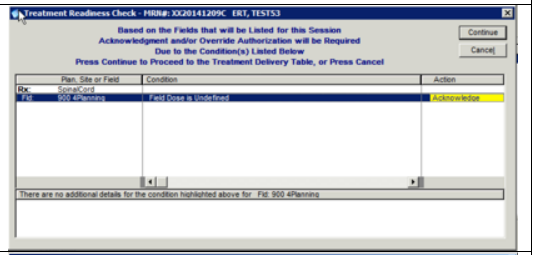 |
| Click “Send Plan” to send the field to Syngo. | 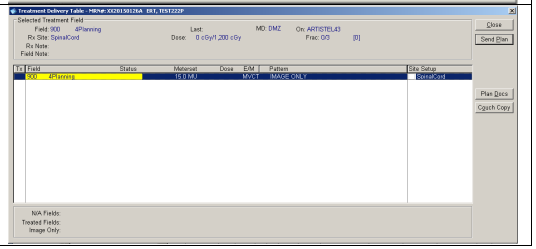 |





| | |
|---|---|
| Acknowledge the conditions and “Continue”. | 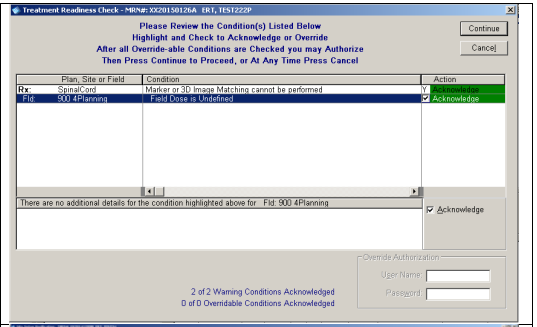 |
| Cancel the Site Setup Verification in this window and confirm with “Yes”.<br><br>MOSAIQ is now sending the field to Syngo. | 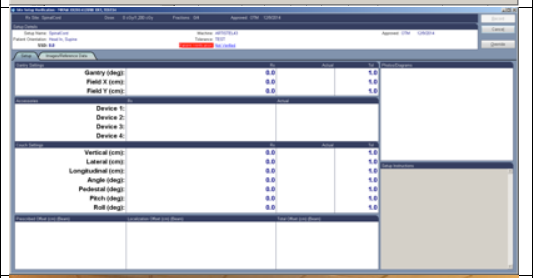 |
| **4. Setup patient**<br>Set up the patient as you expect they will be positioned during treatment. | 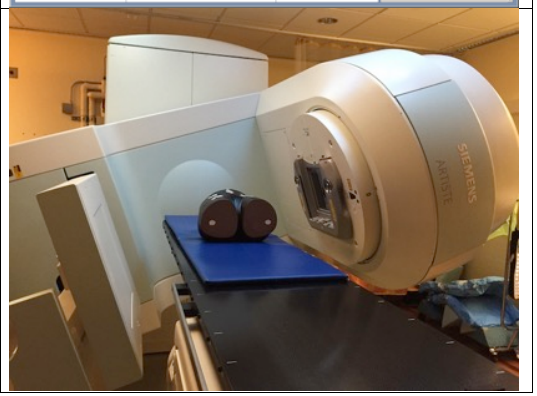 |

**5. Acquire MV CBCT**
On the Syngo computer, confirm to receive the treatment field with “OK”.

Click on the chart symbol at the bottom to select an imaging protocol.

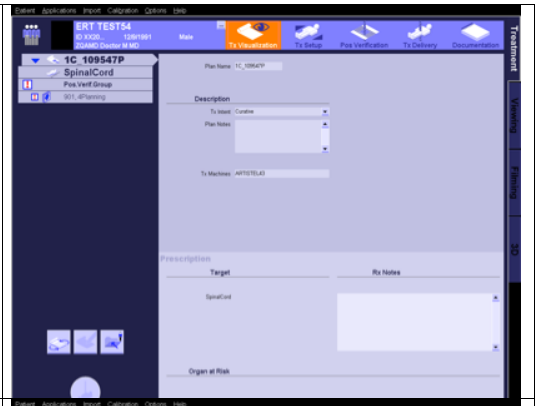

Right mouse click on to the treatment field and choose “Imaging Options”.

Choose the according imaging protocol from the drop down menu, in this case ERT_Pelvis_15MU_ eFOV_256.

(In case of a thorax treatment, use the protocol ERT_Thorax_15MU_ eFOV_256.)

Choosing the correct imaging protocol is important for the correct dose calculation in the TPS.

The patient size is defaulted to Medium. Keep this setting.

Click ‘OK’ and then on the chart at the bottom left to confirm the selection.

Check the box next to Pos.Verif.Group and click the round Treatment button on the bottom.


On the treatment console, use F12 to adjust the gantry and MV flat panel position.

| | |
|---|---|
| Double-click Accept. If necessary, override Longitudinal and Vertical table positions.<br>Wait for the machine to turn to a green ready light, turn the key and hit RAD-ON.<br><br>On the SYNGO RTT PC, the bottom left will show the projection of the patient during CBCT acquisiton.<br><br>The cone beam uses 15 MU and a clock-wise gantry rotation from 181° to 180°. |  |
| Wait until the image acquisition is completed and the images are loaded in Syngo.<br><br>Confirm this warning with “OK” and abort treatment on the X at the bottom.<br>  | 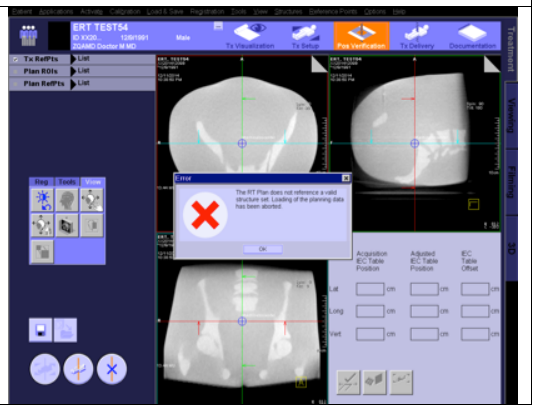 |





| | |
|---|---|
| **6. Export images to Pinnacle**<br>To export the images, open the patient browser by clicking on the “3 people symbol” in the top left corner.<br>  <br>Find the Patient in the Local Database and highlight the latest Cone Beam CT.<br><br>Only choose “Cone Beam CT”. Do **NOT** export any of the other fields.<br><br>In the toolbar on top, find “Transfer”, “Send to…” | 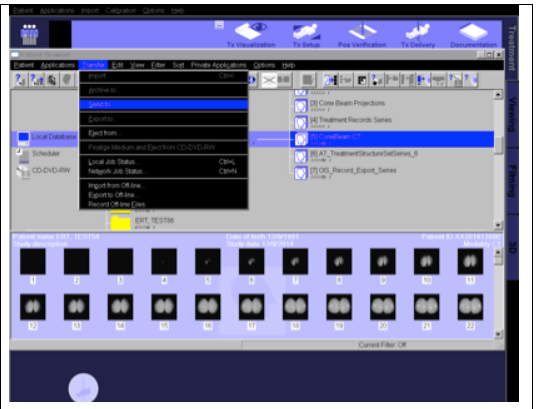 |
| Choose ‘Pinnacle’ from the list and click “Send”.<br><br>You can now close the patient in Syngo. Save changes before the unload. | 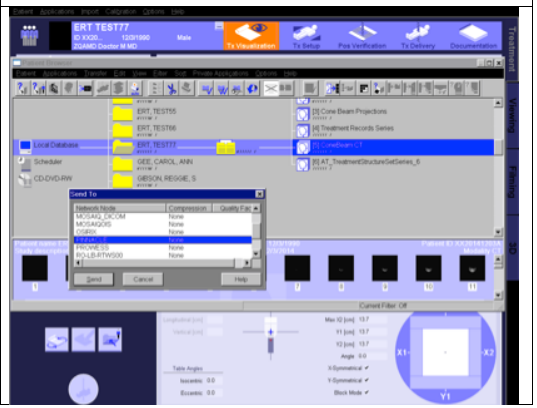 |

| | |
|---|---|
| On the MOSAIQ computer, record the delivered field by clicking on “Record”. | 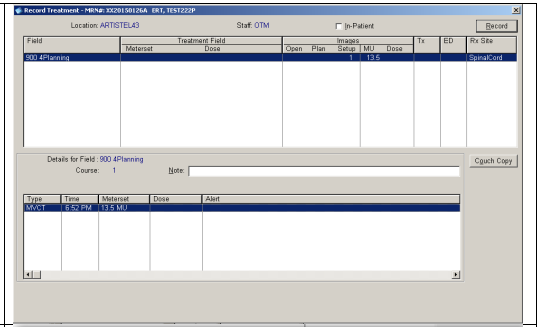 |
| Confirm to exit the dose delivery. | 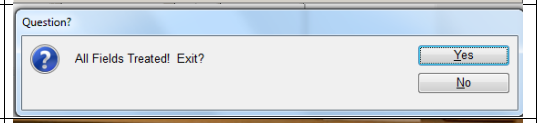 |
| **7. Treatment planning**<br>On the MOSAIQ CLIENT/DAILY QA computer:<br>Start up Oracle Virtual Desktop Client from the Desktop.<br>Log in to Pinnacle and click on the triangle icon to get to the home screen.<br> 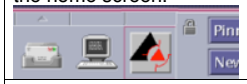 | 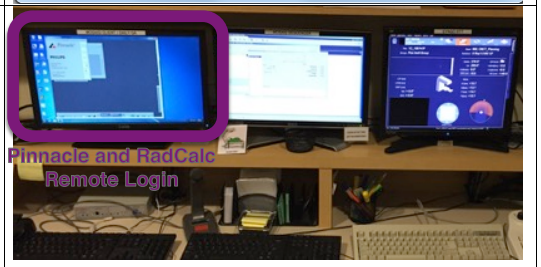 |
| Choose the Emergency_V9.8 Institution by clicking on “Institutions”.<br>  <br>Close window with “Dismiss”. | 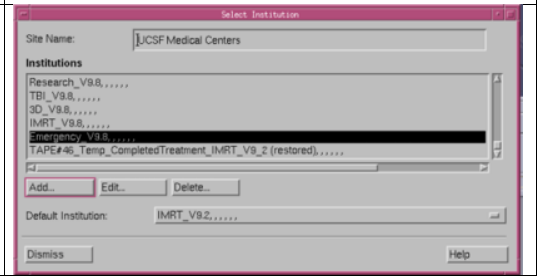 |





| | |
|---|---|
| Go to Planning.<br>  <br>Add a patient by clicking on the “Add” button under ‘Patients’. | 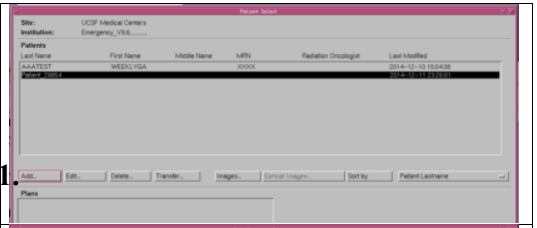 |
| Click on “Import Images”. | 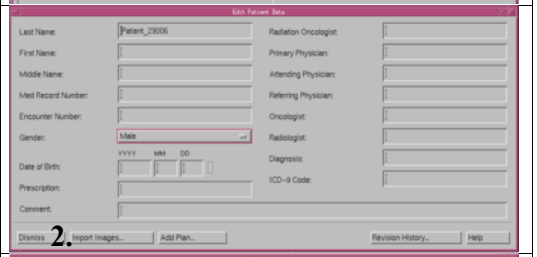 |
| Click “Add”.<br><br>Be patient, it might take a moment for the image library to pop up. | 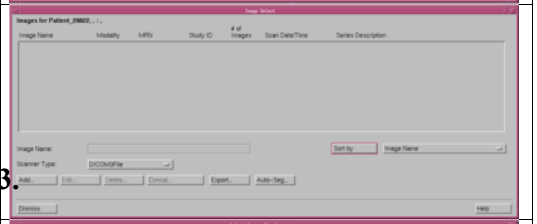 |
| Select the Patient and check the box next to the image set to import.<br><br>At the bottom, click “Import Images and Add Plan”. | 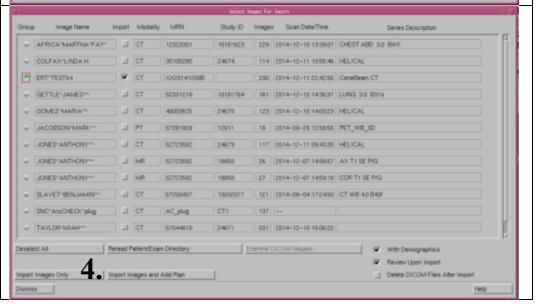 |

| | |
|---|---|
| Click on “Save and Exit” to continue. | 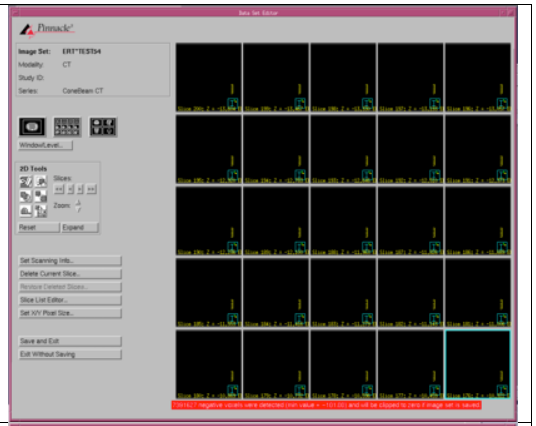 |
| Change the Plan Name to ‘SpinalCord’.<br><br>Under ‘Primary Image Set’, choose the CBCT image from the drop down menu.<br><br>Click “Planning” at the bottom. | 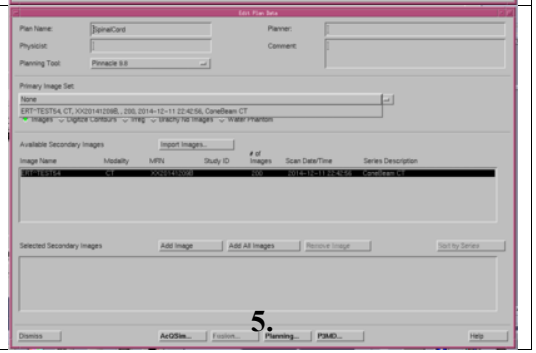 |





| | |
|---|---|
| Choose the ‘CT-Density Table’ corresponding to the imaging protocol that was used during the CBCT imaging. “Accept” at the bottom.<br><br>For a pelvis treatment, that would be Artiste eFOV Pelvis (Syngo imaging protocol ERT_Pelvis_ 15MU_eFOV_256).<br><br>(In case of a thorax treatment where the imaging protocol ERT_Thorax_ 15MU_eFOV_256 was used, use the ‘Artiste eFOV Thorax’ CT density table.) | 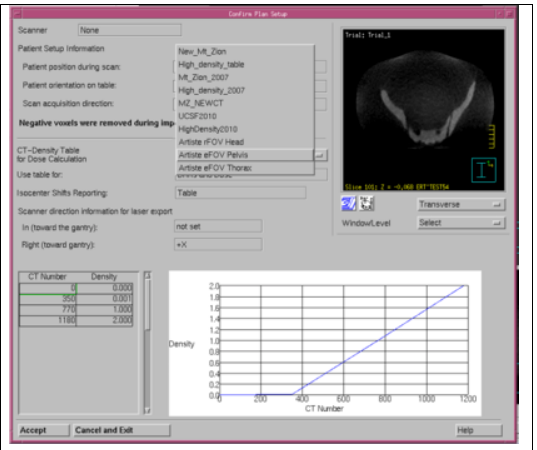 |
| Change the selection under ‘Remove couch from scan’ to “Yes”.<br><br>Click on the little icon next to ‘Location’<br><br>  <br><br>and place the couch (red line) below the posterior end of the patient. | 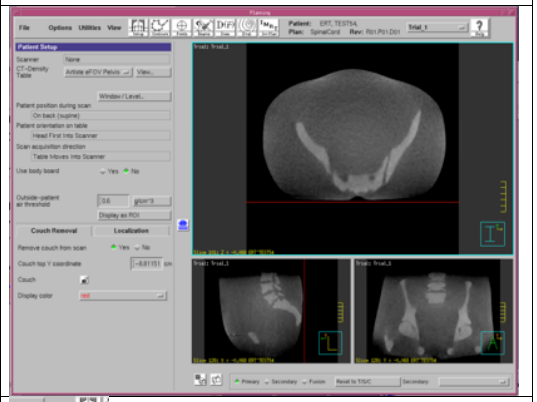 |
| At the top, under ‘Utilities’, choose ‘Scripting’. | 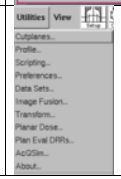 |

| | |
|---|---|
| Click on the HotScript “ERT_APPA_ONE” *2)<br><br>For detailed info on what happens within the script, refer to **Note3** below this procedure.<br><br>The script places necessary points, AP beam, changes the prescription and jumps into BEV. | 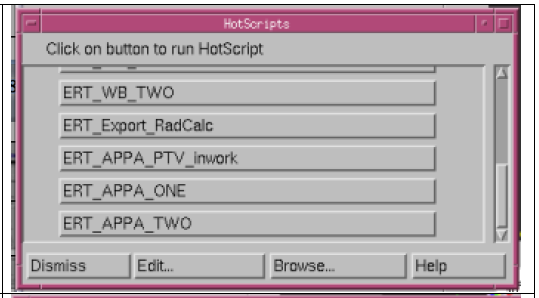 |
| *1)<br>If the script is not on your HotScripts list, click on “Browse”. Enter the directory<br><br>/home/heldma/Scripts<br><br>Select the script on the left hand side and click on “OK” at the bottom.<br><br>Wait for the script to run. | 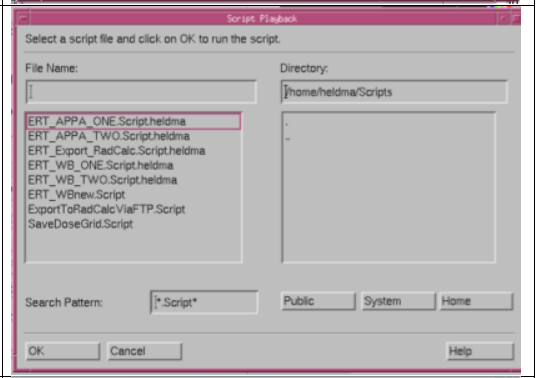 |
| At this point, the system is ready to define the treatment field. | 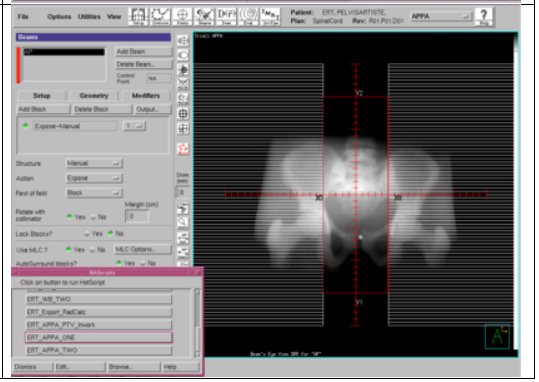 |





| | |
|---|---|
| Once ready, run the second script ERT_APPA_TWO.<br><br>Again, use the browse button if the script is not on the HotScripts list.<br><br>For detailed info on what happens during this script, refer to **Note4** below this procedure. | 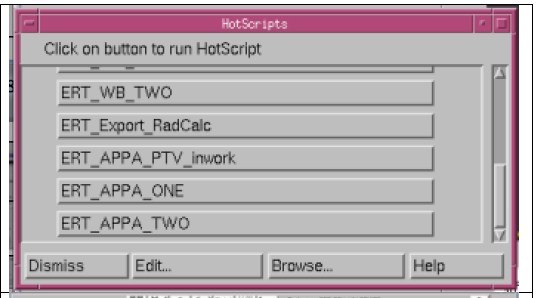 |
| The script uses Copy & Oppose for beam PA, adjusts the beam weighting to 34/66, and computes the dose for both beams.<br>**Isodose lines** are percentage values of 98% (red), 95% (yellow), 90% (green), 80% (blue).<br><br>It opens the ‘Eval’ tab and shows the prescription, MU, and beam weighting window.<br><br>The default prescription is set to 400 cGy per fraction to 100% of point dose at “CalcPt1” for 4 fractions. | 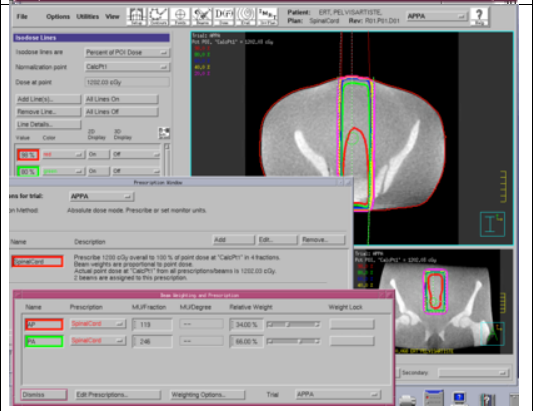 |
| Verify the prescription, beam weighting, dose distribution and MU per beam.<br>**NOTE: If the patient has already been treated previously, make sure that the field ID 11 and 12 are unique. MOSAIQ does not allow importing beams with the same field ID.**<br><br>Change the Field ID if necessary (check in | 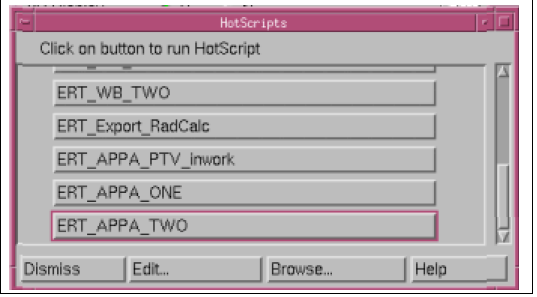 |

MOSAIQ) to unique IDs under the beam tab.


Do so for both LTLAT and RTLAT beams.

Once the plan is ready for second dose check and export, use a script to export the plan to RadCalc.

Under 'Utilities', 'Scripting', choose 'ERT_Export_RadCalc' or use the 'Browse' button to call the script.

It chooses the CalcPt1 as the reference point.

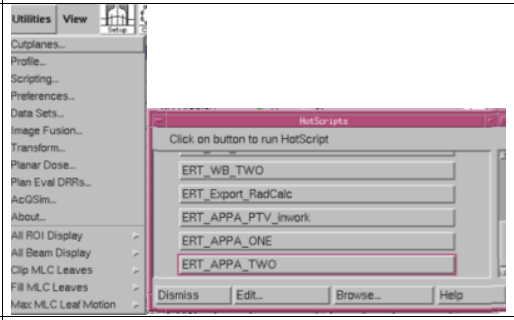


Minimize the Pinnacle window for now.

**8. MU verification**

Open RadCalc using the RadCalc Shortcut on the Desktop.

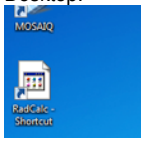


Confirm the Security Warning with "Run".

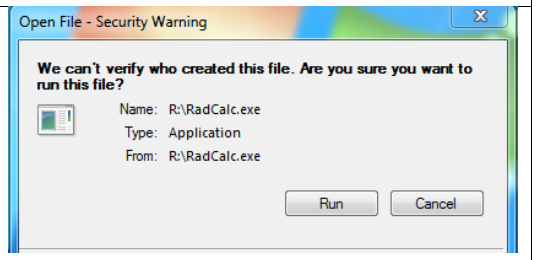


Log in to RadCalc with your username and password.

Click on "Import" to import the patient plan.


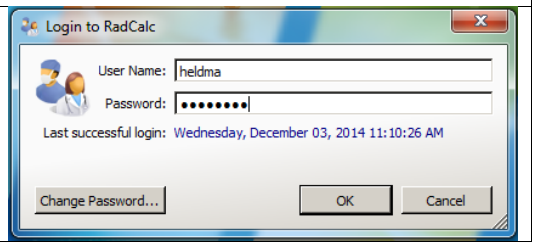






Select patient and click on "Import Selected" at the bottom.

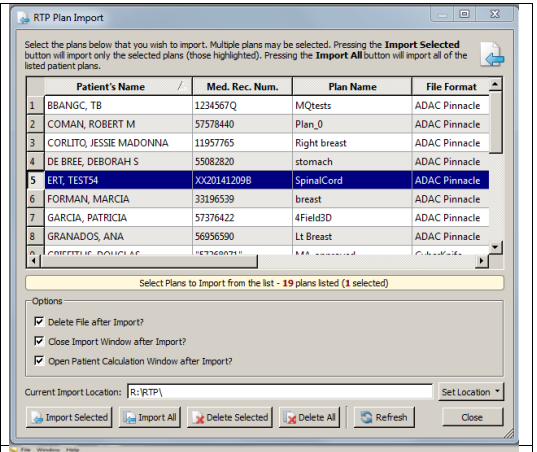


Double-click on the plan to open.

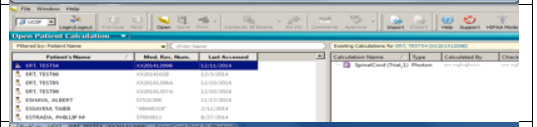

The first window summarizes the prescription.

Prescription Isodose and Scatter Dose are not required.

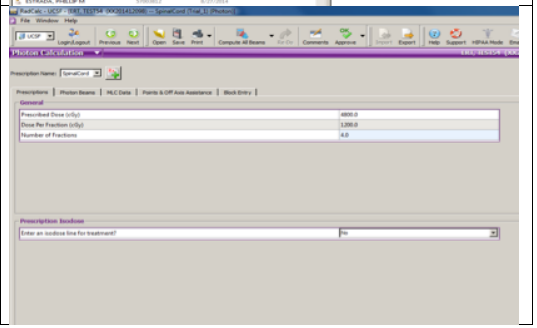

| | |
|---|---|
| Open the second tab 'Photon Beams'.<br><br>Verify that all the information is correct. Under Beam Setup, 'Calc Pt' should be set to 'CalcPt1'.<br><br>In the yellow window in the upper right corner are the MUs calculated for this beam by RadCalc, by Pinnacle, and %Diff. | 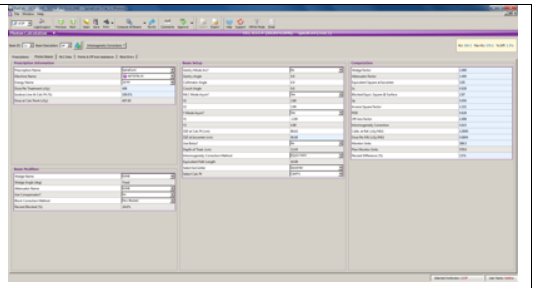 |
| Under 'Beam Description', choose the second beam "PA" from the drop down menu and verify the same way as the first beam.<br><br>The %Diff should be less than 5% for both beams.<br><br>(In case %Diff > 5%, change the placement of the point in Pinnacle away from sharp dose gradients and export to RadCalc again.) | 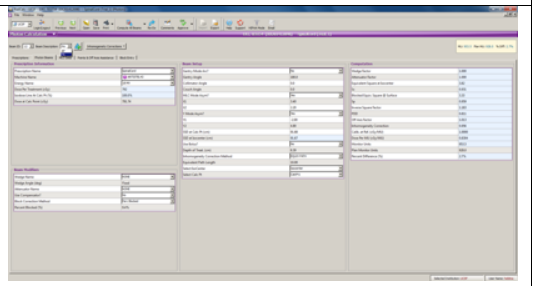 |
| Print the RadCalc check. Under File → Print. | |
| Close RadCalc and maximize the Pinnacle Virtual Desktop Window again. | |









| | |
|---|---|
| **9. Export plan from Pinnacle to MOSAIQ**<br>The 'ERT_Export_RadCalc' script also prepares the export to MOSAIQ and automatically checks the following checkboxes for export:<br>RT Plans<br>Prescription SpinalCord<br>RT Structures<br>DICOM Image<br><br>Destination AE Title: IMPAC_DCM_SCP<br><br>Click on "Transmit Data" and wait until finished.<br> 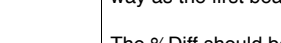 | 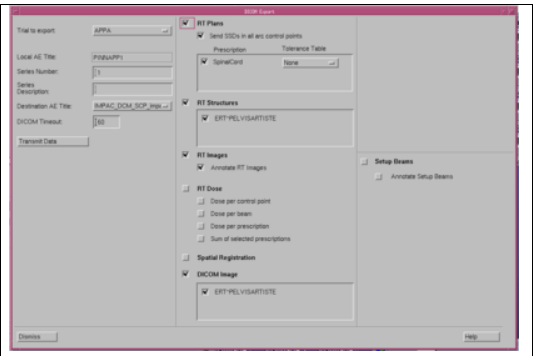 |
| Click "OK" in the pop-up box. | 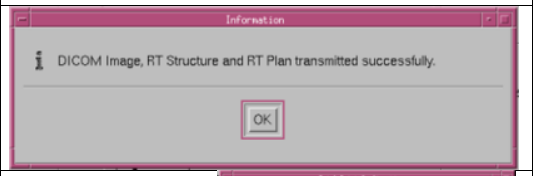 |
| Print the plan.<br>Got to File → Print Plan<br><br>Make sure to select Long Ricoh printer.<br>  | |
| Under File, exit, save and close patient plan and exit | |

| | |
|---|---|
| Pinnacle. | |
| **9.B Create PDF for MOSAIQ** | |
| **10. Import plan to MOSAIQ**<br>In MOSAIQ, go to RTP Import. Either click the symbol on the tool bar<br>  <br><br>or find it under File I Import/Export I RTP Import.. | 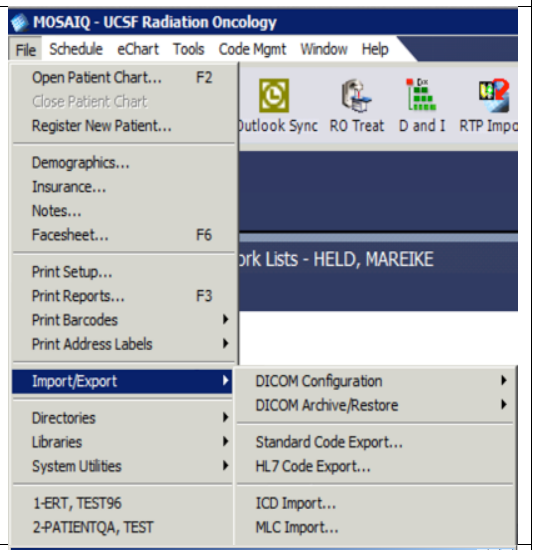 <br> |
| Choose \\Mosaiqapp\ MOSAIQ_APP\UCSF_ APP\RTP from the drop down menu.<br><br>Select the patient to import. | 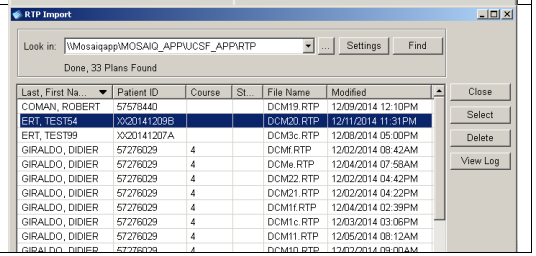 <br> |





| | |
|---|---|
| Click on the red highlighted ?? in the column ‘Action’ next to Radiation Oncology Course.<br>Choose XX - Ignore to ignore this field during import.<br>  <br> | 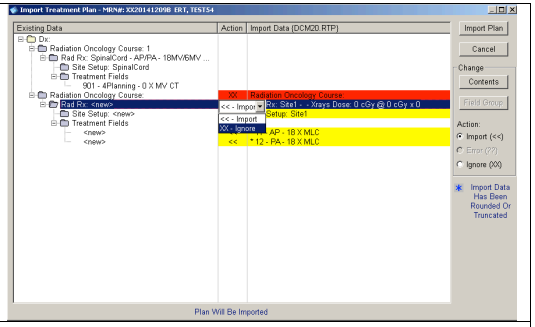 <br> |
| Click on the green << in the column ‘Action’ next to Rad Rx: Site1.<br>Choose XX - Ignore to ignore this field during import.<br>  <br><br><br>Double click on the yellow field “Site Setup: Site1” | |
| In the yellow highlighted line, click on the empty field in the column ‘Import Data’ and choose ’11 TEST’.<br><br>In the top row ‘Rx Site Name’ replace Site1 under ‘Import Data’ with the Rx Site name entered previously when creating the prescription. In this case it is “SpinalCord”.<br><br>Make sure that the Rx Site Name is identical to the previously entered Site Name.<br><br>Confirm with “OK”. | 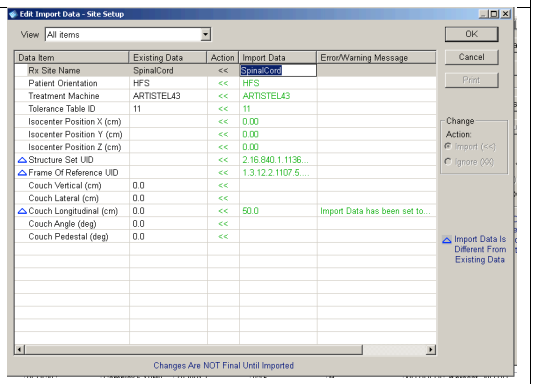 <br> |

| | |
|---|---|
| Highlight the first treatment field. On the right hand side, click on “Field Group”.<br><br>Choose the Site Name ‘SpinalCord’ entered previously from the drop down menu and select the Tolerance Table ‘8 Emergency’.<br><br>Finalize the import by clicking “Import Plan”. | 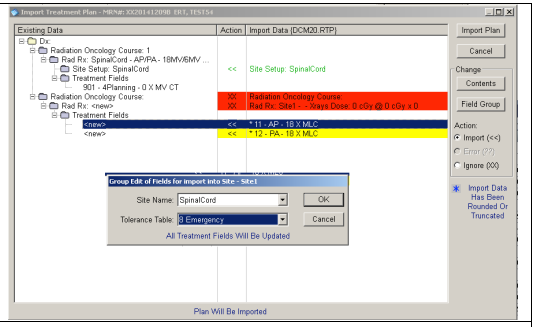 |
| **11. Associate DRR images** screenshots | |
| Close the RTP Import Window and open D&I.<br>  | |
| **12. Approve Site Setup and Treatment Fields**<br>Double click on Site Setup.<br><br>Verify the correct Patient Orientation and Machine are entered and approve the Site Setup. | 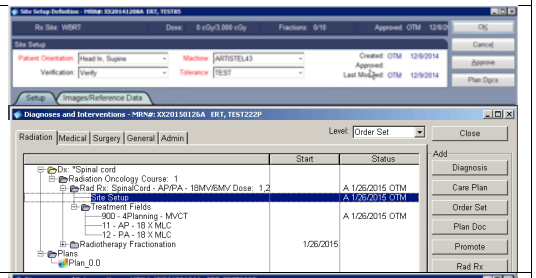 |
| Highlight treatment field 900 4Planning MVCT.<br><br>Click on “Tx Field” on the right side. |  |
| Confirm to copy treatment field with “Yes”. | 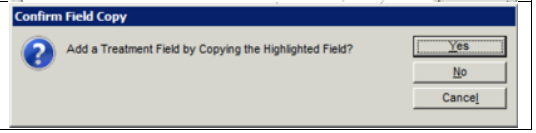 |





| | |
|---|---|
| Enter beam ID 901 4Setup under Field:<br><br>Verify that all beam parameters are correct and Longitudinal Couch Position is 50.00.<br><br>Right click into the window to approve beam 901. Confirm the warning with “Yes”. | 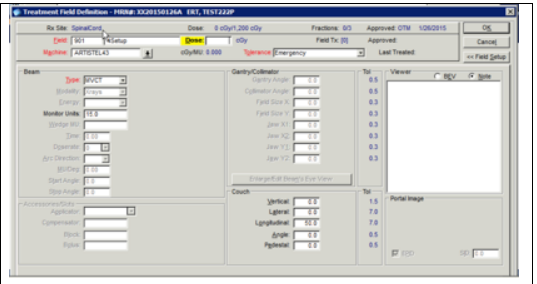 |
| Highlight and right click on the previous treatment field 900. Choose ‘Hidden Tx Field’ to hide this field for delivery.<br><br>It should now have “AH” before the approval stamp under ‘Status’ in the D&I window. | 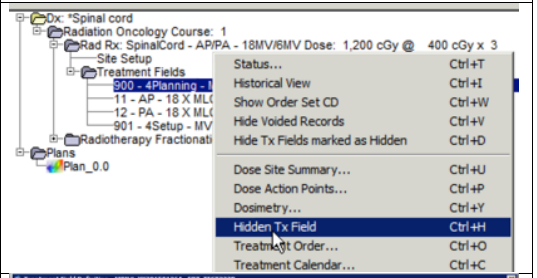 |
| Double-click on the treatment field 11 – AP.<br><br>Verify all beam, Gantry/Collimator, and Couch parameters.<br><br>Then, right click into the window to approve the field.<br><br>Close window with “OK”. | 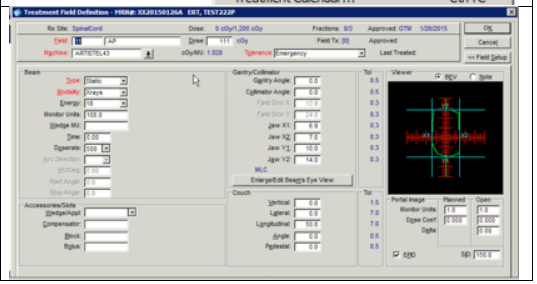 |

| | |
|---|---|
| Accept the new field. | 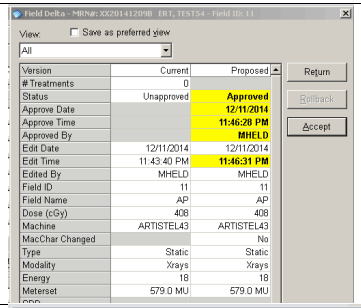 |
| Repeat the same for treatment field 12.<br><br>Double click on the treatment field 12 – PA, verify that all beam parameters are correct and approve the field. Accept in the Field Delta window as above. | 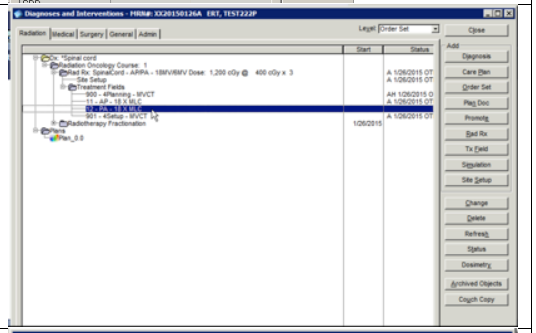 |
| For dose tracking, create the dose coefficient for the new beams by clicking on “Dosimetry”.<br><br>Confirm the Dosimetry Setup Information with “OK”. | 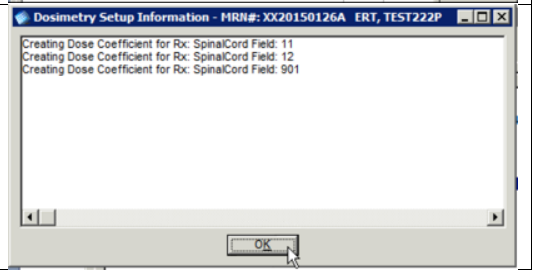 |





| | |
|---|---|
| Close the Dosimetry Setup window. | 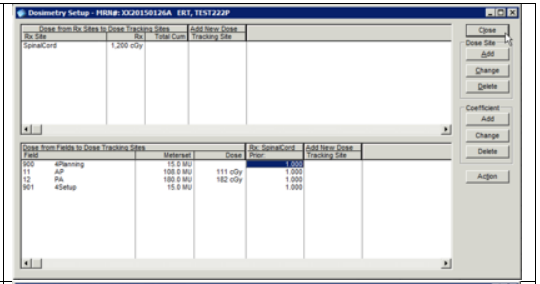 |
| **13. Verify patient position and treatment field delivery**<br>Open the Treatment Chart window by clicking on the “RO Treat” tab.<br>  <br>Open ‘Tx Calendar’ on the right. | 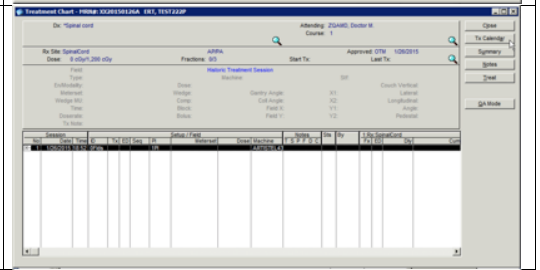 |
| Click on “Add” on the right side to add a new treatment session. | 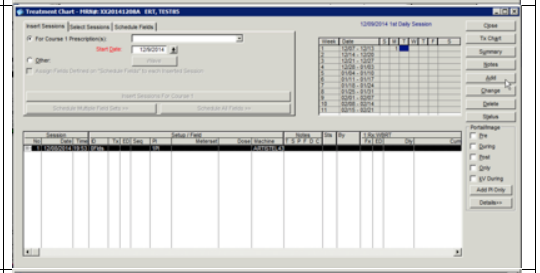 |
| Choose today’s date under ‘Due’ and confirm with “OK”.<br><br>Then, click on “Define”. | 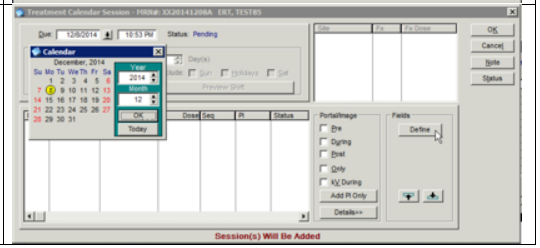 |

| | |
|---|---|
| Add both treatment fields under the prescription SpianlCord from the left to the right by using the “Add>>” button.<br>Confirm with “OK”. | 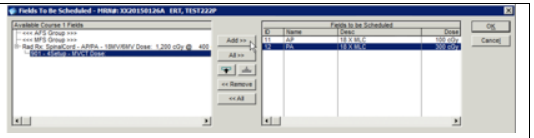 |
| Click on “Details” in this window to enable port imaging. | 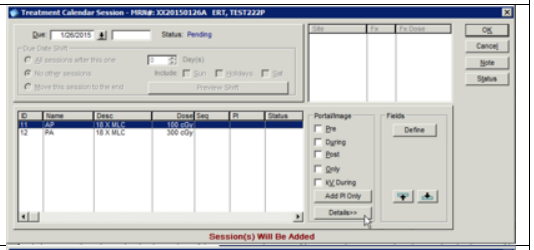 |
| Check the box next to ‘Only’ and choose “Plan-Open”.<br><br>Confirm with “OK”. | 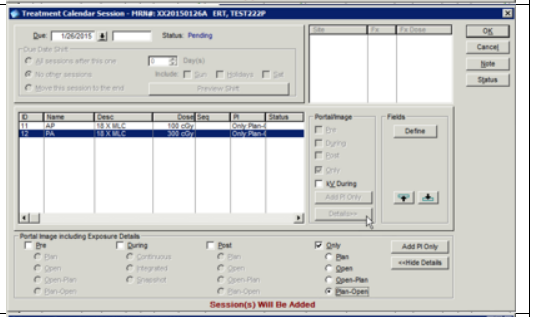 |
| Confirm the next window with “OK”. Return to ‘RO Treat’ by clicking on “Tx Chart”. | 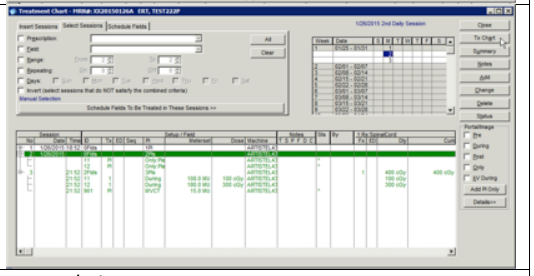 |
| Acquire portal images for both beams. | screenshot |





| | |
|---|---|
| **14. Schedule treatment fields**<br>Open the Treatment Chart window by clicking on the “RO Treat” tab.<br>  <br>Open ‘Tx Calendar’ on the right. | 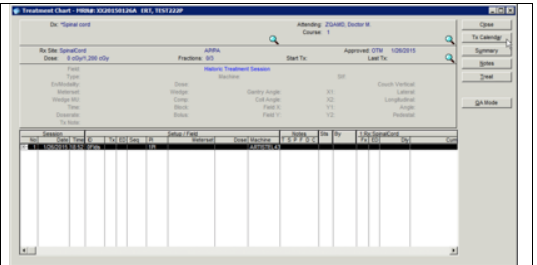 |
| Click on “Add” on the right side to add a new treatment session. | 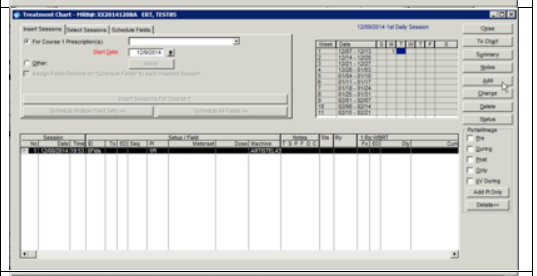 |
| Choose today’s date under ‘Due’ and confirm with “OK”.<br><br>Then, click on “Define”. | 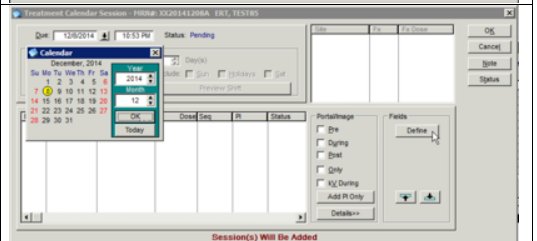 |
| Add all fields under the prescription SpinalCord from the left to the right by using the “Add>>” button.<br>Confirm with “OK”. | 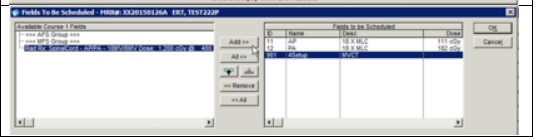 |

| | |
|---|---|
| Confirm the next window with “OK”. Return to ‘RO Treat’ by clicking on “Tx Chart”. | 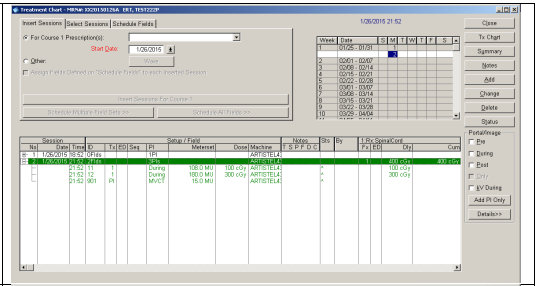 |
| All scheduled treatment fields should be green.<br><br>Click “Treat” to proceed with the treatment. | 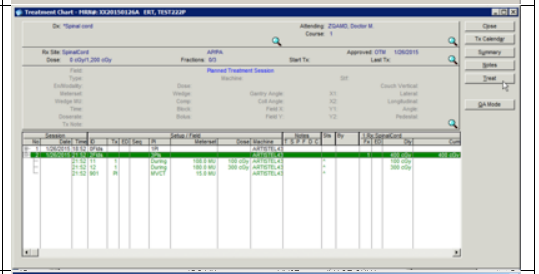 |
| Continue. | 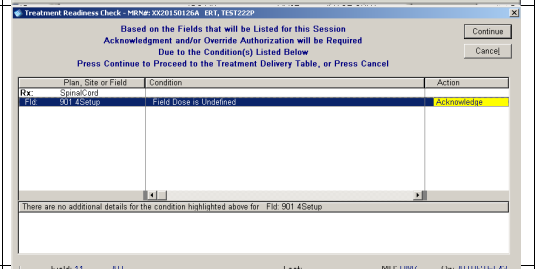 |
| Right click into this window to load the reference data. | 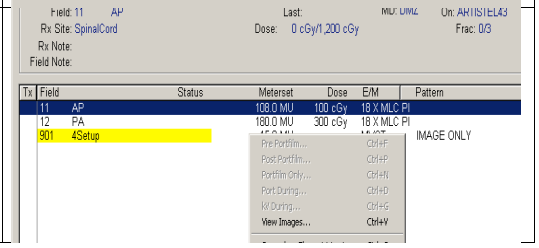 |





| | |
|---|---|
| Wait until DICOM data is sent. | 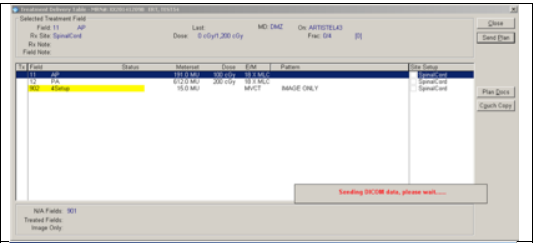 |
| Acknowledge the condition in the Treatment Readiness Check window and click “Continue”. | 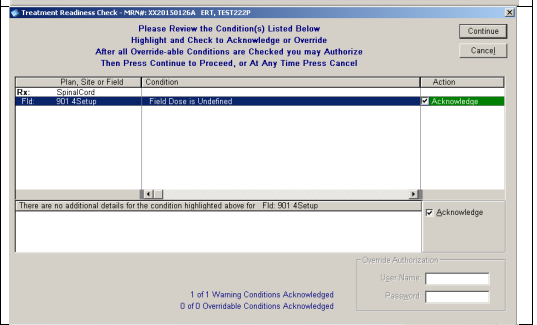 |
| Cancel the Site Setup Verification. | 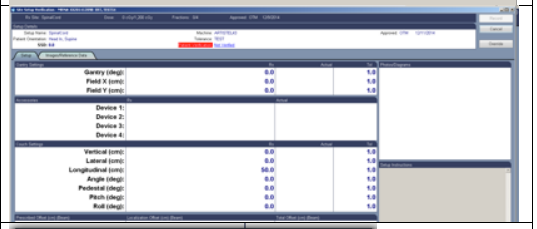 |
| Confirm to cancel. | 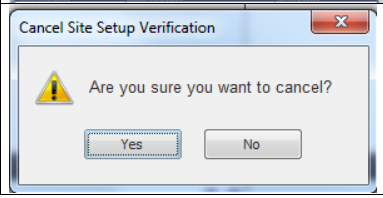 |

| | |
|---|---|
| Retrieve the plan on the Syngo station. | 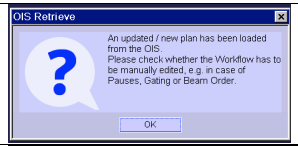 |
| **15. Confirm patient setup with MV CBCT**<br>If necessary for setup, acquire another cone beam.<br><br>To choose a CBCT protocol for the 901 4Setup cone beam, click on the chart symbol in the lower left corner.<br>  | 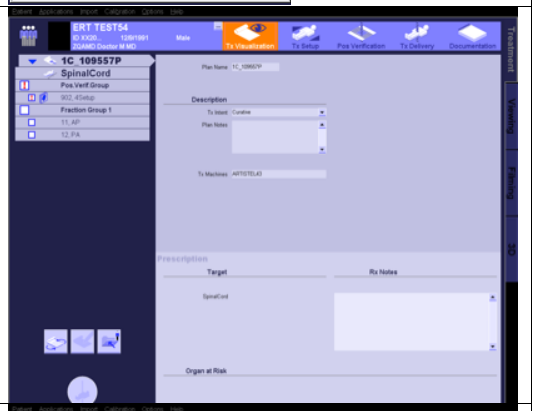 |
| Right click onto the 901 treatment field and choose ‘Imaging Options’.<br><br>Choose any protocol that you think is suitable for patient setup verification. For example ‘8MU Pelvis Bony Setup’.<br><br>Verify with ‘OK’ and click the chart symbol again to return to the field delivery window.<br>  |  |





| | |
|---|---|
| Check the boxes next to both ‘Pos.Verif.Group’ and ‘Fraction Group 1’.<br><br>On the treatment console, move the gantry, collimator, and MV flat panel into position. Double click “Accept”.<br><br>In Syngo, override the table position if necessary and approve with password. |  |
| Acquire the cone beam CT. |  |

| | |
|---|---|
| Once the cone beam is taken, it automatically goes into the 'Pos Verification' tab on the Syngo computer.<br><br>Change the view using any of the tools on the left side of the screen. |  |
| Use automatic alignment or align the cone beam image manually to the reference image.<br> 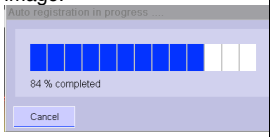 <br><br>Once complete, 'accept offset'.<br>  <br>Apply the offset before treatment. | 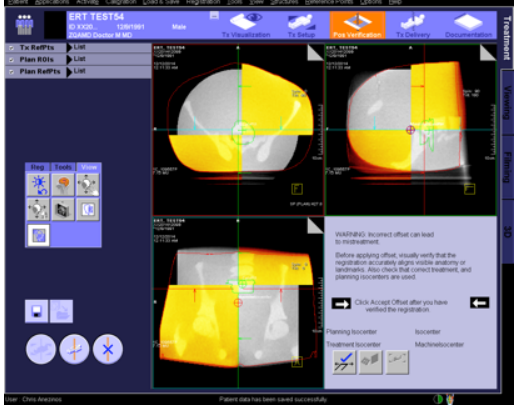 |
| Apply offset<br>  <br>and confirm to 'apply offset' that is shown in the small window. | |





| | |
|---|---|
| **16. Treatment**<br>Press RadOn on the treatment console to proceed with the treatment delivery. | |
| Once all fields are delivered, close out the patient from Syngo<br>  <br>and record the delivered dose in MOSAIQ. | |

**Note3:**
**What script #1 ERT_APPA_ONE does:**

- Changes Trial name to 'APPA'
- Sets localization to 0, 0, 0
- Places point at 0, 0, 0, and names it Isocenter
- Changes POI type to Isocenter
- Places a second point at 0, 0, 0
- Names that point CalcPt1
- Adjusts window level for CBCT view
- Contours external, names it "Tissue", ROI type 'External'
- Cleans up contour
- Adds AP beam with field ID 11
- Chooses the treatment machine ArtisteL43, 18MV and Isocenter
- Adds a block to expose manual contour
- MLCs are enabled
- Jaws are asymmetric and MLCs automatically adjust to the jaw position
- Jaws are opened to 30 cm x 10 cm
- Draws dose grid based on external contour "Tissue"
- Sets default prescription of 1,200 cGy overall dose for 4 fractions
- Names prescription "SpinalCord"
- Dose is prescribed to POI "CalcPt1"
- Goes into BEV and adjusts the window for DRR
- Increases BEV resolution to 555
- Displays DRR in BEV automatically
- Goes to the beam tab, opens BEV and is ready to draw blocks.

**Note4:**

**What script #2 ERT_APPA_TWO does:**

- Copy & Oppose beam
- Beam name, beam ID
- Adjusts beam weighting to 34/66.
- Computes dose for both beams.
- Adjust isodose lines to 'Percent of POI dose' with POI 'CalcPt1'
- Isodose lines are 105% (red), 100% (yellow), 90% (green), 60% (blue), 20% (purple)
- Draws thick lines
- Opens prescription window and beam weighting window
- Jumps to the Evaluation tab for plan review





# RTT Emergency and Urgent RT Checklist

Patient: _____ Date: _____

BEFORE PT ARRIVES:

- ☐ **MOSAIQ** - Patient is entered in MOSAIQ
- ☐ **Diagnosis** is saved and affirmed by MD
- ☐ **Prescription** is signed by MD
- ☐ **MV CBCT** field is in MOSAIQ and scheduled

WHEN PT ARRIVES:

- ☐ **Consent** form must be signed, dated and witnessed
- ☐ **ID checked**
- ☐ **Patient Setup** with machine iso close to treatment iso
- ☐ **MV CBCT protocol** is one of the ERT protocols depending on Tx site

TX PLANNING:

- ☐ **Tx plan** approved by MD
- ☐ **RadCalc** MU check is within 5%

TX DELIVERY:

- ☐ **Rx treatment fields** are checked and MU verified with Pinnacle plan
- ☐ **Pt position verification** with CBCT or portal images
- ☐ **Prescribed daily dose** is carried correctly after first tx delivery
- ☐ **Tx charge** double check. **Capture** all charges and **document** with appropriate notes in MQ

## SIMULATION WORKSHEET

PATIENT _____ DATE _____

Machine _____ MD _____ Sim Tech _____

2 Pt identifiers: Name _____ DoB _____

Treatment Site: _____

Patient Position:

Supine _____ Prone _____ Other _____

Head first _____ Feet first ___ Arm position _____

Positioning Device:

Headrest _____ Mask _____ Mold _____

Knee/ankle sponge: red _____ blue _____ black _____

Comments:

_____

_____

_____

PARAMETERS:

Distance: SSD SAD ODI: _____ Table Top: _____

SFD: _____

Field size: X1 Y1

X2 Y2

Separation: _____

Gantry angle: _____ Collimator angle: _____ Couch angle: _____

# APPENDIX E

## Report on the Installation of the In-Line kView System on the Siemens Artiste Linear Accelerator

UCSF implemented the so called "In-Line kView" system on their Siemens Artiste linac in March 2013. It is a new patient MV CBCT imaging system that reduces the beam energy while acquiring CBCTs. The main technical differences are the use of a carbon target instead of the usual tungsten treatment beam target and the removal of the flattening filter when in imaging mode. The carbon target is chosen because of its lower atomic number. Image quality is improved due to less heavy filtration of the low-energy bremsstrahlung. Additionally, a low-MV beam energy is used, shifting the energy spectrum towards the kV-range, which ultimately results in better image contrast. This is summarized in Figure E.1. Furthermore, Faddegon et al. [61] provide extensive detail on the system.

The installation requires opening up the treatment head to reach the target tray, which makes this a critical procedure on the machine. While the replacement of the target only takes a few hours, the subsequent tuning of the machine to its previous state requires two full days. Siemens engineers from Germany and the US were on site for the installation and subsequent tuning of the beam.

Figure E.2 shows the Siemens Artiste linac at the beginning of the installation with its covers removed. To reach the target tray, heavy lead shielding

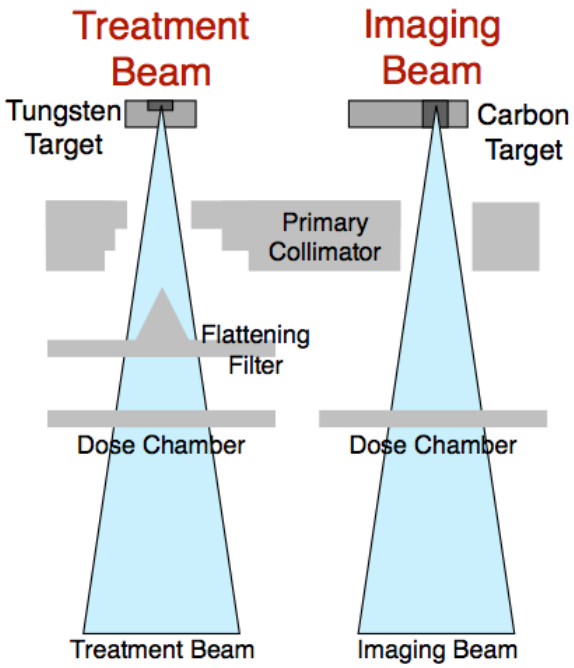


**Figure E.1:** Schematic of the original and the upgraded CBCT imaging system.

needed to be removed. The target tray slides out on the side of the linac head.

**Day 1**

First, the target tray is removed, which is shown in Figure E.3(a). The large circle on the left is the target that is used to produce the photon beam for therapy. The five smaller slots on the left hold electron scatter foils, which are used for electron treatments. The 21 MeV electron scatter foil is removed and replaced with the carbon target. Figure E.3(b) shows the electron scatter foil tray in comparison to the size of a one cent piece. On the left, the carbon target is inserted. In this case, the photon target is replaced as well due to oxidation around the target shown in E.3(a). This was probably caused by a water leakage near the target. The target tray with the replaced tungsten target and the new carbon target is shown in Figure E.3(c).

Next, the high range power supply is updated to enable monitoring the dosimetry of an additionally beam.

**Day 2**

Cables are run to attach the electron chamber, which monitors the beam, to the power supply. A new software is installed to monitor and run the addi-

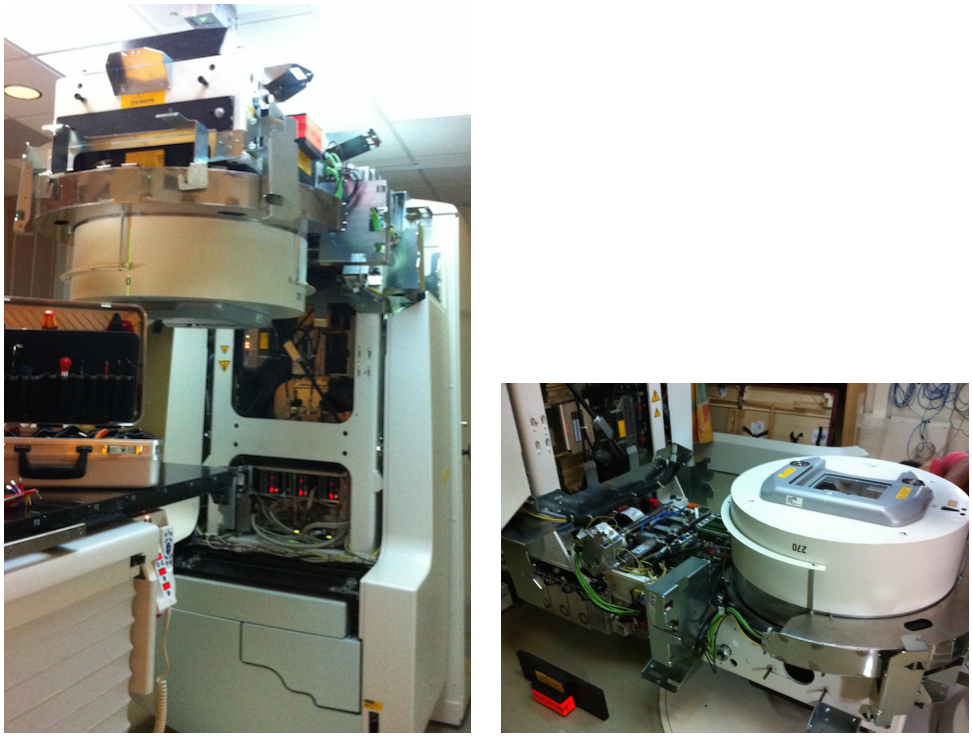

(a) Siemens Artiste without covers and the gantry at 0deg.

(b) Siemens Artiste with the gantry at 180deg.

**Figure E.2:** The Siemens Artiste without its covers while trying to remove the target from the linac head.

tional beam from the treatment console. Also, the hand controller inside the treatment room is updated .

**Day 3**

The imaging beam is tuned to a 4 MeV beam. Since the flattening filter will be removed during imaging, which usually filters out a large amount of the low energy photons, the photon beam past the target will have an energy that is more accurately described as a 1 MV beam. The beam's properties are characterized using the Blue Phantom (IBA, Schwarzenbruck, Germany), which is a 68 cm × 65 cm × 56 cm water phantom. For a field size of 10 cm × 10 cm, the 1 MV beam depth dose at 10 cm depth is 55% of the maximum dose, compared to 67% at 10 cm depth for the 6 MV treatment beam. The dose maximum of the 1 MV beam is at 0.67 cm depth, compared to 1.5 cm maximum depth for the 6 MV beam. Figure E.4 summarizes this in a plot.

Finally, the machine quality assurance was run to ensure that the linac per-

forms the same way in treatment mode as it did previous to the upgrade. The mechanical machine isocenter is re-aligned with the radiation iso center and the light field.

Figure E.5 compares the images produced by the original CBCT system and the new in-line kView system.

(a) The bottom view of the old photon target (left) and electron scatter foils (right). The greenish powder around the photon target shows the oxidation.


(b) The slots containing the electron scatter foils and the carbon target hidden under the silver cover (top)

(c) The top view of the new photon target, the electron scatter foil slots, and the carbon target.

**Figure E.3:** The old and new photon target next to the electron scatter foil slots. The carbon target is taking the spot of one electron scatter foil.

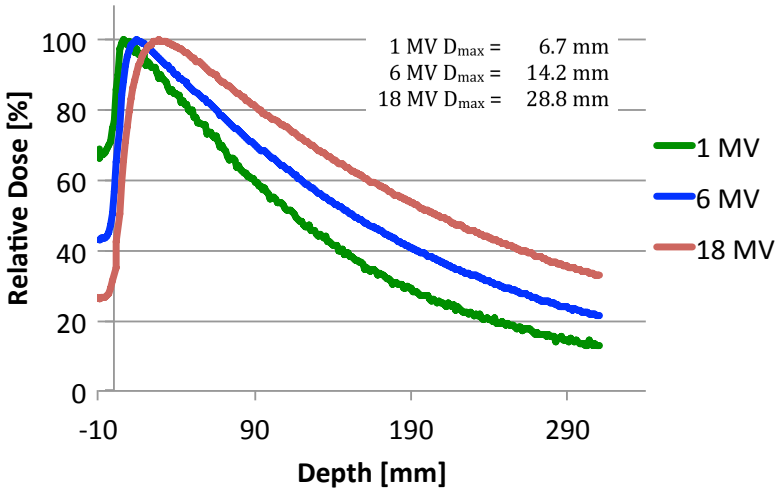


**Figure E.4:** Percentage Depth Dose (PDD) profiles of the 1 MV, 6 MV, and 18 MV photon beam after the installation of the in-line kView system.

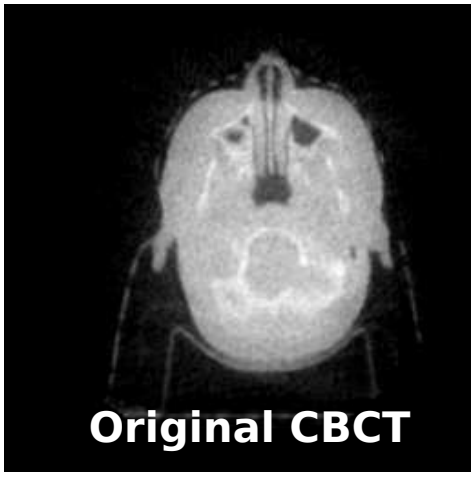


(a) Head CBCT acquired with the original treatment beam line CBCT before the upgrade.


(b) The same patient as in (a) imaged with the new In-Line kView imaging system.

**Figure E.5:** The same patient was imaged on the original treatment beam line before the upgrade and the new In-Line kView system after the upgrade.

# APPENDIX F

## Measured Modulation Transfer Functions for On-Board CT systems

### Purpose

To compare the spatial resolution of different CT systems.

### Materials and Methods

The cylindrical phantom (CatPhan 500, The Phantom Laboratory, Greenwich, NY) contains multiple slices with different properties to measure image quality. The CTP528 module contains between 1 to 21 line pairs per cm. The phantom is imaged on five different CT machines, including the MX8000 kV CT (Philips, Amsterdam, NL), TrueBeam kV CBCT (Varian, Palo Alto, CA), VersaHD kV CBCT (Elekta, Crawley, UK), Artiste MV CBCT (Siemens, Munich, Germany), and Tomotherapy MV CT (Accuray, Sunnyvale, CA) system. For CT acquisition, the most common imaging protocol that would be chosen clinically to image a patient's head is used on each of the machines.

Using the open source software OsiriX Lite, a linear intensity profile is plotted perpendicular to the grid for each image set and each line pair. The difference between the maximum and minimum intensity for the largest line pair, 1 lp/cm, equals a modulation of 1. The intensity amplitudes of all sub-

sequent line pairs are relative to this value and are plotted against each line pair.

The critical frequency at 50% is used to compare the systems qualitatively to each other. The maximum line pair per cm that can be resolved is also considered.

# Results

Figure F.1 shows the relevant CT slice obtained on each imaging system. The table lists the gap size for each line pair per cm. Figure F.2 plots the resulting MTF for each system. The TrueBeam kV CBCT resolved intensity differences up to 8 lp/cm using an intensity profile along a line perpendicular to the grid. Its critical frequency at 50% is 4.7 lp/cm. Both, the Versa kV CBCT and Artiste MV CBCT only resolved up to 4 line pairs per cm. Their cricical frequency at 50% is 2.2 lp/cm and 1.6 lp/cm, respectively. In this setup, kV CT results in a 50% critical frequency of 4.3 lp/cm and the Tomotherapy MV CT system in 2.2 lp/cm. However, the MV CT system resolved up to 5 lp/cm, thus slightly better than the Versa kV CBCT.

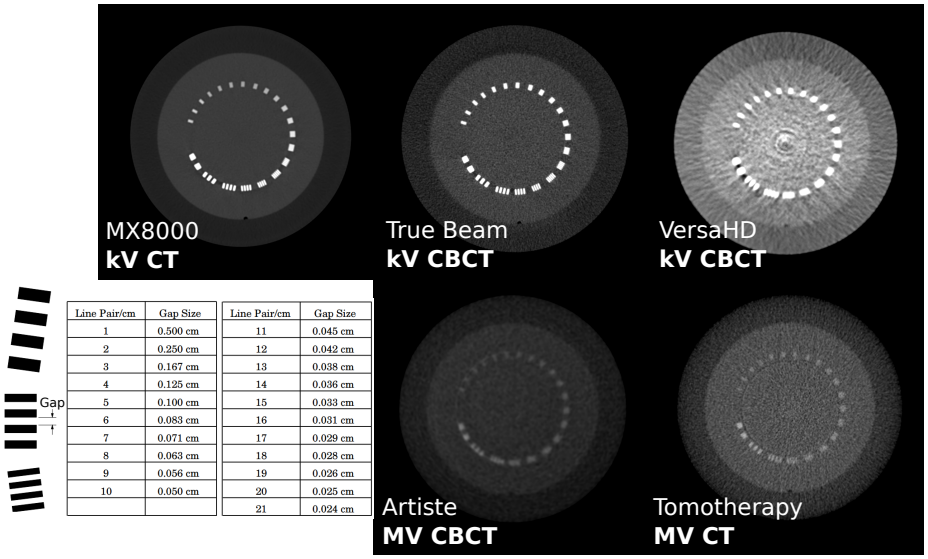


| Line Pair/cm | Gap Size | Line Pair/cm | Gap Size |
|---|---|---|---|
| 1 | 0.500 cm | 11 | 0.045 cm |
| 2 | 0.250 cm | 12 | 0.042 cm |
| 3 | 0.167 cm | 13 | 0.038 cm |
| 4 | 0.125 cm | 14 | 0.036 cm |
| 5 | 0.100 cm | 15 | 0.033 cm |
| 6 | 0.083 cm | 16 | 0.031 cm |
| 7 | 0.071 cm | 17 | 0.029 cm |
| 8 | 0.063 cm | 18 | 0.028 cm |
| 9 | 0.056 cm | 19 | 0.026 cm |
| 10 | 0.050 cm | 20 | 0.025 cm |
| | | 21 | 0.024 cm |

**Figure F.1:** CT images of the CatPhan Phantom that were used to determine the spatial resolution of each imaging system. Image contrast is displayed as the same for each image.

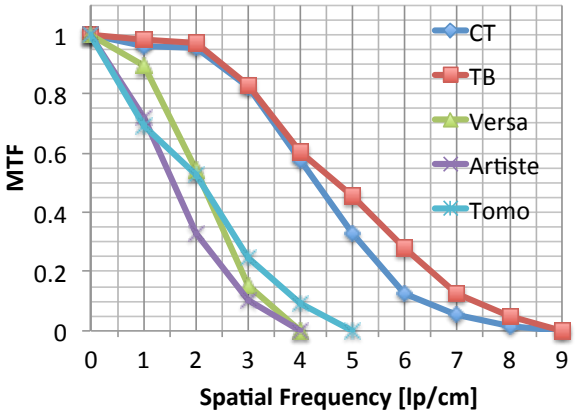


**Figure F.2:** The MTF of each measured CT system.

# Conclusion

According to the image protocols used in this setup, TrueBeam kV CBCT produces the highest spatial resolution. kV CT images have a spatial resolution only slightly smaller. Artiste MV CBCT has the lowest spatial resolution performance. Although the MV CT system and the Versa kV CBCT system have the same critical frequency at 50%, the Tomotherpay system delineates 4 lp/cm at a higher modulation.

# Publications & Presentations on this Subject

### Oral and Poster Presentations

| | | |
|---|---|---|
| 2013 | AAPM Annual Meeting<br>Indianapolis, IN | Poster Presentation |
| 2014 | AAPM Annual Meeting<br>Austin, TX | Poster Presentation |
| 2014 | EPI2K14 conference<br>Århus, Denmark | Oral Presentation |
| 2014 | ASTRO Annual Meeting<br>San Francisco, CA | Poster Presentation |
| 2015 | AAPM Annual Meeting<br>Anaheim, CA | Oral Presentation |

### Publications

Held M, Sneed P K, Fogh S E, Pouliot J, and Morin O, "Feasibility of MV CBCT-based treatment planning for urgent radiation therapy: dosimetric accuracy of MV CBCT-based dose calculations". *J Appl Clin Med Phys* 2015;**16**(6):458-471.

Held M, Cremers F, Sneed P K, Braunstein S, Fogh S E, Nakamura J, Barani I, Perez-Andujar A, Pouliot J, and Morin O, "Assessment of image quality and dose calculation accuracy on kV CBCT, MV CBCT and MV CT images for urgent palliative radiotherapy treatments". *J Appl Clin Med Phys* 2016; (Accepted. In press.)

# Acknowledgments

It has been an exciting and interesting four years of research for me and I would like to express my sincere gratitude and appreciation to all those who contributed to the realization and completion of this dissertation.

In particular, I would like to thank my team of supervisors for making this international project viable. I am grateful to the late Prof. Jean Pouliot who took me on as his student and made it possible for me to work with the amazing RadOnc team at UCSF. Jean introduced me to Asst. Prof. Olivier Morin, who was my go-to person for any questions throughout this project since the first day. I am very lucky to have him as my mentor and I want to thank him for the around-the-clock support he has given me as well as for taking on Jean's responsibilities when he was no longer able to.
I would also like to thank Dr. Florian Cremers for his support over the years and his guidance along the way. It takes special dedication to mentor students over this large distance. Also, I want to thank Prof. Dieter Horns for his commitment to this project and for taking on the responsibilities as the chairman of this committee.

I would like to thank Siemens OCS and DOSIsoft for their financial support, which allowed me to do my research at UCSF.

I would like to take the opportunity to thank Prof. Chris Diederich and Asst. Prof. Martina Descovich for their help on behalf of Jean, especially during the last year, and for freeing up my clinical schedule to focus on finalizing my dissertation. I also want to thank Alan Taniguchi and Mauricio Guerrero for all their administrative efforts and their hard work to get the recurring paperwork sorted out on time.

The clinical success of this project is also owed to the wonderful team I had the pleasure working with and I would like to express my deepest gratitude

to all therapists, dosimetrists, physicists, and physicians who helped me to make this project clinically feasible. I am fortunate to have had the support of a strong physics team who never hesitated to help me overcome any obstacles along the way, discuss issues over a coffee, or take the time to assist me on the machines.

I spent a lot of time with the physics residents and I am thankful they included me in their circle as if I was one of their own and who helped me in every way they could. Many of them became close friends of mine. Special thanks to Neil, Lisa, Atchar, Sarah, Chris, and Joey!

Neil and Atchar both provided critical comments on my dissertation, which I want to thank them for. I want to especially mention Dr. Neil Kirby - although he left UCSF a few years ago to take a position in San Antonio, TX, he will always be my mentor and role model, whether he wants to or not. He seems to never tire of helping me with my questions and I hope that some day I will have the honor of working with him again.

Almost last but not least I want to thank my family: my parents, siblings, siblings in-law, and grandparents. I am incredibly fortunate to have such a supportive and encouraging family!

I would not have been able to keep up the good spirit throughout the PhD research if it was not for my fiance Reuben. His everlasting support and love was the driving force to the completion of this dissertation. Thank you for keeping up with the long nights and weekends spent in the RadOnc 'basement' and making sure I don't forget to eat over the last few weeks.

**Thank you all!**

# Bibliography


[1] D. Yan et al., "Adaptive Radiation Therapy," *Phys Med Biol*, vol. 42, pp. 123–132, January 1997.

[2] U. Oelfke, "Image Guided Radiotherapy," in *Radiotherapy and Brachytherapy* (Y. Lemoigne and A. Caner, eds.), Springer Science + Business Media B.V., 2009.

[3] M. Gabel, "Palliation and Oncologic Emergencies," in *Handbook of Radiation Oncology* (B. G. Haffty and L. D. Wilson, eds.), ch. 7, Jones and Bartlett Publishers, LLC, 2007.

[4] D. Hoegler, "Radiotherapy for palliation of symptoms in incurable cancer," *Current Problems in Cancer*, vol. 21, pp. 129–183, May/June 1997.

[5] L. C. Lim et al., "Management of brain metastases," *Internal Medicine Journal*, vol. 34, pp. 270–278, May 2004.

[6] A. Konski et al., "Palliative radiation therapy," *Seminars in Oncology*, vol. 32, pp. 156–164, November 2005.

[7] B. van Oorschot et al., "Palliative Radiotherapy - New Approaches," *Seminars in Oncology*, vol. 38, pp. 443–449, June 2011.

[8] J. P. Gibbons et al., "Monitor unit calculations for external photon and electron beams: Report of the AAPM Therapy

Physics Committee Task Group No. 71," *Med Phys*, vol. 41, pp. 031501–1 – 031501–34, March 2014.

[9] P. Koulouvaris et al., "Incidence of heterotopic ossification in patients receiving radiation therapy following total hip arthroplasty," *Advances in Orthopedic Surgery*, p. 4, 2014.

[10] A. K. Hedley et al., "The prevention of heterotopic bone formation following total hip arthroplasty using 600 rad in a single dose," *The Journal of Arthroplasty*, vol. 4, pp. 319–325, December 1989.

[11] W. L. Healy et al., "Single-dose radiation therapy for prevention of heterotopic ossification after total hip arthroplasty," *The Journal of Arthroplasty*, vol. 5, pp. 369–375, December 1990.

[12] P. N. McDermott and C. G. Orton, *The Physics & Technology of Radiation Therapy*, ch. 9. Medical Physics Publishing, Madison, WI, 1st ed., 2010.

[13] P. R. Almond et al., "AAPMs TG-51 protocol for clinical reference dosimetry of high-energy photon and electron beams," *Med Phys*, vol. 26, pp. 1847–1870, September 1999.

[14] F. H. Attix, *Introduction to Radiological Physics and Radiation Dosimetry*. Wiley-VCH, 2004.

[15] F. M. Khan, *The physics of radiation therapy*. Lippincott Williams & Wilkins, 3rd ed., 2003.

[16] C. M. Prado and K. L. Prado, "Photon dose distributions," in *Principles and Practice of Radiation Therapy* (C. M. Washington and D. Leaver, eds.), ch. 24, Elsevier Mosby, 4th ed., 2015.

[17] M. J. Day, "A note on the calculation of dose in x-ray fields," *Br J Radiol*, vol. 23, pp. 368–369, June 1950.

[18] T. D. Sterling et al., "Derivation of a mathematical expression for the percent depth dose surface of cobalt 60 beams and visualization of multiple field dose distributions," *Br J Radiol*, vol. 37, p. 544, 1964.

[19] J. A. Purdy et al., "Three-dimensional treatment planning and conformal therapy," in *Technical Basis of Radiation Therapy* (C. A. P. S. H. Levitt, J. A. Purdy and S. Vijayakumar, eds.), ch. 9, Springer, 4th ed., 2006.

[20] U. Oelfke and C. Scholz, "Dose Calculation Algorithms," in *New Technologies in Radiation Oncology* (W. Schlegel et al., ed.), ch. 15, Springer, 2006.

[21] T. R. Mackie et al., "A convolution method of calculating dose for 15 mv x-ray," *Med Phys*, vol. 12, pp. 188–196, March/April 1985.

[22] A. Ahnesjö, "Collapsed cone convolution of radiant energy for photon dose calculation in heterogeneous media," *Med Phys*, vol. 16, pp. 577–592, July/August 1989.

[23] T. McNutt, "Dose Calculations - Collapsed Cone Convolution Superposition and Delta Pixwl Beam." `http://incenter.medical.philips.com/doclib/enc/5161735/Dose_Calculations-_Collapsed_Cone_Convolution.pdf%3Ffunc%3Ddoc.Fetch%26nodeid%3D5161735%26vernum%3D2`, December 2007. Philips Medical Systems. Retrieved January 20, 2016.

[24] N. Uricchio et al., "Simulator design," in *Principles and Practice of Radiation Therapy* (C. M. Washington and D. Leaver, eds.), ch. 21, Elsevier Mosby, 4th ed., 2015.

[25] International Commission on Radiation Units and Measurements (ICRU), "Determination of absorbed dose in a pa-

tient irradiated by beams of X or gamma rays in radiotherapy procedures," 1976. ICRU Report No. 24.

[26] A. Needham, "Simulation equipment," in *Practical Radiotherapy: Physics and Equipment* (P. Cherry and A. Duxbury, eds.), ch. 6, John Wiley & Sons, 2009.

[27] J. Cheung et al., "Dose Recalculation and the Dose-Guided Radiation Therapy (DGRT) Process Using Megavoltage Cone-Beam CT," *Int J Radiation Oncology Biol Phys*, vol. 74, pp. 583–592, December 2008.

[28] J. Van Dyk, *The Modern Technology of Radiation Oncology.* Medical Physics Publishing, 1st ed., 1999.

[29] J. T. Bushberg et al., *Essential Physics of Medical Imaging.* Lippincott Williams & Wilkins, 2nd ed., 2001.

[30] O. A. Zeidan et al., "Megavoltage computed tomography," in *Cancer Imaging* (M. A. Hayat, ed.), ch. 9, Elsevier Academic Press, 2008.

[31] M. G. Herman et al., "Clinical use of electronic portal imaging: Report of AAPM Radiation Therapy Committee Task Group 58," *Med Phys*, vol. 28, pp. 712–737, May 2001.

[32] L. E. Antonuk, "Electronic portal imaging devices: a review and historical perspective of contemporary technologies and research," *Phys Med Biol*, vol. 47, pp. R31–R65, 2002.

[33] B. A. Groh et al., "A performance comparison of flat-panel imager-based mv and kv cone-beam ct," *Med Phys*, vol. 29, pp. 900–907, June 2002.

[34] UCSF Comprehensive Cancer Center, "Tutorial on Portal Imaging." `http://radonc.ucsf.edu/research_group/jpouliot/tutorial/main.htm`, February 2005. Retrieved January 18, 2016.

[35] O. Morin, *The Development and Role of Megavoltage Cone Beam Computerized Tomography in Radiation Oncology.* PhD thesis, Laval University, Québec City, Canada, 2007.

[36] P. Suetens, *Fundamentals of Medical Imaging.* Cambridge, UK: Cambridge University Press, 2nd ed., 2009.

[37] S. Xie et al., "A level set method for cupping artifact correction in cone-beam ct," *Med Phys*, vol. 42, pp. 4888–4895, August 2015.

[38] J. H. Siewerdsen and J.-J. Sonke, "Kilovoltage cone-beam ct guidance of radiation therapy," in *Image-Guided Radiation Therapy* (J. D. Bourland, ed.), CRC Press, Taylor & Francis Group, 2012.

[39] V. Wu et al., "Dosimetric impact of image artifact from a wide-bore CT scanner in radiotherapy treatment planning," *Med Phys*, vol. 38, pp. 4451–4463, July 2011.

[40] D. L. Parker, "Optimal short scan convolution reconstruction for fanbeam CT," *Med Phys*, vol. 9, pp. 254–257, March/April 1982.

[41] M. F. Chan et al., "Evaluation of imaging performance of major image," *Biomed Imaging Interv J*, vol. 7, no. 2, 2011.

[42] M. Held et al., "Assessment of image quality and dose calculation accuracy on kV CBCT, MV CBCT and MV CT images for urgent palliative radiotherapy treatments," *J Appl Clin Med Phys*, In Press.

[43] J. Chen et al., "Dose-guided radiation therapy with megavoltage cone-beam ct," *Br J Radiol*, vol. 79, pp. S87–S98, 2006.

[44] O. Morin et al., "Dose calculation using megavoltage cone-beam CT," *Int J Radiation Oncology Biol Phys*, vol. 67, pp. 1201–1210, April 2007.

[45] J.-F. Aubry et al., "Correction of megavoltage cone-beam CT images for dose calculation in the head and neck region," *Med Phys*, vol. 35, pp. 900–907, March 2008.

[46] D. Létourneau et al., "Online planning and delivery technique for radiotherapy of spinal metastases using cone-beam CT: image quality and system performance," *Int J Radiation Oncology Biol Phys*, vol. 67, no. 4, pp. 1229–1237, 2006.

[47] S. Yoo and F.-F. Yin, "Dosimetric feasibility of cone-beam CT-based treatment planning compared to CT-based treatment planning," *Int J Radiation Oncology Biol Phys*, vol. 66, pp. 1553– 1561, 2006.

[48] Y. Yang et al., "Evaluation of on-board kV cone beam CT (CBCT)-based dose calculation," *Phys Med Biol*, vol. 52, pp. 685–705, 2007.

[49] S. F. Petit et al., "Calibration of megavoltage cone-beam CT for radiotherapy dose calculations: Correction of cupping artifacts and conversion of CT numbers to electron density," *Med Phys*, vol. 35, pp. 849–865, March 2008.

[50] H. Guan and H. Dong, "Dose calculation accuracy using cone-beam CT (CBCT) for pelvic adaptive radiotherapy," *Phys Med Biol*, vol. 54, pp. 6239–6250, 2009.

[51] T. H. Thomas et al., "The adaptation of megavoltage cone beam CT for use in standard radiotherapy treatment planning," *Phys Med Biol*, vol. 54, no. 7, pp. 2067–2077, 2009.

[52] A. McIntosh et al., "Helical tomotherapy-based STAT RT: dosimetric evaluation for clinical implementation of a rapid

radiation palliation program," *Med Dosim*, vol. 35, no. 4, pp. 280–286, 2010.

[53] S. L. Mahan et al., "Evaluation of image-guided helical tomotherapy for retreatment of spinal metastasis," *Int J Radiat Oncol Biol Phys*, vol. 63, no. 5, pp. 1576–83, 2005.

[54] B. Kim et al., "Image-guided helical tomotherapy for treatment of spine tumors," *Clin Neurol Neurosurg*, vol. 110, no. 4, pp. 357–263, 2008.

[55] M. MacPherson et al., "On-line rapid palliation using helical tomotherapy: a prospective feasibility study," *Radiother Oncol*, vol. 87, no. 1, pp. 116–118, 2008.

[56] Y. Rong et al., "A planning study for palliative spine treatment using StatRT and megavoltage simulation," *J Appl Clon Med Phys*, vol. 12, no. 1, pp. 97–107, 2011.

[57] B. A. Faddegon et al., "Comparison of patient megavoltage cone beam CT images acquired with an unflattened beam from a carbon target and a flattened treatment beam," *Med Phys*, vol. 37, pp. 1737–1741, April 2010.

[58] Z. A. Alrowaili et al., "2D mapping of the MV photon fluence and 3D dose reconstruction in real time for quality assurance during radiotherapy treatment," *Journal of Instrumentation*, vol. 10, September 2015.

[59] P. Francois et al., "In vivo dose verification from back projection of a transit dose measurement on the central axis of photon beams," *Physica Medica*, vol. 27, pp. 1–10, January 2011.

[60] M. Ginsberg, "Varian unveils VitalBeam™ for affordable advanced radiotherapy." `http://investors.varian.com/2015-04-27-Varian-Unveils-VitalBeam-for-\`

Affordable-Advanced-Radiotherapy, April 2015. Retrieved December 23, 2015.

[61] B. A. Faddegon et al., "Low dose megavoltage cone beam computed tomography with an unflattened 4 MV beam from a carbon target," *Med Phys*, vol. 35, pp. 5777–5786, December 2008.

CURRICULUM VITAE

# MAREIKE HELD

47A Landers St, San Francisco, CA 94114
Phone (415) 678-9618 Office (415) 353-9847
mareike@lauterhelden.com

## EDUCATION

| | | |
|---|---|---|
| 2012 – present | Universität Hamburg, Hamburg, Germany | PhD Candidate – (Medical) Physics |
| 2006 – 2011 | Universität Hamburg, Hamburg, Germany | Diplom – Physics (M.Sc. equivalent) |
| 2003 – 2005 | Graf-Anthon-Günther Gymnasium, Oldenburg, Germany | Abitur (High School Graduation Certificate) |
| 2002 – 2003 | Eden Valley Watkins High School, MN, USA | High School Diploma |

## RESEARCH

2011 – present Graduate Research Scholar at the University of California San Francisco, Department of Radiation Oncology
PhD dissertation research: *A New On-Board Treatment Technique for Palliative and Emergency Treatments in Radiation Oncology*
Advisors: Prof. J. Pouliot, PhD (UCSF)
Asst. Prof. O. Morin, PhD (UCSF)
F. Cremers, PhD (U Schleswig-Holstein)
Prof. D. Horns, PhD (U Hamburg)

2010 – 2011 Research Scholar at the University of California San Francisco, Department of Radiation Oncology
Master's thesis research: *A New Modulated-Arc Inverse-Planned Total Body Irradiation Technique*
Advisors: Prof. J. Pouliot, PhD (UCSF)
F. Cremers, PhD (U Hamburg)

## Research and Internship Positions Held

| | |
|---|---|
| 2012 – present | Assistant Specialist (Step 1 - 3) at the University of California San Francisco, Department of Radiation Oncology |
| 2010 – 2011 | Junior Specialist at the University of California San Francisco, Department of Radiation Oncology |
| 2008 – 2009 | Student Assistant at the Nano Science and Solid State Physics Laboratory, group for magnetic force microscopy (group of Prof. R. Wiesendanger), Universität Hamburg |
| 2005 – 2006 | 3-month internship for patient care training at Klinikum Kreyenbrück, Oldenburg, Germany |

## Professional Organizations

Memberships

| | |
|---|---|
| 2012 – present | American Association of Physicists in Medicine (AAPM) |
| 2006 – present | Deutsche Physikalische Gesellschaft (DPG) |

Service to Professional Organizations

| | |
|---|---|
| 2013 – present | AAPM's Student and Trainees Work Group Volunteer |

## Presentations

International

| | | |
|---|---|---|
| 2014 | EPI2K14 International Conference on Electronic Patient Imaging, Aarhus, Denmark | Oral Presentation |
| 2013 | University of Hamburg, Department of Radiation Oncology, Hamburg, Germany | Oral Presentation |

| | | |
|---|---|---|
| 2012 | University of Hamburg, Department of Radiation Oncology, Hamburg, Germany | Oral Presentation |
| 2011 | AAPM/COMP Joint Annual Meeting, Vancouver, Canada | Oral Presentation |
| 2011 | University of Hamburg, Department of Radiation Oncology, Hamburg, Germany | Oral Presentation |

National

| | | |
|---|---|---|
| 2015 | AAPM Annual Meeting, Anaheim, CA | Oral Presentation |
| 2014 | AAPM Annual Meeting, Austin, TX | Poster Presentation |
| 2014 | ASTRO Annual Meeting San Francisco, CA | Poster Presentation |
| 2013 | AAPM Annual Meeting, Indianapolis, IN | Poster Presentation |
| 2012 | AAPM Annual Meeting, Charlotte, NC | Oral Presentation |

Regional

| | | |
|---|---|---|
| 2015 | AAPM Bay Area Chapter Meeting – Young Investigator's Symposium Berkeley, CA | Oral Presentation |
| 2014 | AAPM Bay Area Chapter Meeting – Young Investigator's Symposium San Francisco, CA | Oral Presentation |

## PEER REVIEWED PUBLICATIONS

Kim H, Chen J, Chuang C, Held M, Pouliot P, *Non-local total-variation (NLTV) combined with reweighted L1-norm for compressed sensing CT reconstruction,* Phys Med Bio. Submitted.

Held M, Cremers F, Sneed P K, Braunstein S, Fogh S E, Nakamura J, Barani I, Perez-Andujar A, Pouliot J, Morin O, *Assessment of image quality and dose calculation accuracy on kV CBCT, MV CBCT and MV CT images for urgent palliative radiotherapy treatments.* J Appl Clin Med Phys 2016. In press.

Held M, Sneed P K, Fogh S E, Pouliot J, Morin O, *Feasibility of MV CBCT-based treatment planning for urgent radiation therapy: dosimetric accuracy of MV CBCT-based dose calculations.* J Appl Clin Med Phys 2015 Nov;16(6):458-471.

Held M, Kirby N, Morin O, Pouliot J, *Dosimetric aspects of inverse-planned modulated-arc total-body irradiation.* Med Phys 2012 Aug;39(8):5263-71.

Kirby N, Held M, Morin O, Fogh S, Pouliot J, *Inverse-planned modulated-arc total-body irradiation.* Med Phys 2012 May;39(5):2761-4.

Other Publications

Held M, *A New Modulated-Arc Inverse-Planned Total-Body Irradiation Technique.* Master's thesis, Universität Hamburg (2011).

The thesis contains six chapters summarizing my research project I performed to receive the master-equivalent german "Diplom" degree. It describes the newly developed treatment technique, which is being used clinically at UCSF since 2011, in detail and presents all measurements that were performed during the one-year research project. The thesis was awarded the grade of *excellent*, the highest distinction at a German university.

Significant Publications

Kirby N, Held M, Morin O, Fogh S, Pouliot J, *Inverse-planned modulated-arc total-body irradiation.* Med Phys 2012 May;39(5):2761-4.

This manuscript describes the new technique for modulated-arc total-body irradiation. Figure 2 was chosen as the cover image in the May 2012 issue of the Medical Physics journal. This was the topic of my master's thesis at the time and I contributed my measurements data and ideas to this publication. It was the first publication of two that introduced MATBI as a new treatment procedure for total-body irradiation using linear accelerators in standard sized treatment vaults. Since then, many institutions all over the world have shown interest in implementing the technique at their clinic.

## HONORS AND AWARDS

2010 STIP-OUT travel grant by Universität Hamburg